The Characteristics of Ribbed Moraine and Assessment of Theories for Their Genesis.

Volume 1

Paul Dunlop

A Thesis Submitted for the Degree of Doctor of Philosophy

The University of Sheffield
Department of Geography

January 2004

CONTAINS

PULLOUTS

Abstract

Ribbed (Rogen) moraines are large subglacially formed transverse ridges that cover extensive areas of the beds of the former Laurentide, Fennoscandian and Irish ice sheets. Since the flow speeds and stability of ice sheets are known to be sensitive to conditions operating at the bed, a full understanding of the processes of ribbed moraine genesis are critical if we are to appreciate their role in ice sheet dynamics.

Several theories of ribbed moraine genesis have been published, however, these could not be tested due to the paucity of data on ribbed moraines. This thesis addresses this deficit by producing the first representative data set on ribbed moraine characteristics. Various remote sensing and GIS techniques were used to record the morphological, morphometric and spatial characteristics of ribbed moraines in Ireland, Canada and Sweden, over a combined area of 81,000 km^2. This established that some published accounts were inaccurate or untrue, and that ribbed moraine morphology is more complex than was hitherto reported. This thesis demonstrates that ribbed moraines form independent of topographic influences, are not always curved down-ice, do not have accordant summits, can have both steep proximal and distal sides, have undulating crests and resemble waves, are not always anastomosing and do not necessarily fit neatly together like a jigsaw. This thesis also provides the first quantitative database of ribbed moraine ridge length, width, height and wavelength, and demonstrates they exist over a larger scale range than was previously thought.

The above data were used to test the various ribbed moraine theories. This led to the rejection of the topographic model of shear and stack and undermined the credibility of all other shear and stack hypotheses, the two-step hypothesis, the megaflood hypothesis and the thermal fracturing model of formation. Ribbed moraine wavelength data were used to test the only numerical computer model of ribbed moraine formation, which argues that they are the product of instability in a deforming subglacial till. Extensive tests failed to falsify the model and it is concluded that it remains the prime candidate of explanation. However, if future tests or observations do falsify this model, we argue that because ribbed moraines share many common properties of other natural instabilities, it will be another instability mechanism that will emerge as being successful is explaining their genesis.

Abstract

Ribbed (Rogen) moraines are large subglacially formed transverse ridges that cover extensive areas of the beds of the former Laurentide, Fennoscandian and Irish ice sheets. Since the flow speeds and stability of ice sheets are known to be sensitive to conditions operating at the bed, a full understanding of the processes of ribbed moraine genesis are critical if we are to appreciate their role in ice sheet dynamics.

Several theories of ribbed moraine genesis have been published, however, these could not be tested due to the paucity of data on ribbed moraines. This thesis addresses this deficit by producing the first representative data set on ribbed moraine characteristics. Various remote sensing and GIS techniques were used to record the morphological, morphometric and spatial characteristics of ribbed moraines in Ireland, Canada and Sweden, over a combined area of 81,000 km^2. This established that some published accounts were inaccurate or untrue, and that ribbed moraine morphology is more complex than was hitherto reported. This thesis demonstrates that ribbed moraines form independent of topographic influences, are not always curved down-ice, do not have accordant summits, can have both steep proximal and distal sides, have undulating crests and resemble waves, are not always anastomosing and do not necessarily fit neatly together like a jigsaw. This thesis also provides the first quantitative database of ribbed moraine ridge length, width, height and wavelength, and demonstrates they exist over a larger scale range than was previously thought.

The above data were used to test the various ribbed moraine theories. This led to the rejection of the topographic model of shear and stack and undermined the credibility of all other shear and stack hypotheses, the two-step hypothesis, the megaflood hypothesis and the thermal fracturing model of formation. Ribbed moraine wavelength data were used to test the only numerical computer model of ribbed moraine formation, which argues that they are the product of instability in a deforming subglacial till. Extensive tests failed to falsify the model and it is concluded that it remains the prime candidate of explanation. However, if future tests or observations do falsify this model, we argue that because ribbed moraines share many common properties of other natural instabilities, it will be another instability mechanism that will emerge as being successful is explaining their genesis.

Acknowledgements

The preparation and writing of this thesis became somewhat of a geographical odyssey for me. I guess the beauty of being a remote sensor is that you are free to conduct your research anywhere you please, so long as you can plug in a PC, or are able to stare into a stereoscope, and I have fond memories of mapping and writing about ribbed moraines in Sheffield, Cambridge, the Outer Hebrides and in various parts of Ireland. Throughout my travels, I have had the pleasure of meeting some really excellent people, who not only made this thesis possible, but ultimately ensured I had a more enjoyable experience.

I cannot extend enough thanks to my supervisor Chris Clark, for all his support and encouragement during my time as his research student. They say a lot can happen in four years, but neither of us would have predicted the arrival of baby Molly and baby Rio, and it was great working alongside someone who personally understood both the joys and the trials and tribulations of being a new parent. I can honestly say that I had as much fun discussing babies with him as I did drumlins and ribbed moraine! Thank you for being a risk taker. Special thanks also goes to my co-supervisor Richard Hindmarsh for patiently guiding me into the realm of ice sheet modelling, and for spending long periods away from his own work at the British Antarctic Survey to do hard sums with me and run computer models. I also wish to acknowledge the help of Clas Hättestrand from Stockholm University, who unselfishly lent me his extensive collection of aerial photographs of Swedish ribbed moraine.

I am very grateful to the Department of Geography at the University of Sheffield for funding my project, and wish to acknowledge the help I received from all the staff and postgraduates during my time in Sheffield. I would particularly like to thank Rob Ferguson for helping me with the philosophy of numerical modelling, Paul Brindley and Young-Hoon Kim for help in all things relating to GIS, and to Monica Winsborrow for reading this thesis and providing some helpful comments. To all of the good friends I met at Sheffield, I extend my warmest appreciation, but special thanks go to Brian Garvey, Stuart MacQuarrie, Chris Stokes, Mike Smith, Paulo Fernandez Da Silva, Helen Howard, Janet O Sullivan, Julie Pedlar, and to my climbing partners, Niall Grimes, Donie O Sullivan, Pat Nolan and John Godding; the craic was always good when you were around.

During the final stages of this thesis I found myself back in Ireland in the Department of Geography at NUI Galway. I am particularly grateful to Kieran Hickey for introducing me to the department and to all the members of staff who encouraged me to keep going during the final stages.

Finally, I wish to acknowledge the unwavering support of my partner Siobhan Kenny and wonderful daughter Molly. You sacrificed a lot during the past few years; I can only hope that the completion of this thesis in some small way makes up for the countless hours spent away from you both. With my warmest love and affection I dedicate this work to you. Paul.

Contents

Volume 2

Chapter 1: Introduction

1.1. The significance of ice sheets

Glaciers and ice sheets are spectacular features that cover approximately 10 % of the Earth's surface. They are currently estimated to hold up to 33 million km^3 of fresh water, enough to raise global sea levels by 70 m if they were to melt (Benn and Evans, 1998). During the Quaternary Period, ice coverage is known to have been more extensive than it is today, with approximately one third of the globe estimated to have been covered by ice. During this period, the waxing and waning of the world's ice sheets and glaciers interacted with the Earth's surface creating visually stunning landscapes. Clearly, a thorough understanding of these interactions is essential for anyone who wants to fully understand the operation of ice sheets.

Ice sheets also affect the Earth in a variety of important ways. Their growth and disappearance both compresses and causes substantial rebound of the Earth's surface, which in turn influences relative sea levels. Ice loading is known to have resulted in large areas of the land surface beneath the Antarctic and Greenland ice sheets being depressed below current seal levels (e.g. Denton *et al.*, 1993). We also know that ice sheets are a critical component of the ocean-climate system and influence it in a number of important ways (Fig. 1.1). They have a high surface albedo, which reduces the overall amount of incoming solar radiation received at the Earths surface. This accentuates the thermal contrasts that already exist between the poles and equatorial regions and regulates the meridional transfer of heat from the tropics to the poles (Benn and Evans, 1998). Palaeo-ice sheets have recently been implicated in adversely affecting the Earth's thermohaline circulation pattern. The ocean sedimentological record has shown evidence of increased pulses of iceberg rafted debris into the North Atlantic Ocean, indicating rapid collapse of portions of the Laurentide Ice Sheet (Heinrich, 1988; Andrews and Tedesco, 1992, Bond *et al.*, 1992). These so called Heinrich events are known to have created massive influxes of fresh water from melting icebergs and have been implicated in shutting down the North Atlantic Drift, which triggered changes in atmospheric circulation in the North Atlantic region and other parts of the globe (e.g. Charles and Fairbanks, 1992; Street-Perrot and Perrot, 1992).

Obviously, a full understanding of the processes that control ice sheet motion is critical in helping to evaluate the role of such unstable glacier behaviour within the ice sheet-ocean-atmosphere system.

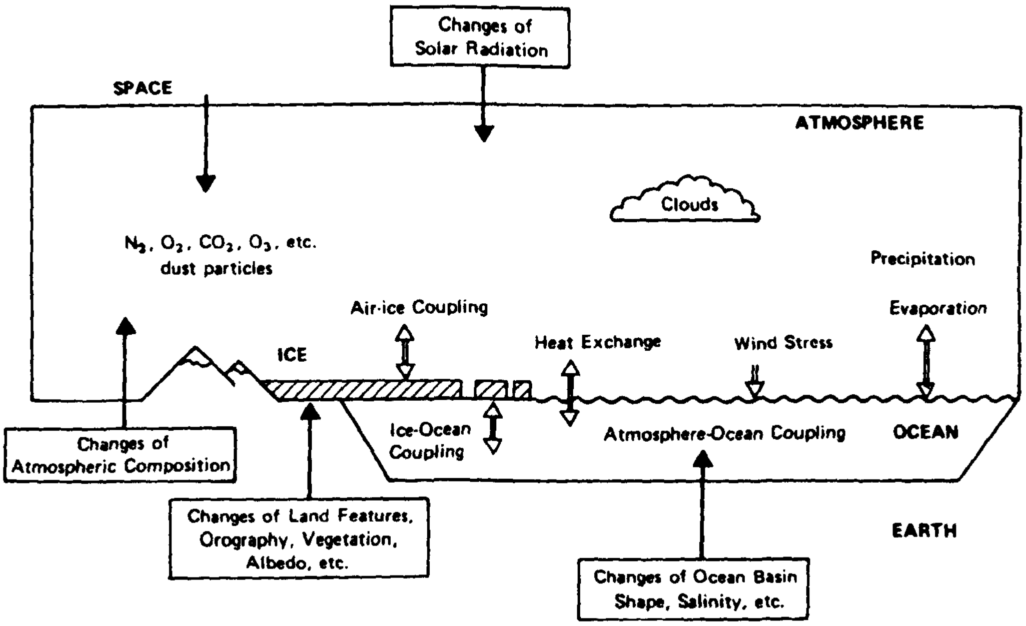

Figure 1.1. Schematic diagram showing the major components of the Earth's climate system. Feedbacks between various components play an important role in climatic variations. (After Bradley, 1995).

Currently there is some concern regarding the stability of contemporary ice sheets and how changes in their state might influence both global climate and sea levels. Of particular interest is the West Antarctic Ice Sheet (WAIS), which is mostly grounded below sea level. Presently, the midsummer temperatures at the outer limits of the ice sheet are a few degrees below freezing point. Thus, there is the possibility that the effects of increasing anthropogenic greenhouse gases in the atmosphere may lead to an ocean temperature increase large enough to begin to melt the ice sheet. The immediate consequence would be to raise global sea level by some 5 m (Vaughan and Spouge, 2002). Furthermore, the WAIS is drained by several large ice streams. These arteries of fast flowing ice are known to discharge up to 40 % of the ice from the WAIS (Bennett, 2003) and emphasises their crucial role in the overall dynamics of the ice sheet. These ice streams are controlled largely by unlithified subglacial sediments that are actively deforming. As of yet there is no consensus regarding how this process operates and until it is fully understood our ability to predict the stability of contemporary ice sheets is currently limited.

1.2. The importance of subglacial bedforms

A fundamental characteristic of glaciers and ice sheets is their ability to move. Ice movement is initiated by a variety of processes, such as internal deformation of the ice. However, it is now clear that much of the forward motion can be controlled largely by processes that operate at the bed (e.g. Lliboutry, 1968; Weertman, 1964; Nye, 1969) Boulton and Jones, 1979). Because of this, the basal area of an ice sheet can be viewed as a shear zone that includes the lower layers of the ice, the ice-bed interface, and deformable parts of the substratum where the greater part of glacier motion occurs by deformation and slip in this zone (Benn and Evans, 1998). The subglacial shear zone is of extreme importance for glacial erosion, transport and deposition, for it is here that the ice sheet interacts directly with the landscape, creating striking landforms such as *ribbed moraine*, drumlins and mega-scale glacial lineations. Since ice sheet motion can be controlled by processes operating at the bed and it is in this zone where subglacial bedforms are created, it seems logical to assume that such bedforms must be intrinsic to ice sheet motion. If one considers the areal extent of subglacial bedforms in formerly glaciated terrains is extensive, then their role in controlling ice sheet dynamics must have been significant (Fig. 1.2). Clearly until we fully understand the processes responsible for the formation of these landforms our knowledge of ice sheet dynamics remains incomplete.

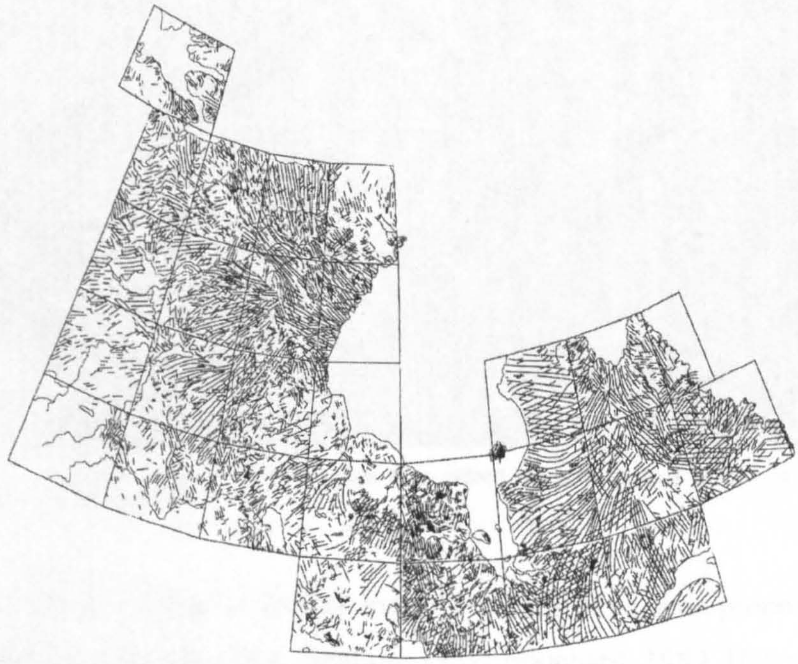

Figure 1.2. Pattern of glacial lineations mapped from satellite imagery of the area of most of Canada covered by the Laurentide Ice Sheet. Note the ubiquity of the subglacial bedforms across the bed of the ice sheet indicating their significance in controlling ice sheet motion. (After Boulton and Clark, 1990b).

Over the past few decades, much work has been conducted to try to decipher how these landforms are generated. Most of the research has focussed on explaining the formation of drumlins. Although much has been learnt about this bedform, a general theory of formation remains elusive and current ideas range from generation by deforming glacier beds (e.g. Boulton, 1987) to mega-scale subglacial sheet floods (e.g. Shaw, 1983). Ribbed (Rogen) moraine can be described as coalescent crescentic subglacially formed ridges that lie transverse to the former ice flow (Fig. 1.3). Typical size values reported in the literature range from 300-1200 m long, 150-300 m wide and 10-30 m in height (Hättestrand and Kleman, 1999). This landform has received less attention in the literature, which seems surprising considering they cover sizable portions of the beds of former ice sheets and are considered by some researchers to represent the initial phase of drumlin formation (e.g. Boulton, 1987; Hindmarsh, 1998a,b, 1999).

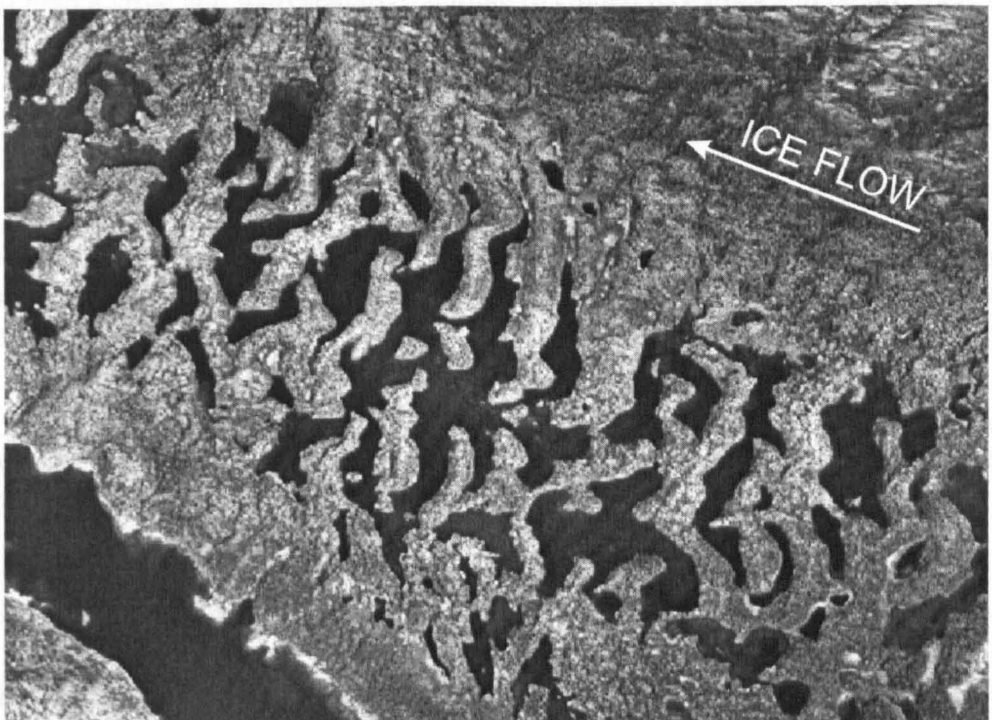

Figure 1.3. 1:60,000 scale aerial photograph of a ribbed moraine at Lake Rogen in southwest Härjedalen, central Sweden.

As with drumlins, a number of formational hypotheses have been proposed to explain the genesis of ribbed moraine (e.g. Boulton, 1987; Bouchard, 1989, Hättestrand, 1997b, Hindmarsh, 1998a,b; 1999). Clearly, if we are to appreciate their role in influencing ice sheet dynamics it is in our interest to rigorously test these ideas to determine whether they feasibly account for ribbed moraine formation. One way of testing these hypotheses is to use data on the characteristics of ribbed moraine to determine whether the competing theories explain their unique properties. However, it is clear from the literature that most observations of ribbed moraine characteristics are limited to small areas and with small sample sizes, and as such cannot be regarded as being generally applicable to all ribbed moraine. This thesis aims to address this shortfall by sampling ribbed moraines from the global population, recording their characteristics and producing the first comprehensive morphometric data set on ribbed moraine, which will be used to test the various theories of ribbed moraine genesis.

1.3. Specific aims of the research

The specific aims of this research are as follows;

1. To map a large and representative sample of ribbed moraines and record their spatial, morphological and morphometric characteristics.

2. To produce the first morphometric database on ribbed moraine ridge length, height, width and wavelength.

3. Use these data from (1) and (2) to examine each formational theory and make an assessment regarding whether or not they can be considered valid in light of the data gathered during this study.

4. Use the wavelength data from (2) to test a numerical computer model of ribbed moraine formation (Hindmarsh, 1998a,b, 1999), which specifically predicts the wavelength of ribbed moraine ridges.

1.4. Thesis structure

This chapter briefly discussed the significance of ice sheets and the importance of how subglacial processes create bedforms that in some way control ice sheet motion. Deforming glacier beds is just one of the processes that has been implicated in bedform generation and **Chapter 2** reviews what is currently known about this complex process. The chapter also introduces the reader to one of the most controversial ongoing debates within contemporary glaciology; do deforming subglacial sediments behave like a viscous or plastic material? Since subglacial bedforms, such as ribbed moraine and drumlins, are seen by many as being the geological product of this process, the ability to explain subglacial bedforms can be seen as a key test for any theory of subglacial sediment deformation. A recent theory of ribbed moraine genesis by a deforming bed mechanism has been presented by Hindmarsh (1998a,b, 1999). This author has produced the only numerical computer model of ribbed moraine genesis that makes quantitative predictions of ribbed moraine wavelength. A major part of this thesis will involve testing this model to assess whether its predictions are consistent with those observed in nature.

Chapter 3 describes the major types of subglacial bedforms and reviews some of the current theories of formation. Since ribbed moraines are the primary concern of this thesis a more thorough review of this landform is presented. The chapter finishes with a list summarising ribbed moraine characteristics based on information in the literature. **Chapter 4** outlines the basic methodology used during this thesis to investigate whether the reported characteristics are true. Remote sensing provides an excellent tool for doing this and the methods employed for investigating ribbed moraine properties are described in detail.

Chapters 5-8 use the methods outlined in Chapter 4 to explore the characteristics of ribbed moraines in four study sites; two in Canada and one in Sweden and Ireland. A variety of ribbed moraine characteristics are examined at each locality including;

1. The regional distribution,
2. Ribbed moraine field size and morphology,
3. Individual ribbed moraine ridge morphology,
4. Relationships with topography,
5. Relationships with other subglacial bedforms,
6. Detailed morphometric measures.

Chapter 9 summarises the results of the previous four chapters and compares them with the published accounts of ribbed moraine characteristics. The assertions made about ribbed moraines in the literature are critically evaluated. This established that many of the previous assertions made about ribbed moraines are either inaccurate or untrue, and it is argued that the competing ribbed moraine theories need to be reassessed in light of this new evidence. **Chapter 10** examines each formational theory in turn and makes an assessment regarding whether or not they can be considered valid in light of the new data discovered during this study.

The Hindmarsh theory of ribbed moraine formation is outlined briefly in Chapter 3. This theory is reviewed more fully in **Chapter 11**. It discusses the nature of the environment being modelled, provides a description of the numerical computer model, describes the input parameters, and explains how to interpret output from model runs. It introduces the reader to the style of tests conducted with the model to try to falsify it and explains the logic for choosing the parameter values that were used to constrain parameter space. Quantitative measures of ribbed moraine wavelength (presented in Chapters 5-8 and summarised in Chapter 9) are then compared against the model runs. The chapter concludes by assessing whether the Hindmarsh model can be considered a valid explanation of ribbed moraine genesis. Concluding remarks outlining the key discoveries made during this thesis are considered in **Chapter 12**.

***

Chapter 2: Deforming Glacier Beds

2.1. Introduction

It is well established that the flow speeds and stability of ice sheets is highly sensitive to conditions operating at the bed (e.g. Lliboutry, 1968; Weertman, 1964; Nye, 1969). Prior to the mid 1980s, most scientists believed that ice masses moved solely over hard bedrock with resistance to motion provided by bumps at the bed. Investigations of glaciers in Iceland however, (Boulton and Jones, 1979; Boulton and Hindmarsh, 1987), and results from high resolution seismic surveys from ice streams in Antarctica (Blankenship *et al.*, 1986), clearly demonstrated that some glaciers were underlain by unlithified sediments that were actively deforming. This realisation marked what has been described as a paradigm shift in glaciology (Boulton, 1986) and caused an immediate change in research focus for many glaciologists, as the process of subglacial deformation provided an explanation for unstable glacier behaviour and for the fast flow of some ice streams and outlet glaciers (Boulton and Jones, 1979; Clarke, 1987; Alley *et al.*, 1987). In some cases (e.g. Boulton and Hindmarsh, 1987), it has been established that deforming beds are responsible for up to 95 per cent of the forward motion of the ice mass, indicating the importance of deformation as a process of glacier motion and ice sheet stability.

Currently there is a large research drive directed towards understanding how deforming subglacial sediments behave. The main objective of this research is to establish a flow law for till that can be used to model the flow of glaciers and ice streams that are underlain by soft beds. This is extremely important in regard to the stability of the West Antarctic Ice Sheet (WAIS) and its possible effects on climate change and worldwide sea levels (Oppenheimer, 1998, Vaughan and Spouge, 2002). The WAIS is drained by several large fast flowing ice streams, whose flow rates are controlled largely by deforming sediment (Blankenship *et al.*, 1986; Kamb, 2001). Clearly, a full understanding of how this process operates is critical if we are to understand and predict the stability of contemporary ice sheets. Many glacial geomorphologists also argue that subglacial bedforms, such as ribbed (Rogen) moraine and drumlins, are the geological product of a deforming glacier bed (e.g. Boulton, 1987; Clark, 1993; Hindmarsh, 1998a,b,c, 1999; Hart, 1997). Therefore, an understanding of how bedforms are generated is also crucial if we are to fully understand the processes contributing to ice sheet dynamics. This clearly has implications for scientists searching for a flow law for till, because the ability to explain subglacial bedforms can be seen as a key test for any theory of subglacial sediment deformation (Hindmarsh, 1998a). This chapter briefly reviews what is known about deformable glacier beds since their discovery more than thirty years ago. It also introduces the reader to one of the most controversial ongoing debates of recent times within glaciology and glacial geomorphology; does subglacial deforming sediment behave as a viscous or a plastic material? These are two apparently contradictory statements about how till deforms in response to applied stress. If the rate of deformation increases continuously with the applied stress, the material is regarded as viscous. If, on the other hand, the rate of deformation changes discontinuously from practically nothing to a large amount at a given stress, the material is regarded as plastic (Fig. 2.1).

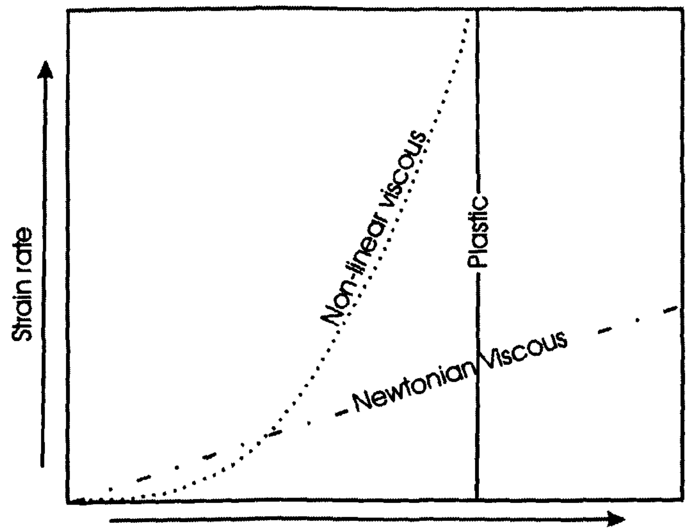

Figure 2.1. Schematic graph showing the relationship between strain rate and stress, and the difference between a viscous and a plastic rheology. In sediments with a viscous rheology, the rate of deformation increases with the applied stress in a non-linear fashion. Sediments that have a plastic rheology have a finite strength known as the yield strength above which they fail. In plastic materials the rate of deformation (strain rate) is in-dependent of the stress applied. In practice the rate of plastic deformation is limited by some other unspecified process, unrelated to the properties of the till, and generally the rate of deformation of ice. The viscous rheological relationship for till includes a dependence on the effective pressure, which is not illustrated in this diagram. (After Bennett, 2003).

These ideas can be expressed mathematically by the equations

$$\dot{\varepsilon} = A\frac{\tau^{b}}{p_e^{b}}, \qquad (2.1)$$

and

$$\tau = \eta p_e. \qquad (2.2).$$

In these equations $\dot{\varepsilon}$ is the strain rate, A is the viscous coefficient, τ is the shear stress, p_e is the effective pressure, b is the rheological exponent and η is the coefficient of friction. Equation (2.1) is a viscous relationship, while (2.2) is the plastic relationship, showing that the shear stress can never exceed the product of the coefficient of friction and the effective pressure. Thus, as illustrated in Figure 2.1, for the viscous relationship the strain-rate increases as the stress increases (the strain-rate is proportional to the stress raised to the power b), while in the plastic relationship the stress can never exceed the strength ηp_e.

2.2. Evidence of deforming glacier beds

The obvious way to settle this controversy is to observe and measure the bed of a glacier. However, gaining access to the beds of contemporary glaciers is extremely difficult, and consequently different novel approaches have been adopted in order to glean information on the behaviour of the till as it undergoes deformation. This section discusses some of these approaches and reviews what has been discovered by these investigations.

2.2.1. Field experiments – evidence of viscous behaviour

The first experiments to yield any information on the nature of how deforming subglacial sediment behaves came from a series of investigations conducted on Breidamerkurjökull, an outlet tongue of the Vatnajökull ice cap in southeast Iceland (Boulton, 1979; Boulton and Hindmarsh, 1987). These authors gained access to the glacier bed via a series of tunnels cut in from the margin where they inserted strain markers into the till beneath the ice. When these were excavated 136 hours later, the rod segments had been displaced downglacier by varying amounts, clearly revealing that the till was deforming (Fig. 2.2). The experiment established the till had a two-layered structure with a dilated upper A-horizon approximately 0.5 m thick and a denser lower B-horizon. Most of the observed deformation was by ductile flow of the upper till, which was responsible for 80-95 per cent of the observed surface motion of the glacier. The low strength of the A-horizon is partly due to its high porosity, only 40-45 per cent of the volume of the till was occupied by mineral grains, the rest consisting of water-filled pores. Measurements over a ten-day period demonstrated a strong relationship between pore water pressures and strain rates in the till, with peak strain rates lagging behind peaks in pore water pressures by a few hours. Boulton and Hindmarsh (1987) argued that high pore water pressures acted to reduce effective pressure, which created favourable conditions for deformation. The effective pressure is important in till mechanics because it determines the overall strength of the sediment. In subglacial till, effective pressure is the amount by which the overburden pressure, caused by the overlying ice and sediment, exceeds the pore water pressure.

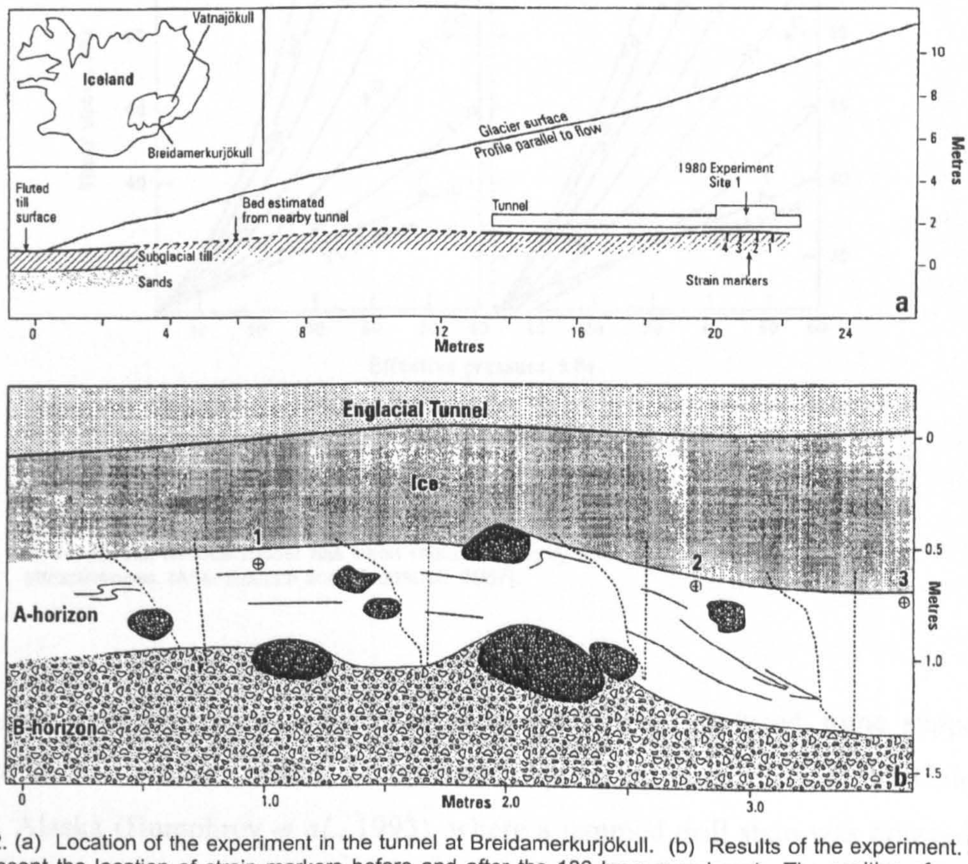

Figure 2.2. (a) Location of the experiment in the tunnel at Breidamerkurjökull. (b) Results of the experiment. Dashed lines represent the location of strain markers before and after the 136 hour experiment. The position of pore water transducers are marked 1-3. Large boulders and sand wisps are also shown. Two distinct horizons were found. The A-horizon (clear) is dilated and undergoing pervasive deformation. The sediment beneath in the B-horizon is consolidated and shearing only occurred along discrete shear zones. (After Boulton and Hindmarsh, 1987).

It measures how strongly the grains in the till are pushed together. As the effective pressure decreases, the till becomes less cohesive, allowing more rapid rates of deformation. Boulton and Hindmarsh (1987) argued that the strain patterns recorded by the markers were similar to patterns expected from a non-linearly viscous material, or Bingham material with a finite yield strength, whereby the rate of deformation increases with the applied stress (Fig. 2.1). They modelled the till using a viscous rheology and argued the model predicted strain rates consistent with their field measurements (Fig. 2.3). This type of viscous model has been used effectively to predict the large-scale patterns of erosion and sedimentation induced by subglacial deformation within ice sheets and to explain a range of geological observations in the field (e.g. Alley *et al.*, 1987; Hart *et al.*, 1990; Hart and Boulton, 1991; Boulton, 1996a,b).

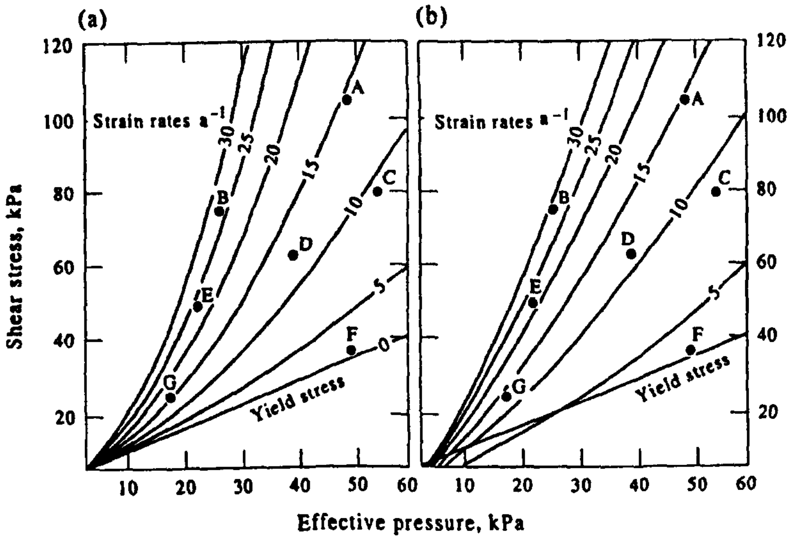

Figure 2.3. Relationships between shear stress, strain rate and effective pressure at Breidamerkurjökull. Measured values of the three parameters (points with letters) are compared to modelled strain rates using a visco-plastic Bingham rheology (a) and a purely viscous till rheology (b). The Mohr-Coulomb failure criterion for the till is also plotted (Yield stress). Measured strain rates in a^{-1} for these points are A: 14.17; B: 27.8; C: 9.35; D: 12.8; E: 24.58; F: 2.12; G: 12.16. Neither model can be preferred on the basis of the few data points, however, the viscous model has been more commonly used due its greater mathematical attractiveness. (After Boulton and Hindmarsh, 1987).

Subsequent field experiments by other investigators has produced some supporting evidence for the viscous model. A borehole experiment conducted on the Columbia Glacier, Alaska (Humphrey *et al.*, 1993), where a jammed drill stem was dragged over the glacier bed for five days yielded important data on the yield strength and viscosity of the till. The bed was inferred to be sediment and striations on the drill stem suggested differential motion between the upper and lower portions of the till, which is consistent with the till behaving either as a viscous or as a plastic medium. Humphrey *et al.* (1993) argued that by measuring the curvature of the drill stem, and calculating the force distribution by which it was bent it was possible to infer sediment properties. An assumption of plasticity led to an estimate of the sediment's yield strength of 5.5 kPa, while the assumption of viscosity led to an estimate of the viscosity of 2 x 10 Pa.s. Neither would be sufficient enough to support the calculated basal shear stress of 100 kPa.

Other field experiments however reveal a more complex pattern of deformation. Tilt-cells inserted into the bed of Trapridge Glacier, Yukon Alaska in 1988 and 1989 yielded widely different results from those above (Blake, 1992; Blake *et al.*, 1992). In 1988, measurements averaged over four days gave values of shear strain rate of 36 a^{-1} and effective pressure 292 kPa, and in 1989, six days of measurement recorded a dramatic drop in both parameters this time the shear strain rate was 4.1 a^{-1} and effective pressure was 78 kPa. Basal shear stress in both cases calculated from the local slope was 77 kPa. Murray (1997) argued these values are not in good agreement with the Boulton-Hindmarsh rheology, and Patterson (1994) noted that they conflict with the idea that deformation is rapid when effective pressures are low (Boulton and Hindmarsh, 1987). The 1988 measurements show a much higher strain rate in the till compared to that recorded in 1989 even though the effective pressure is almost four times higher. However, it is not clear whether computing the shear stress from the local slope is a sufficiently accurate procedure to warrant this conclusion.

2.2.2. Laboratory and field experiments – evidence of plastic behaviour

The idea of a viscous rheology for till has been fiercely contested by several researchers (e.g. Englehardt *et al.*, 1990; Kamb, 1991; Iverson *et al.*, 1998; Tulaczyk *et al.*, 2000). These authors argue that laboratory tests conducted on till retrieved from deforming glacier beds demonstrate failure in a plastic fashion and that in consequence tills have a Coulomb rheology. All of these experiments subjected the tills to varying values of shear stress under controlled conditions in a laboratory using a shear device. Till samples recovered from beneath ice streams of the WAIS (Fig. 2.4) have been extensively studied using these techniques since the early 1990's. Early experiments by

Kamb (1991) on till from Ice Stream B demonstrated that the till had a nearly plastic rheology, with almost no dependence of strength on the strain rate. At stresses below 2 kPa, the till showed transient creep, decreasing with time. Above this, it showed accelerated creep leading promptly to catastrophic failure, which increased drastically with attempts to apply shear loadings greater than 2 kPa. Kamb argued this is typical plastic behaviour (see Figure 2.1). The experiment indicated that till from Ice Stream B had a shear strength of 2 ± .2 kPa. Kamb (1991) also found that till from Ice Stream D behaved similarly and had a shear strength of 1 ± .2 kPa.

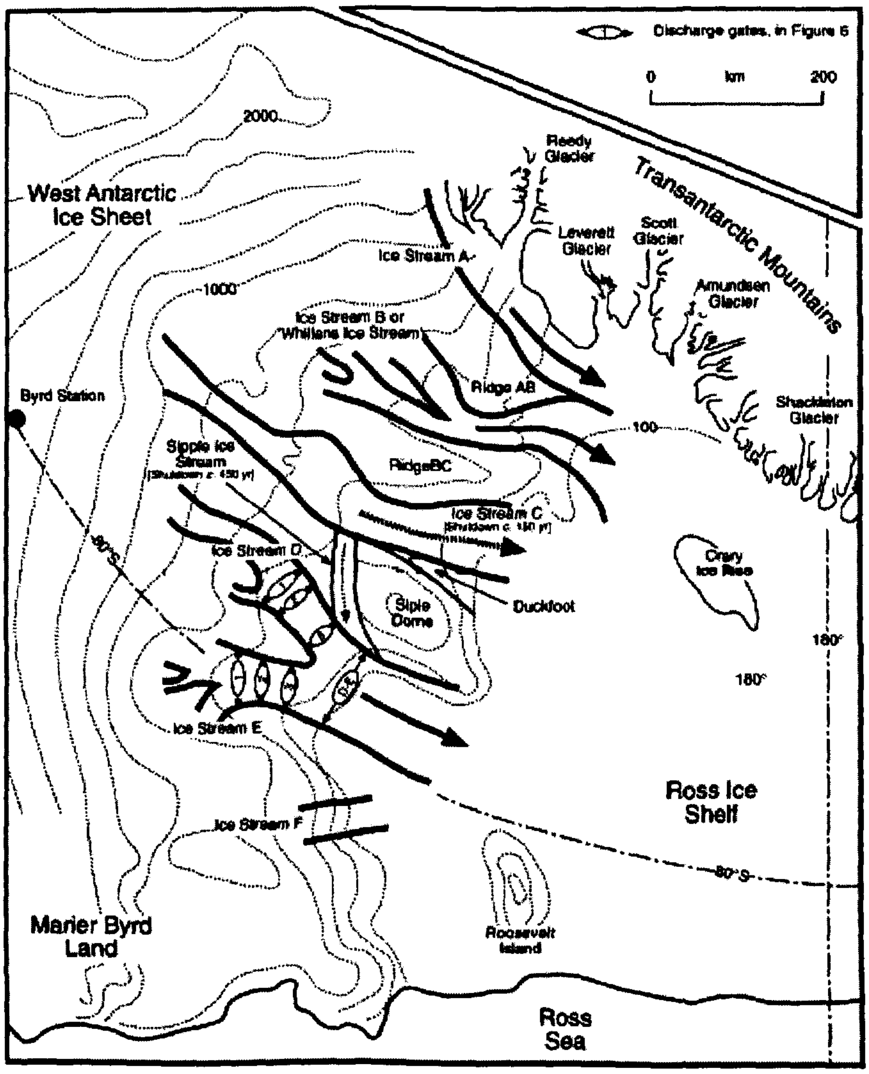

Figure 2.4. Sketch map showing the location Ice Streams A-F on the West Antarctic Ice Sheet. (After Bennett, 2003).

Other shear-box tests conducted by Englehardt *et al.* (1990) on till samples from Ice Stream B support the findings of Kamb (1991). In 16 tests carried out in the laboratory, they found the strength of the till was nearly constant at about 1.7 kPa. Above this, the till could withstand no shear stress and failed in a manner consistent of a till with a plastic rheology (Fig. 2.5). This result was criticised on the basis of assumptions that a relevant till rheology can only be obtained if samples are sheared to the higher strain typical of ice sheets than can be achieved using a shear-box (Tulaczyk, 1998).

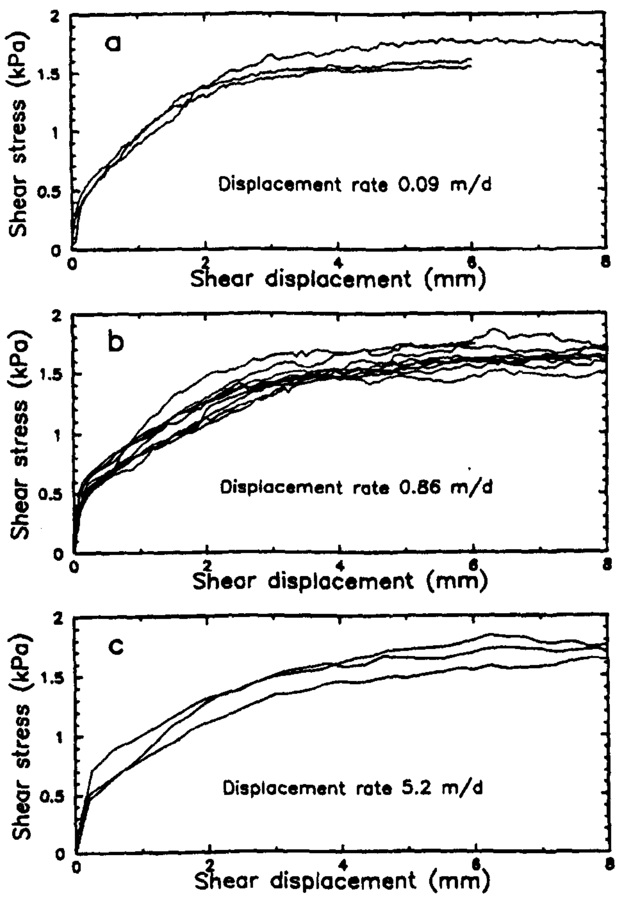

Figure 2.5. Shear displacement results using a shear-box device on till from Ice Stream B. Shear rates (a) 0.09 m day^{-1}; (b) 0.86 m day^{-1}; (c) 5.2 m day^{-1}. The graphs show that at very low shear stresses (i.e. <1.5 kPa) there is a small amount of viscous deformation. At shear stresses higher than this, the till fails catastrophically indicating plastic behaviour. The small viscous deformation events are ignored by this author since the low shear stresses are not glaciologically relevant. In other words shear stresses are usually much higher than this in a glacier. (After Kamb, 2001)

This deficit was overcome by using ring-shear devices, which can shear the till to much higher strains. These tests confirmed that at much higher levels of strain and effective stress, samples of till from Ice Stream B still behaved like a Coulomb-plastic material with no significant strain rate dependence of strength (Tulaczyck *et al.*, 2000). Tills from Antarctic ice streams appear not to be unique in this characteristic. Laboratory tests conducted on subglacial sediments from other glaciers also indicate a plastic, rather than a viscous rheology (e.g. Iverson *et al.*, 1995, 1998; Hooke *et al.*, 1997; Murray, 1997).

Storglaciären is mainly a warm-based glacier in northern Sweden that overlies soft sediments in its ablation zone (Brand *et al.*, 1987; Iverson *et al.*, 1995). Tilt-cells inserted into the till in 1992 and 1993 showed the till was deforming in a 0.33 m layer with a mean strain rate of 25 a^{-1} (Iverson *et al.*, 1995). An important observation was that the sediment was deforming in a localised manner rather than throughout the thickness of the sediment, which is more consistent with a plastic model of deformation.

2.2.3. Can plastic and viscous behaviour be reconciled?

The above discussion highlights a clear problem for glaciologists. Which rheology should be used for modelling the flow of deforming till? Experiments conducted in the field suggest the possibility of a non-linearly viscous rheology, whilst small-scale studies in the laboratory clearly show till behaves like a plastic material. Hindmarsh (1997) recently tried to reconcile both schools of thought by suggesting the behaviour of subglacial till may be scale dependent. His argument is that as the dimensional scale of deformation increases, till rheology undergoes a transition from plastic to viscous at a scale much larger than the grain scale, but smaller than the scale of deformation in large ice-sheet models (Kamb, 2001). Hindmarsh (1997) argued that above the cross-over scale between plastic and viscous deformation, till will flow like a viscous fluid. Like most authors, Hindmarsh (1997) acknowledges that at a small-scale, till fails by plastic failure, and that during such events, the rate of deformation is independent of the stress regime. However, he argues that the net integration of multiple small-scale plastic failures is best approximated by a viscous flow law. Hindmarsh (1997) drew an analogy with glacier ice, which on an atomic-scale behaves in a manner that is similar to plastic deformation, crystals deform by the migration of dislocations through the lattice (i.e. individual plastic failures). However, the net effect of multiple dislocations at a larger-scale is the nonlinear viscous-type behaviour, which is an accepted characteristic of ice flow as defined by Glen's Flow Law (Bennett, 2003). Hindmarsh (1997) argued that the same is true of subglacial till in which point-specific subglacial experiments and laboratory tests describe individual dislocations, the sum of which produces a viscous-type behaviour when viewed at a larger scale. Essentially, the two alternative models are reconciled by placing them at different ends of a scale spectrum. The idea by Hindmarsh (1997) of there being a cross-over in scale between plastic and viscous deformation is a novel idea, however it is not without its critics. Kamb (2001) for example correctly highlights Hindmarsh's acknowledgement that "the key theoretical problem which is yet to be solved is how multiple small scale failure events combine into a viscous type flow" (Hindmarsh, 1997, p. 1039).

As was noted earlier, as well as being able to simulate realistic ice sheet behaviour, a key test for any theory of subglacial sediment deformation will be its ability to account for subglacial bedforms such as ribbed moraine and drumlins. Hindmarsh (1998a,b,c, 1999) has produced two physically-based numerical computer models that use a viscous rheology for the till, and which he argues explains the formation and characteristics of drumlins and ribbed moraine. These are the only numerical models of bedform generation to date and are an important advance in the science because they make predictions of bedform characteristics that can be quantitatively tested (see Section 3.2.2.3). Clearly, a critical test for these models will be to what extent they can predict bedform characteristics that are consistent with those observed in nature. A major part of this thesis is concerned with gathering quantitative data on ribbed moraines that will be used to test the Hindmarsh model of ribbed moraine genesis (see Chapter 11).

2.3. Summary and conclusions

It is clear from the above discussion that there is currently no consensus as to the type of flow law which best approximates deforming subglacial sediment. Consequently, two broad schools of thought have emerged. One school fully embraces a plastic description of subglacial sediments (e.g. Englehardt *et al.*, 1990; Kamb, 1991; Iverson *et al.*, 1998; Tulaczyk *et al.*, 2000), whilst the other maintains that, although tills may deform in a plastic fashion at a small-scale, their gross behaviour at larger-scales still approximates a quasi-viscous flow rheology (Hindmarsh, 1997). Clearly if a flow law is to be considered reliable it must explain the laboratory, geomorphological and sedimentological properties of till and also be able to simulate realistic ice sheet behaviour. Some of these aspects are only beginning to be answered, with controversy raging between plastic and viscous behaviour, each providing only a partial explanation of the above. The plastic model can explain the laboratory properties of till, however the theory has yet to be developed to explain the formation of subglacial bedforms. Viscous behaviour has never been measured in the laboratory, however it has been widely adopted because it seems to explain many of the observations of geomorphology and sedimentology (e.g. Boulton, 1987; Hart, 1997). The development of two numerical computer models of bedform generation by Hindmarsh (1998a,b,c, 1999) marks an advancement in the field because for the first time the viscous theory can be quantitatively tested If rigorous tests fail to falsify these models then clearly weight will be added to the viscous side of the debate. The onus will then be placed on those who advocate plastic theory to develop numerical models that can account for the widespread generation of subglacial bedforms that take account of their morphological properties.

The next chapter introduces the reader to the major subglacial bedforms in more detail and reviews some of the more current formational theories.

***

Chapter 3: Subglacial Bedforms

3.1. Introduction

The previous chapters discussed how ice sheet motion is controlled partly by processes that operate at the bed and noted that the formation of subglacial bedforms must in some way influence ice sheet motion. This chapter discusses the major bedforms that are produced by processes in the subglacial zone and briefly reviews some of the current formational theories. Since ribbed moraines are the primary focus of this thesis, a more comprehensive review of this landform is presented.

3.2. Subglacial bedforms

Subglacial bedforms are either longitudinal or transverse accumulations of sediment that were formed beneath active ice (Rose, 1987; Menzies and Rose, 1987). The longitudinal bedforms, collectively termed glacial lineations, are streamlined features that are aligned parallel to ice flow direction and can be separated into four general categories; flutings, drumlins, megaflutes and mega-scale glacial lineations. The most significant of the transverse bedforms are ribbed moraine, which are also known as Rogen moraine (e.g. Lundqvist, 1969). The main distinction between the glacial lineations is based upon their length and elongation ratio. The elongation ratio is defined as:

$$E = l/w$$

Where E is the elongation ratio, l is the maximum length of the bedform and w is maximum bedform width. Elongation ratios and lengths of some streamlined features have been plotted by Rose (1987) and are shown in Figure 3.1. Generally, drumlins are large forms (> 100 m long axis) with elongation ratios up to about 7:1; flutings are much smaller lineations and are normally less than 100 m long with elongation ratios in the range of 2:1 to 60:1 or even more. Megaflutes are elongate bedforms with long axes usually greater than 100 m. Drumlinoid features longer than 1000 m are classified as streamlined hills (Benn and Evans 1998). Extremely large elongate bedforms many tens of kilometres long, hundreds of metres wide and over 25 m high have been recognised using satellite imagery and are classified as mega-scale glacial lineations

(Clark, 1993). The following sections examine in more detail the morphology and composition of these bedforms and discusses some of the more up to date formational theories.

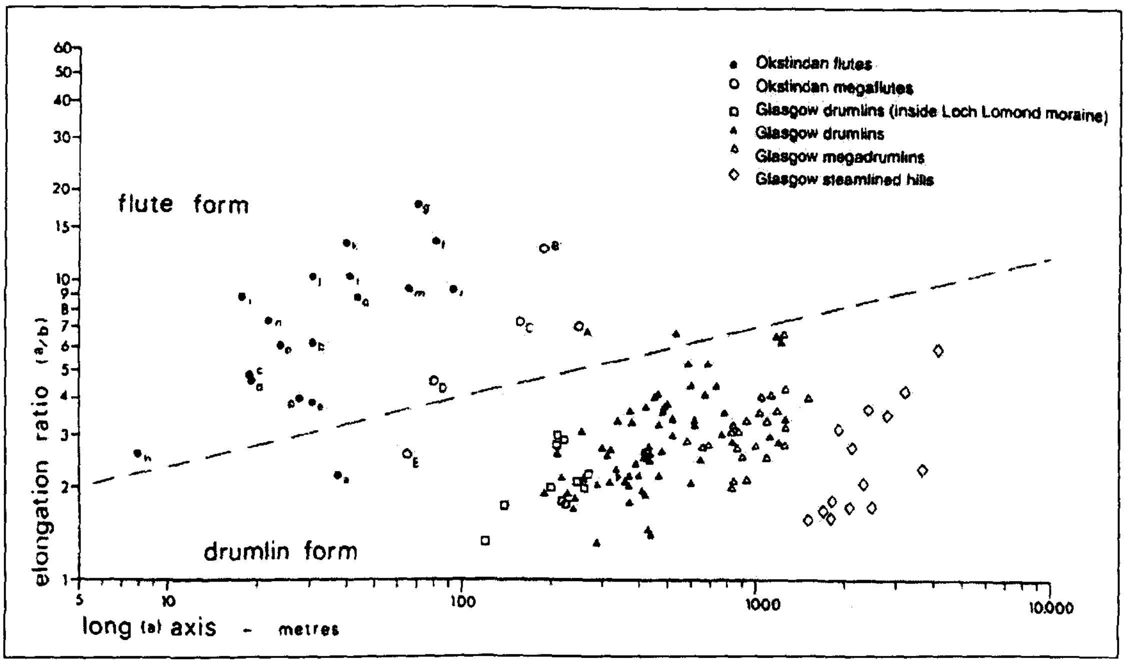

Figure 3.1 The relationship between length and elongation ratio of flutes, megaflutes, drumlins, mega-drumlins and streamlined hills from central Scotland (Glasgow area) and Scandinavia (O'kstindan). The dashed diagonal line reflects the possible quantitative differentiation of flutes and drumlins. (After Rose, 1987)

3.2.1. Flutings

Flutings or flutes are elongate streamlined subglacial ridges that are orientated in the direction of glacier flow, giving a corrugated appearance to many contemporary glacial forelands (Fig. 3.2). Like other subglacial bedforms, flutes form at a variety of scales and are common in a wide range of glacial environments. They have been observed in front of drumlin belts (Miller, 1972), superimposed on top of drumlins (Rose, 1989) and ribbed moraine (Lundqvist, 1969; Bouchard, 1989) and found in isolation in the proglacial zone of many present-day glaciers (Benn, 1994). Compared to other subglacial bedforms they are relatively small, being generally a few tens of centimetres to several metres high and wide (Table 3.1). Several theories of flute formation have been proposed, however, according to Benn and Evans (1998) the most widely accepted model regards flutings as the product of subglacial sediment deformation in the lee of obstructions at the bed such as large boulders (Dyson, 1952; Boulton, 1976; Benn, 1994; Eklund and Hart, 1996).

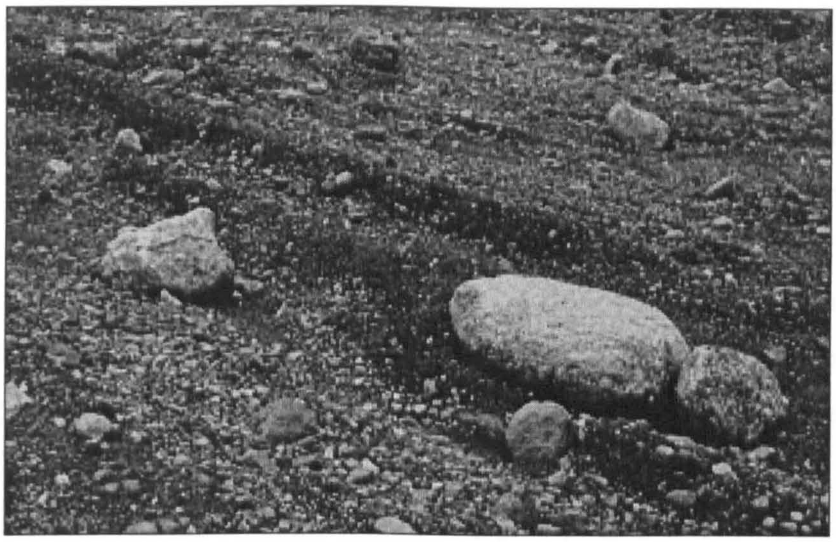

Figure 3.2. Fresh flutings at Breidamerkurjökull, Iceland. Note deflection of the nearest flute around the boulder (After Benn and Evans, 1998).

Table 3.1. Maximum height of flutes observed by various authors. (After Menzies and Shilts, 1996)

Reference	Locality	Height (m)
Grant and Higgens (1913)	Petrof Glacier, Alaska	0.45
Paul and Evans (1974)	Blomstrandbreen, Spitsbergen	0.1, 0.2
Boulton and Dent (1974)	Breidamerkurjökull, Iceland	0.5
Ray (1935)	Mendenhall Glacier, Alaska	0.075
Todtmann (1952)	Bruarjökull, Iceland	2.0
Hoppe and Schytt (1953)	Bruarjökull, Iceland	1.0
Kozarski and Szpryczynski	Sidujökull, Iceland	1.3
Baranowski (1970)	Werenskioldbreen, Spitsbergen	0.3
Dyson (1952)	Grinnell Glacier/Sperry Glacier, Montana	0.9

3.2.2. Drumlins, megaflutes and mega-scale glacial lineations

Drumlins are arguably the most studied subglacial bedform and interest in their formation has produced a large number of publications and almost as many formational theories (e.g. Upham, 1892; Alden, 1905; Fairchild, 1929; Menzies, 1984; Boulton, 1987; Shaw, 1983). Nonetheless, despite this large body of knowledge, drumlins remain enigmatic and many questions regarding their formation remain unanswered. Considering that ice sheet motion is largely controlled by processes operating at the bed, and that this is the zone where drumlins are initiated, then it follows that drumlins must in some way influence ice sheet motion. As stated previously, considering that the areal extent of glacial lineations in formerly glaciated terrains is extensive then this role must have been significant.

The term drumlin was derived in 1867 by M. H. Close in Ireland, who took the name from the Gaelic *druim*, meaning a rounded hill. According to Menzies (1979), drumlins are typically smooth, oval shaped hills or hillocks of glacial drift resembling in morphology an inverted spoon or an egg half buried along its long axis. Generally, but not always, the steep blunter end points in the up-ice direction and the gentler sloping pointed end faces in the down-ice direction, these two ends being respectively known as the stoss and lee sides (Fig. 3.3). The long axes of drumlins are usually oriented parallel to the direction of ice flow. Although a classic description of a "typical" drumlin, this is somewhat over simplified and in reality drumlin morphology shows a high degree of variability (Fig. 3.4). Long, narrow drumlins have been termed spindle forms, and broader, often asymmetrical drumlins are called parabolic drumlins (Shaw, 1983; Shaw *et al.*, 1989). More complex forms also exist, such as asymmetrical drumlins (Claperton, 1989) and Rose and Letzer (1977) researching drumlins in east Cumbria and central Scotland, describe mega-drumlins and superimposed drumlins, which are smaller bedforms situated on the surface of the mega-drumlins. Knight (1997), studying drumlins in the Omagh Basin, north central Ireland, also identified superimposed drumlins and classified several other types:

1. *Shield drumlins*, having low elongation ratios.

2. *Barchanoid drumlins*, these show down-ice trending horns of sediment that tail from the from the drumlin lee side.

3. *Compound drumlins*, of which there are two type, **(a)** *fused drumlins*, composed of a number (two to five) of smaller forms which are generally of similar size and stacked side by side as serrated ridges and **(b)** *superimposed* drumlins, which are larger (mainly shield and barchanoid) rock cored drumlins upon which smaller areas of diamict are superimposed.

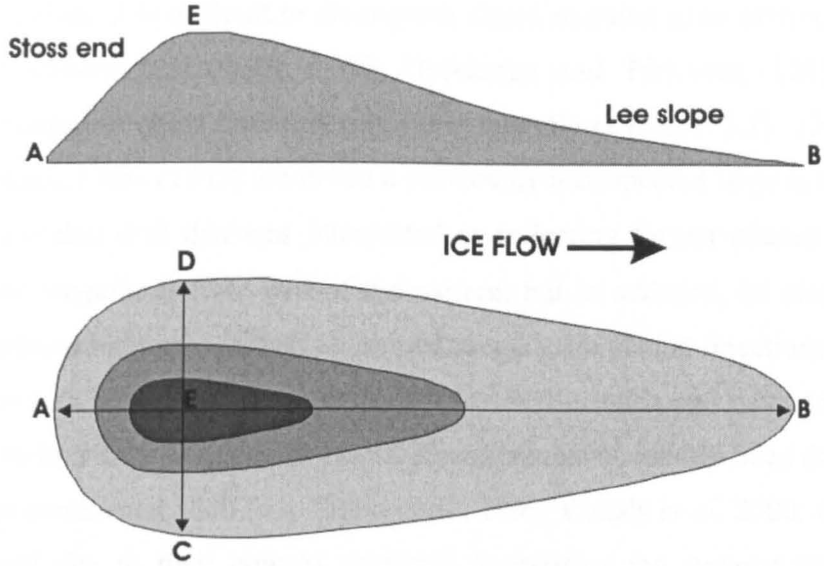

Figure 3.3. Schematic drawing of a classic type drumlin showing the characteristic steep upstream facing stoss end and a tapering lee that points downstream.

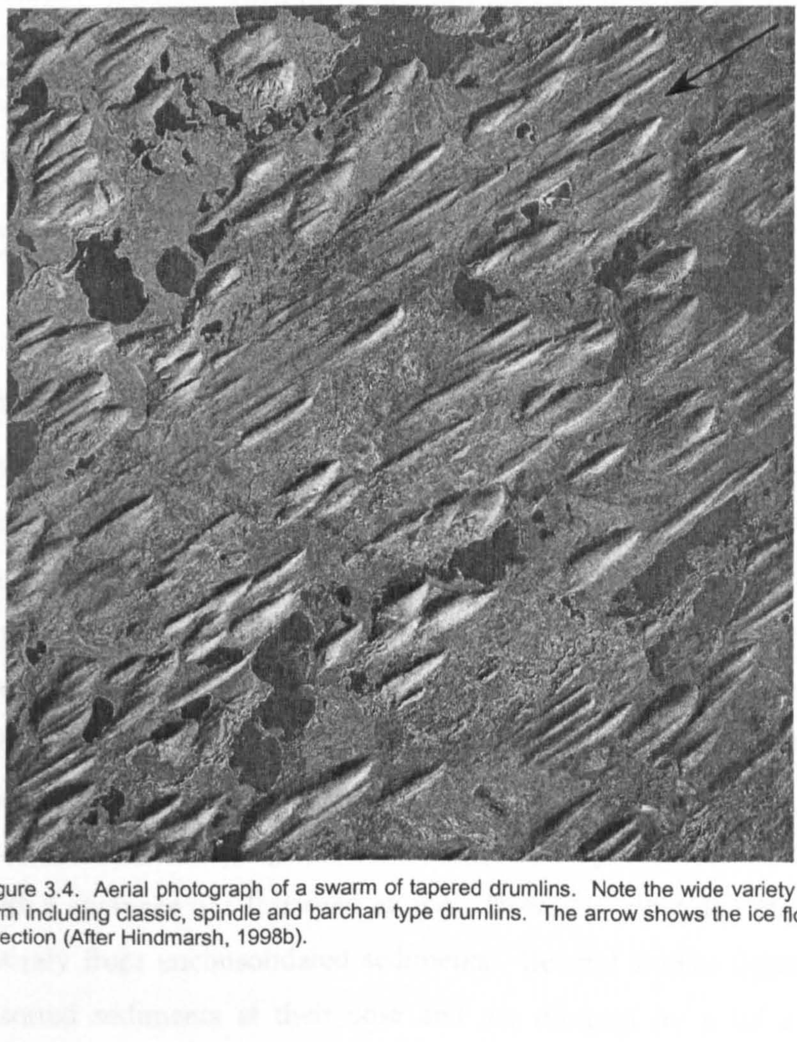

Figure 3.4. Aerial photograph of a swarm of tapered drumlins. Note the wide variety of form including classic, spindle and barchan type drumlins. The arrow shows the ice flow direction (After Hindmarsh, 1998b).

In certain locations it is difficult to distinguish fluted moraine from extremely elongate drumlins (Aylsworth and Shilts, 1989; Heikkinen and Tikkanen, 1989) and with increasing elongation ratios drumlins grade into megaflutes (Table 3.2). Using Landsat satellite imagery, Clark (1993) identified a previously unsuspected large-scale pattern of streamlining within drift that was interpreted as reflecting former phases of ice flow. Drumlins and megaflutes form part of the pattern, but in addition, he identified much larger streamlined bedforms, which he termed mega-scale glacial lineations. Typically, they range in size from 8 to 70 km long, 200 to 1300 m wide and have spacings from around 300 m to 5 km. Mega-scale glacial lineations have recently been discovered on the Antarctic continental shelf (e.g. Shipp *et al.*, 1999; Canals *et al*, 2000; O Cofaigh *et al.*, 2002) and due to their context proximal to existing ice streams confirms their previously inferred association with fast ice flow (Clark, 1993).

Table 3.2. Dimensions and form of megaflutes, Austre Okstindbreen, north Norway. (After Rose, 1989)

Megaflute	Length (m)	Width (m)	ER (L/W)	Height (m)
A	250	35.0	7.1	3.1
B	189	14.5	13.0	2.5
C	157	24.4	7.3	1.4
D	80	17.5	4.6	2.3
E	65	25.0	2.6	3.0
Mean	148	23.3	6.9	2.5

3.2.2.1. Distribution and composition

Drumlins generally tend to be concentrated in fields or swarms, often numbering several thousand individual landforms. Within such fields, they may occur in close association with other bedforms such as rock drumlins and ribbed moraines. Drumlin fields form broad bands that can be aligned transverse or parallel to former glacial flow directions. Although some studies have shown drumlin distribution within a field to be regular (e.g. Vernon, 1966; Hill, 1973; Mills, 1980), the more usual scenario is for them to be distributed randomly throughout the field (Smalley and Unwin, 1968). The internal composition of drumlins and megaflutes is known to vary considerably. Some have rock cores with a carapace of till draped on top. However, most do not and many are composed entirely from unconsolidated sediments. Several studies describe drumlins which have sorted sediments at their core and are covered by a till carapace (e.g.

Lemke, 1958; Krüger and Thomsen, 1984; Boulton, 1987; Boyce and Eyles, 1991). In some drumlins, the sediment cores have been found to consist of overridden pre-existing materials (Krüger and Thomsen, 1984; Boyce and Eyles, 1991) but in other drumlins the age relationships between the sediment and drumlinization are ambiguous. Some researchers have explained this by suggesting the sorted sediments within the drumlin were laid down contemporaneously during drumlin formation (e.g. Dardis and McCabe, 1983; Dardis, 1985; Dardis *et al.*, 1984; Hanvey, 1987).

3.2.2.2. Discussion of formational theories

A myriad of theories explaining the formation of drumlins and megaflutes exist in the literature and it is beyond the scope of this review to assess them all. However, as Benn and Evans (1998) state, in essence they can be explained as the result of either (a) erosion of the intervening hollows, (b) accretion of sediment in hills, or (c) some combination of the two. Erosion of material from hollows and swales could produce drumlins from the remnants of pre-existing sediments. Early advocates of drumlin accretion theory argued that drumlins might be built up by successive additions of till as a series of concentric shells (Fairchild, 1929; Flint, 1947). Although this model of formation can explain drumlins consisting of concentric layers and rock-cored drumlins with a till carapace, it does not explain why some drumlins have sorted sediments at their core or address the question of why drumlins should begin to grow in some areas and not in others. Other theories of drumlin formation through accretion have been proposed including differential sediment dilation (Smalley and Unwin, 1968), frost heaving (Baranowski, 1969), and deposition below helicoidal flow cells in basal ice (Shaw and Freschauf, 1973). However, modern research has now shown that such models are physically implausible and find little support today (Benn and Evans, 1998).

3.2.2.3. Sediment deformation model

The discovery that glaciers and ice sheets were underlain by actively deforming sediments (Boulton and Jones, 1979; Blankenship *et al.*, 1986) re-ignited interest in subglacial bedforms because the process of sediment deformation could explain many of the features found within these landforms. A widely accepted model of drumlin formation based on this process was proposed by Boulton (1987). The essence of his theory centres on how deforming till reacts to different stresses and strains set up at the bed due to various factors, such as the presence of protruding bedrock, or variations in till rheology at the bed. According to this model, regions within a deforming layer that are stronger and stiffer than average will remain static or deform slowly, in contrast with the intervening weaker areas, which will undergo higher strain rates. The various ways in which drumlins are envisaged to form by this process are summarised schematically in Figure 3.5.

Mega-scale glacial lineations have also been explained using the deforming bed model. According to Clark (1993), mega-scale glacial lineations form by differential patterns of subglacial sediment deformation set up by variations in bed characteristics and their great lengths reflect rapid ice flow and/or long periods of time for development. Clark (1993) calculated typical maximum estimates of the periods of time available for the production of these landforms and concluded that they are a product of fast glacier flow (400-1600 m yr^{-1}), at velocities typical of modern ice streams. Evans (1996) also invokes ice stream activity to explain megaflutes over 50 km long in southern Alberta Canada.

More recently, Hindmarsh (1998a,b,c, 1999) developed the deformation theory by numerically modelling the behaviour of deforming subglacial till. According to Hindmarsh, a theory of drumlin formation must have three ingredients. There must be a mechanism for promoting relief, a mechanism for quenching the unstable amplification once drumlins have reached a critical stage and a mechanism that produces drumlinoid forms. Hindmarsh tackled these problems by producing two physically-based numerical computer models. The first model, termed here, the Bed Ribbing Instability Explanation (BRIE), takes a linearised approach and predicts under which conditions sediment amplification in a viscously deforming till sheet can be initiated. The second model, termed here, the Shock Formation Model, is a non-linear model and predicts under which circumstances drumlins can be formed in a viscously deforming till after amplification has occurred. His contributions are significant because it is the first real quantitative formational theory of bedform generation that makes predictions which can be quantitatively tested.

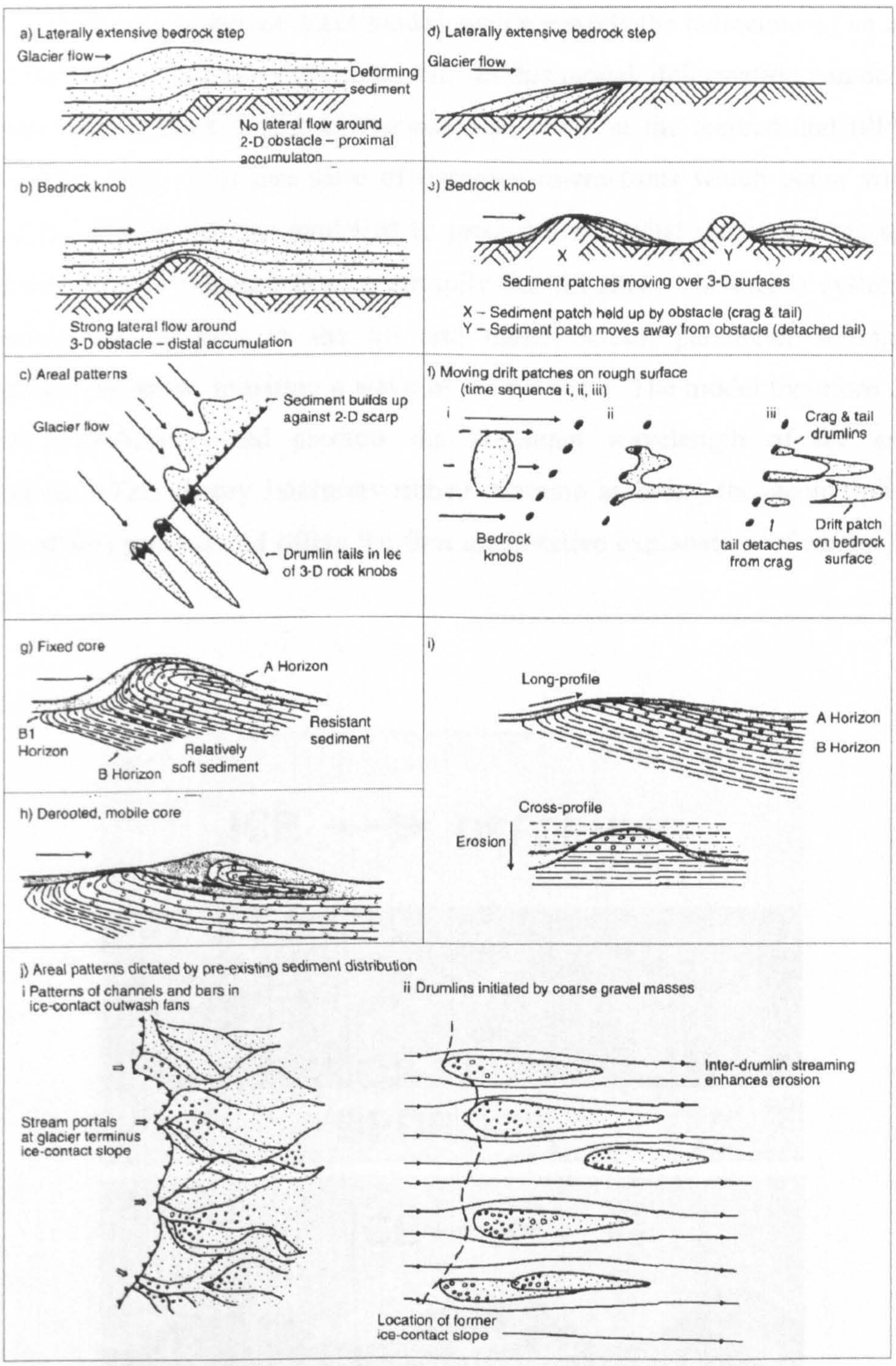

Figure 3.5. Summary schematic diagram showing drumlin-forming processes, internal structures and distribution patterns according to the deforming bed model. (a), (d) Streamlined nose builds up on the proximal side of a laterally extensive bedrock step. (b), (e) Streamlined tail builds up on the distal side of a bedrock knob, owing to enhanced flow around the flanks. The drumlin forms a standing wave when the subglacial sediment is thick, although sediment does flow through the drumlin. When subglacial sediment (drift) patches move over the rock substrate, the drumlin can move past the retarding knob. (c) Drumlin nose builds up on the proximal side of a step of uniform height. The locations of noses reflect subglacial sediment "streams". Where gaps occur in the scarp, sediment streams over and flows into low-pressure points in the lee of the inter-gap knobs. (f) Subglacial sediment patches moving over bedrock are retarded by crags to produce crag and tails and detached tails. (g), (h) Drumlins initiated by stiff sediment obstacles that form deforming cores and which may be fixed or mobile. (i) Drumlins initiated by stiff sediment obstacles which form rigid, fixed cores. Weaker sediment to either side is eroded by subsole deformation. (j) An example of how drumlin distribution patterns can reflect original sedimentary inhomogeneities (e.g. coarse gravels at ice-contact outwash fan apices and gravel bars). Such drumlins can become derooted and mobile. (After Boulton, 1987)

BRIE is a physically based ice sheet model, which models the behaviour of an ice mass that is coupled to a viscously deforming till. In this model, deformation can occur both within the ice and the till, and sliding can also occur at the ice/bed and till/bedrock interface (Fig. 3.6). It is this suite of complex interactions which occur within the whole of the system that are modelled to predict under what circumstances sediment amplification can be initiated from a virtually flat till sheet. In such a system, small perturbations are inherent in the till and under certain parameter settings these perturbations can grow, initiating a wave in the till sheet. The model therefore explains sediment amplification and predicts the dominant wavelength of the amplified perturbations. This theory interprets ribbed moraine as being the geomorphological signature of this process and offers the first quantitative explanation of ribbed moraine genesis.

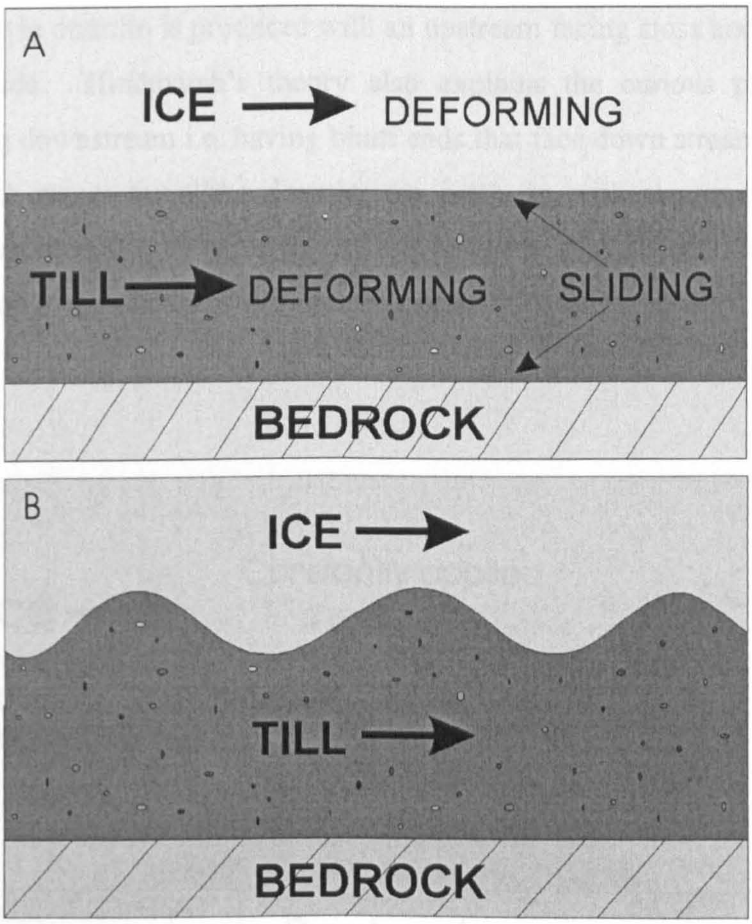

Figure 3.6. (A) Showing ice/till coupling, deformation occurs within the ice and till and sliding can occur at the ice/bed and till/bedrock interface. (B) Under certain parameter space, perturbations can preferentially grow and a wave is initiated in the till.

The Shock Formation Model (SFM) is similar to BRIE in that it also models the behaviour of an ice sheet that is coupled to a viscously deforming till (Fig. 3.7). However, unlike BRIE, spontaneous relief cannot be produced (for mathematical reasons) and model runs must begin with an existing sediment body already in place. The model predicts the outcome of the interactions that occur between sliding and deforming till as the sediment meets with the obstruction. Sediment flux is a function of sliding and internal deformation, and kinematic waves are propagated in the till sheet as the travelling sediment interacts with the pre-programmed sediment relief. These kinematic waves can migrate both up and downstream and their coalescence with other kinematic waves in the till can result in shock formation (Fig. 3.8). These "shocks" are directly analogous to hydraulic jumps or standing waves in a river and is the mechanism by which sediment amplification is quenched, resulting in steep blunt faces being produced in the sediment body. This theory interprets the steep sides as being the stoss end of drumlins, which is an essential component to any drumlinoid form. In Figure 3.8, a classic style drumlin is produced with an upstream facing stoss and a downstream pointing lee side. Hindmarsh's theory also explains the curious phenomenon of drumlins facing downstream i.e. having blunt ends that face down stream. These occur when kinematic waves travelling downstream catch up with slower moving waves. When this happens sediment piles up on the downstream side and shock formation occurs producing a blunt downstream facing drumlin.

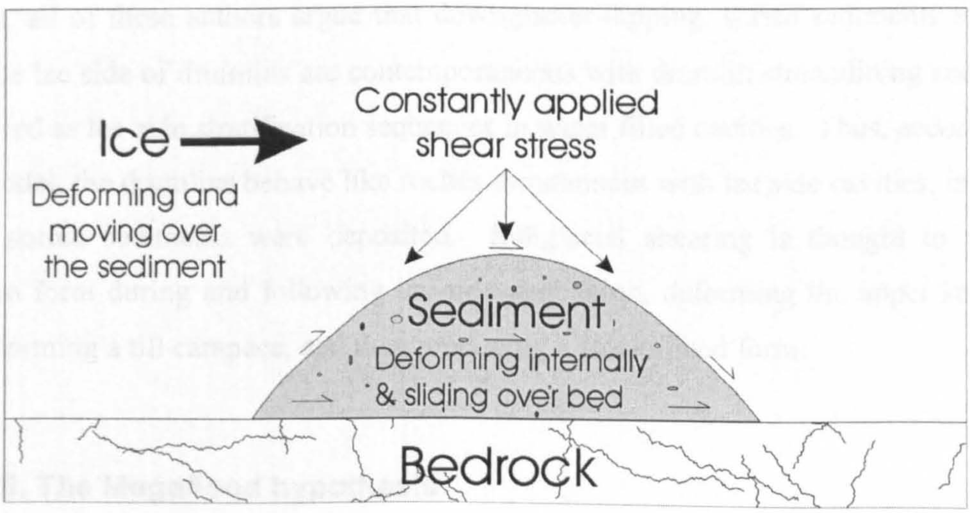

Figure 3.7. Conceptual diagram of the environment modelled in the Shock Formation Model. Ice is deforming and moving over the sediment body, which in turn is also deforming and sliding over the bed.

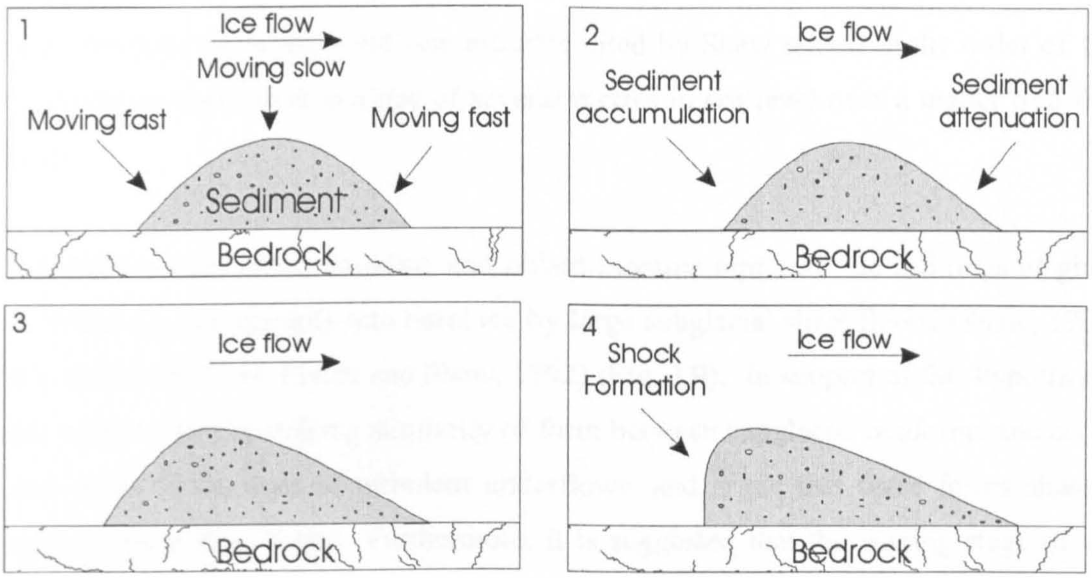

Figure 3.8. Schematic diagram of shock formation in a viscously deforming sediment body. 1. Sediment begins to deform and slide under shear. In this example, the thinner portions of the sediment body are moving faster than the thicker inner part. 2. Faster moving upstream sediment flux begins to catch slower moving downstream flow. Sediment begins to pile up against the upstream side, which begins to become steep, faster moving sediment on the lee side begins to attenuate. 3. Upstream face continues to get steeper as sediment piles against the upstream side. Faster moving sediment on the lee side becomes more attenuated. 4. Shock formation has now occurred as the thinner outer sediment on the upstream side has caught up with the slower inner part. A stoss end has been formed in the sediment. The faster moving sediment on the downstream side is now stretched out forming a tapering lee side.

3.2.2.4. Glacifluvial origins

Stratified sediments found in numerous drumlins in Ireland have been interpreted as subglacial glacifluvial deposits, rather than pre-existing cores of sediment (Dardis and McCabe, 1983, 1987; Dardis, *et al.*, 1984; Dardis, 1985, 1987; Hanvey, 1987, 1989; McCabe and Dardis, 1989; Dardis and Hanvey, 1994). According to Benn and Evans (1998), all of these authors argue that downglacier-dipping, sorted sediments exposed near the lee side of drumlins are contemporaneous with drumlin streamlining and, were deposited as lee-side stratification sequences in water filled cavities. Thus, according to this model, the drumlins behave like roches moutonnées with lee side cavities, in which water sorted sediments were deposited. Subglacial shearing is thought to modify drumlin form during and following lee-side deposition, deforming the upper stratified beds, forming a till carapace, and then producing a streamlined form.

3.2.2.5. The Megaflood hypothesis

One of the most controversial theories to have emerged of late is John Shaw's megaflood hypothesis. In this model, subglacial bedforms are radically reinterpreted as being products of mega-scale subglacial floods. The volume of water involved in these events are quite impressive and one estimate cited by Shaw puts it in the order of 10^6 km^3, which is equivalent to a rise of several metres in sea level over a matter of a few weeks.

According to this model, drumlins and ribbed moraine represent the infillings of giant scours that are cut upwards into basal ice by large subglacial sheet floods (Shaw, 1983; Shaw and Kvill, 1984, Fisher and Shaw, 1992) (Fig. 3.9). In support of this hypothesis, these authors cite the striking similarity of form between subglacial bedforms and scour marks made at the base of turbulent underflows, and argue that these forms share a common origin (Fig. 3.10). Furthermore, it is suggested that the waning stage of the flood event fills the eroded cavity with stratified sediments (Shaw, 1983; Shaw and Kvill, 1984; Sharpe, 1987). Shaw *et al.* (1989) and Shaw (1993) also state that drumlins can be erosional remnants of pre-existing sediments whereby meltwater from the flood excavated the substrate between the sediments leaving streamlined bedforms behind.

Thus, the megaflood hypothesis attempts to explain the diverse characteristics of subglacial bedforms by an assortment of mechanisms. If bedforms contain sorted sediments, they are interpreted as scour infillings and if they do not, they are interpreted as erosional remnants that survived the floods. Because of this, Benn and Evans (1998) state that it is an example of an unfalsifiable hypothesis: no matter what the evidence, a way can be found to explain it in terms of the flood. These authors also state that form analogy may not always be the best criterion upon which to base genetic interpretations and streamlined and rippled forms are produced in a wide range of environments wherever two media shear past each other. They can be observed in cloud formations, riverbeds, wind blown sand dunes and snow, at the base of turbidity currents and other mass movements, and on glacier beds. The hypothesis also requires vast amounts of water and thus possible reservoirs need to be identified and validated by independent evidence.

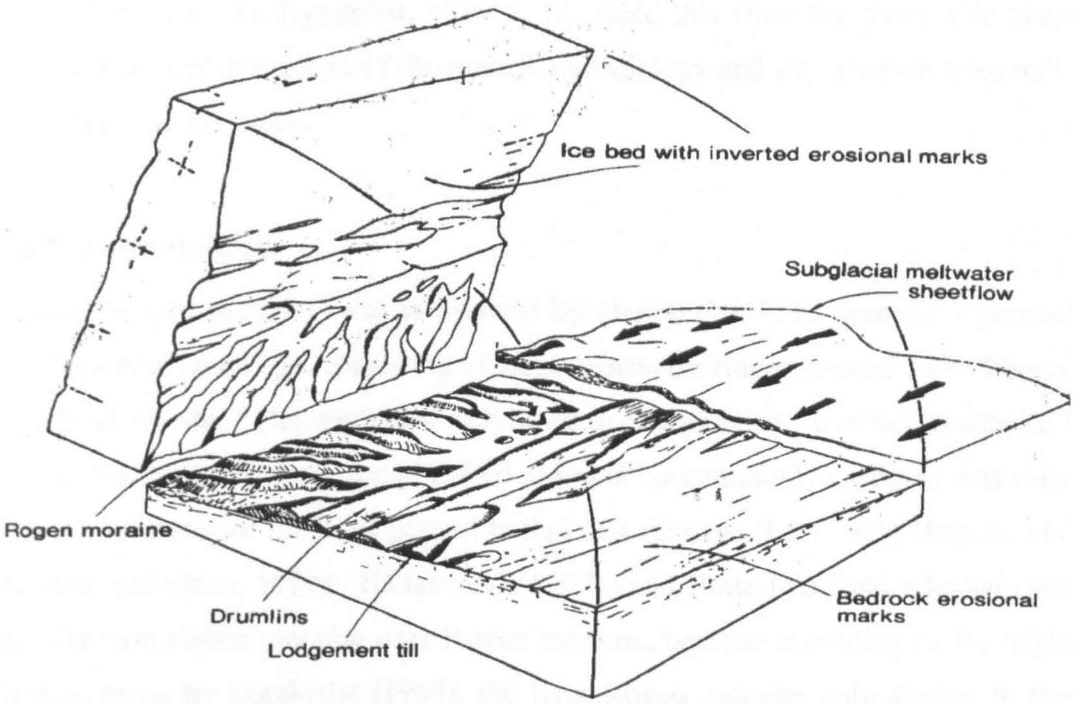

Figure 3.9. Schematic reconstruction of flow conditions during the formation of subglacial bedforms by large-scale subglacial outburst floods (After Fisher and Shaw, 1992).

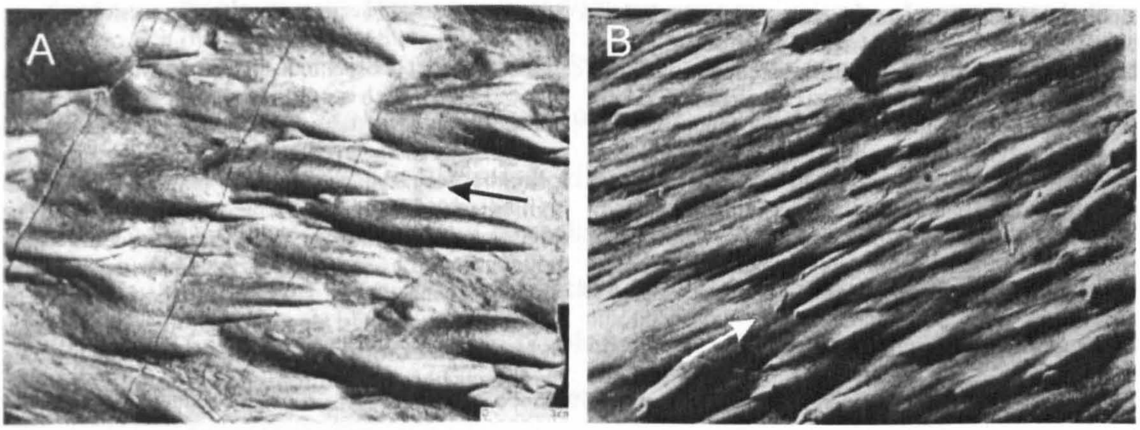

Figure 3.10. Streamlined erosional marks associated with turbidites: (a) narrow, parabolic and spindle flute castes; (b) longitudinal obstacle scour moulds cut behind small tool marks. Arrows indicate flow direction. (After Shaw, 1983)

3.2.3. Ribbed (Rogen) moraine

An excellent, comprehensive review on ribbed moraines was published recently by Hättestrand and Kleman (1999) and this section draws heavily on their work. Their paper offers a detailed discussion of the known characteristics and spatial distribution of ribbed moraine and reviews the major competing formational theories. In the literature, there appears to be some ambiguity regarding the correct name to use when referring to this landform (e.g. see Lundqvist, 1989). To avoid this from the onset, this chapter begins with a brief discussion of the present terminology and states which term will be used throughout this thesis.

3.2.3.1. Terminology

The term "Rogen moraine" was introduced by Hoppe (1959) to describe a particular type of moraine landscape, consisting of large transverse ridges, around Lake Rogen in west-central Sweden. This term is widely used in Scandinavia. In other countries, for example, North America, the term "ribbed moraine" is commonly used and was chosen due to the similarity of the ridge pattern to that of a rib cage (Lee, 1959; Hughes, 1964; Aylsworth and Shilts, 1989). Hättestrand (1997b) and Hättestrand and Kleman (1999) prefer the term ribbed moraine over Rogen moraine, because according to the original definition given by Lundqvist (1969), the term Rogen moraine only applies to those ridges that have drumlinoid elements or superimposed flutings. It therefore excludes all non-drumlinized ribbed moraines, and since it has not yet been shown that drumlinization is directly linked to the ridge construction, the term ribbed moraine is preferable. Furthermore, Hättestrand (1997b) has convincingly demonstrated four different categories of ribbed moraine in Sweden; Blattnick moraine (Markgren and Lassila, 1980); Rogen moraine (Hoppe, 1959; Lundqvist, 1969); hummocky ribbed moraine (Hättestrand, 1997b); and minor ribbed moraine (Minell, 1977; Hättestrand, 1997b), which share characteristics indicative of a common subglacial origin. Therefore, in this thesis, no distinction is made between the various classifications and all are treated as one genetic type of morphology, i.e. ridges composed of drift that were formed transverse to the known ice flow direction, and as such will be referred to herein as ribbed moraine.

3.2.3.2. Known characteristics of ribbed moraine

The following sections discuss the known characteristics of ribbed moraines that have been reported in the literature.

3.2.3.3. Global distribution

Ribbed moraines are restricted to areas of the late Pleistocene glaciations in the Northern Hemisphere (Fig. 3.11). They are found in the Keewatin and Québec sectors of the Laurentide Ice Sheet, on Newfoundland and in Norway, Sweden and Finland. Some isolated fields have also been reported in Maine, USA (Thompson and Borns, 1985), Wisconsin, USA (Attig, 1985) and on Prince of Wales Island, Arctic Canada (Dyke *et al.*, 1992). More recently, Knight and McCabe (1997) and Clark and Meehan (2001) extended the known global distribution by finding ribbed moraines in Ireland. So far, ribbed moraines only occur in formerly glaciated areas, and they have not been found in association with contemporary glaciers or ice sheets.

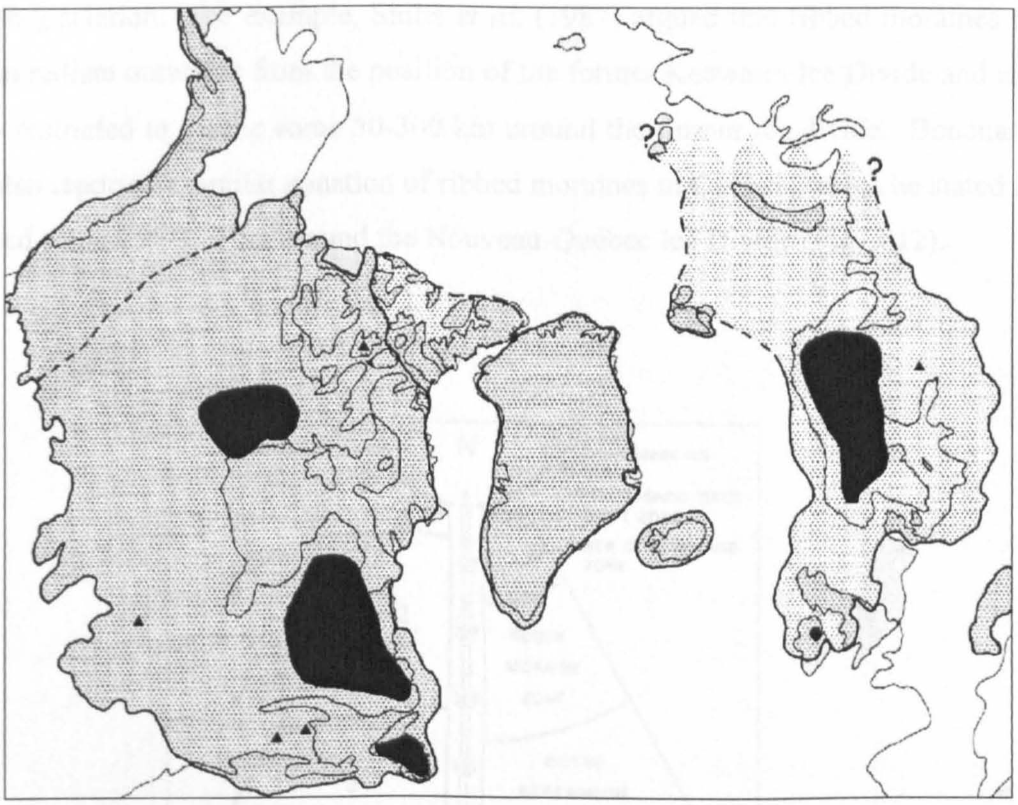

Figure 3.11. Currently known worldwide distribution of ribbed moraines. Light shaded regions show the Last Glacial Maximum ice sheet distribution. Dark shaded regions are where ribbed moraine occurs commonly. In addition, a few outliers of ribbed moraine have found outside the core areas and these are marked with triangles. The ribbed moraines recently recognised in Ireland are also included. (Modified from Hättestrand, 1997b)

Hättestrand and Kleman (1999) estimate that ribbed moraines occur in only 10 % of the area covered by the Laurentide Ice Sheet and in 20 % of the area covered by the Fennoscandian Ice Sheet. They appear to occupy roughly 15 % of the area covered by the Irish Ice Sheet. According to these authors, the limited distribution, often with a sharp boundary to areas lacking ribbed moraines, does not appear to coincide with a specific topography, bedrock geology, the position of the marine limit, or the ice-marginal position at a specific time. For example, the ribbed moraine limit coincides with the 12 thousand B.P. (Ka) ice marginal position in Newfoundland, the 10 Ka ice margin in Fennoscandia, the 9 Ka ice margin in Keewatin, and the 8 Ka ice margin in Québec.

3.2.3.4. Regional distribution

Ribbed moraines are widely reported to occur in core areas of former ice sheets close to the region of the former ice divide, or in regions to which the ice sheet retreated to during de-glaciation. For example, Shilts *et al.* (1987) argued that ribbed moraines in Keewatin radiate outwards from the position of the former Keewatin Ice Divide and are spatially restricted to a zone some 50-300 km around the former ice divide. Bouchard (1989) also reported a similar zonation of ribbed moraines in Québec, which he stated is distributed some 150-350 km around the Nouveau-Québec Ice Divide (Fig. 3.12).

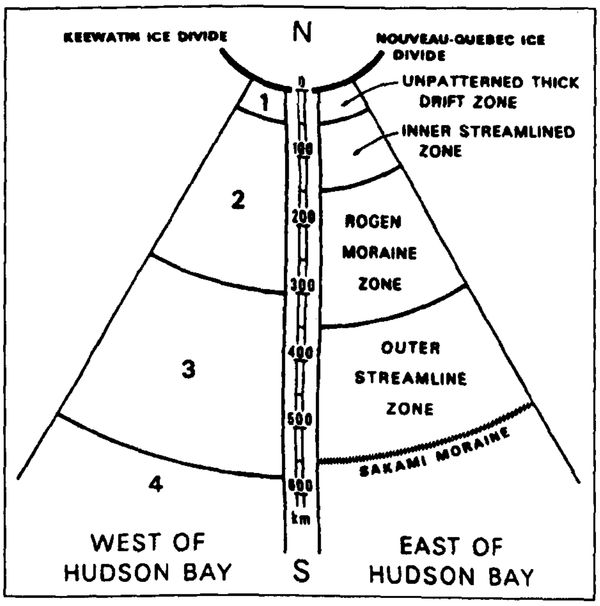

Figure 3.12. Compared geomorphic zonation around the Keewatin Ice Divide, west of Hudson Bay and around the Nouveau-Québec Ice Divide, east of Hudson Bay. In Keewatin ribbed moraine are found in a zone 50-300 km from the ice divide, termed Zone 2, in Québec ribbed moraines begin slightly further from the divide (150-350 km) (After Bouchard, 1989)

Kleman and Hättestrand (1999) claim that maps of glacial landforms made from aerial photographs of Canada and Sweden demonstrate that ribbed moraines are concentrated around the ice-sheet retreat centres of Québec, Keewatin, Newfoundland and west-central Fennoscandia.

3.2.3.5. Local distribution

At a more local level, many authors state that ribbed moraines are a feature commonly associated with topographic depressions such as concave basins, swales and hollows (Shaw, 1979; Markgren and Lassila, 1980; Minell, 1980; Mollard and James, 1984; Bouchard, 1989; Lundqvist, 1989; Sollid and Sørbel, 1994). Hättestrand and Kleman (1999) state they are also found in a variety of settings including plains, upland plateaux and the fact that they are found on islands in the Replot area off the western coast of Finland, suggests they are situated on convex parts of the sea floor. Aylsworth and Shilts (1989) also noted that ribbed moraine in Keewatin is developed largely independently of topography.

3.2.3.6. Relation to other landforms

The original definition of Rogen moraine (Lundqvist, 1969, 1981) included the presence of drumlinoid elements in the ridge field, or fluting of the ridges. Hättestrand and Kleman (1999) state that this is a common feature of ribbed moraines in general. Normally the drumlinization is at right angles to the ridges and can thus be associated with an ice flow similar to (and probably at a time of formation close to) the genesis of the ribbed moraine ridges. There are several cases where drumlinization is at oblique angles (Watenson, 1983; Borgström, 1989) and parallel to the ridges (Soyez, 1974). In these cases, the drumlinization is clearly a later feature, separated from the formation of the ribbed moraine.

In Sweden, Lundqvist (1969) developed a widely reproduced model showing the relationship of drumlins and ribbed moraine to be one which one form passes through a transition zone into the other down-ice. In this model, drumlins occupy higher parts of the terrain (zones of extensional glacial flow) and ribbed moraine occupies depressions (zones of compression). Aylsworth and Shilts (1989) noted that this down-ice transition in Keewatin was rare and observed that an abrupt lateral transition between the two bedforms was more usual. Nonetheless, down-ice transitions have been noted in other parts of Canada and Bouchard (1989) describes down-ice transitional forms occurring at the margins of ribbed moraine fields in Québec.

There are many reports of eskers superimposed on ribbed moraines, either running across ridges, or running through meltwater cuts in the ridges. However, there are no observations where ribbed moraines are superimposed on eskers. Hättestrand and Kleman (1999) suggest that the formation of ribbed moraine precedes the presence of abundant meltwater at the base of an ice sheet.

3.2.3.7. Morphology

Ribbed moraines can be described as coalescent crescentic ridges that lie transverse to the former ice flow (Fig. 3.13). According to Hättestrand and Kleman (1999), the morphology of individual ridges is generally consistent in well-developed ribbed moraines and they tend to be of similar size throughout the field. Typical size values range from 300-1200 m long, 150-300 m wide and 10-30 m in height. These authors state the spacing between the ridges, or wavelength, is also very regular and although this appears to be true, the literature reveals that ridge spacing does vary between different ribbed moraine localities (Table 3.3). They state that if the water bodies, mires and sediments filling the inter-ridge basins are ignored, a longitudinal profile taken across a ribbed moraine field would show a rather asymmetric wave form.

Table 3.3. Typical spacing (wavelength) of ribbed moraine ridges reported in the literature

Ridge spacing (m)	Locality	Reference
100-300	Sweden	Lundqvist (1989)
30-100	Ireland	Knight and McCabe (1997)
300-700	Québec, Canada	Mollard and James (1984)
275-1925	Ireland	Clark and Meehan (2001)

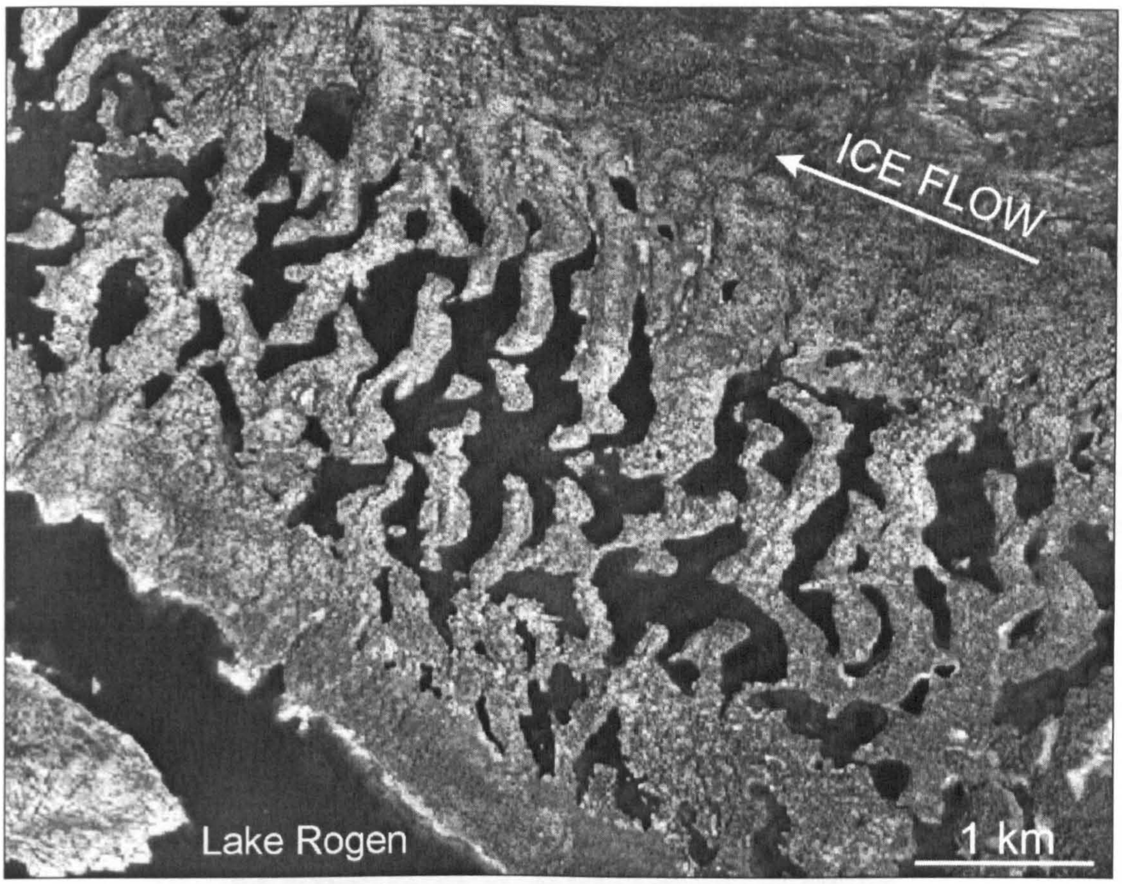

Figure 3.13. 1:60,000 scale aerial photograph of ribbed moraine from the type locality of Rogen moraine, at Lake Rogen in southwest Härjedalen, Sweden.

Both Bouchard (1989) and Hättestrand and Kleman (1999) strongly assert that in many cases the crest height across a ribbed moraine field is very consistent producing or accordant summits. Bouchard (1989) demonstrated this accordant summit characteristic with a measured profile of the crest heights across a ribbed moraine field in Québec, showing a variability of less than 3 m over a distance of 1 km. Bouchard (1989) argued that this was the result of post-formational truncation, as a shear plane developed in the basal parts of the ice sheet, along a plane following the crests. However, Hättestrand and Kleman (1999) note that post-formational planning cannot account for all examples of the accordant summit characteristics, because it is not confined to ribbed moraines that were smoothed or drumlinized, but is common with ribbed moraines with rather sharp crests.

Hättestrand and Kleman (1999) state that the regularity in ridge morphology is generally confined to longitudinal profiles in the ice flow direction. Transverse to ice flow (i.e. parallel to the ridges), it is claimed that the morphology is less regular. They state that ribbed moraine ridges are often anastomosing, frequently have crescentic segments and when situated in a valley, there is commonly a gap in the centre of the ridges along the valley axis (Lundqvist, 1969; Markgren and Lassila, 1980; Borgström, 1989). The ridges bordering this gap tend to have spurs that point in the down ice direction. Hättestrand and Kleman (1999) also note that in cross section, individual ridges are commonly asymmetric and are usually steeper on their distal side. The ridges occasionally have multiple sub-crests, or have flat crest, giving the ridges a tabular appearance in cross-profile. Lundqvist (1969), Bouchard (1989) and Hättestrand (1997b) have all noted that ribbed moraine ridges appear to fit together like a jigsaw puzzle. Hättestrand and Kleman cite the type locality of Rogen moraine, at Lake Rogen in west-central Sweden, as a good example where the detailed morphology of individual ridges fit together (Fig. 3.14).

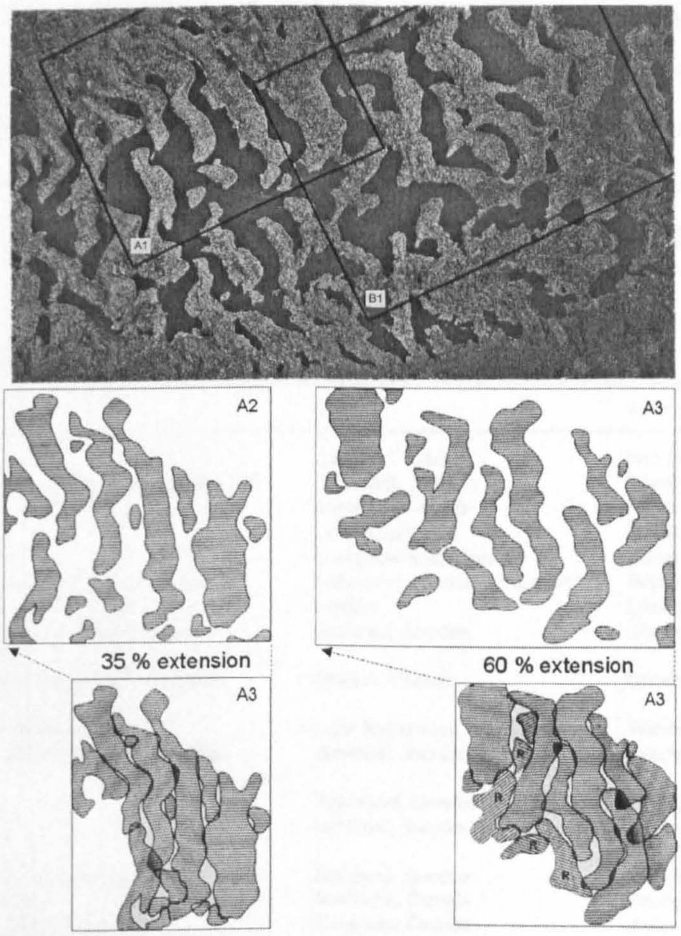

Figure 3.14. Jigsaw puzzle matching of ribbed moraine ridges at Lake Rogen in west-central Sweden presented by Hättestrand and Kleman (1999). These authors state the morphology indicates the predominant process in the formation of the ribbed moraine is by fracturing of a pre-existing till sheet. The direction of the lines in the shading of the ridges (A2, A3) and (B2, B3) corresponds to the faint overprinted fluting direction. The areas overlapping ridges in (A3) and (B3) are confined to "horns" which are interpreted to be formed by post-ridge formational drumlinization processes. The ridges marked R in (B3) are elements, which are interpreted to have been slightly rotated during the fracturing process.

The apparent close fit, they state, is evidence that these ridges were once joined, and in this example, they believe the ice sheet has pulled apart and extended two slabs of till by 35 % and 60 %.

3.2.3.8. Composition

The internal stratigraphy of ribbed moraine ridges is documented in a number of studies (Table 3.4). However, the results are very divergent and there is a large variability in internal composition, the ridges can contain anything from well sorted sediments to disaggregated bedrock (Hättestrand, 1997b). Hättestrand and Kleman (1999), suggest that this feature appears to be related to the fact that ribbed moraines are commonly composed of the same material as the surrounding terrain. Although authors have noted this diversity in ridge composition, few describe the stratigraphy throughout the ridges. Often, pits one or two metres deep have been used to draw conclusions on the overall composition of the ridges. Internal structure also varies, however the presence of steeply inclined layers and various signs of glacitectonic activity appear to be common features (Hoppe, 1952; Cowan, 1968; Minell, 1977, 1979; Shaw, 1979; Dredge *et al.*, 1986; Bouchard, 1989; Lundqvist, 1989, 1997; Fisher and Shaw, 1992).

Table 3.4. Internal composition of ribbed moraines (After Hättestrand, 1997b).

Material	Locality	Reference
Medium to coarse sand	Québec, Canada	Ives (1956)
Glaciofluvial sand, interbedded in ablation and basal till	Värmland, Sweden	Lundqvist (1958)
Gravely sediments	Keewatin, Canada	Aylsworth and Shilts (1989)
Glaciofluvial gravel	Lake Rogen area	Lundqvist (1937)
Sandy-muddy gravel	Newfoundland, Canada	Fisher and Shaw (1992)
Kalix till, slightly disturbed, water deposit sediments	Norrbotten, Sweden, Värmland Sweden	Hoppe (1948); Fromm (1965) Lundqvist (1969)
Sveg till, diamicton with layers of sorted material ("subglacial melt-out till")	Jämtland, Sweden	Shaw (1979)
Stratified, matrix-supported, fine grained diamicton ("basal meltout till")	Québec, Canada	Bouchard (1989)
Sandy-silty till with sorted sediment lenses	Lake Rogen area, Sweden	Watenson (1983)
Sandy till (clayey till underneath and in surrounding areas)	Jämtland, Sweden	Lundqvist (1969)
Loose ablation till	Värmland, Sweden	Lundqvist (1958)
Very hard-packed basal till	Jämtland, Sweden	Rasmusson and Tarras-Wahlberg (1951)
Silty till with folded beds of shattered bedrock	Jämtland, Sweden	Minell (1977)
Broken rock with little matrix	Manitoba, Canada	Dredge *et al.* (1986)
Disaggregated sandstone, without fines	Keewatin, Canada	Aylsworth and Shilts (1989)
"Great variation in internal structure and bedding"	Sweden in general	Lundqvist (1969; 1995)

3.2.3.9. Formational theories

According to Hättestrand and Kleman (1999) ribbed moraines were first described in central Sweden by Högbom (1885, 1894), who did not try to explain their genesis but noted the highly varied internal composition. The first formational theories suggested that they had a frontal origin, as series of end moraines (Frödin, 1913; 1925; Högbom, 1920; Beskow, 1935). Several later studies also proposed a marginal or near marginal formation (Frödin, 1954; Fromm, 1965; Cowan, 1968), possibly in association with calving ice margins in glacial lakes (Hughes, 1964). However, Lundqvist (1935, 1937, 1943, 1951) rejected a marginal explanation on the basis that the large quantities of material found in the ribbed moraines were unlikely to be deposited by active ice close to the last small remnants, where the most proximal ribbed moraines are found (with respect to deglacial ice flow). Lundqvist instead advocated a dead-ice explanation where supraglacial material slumped into transverse crevasses, forming the characteristic ribbed pattern. Mannerfelt (1942, 1945), Granlund (1943), Tanner (1944), and Kurimo (1980) followed this idea of ribbed moraine genesis during areal stagnation towards the end of glaciation. Hoppe (1948) appealed to a near marginal deposition of material followed by remoulding by smaller ice-front oscillations for the Kalix-pinnmo ridges in northern Sweden, as their interiors showed clear signs of glacial deformation.

As investigations continued, a subglacial origin was put forward as studies began to reveal the subglacial characteristics of ribbed moraine (Lundqvist, 1969). Evidence for this included the lodgement character of the till, eskers overlying ribbed moraine and drumlinization and fluting of the ridges. The more recent hypotheses almost exclusively invoke a subglacial origin. According to Hättestrand and Kleman (1999), most of these studies explain ribbed moraine formation due to shearing and stacking of slabs of near-base englacial or subglacial debris, as a result of localised compressive stresses, followed by subglacial melt-out of the till ridges. The shear and stack model is most extensively outlined in Shaw (1979) and Bouchard, (1980, 1989) (Fig. 3.15), but is also inferred by Lee (1959), Kurimo (1977), Minell (1977,1980), Shilts (1977), Markgren and Lassila (1980), Punkari (1982, 1984), Sollid and Sørbel (1984, 1990, 1994), Dredge *et al.* (1986), Aylsworth and Shilts (1989) and Dyke *et al.* (1992). The papers differ primarily in terms of the origin of the compressive flow and the glaciodynamic environment in which the ribbed moraine were suggested to form. Bouchard (1980, 1989), Minell (1980), and Sollid and Sørbel (1984) suggested the compressive flow resulted when ice flowed against topographic obstructions at the down-stream end of rock basins. Dredge *el al.* (1986) and Shilts and Aylsworth (1989) argued that high concentrations of near-basal debris caused a decrease in the plastic behaviour of the ice, inducing compression and basal shearing of debris-rich ice, possibly in association with a low surface gradient and climatic deterioration. Sollid and Sørbel (1984, 1990, 1994) argue ribbed moraines are formed far behind the margin in areas where trapped, water soaked debris lying in depressions are entrained by freezing on to the glacier sole and are subsequently sheared up into ridges during an expansion of a frozen core area beneath the ice sheet. Shaw (1979), Punkari (1984), Bouchard and Salonen (1989) propose formation under similar conditions, however they place ribbed moraine genesis closer to the ice margin. These studies infer a frozen outer margin of the ice sheet, causing compressive stresses leading to shearing and stacking. Dyke *et al.* (1992) inferred that ribbed moraine genesis occurred along a transition from cold to warm-based ice which caused alternate sticking and slipping conditions leading to the infolding and stacking of basal debris.

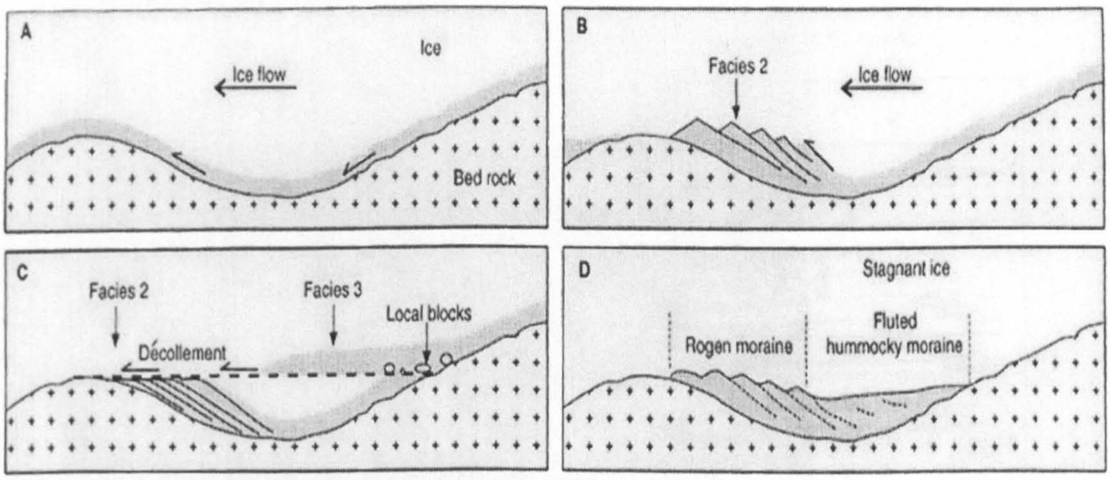

Figure. 3.15. Formation of ribbed moraine envisaged by Bouchard (1989) by processes of shearing and stacking of debris-laden ice under compressive ice flow, as basal ice flows towards the down-ice end of rock basins (A-B). When the basin fills with immobilised debris-laden ice, or when the height of the obstacle impeding ice flow is reduced by erosion, the glacier is able to overcome the resistance to flow through the development of a sub-horizontal shear plane of décollement which shears across the top of the ridges. This increases ice flow, which leads to plucking of the glacier floor and the formation of blocks at the upglacier end of the rock basin (C). When the overlying ice melts two landforms emerge. In places where the underlying mass was sheared and stacked, fluted ribbed moraine with a bouldery cover can be seen, where the immobilised deposit was undeformed, the resultant landform is bouldery fluted hummocky moraine (D). (After, Bouchard, 1989).

Several recent theories differ from the shear and stack model. Lundqvist (1989, 1997) stated ribbed moraines may be formed in two stages. He suggested the primary ridge structure in ribbed moraines reflects pre-existing features that are later remoulded to various degrees by the overriding ice into drumlinized elements of Rogen moraine. Hättestrand and Kleman (1999) correctly note that Lundqvist however failed to specify the origin of the primary ridges. Boulton (1987) proposed a similar idea, and suggested the primary ridges could have been subglacial fold structures, flutes, or drumlins previously produced at right angles to the secondary ice flow direction. Boulton (1987) argued the deformation of weak bed materials around the transverse ridges results in the preferential downglacier transport of the ridge extremities, producing the characteristic concave downglacier planform (Fig. 3.16). Aario (1977, 1987) related ribbed moraine genesis to primary till deposition under a wavy ice motion operating at the bed of an ice sheet, whilst fluting and drumlins were proposed to form under spiral ice flow. As mentioned previously, Fisher and Shaw (1992) suggested that ribbed moraines are part of a landform assemblage formed during mega-scale subglacial floods. These authors suggest that subglacial sheet floods eroded the underside of glaciers forming transverse cavities that served as moulds for ribbed moraine ridges. These moulds are subsequently filled with subglacial sediment leaving transverse ridges once the ice sheet melted.

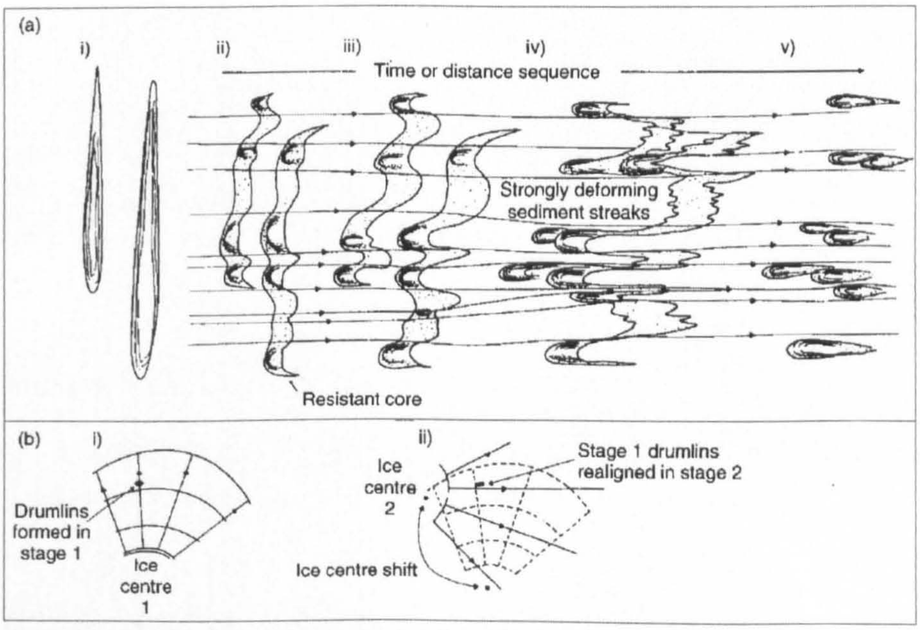

Figure 3.16. Schematic reconstruction of the progressive transformation of flutings to ribbed moraine and drumlins by subglacial deformation. (a) I) Original flutings produced by earlier ice flow direction; ii-iii) ribbed moraine stage; iv-v) drumlin stage. This can be either a time or distance sequence. (b) Explanation of the change in ice flow direction in (a) by a shift in the ice dispersal centre (After Boulton (1987).

Several theories have been presented that associate ribbed moraine formation with extensional flow at the base of an ice sheet. Lundqvist (1969) was the first author to suggest this and stated that less plastic till-loaded basal ice fractured into transverse elements by tensional forces induced primarily by topography. Hättestrand and Kleman (1999) note however, that in later discussions Lundqvist (1981, 1989) disassociated himself with this theory because it was difficult to explain the origin of the tensional forces. Hättestrand (1997b) however proposed that tensional stresses were coupled to the contraction of a frozen-bed core area of a retreating ice sheet. At the transition from proximal (non-sliding) conditions to distal melting (sliding) conditions, high tensional stresses and extensional ice flow will occur, as the basal ice velocity increases across the boundary of basal thermal regime. He suggested that these tensional stresses lead to detachment and "boudinage-like" fracturing of a pre-existing frozen till sheet into ribbed moraine (Fig. 3.17). A key element in this theory is the presence of alternating competent and incompetent materials, exhibiting brittle and ductile deformation characteristics respectively. In contrast to Lundqvist (1969), who inferred ribbed moraine formation from debris-loaded basal ice, Hättestrand (1997b) explained ribbed moraine ridges as fractured subglacial sedimentary sequences.

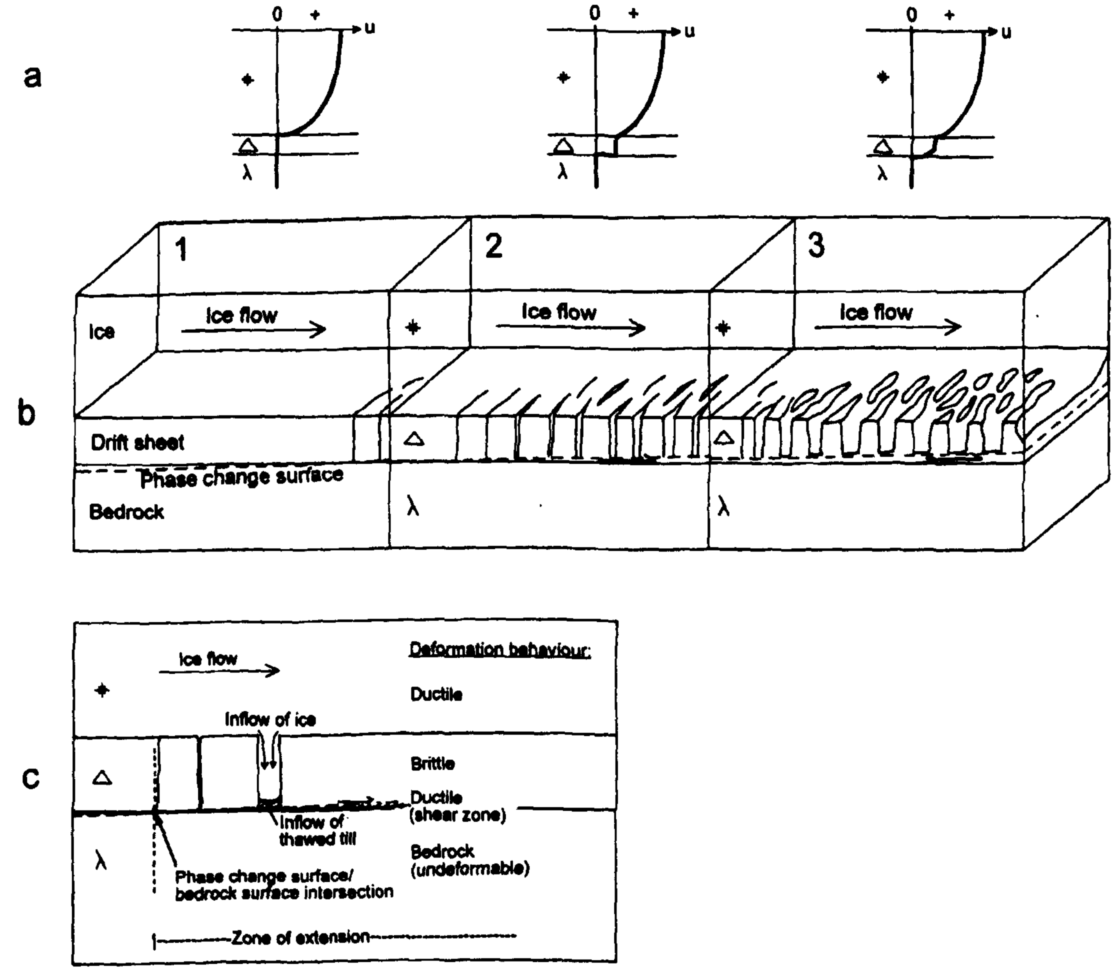

Figure 3.17. Model of ribbed moraine formation illustrated in Hättestrand (1997b) showing the envisaged stages of the fracturing of a pre-existing till sheet during a transition from cold to warm-based conditions under a deglaciating ice sheet. At this transition, basal ice velocity increases as the ice starts to slide over and deform its bed. This highly localised increase in ice velocity (acceleration) induces extensional ice flow. The phase change surface (a pressure melting isotherm), separating frozen material above from thawed below, rises through the bedrock/drift/ice-sequence during thawing of the ice sheet bed. When the phase change surface is located in the lower part of the drift sheet, still-frozen drift is underlain by a deforming layer of thawed drift and overlain by deforming basal ice. Under extensional flow, the frozen upper part of the drift sheet breaks up into ribs in a boudinage-like fashion. a/ Ice flow velocity profiles in the lower part of the ice mass for stages 1-3 in b. b/ Time slice boxes(1-3), showing the successive evolution from a pre-existing frozen drift sheet to a ribbed moraine. Detachment of frozen drift ribs will start to occur when the pressure melting isotherm intersects the bedrock surface. C/ Close up of the fracturing zone showing the fracturing process and the deformational behaviour of the layers. During, and after, deglaciation, mass movement processes decrease the slope angles of the ridges and degrade their tabular morphology. The ribbed moraine fields form successively as the cold-/warm-based transition zone migrates up-glacier. (After Hättestrand and Kleman, 1999)

3.2.3.10. Proximity to cold-based areas

In support of this theory Hättestrand (1997b) and Hättestrand and Kleman (1999) noted that the most abundant and best developed ribbed moraine areas occur in close connection to areas that were cold-based during the last glaciation, whereas areas that were warm-based appear to lack ribbed moraines. Kleman *et al.* (1997) reconstructed the extent of frozen bed conditions in Fennoscandia during the Last Glacial Maximum (LGM) using pre-late Weichselian landforms and deposits. Hättestrand and Kleman

(1999) compared this map to the distribution of ribbed moraines in the region and stated that the match between the two areas appears salient (Fig. 3.18).

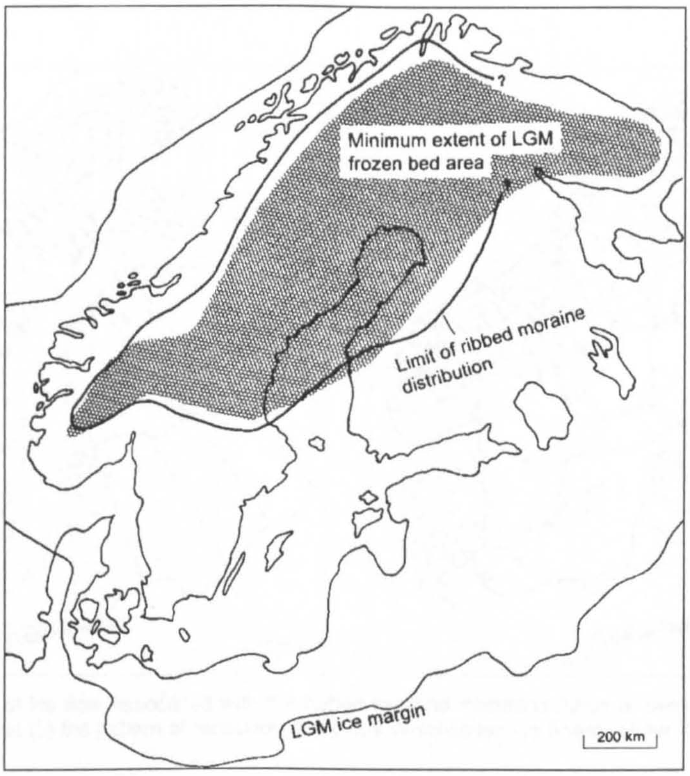

Figure 3.18. The distribution of ribbed moraines compared with the LGM ice sheet margin and frozen bed extent in Fennoscandia. The ribbed moraine distribution is enclosed by a heavy line and the minimum extent of the Last Glacial Maximum frozen bed area is shaded. The frozen bed area is based on the distribution of pre-late Weichselian landforms and sediments (After Hättestrand and Kleman, 1999).

Kleman *et al.* (1994) argued that on a regional scale, ribbed moraines are located in areas that experienced a transition from cold to warm-based conditions, as the frozen core areas reduced in size and warm-based zones migrated inwards towards the deglaciation centre. In areas that were continually cold-based during the final retreat of the ice sheet, no ribbed moraines exist, apart from some that Hättestrand (1997b) suggests are most likely correlated with earlier deglaciations.

3.2.3.11. Direction of ribbed moraine ridges

Hättestrand and Kleman (1999) also argued that the orientation of the ribbed moraine ridges does not match with the LGM ice flow patterns, but broadly mimics the retreat geometry of the late Weichselian Ice Sheet (Fig. 3.19). Hättestrand and Kleman (1999) state that because ice divides, and hence, ice-flow directions, shifted continuously during the decay phase, the implication is that ribbed moraines must have formed in a late stage of deglaciation. In Fennoscandia and North America, this refers to the last (Late Wisconsinan/Weichselian) glaciation.

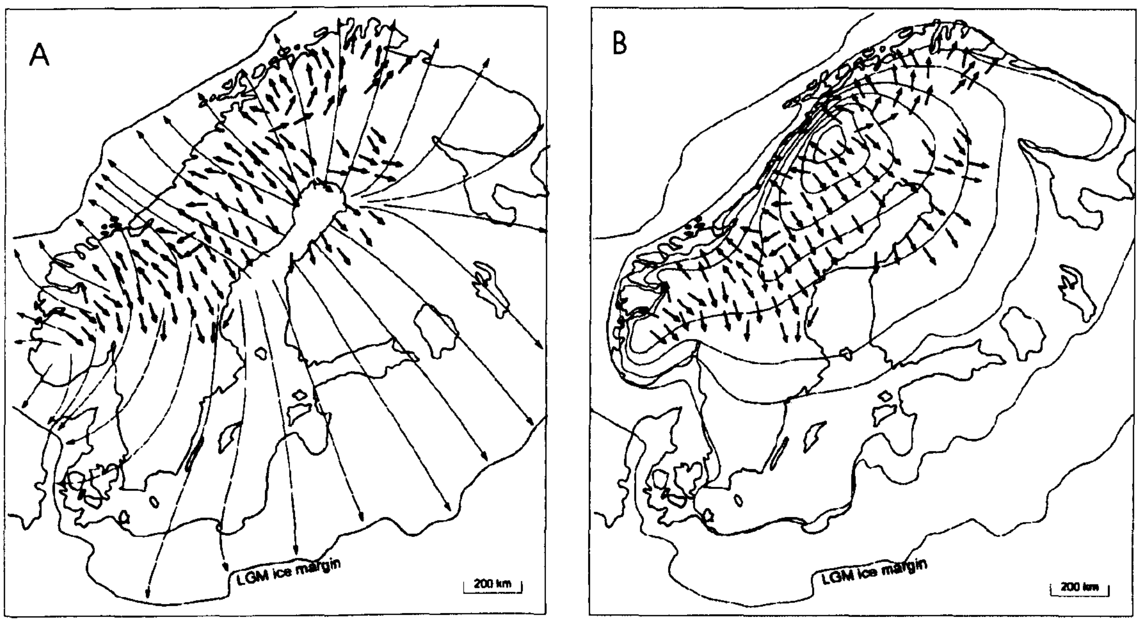

Figure 3.19. Direction of ice flow associated with the ribbed moraine formation (short arrows), compared with (a) the LGM ice flow pattern, and (b) the pattern of recession of the late Weichselian Ice Sheet. (After Kleman *et al.*, 1997).

3.3. The bedform continuum theory

The above discussion highlights that in most instances each bedform type rarely exists in isolation, but rather, there appears to be strong spatial associations between all subglacial bedforms. This phenomenon has steered researchers towards seeing them as being part of an evolving assemblage in a bedform continuum (Aario, 1977; Boulton, 1987; Menzies, 1987; Rose, 1987; Boulton and Clark, 1990a,b; Clark, 1993, Hindmarsh, 1998a,b,c, 1999). In this model, ribbed moraine are the first bedforms in the sequence which are broken up further downstream into drumlins which in turn grade into megaflutes and mega-scale glacial lineations (Fig. 3.20). If this is the case, then it should be possible to identify the sequence and is something that might be resolved using remote sensing techniques.

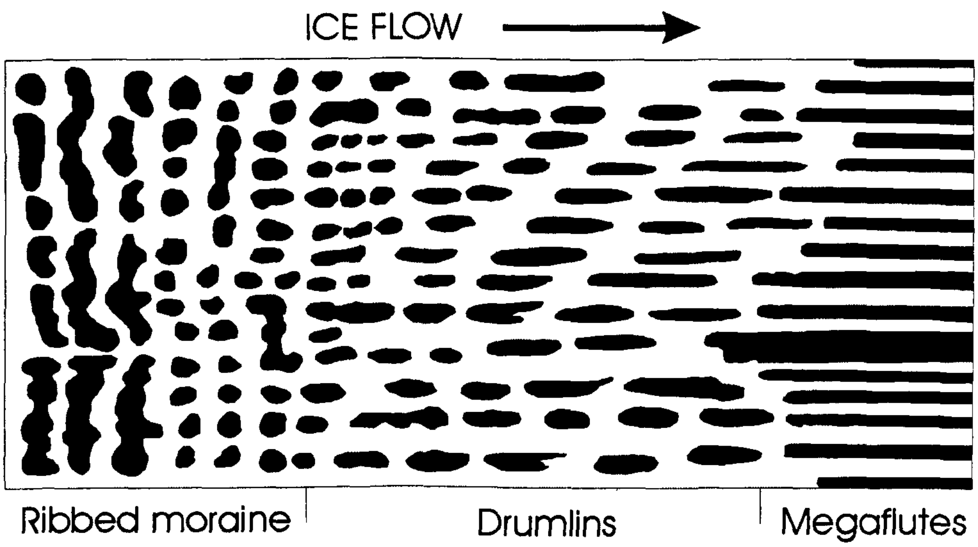

Figure 3.20. Conceptual diagram of the bedform continuum from ribbed moraine to drumlins to mega-scale glacial lineations (Adapted from Aario, 1977).

3.4. Summary and conclusions

Subglacial bedforms are either longitudinal or transverse accumulations of sediment that were formed beneath active ice. Flutes, drumlins, megaflutes and mega-scale glacial lineations are longitudinal bedforms that are streamlined and aligned parallel to the regional ice flow pattern. Ribbed moraines form transverse to ice flow. The main distinction between the glacial lineations is based on their length and elongation ratios (see Figure 3.1).

Flutes are the smallest of the subglacial bedforms and are found in a variety of settings including in front of drumlin belts, superimposed on top of other bedforms and in isolation in contemporary proglacial zones. The most widely accepted theory of flute formation regards them as a product of sediment deformation in the lee of obstructions in the bed.

Drumlins are arguably the most studied of all the subglacial bedforms and a substantial body of literature has been produced by scientists over the last 100 years. In spite of this, many questions regarding their formation remain unanswered. Although many drumlin theories have been published, only several of the more recent theories were reviewed. As was shown, various mechanisms and subglacial conditions have been invoked in order to explain their genesis. The discovery several decades ago of deformable glacier beds regenerated interest in explaining subglacial bedforms and lead to a widely accepted view of drumlin formation proposed by Boulton (1987). This theory describes a number of scenarios by which drumlins may be formed by deforming sediment (Figure 3.5). His ideas account for many of the characteristics of drumlins and the internal structures of both hard and soft-cored drumlins. One problem though is that the theory is qualitative and is therefore very difficult to test. However, the development of two numerical computer models by Hindmarsh (1998a,b,c, 1999), helped usher in a new era in the quest to explain drumlin formation by a deforming bed mechanism, because for the first time, there is a theory that makes quantitative predictions about bedform generation that can be quantitatively tested. Although Hindmarsh's theory accounts for several facets of drumlin formation; spontaneous relief amplification; blunt faces of drumlins; streamlined shapes, it does not explain the internal structure of drumlins and the theory has yet to link both BRIE and the Shock Formation Model. This is mainly a mathematical problem as one model is linear and the other is non-linear, however plans are currently underway to resolve this issue and it is envisaged that both models will soon be combined (Hindmarsh, pers. comm.) However, as it stands, the theory is incomplete, because it cannot explain drumlin formation as a 3-dimensional instability phenomenon; i.e. it cannot produce a drumlin from a flat till sheet.

Other authors have stressed a glacifluvial origin for drumlins. Although this model accounts for the build up and presence of stratified sediments in drumlins, it does not explain how the drumlin was initiated. This theory requires a protuberance to be in place to allow the drumlin to evolve and since most drumlins are soft cored and consist of unconsolidated sediments, it only offers a partial explanation, as it does not account for the initial amplification. As it stands it, it might only explain some local occurrences and is therefore not a general formational theory.

The most controversial theory to have emerged in recent years is the megaflood hypothesis. This theory states that all subglacial bedforms are produced by mega-scale subglacial floods. It is essentially a form analogy theory and the various authors cite the striking similarity of form between subglacial bedforms and scour marks made at the base of turbulent underflows. They argue from the premise that because they look the same they must also share a common origin. However, as was highlighted earlier, form analogy may not always be the best criterion upon which to base genetic interpretations and there is also problems in trying to compare small-scale erosional marks to large-scale subglacial bedforms. As was previously discussed, there are also issues relating to identifying suitable water reservoirs large enough to be involved in floods on the scale proposed by the hypothesis. Nonetheless, it cannot be dismissed out of hand because we know that ice sheets can store large amounts of water and the discovery of Lake Vostok, which is roughly the size of Lake Ontario, is proof of this. Furthermore, subglacial drainage events of large ice-marginal, supraglacial and subglacial lakes are well known from modern environments and it is clear that some Pleistocene Jökulhlaups were of much higher magnitude than any observed in historical times (Benn and Evans, 1998). Because the potential for large-scale floods beneath ice sheets appears to exist, the onus is placed firmly back on the shoulders of the scientific community to either rigorously test the hypothesis and try and falsify it, or else satisfactorily explain subglacial bedform generation and preservation through entirely glacial processes.

As well as introducing the major subglacial bedforms, a more thorough review on the characteristics of ribbed moraine was also presented. As Hättestrand and Kleman (1999) state, "any theory of ribbed moraine formation must be compatible with, and be able to explain, the observations described above. In summary, ribbed moraines:

1. occur only in core areas of former glaciation
2. commonly occur close to and distal of inferred frozen-bed areas
3. are formed during deglaciation of ice sheets (according to Hättestrand and Kleman (1999), but not universally accepted)
4. are most common on concave or flat surfaces in the terrain
5. are commonly drumlinized
6. are rarely found superimposed on aligned drumlins
7. have eskers superimposed on them, not vice versa
8. are commonly regular in ridge height and spacing
9. may have flat, or sometimes multiple, crests of individual ridges
10. are commonly asymmetric, with a steeper lee face
11. often display a "jigsaw puzzle matching" of the ridges
12. are composed of a variety of materials

13. commonly consist of material also found in its surroundings
14. commonly display glaciotectonic structures

In addition to these observations, a theory of ribbed moraine genesis must also be theoretically sound with respect to existing glaciological knowledge" (Hättestrand and Kleman, 1999, pp. 13-14).

***

Chapter 4: Methodology – Remote Sensing of Ribbed Moraine and Ribbed Moraine Wavelength Measurement

4.1. Introduction - ribbed moraine morphometry

Morphometric analysis of glacial landforms has been widely employed by geomorphologists (e.g. Alden, 1905; Hollingsworth, 1931; Charlesworth, 1939) and is a useful tool for several reasons. It provides us with quantitative data regarding the morphology of the landform under consideration, it can be used to establish spatial patterns, and importantly, it helps establish relationships between the measured variables of the landform and the process that created them. Trenhaile (1971) suggested drumlins as being the most suitable glacial landform for conducting morphometric analysis and is the glacial landform that has received most attention in the literature (e.g. Chorley, 1959; Smalley and Unwin, 1968; Piotrowski, 1989; Knight, 1997). Other subglacial bedforms such as ribbed moraine, which are thought by some to be the initial phase of drumlin formation, have received less attention. Many papers dealing with ribbed moraine normally cite a range of dimensions such as height, length and width, and qualitatively describe the shape of the ridges (e.g. Lundqvist, 1969; Hättestrand, 1997b; Knight and McCabe, 1997). However, there is no detailed morphometric data set on ribbed moraine in the current literature that can be used to check if these often quoted dimensions are accurate, site specific or are typical for all ribbed moraine areas. This thesis directly addresses this shortfall by producing the first comprehensive morphometric data set on ribbed moraine. This chapter outlines the methods that were used in this thesis to map areas of ribbed moraine utilising a variety of remote sensing techniques. It also describes the methods that were followed to obtain one aspect of ribbed moraine morphometry, the wavelength, which is defined as the distance between consecutive ribbed moraine ridge crests (Fig. 4.1). The wavelength database was compiled mainly to test the Hindmarsh (1998a,b, 1999) model of ribbed moraine formation, which specifically predicts ribbed moraine wavelength. However, it should be of value on its own as the first quantitative analysis of ribbed moraine made available for evaluating other formative theories.

4.2. Data sources

To ensure any morphometric tests conducted were credible, the data set would have to be representative of the global ribbed moraine population. The best way of ensuring this was to obtain very large sample sizes of ribbed moraine ridges, (in the order of tens of thousands) from a variety of geographical, topographical and ice dynamical settings. The use of remote sensing suited this aim well for several reasons;

1. Satellite imagery and aerial photograph mosaics allows a single user to map geomorphology over very large regions.

2. Satellites provide a widespread source of digital imagery for previously glaciated terrains, which makes it easy to obtain images of ribbed moraine from a variety of geographical and glaciological contexts.

3. It is much quicker and cheaper to map glacial landforms using remote sensing than by traditional field methods, leading to appropriate sample sizes for the aims of this thesis.

Detailed small-scale mapping was conducted using 1:60 000 aerial photographs. Larger regions were mapped using a high resolution Digital Elevation Model (DEM) and both Landsat Multi-Spectral Scanner (MSS) and Landsat Enhanced Thematic Mapper (ETM+) satellite imagery. Towards the end of this study, newly released imagery became available from an imaging instrument on the Terra satellite known as the Advanced Spaceborne Thermal Emission and Reflection Radiometer (ASTER) and ASTER images covering the Lake Rogen site in Sweden (Section 4.3.4) and the Lac Naococane region in Québec (Section 4.3.6) were obtained. The images were acquired after the ribbed moraine had been mapped in the Lac Naococane area and because of this, were not used for this purpose. Instead, they were used to check the accuracy of the mapping that was conducted in this site using an MSS image and also for making detailed observations, because this higher resolution imagery gave a more detailed view of the terrain than was offered by the MSS image. In the Lake Rogen area, the ribbed moraine ridges were originally mapped by tracing the ridge crests directly onto plastic acetate sheets using stereo aerial photographs, which meant the data was not in digital format (Section 4.3.4). Although this was adequate for the purpose of making an accurate map for measuring ribbed moraine wavelength, it proved restrictive because the finished map could not be displayed in a GIS, which was a powerful tool for analysing the characteristics of the mapped ridges (e.g. Sections 5.5.1 & 5.5.2). For this reason, it was thought desirable to have a digital map of the region and for this purpose an ASTER image was also used to map the ribbed moraine in this area. The ASTER DEM's that were acquired were used to conduct detailed topographical analysis (e.g. Section 5.5). Table 4.1 shows the spatial coverage and the resolution of each of type of image.

Table 4.1. Spatial Resolution and Coverage of imagery used in the thesis

Imagery	Spatial Coverage (km)	Spatial Resolution (m)
Landsat MSS	185 x 185	80
Landsat ETM+ (Panchromatic band)	185 x 185	15
ASTER image	60 x 60	15
ASTER DEM	60 x 60	30
DEM of northeast-central Ireland (Compiled by aerial photogrammetry)	100 x 90	25
Aerial Photographs (1:60,000)	3 x 13	1.5

4.2.1. Landsat MSS and Landsat ETM+

The MSS sensor of the Landsat series of satellites provides 4 wavebands in the visible portion of the spectrum (1, 2, 3 and 4) and has a spatial resolution of 80 m. This allows mapping to be conducted at a scale of up to 1:120,000. The ETM+ sensor is an improved version of the Thematic Mapper (TM) instruments and like the earlier TM sensor, the ETM+ acquires data for 7 spectral bands from visible to thermal infrared with a spatial resolution of 30 meters. The ETM+ sensor also incorporates a panchromatic band, which extends over the ultra violet and visible portions of the spectrum, and has a spatial resolution of 15 m.

When mapping ribbed moraine ridges using MSS imagery it was found that a combination of bands 4, 2 and 1 were best for identifying the ridges. Because of its high-resolution capabilities, the panchromatic band of the ETM+ sensor was chosen for use in this thesis. Using this band meant that ribbed moraine ridges too small to be resolved by the MSS sensor could be identified and their characteristics recorded.

4.2.2. Digital Elevation Models

Digital elevation models, or DEM's, are raster-based models of topography consisting of points of elevation that have been sampled systematically at equally spaced intervals. Each individual grid cell or pixel of the DEM represents the elevation within the area that it covers. They are usually derived from data taken from maps or directly from stereo aerial photographs, and where available, high resolution DEM's are often superior to satellite imagery for mapping glacial geomorphology (Clark, 1997). This is partly because DEM's can be manipulated in variety of ways to preferentially enhance the appearance of glacial bedforms (e.g. Clark, 1997 and Clark and Meehan, 2001). For the purpose of this study, a high resolution 25 m DEM of north-central Ireland, compiled by aerial photogrammetry was acquired and viewed vertically as a grey scale elevation image. This proved a sufficient method of preferentially enhancing the ribbed moraine on the DEM and made them easily distinguishable from other topographic features on the image.

4.2.3. Aerial photographs

The use of vertical aerial photographs proved a valuable method for identifying and mapping ribbed moraine ridges of different scales. Using a mirror stereoscope to view the aerial photographs made the ribbed moraine stand out very clearly from the surrounding terrain. This made locating and identifying the ridges easy. Viewing in stereo also made it possible to map the actual crest of each ribbed moraine ridge, which was important when measuring their wavelength, as the wavelength measurement is taken from the crest of one ridge to the crest of the next ridge and therefore accuracy was improved. The extremely good spatial resolution of the aerial photographs also permitted the identification of smaller scale ribbed moraine, known as minor ribbed moraine, which was not possible using MSS imagery.

4.2.4. Advanced Spaceborne Thermal Emission and Reflection Radiometer (ASTER)

The Advanced Spaceborne Thermal Emission and Reflection Radiometer (ASTER) is a multispectral imager that was launched on board NASA's Terra spacecraft in December, 1999. ASTER covers a wide spectral region with 14 bands from the visible to the thermal infrared with high spatial, spectral and radiometric resolution. An additional backward-looking near-infrared band provides stereo coverage. The spatial resolution varies with wavelength: 15 m in the visible and near-infrared (VNIR), 30 m in the short wave infrared SWIR), and 90 m in the thermal infrared (TIR). Each ASTER scene covers an area of 60 x 60 km. As was stated previously, the images were not used to map the ribbed moraine at the Lac Naococane site but for checking the accuracy of the mapping done using the much lower resolution MSS image and also for making detailed observations at this site (see Chapter 5). One ASTER image was also used to map the ribbed moraine in the Lake Rogen region to obtain a digital map of the ribbed moraine in this location so that further analysis of the data set could be done in a GIS (see Chapter 8).

4.3. Methodology: mapping ribbed moraine and measuring their wavelength

4.3.1. Terminology and assumptions

This section outlines the basic procedures followed to map the ribbed moraine ridges using the different types of remotely sensed data discussed above. It also explains the various methods used to obtain ribbed moraine wavelength data from each of the locations. For the purpose of this thesis, ribbed moraine ridges are defined as large, regularly spaced transverse ridges that range between 100 m to several kilometres in length, and are between 25 m to just over 1 km wide. A ribbed moraine field, or a ribbed moraine, is defined as a group of these ridges with the same orientation, which can be clearly delimited from other groups of ribbed moraine ridges in their vicinity (see Figure 4.5). When mapping the ridges, no distinction was made between the various morphological types of ribbed moraine reported in the literature (see Section 3.2.3.1) and all were treated as one genetic type of morphology, i.e. ridges composed of drift that were formed transverse to the known ice flow direction. This was due to the findings of Hättestrand (1997b), who after investigating the characteristics of four different types of ribbed moraine in Sweden, concluded their shared characteristics were indicative of a common subglacial origin. Ribbed moraine wavelength is defined as simply the distance between the crest of each consecutive ribbed moraine ridge and is measured in a down ice direction (Fig. 4.1).

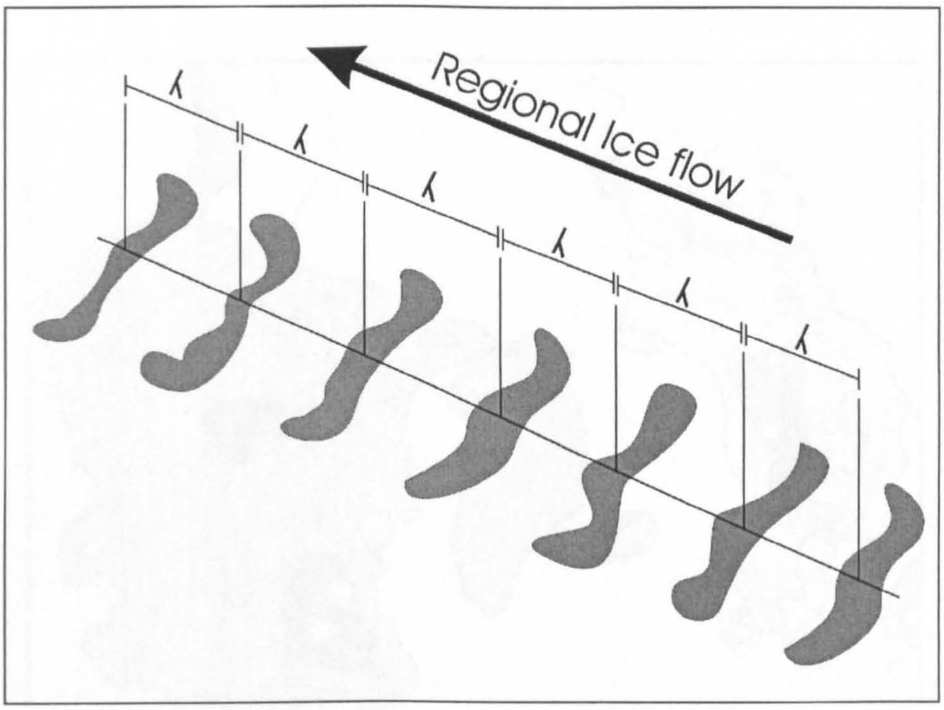

Figure 4.1. Demonstration of how ribbed moraine wavelength is defined. The measurement is taken between the crests of consecutive ribbed moraine ridges and is always made in a down ice direction, as this is the orientation the ridges were formed at.

4.3.2. Sampling ribbed moraines from the global population

The currently known worldwide distribution of ribbed moraine can be seen in Figure 4.2. Presently, all occurrences of ribbed moraine are in the Northern Hemisphere (see Section 3.2.3.3). The large aerial extent of ribbed moraine meant it would be unfeasible to try and map the entire population for this thesis. Therefore, samples of ribbed moraine had to be taken. To try and ensure these samples would be representative of the global population several factors were taken into consideration. Firstly, to be considered globally representative, the sample would have to include ribbed moraine from various parts of the world. Secondly, the areas would have to be from as wide a variety of topographical and ice dynamical settings as possible. Finally, large numbers of ribbed moraine ridges would need to be mapped if the study was to fulfil the expectation of building a database of ribbed moraine wavelength that could be considered credible and reliable.

To help satisfy the above conditions, areas of ribbed moraine were mapped in Canada, Sweden and Ireland. This ensured that ribbed moraine formed beneath three separate ice sheets would be included in the sample (Fig. 4.2). In Québec, two sites were

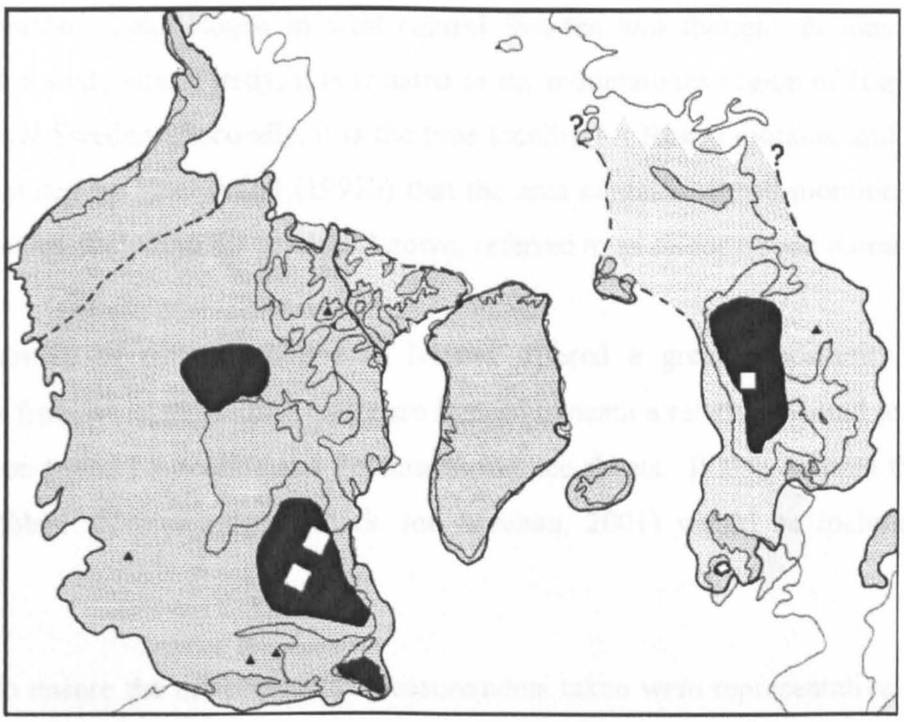

Figure 4.2. Currently known World-wide distribution of ribbed moraine (modified from Hättestrand, 1997b). Light shaded is the Last Glacial Maximum ice sheet distribution. Dark shaded regions are where ribbed moraine occurs commonly. In addition, a few outliers of ribbed moraine have found outside the core areas and these are marked with triangles. The white boxes mark the location where ribbed moraine was sampled and can be seen in greater detail in Figures 4.6, 4.8 and 4.13.

chosen, one just south of Ungava Bay, in the River Kaniapiskau region and the other in the centre of Québec in the Lac Naococane area (see Figure 4.13). These areas of ribbed moraine were selected because they were formed by the same ice sheet but are situated on the opposite sides of the ice divide (see Figures 5.2 and 6.2) and as such, provided an opportunity to investigate whether this affected their characteristics in any way. In addition, both areas have quite different topographical settings. The River Kaniapiskau site is an area where the terrain slopes towards the bay on all sides, resembling a large shallow amphitheatre and there are no real topographical barriers that would have impeded ice flow across this region. The other site is situated in an upland part of Québec and has a more complex topography as it crosses partly over a plateau, several large basins and incorporates the Mount Ottish mountain range (see Figure 5.28).

In Sweden, ribbed moraine can be seen in a variety of topographic settings. However, it is the only place in the world where they can be found nestled among 1000 m mountains. The topographic setting of these ribbed moraine sets them apart from other ribbed moraine areas and it was therefore desirable to include them in the sample. For several reasons, Lake Rogen in west central Sweden was thought an ideal place to choose as a study site. Firstly, it is situated in the mountainous region of Härjedelan in west-central Sweden. Secondly, it is the type locality for Rogen moraine and finally, it has been noted by Hättestrand (1997b) that the area contains ribbed moraine ridges of various scales, including the smallest known, referred to as minor ribbed moraine.

The discovery of ribbed moraine in Ireland offered a great opportunity to study examples from an island setting that were formed beneath a relatively small ice sheet in comparison to the Laurentide and Fennoscandian ice sheets. It also ensured the largest known ribbed moraine ridges (Clark and Meehan, 2001) would be included in the sample.

Finally, to ensure the morphometric measurements taken were representative of ribbed moraine in general, this thesis required large numbers of ribbed moraine ridges to be mapped. Using the various sources of imagery, a combined area of 81,000 km^2 was covered from which approximately 36,000 individual ribbed moraine ridges were mapped. This is the largest sample of ribbed moraine ridges ever mapped and because the final figure was in the order of tens of thousands, it gave confidence that the sample was large enough for the requirements set out in this thesis.

4.3.3. Wavelength sampling design

The main objective here was to obtain a database of wavelength data that would be representative of the global ribbed moraine population. For this purpose, a high sampling rate would be required in order to capture as many wavelengths as exist in nature as possible. This ruled out a random sampling method, as it was thought this approach would have a higher probability of missing out important wavelength data, which in turn might result in an unrepresentative database. Therefore, a systematic approach was seen as a more appropriate, because the sampling strategy could be designed to include as many different ribbed moraine fields as possible in each sample. The method decided upon, was to superimpose evenly spaced transect lines across the ribbed moraine fields, which would then act as a guideline for sampling the wavelength. Because ribbed moraine ridges formed transverse to ice flow, the transects would have to be aligned with the regional ice flow direction to ensure the wavelength was properly sampled. Therefore, the first stage involved determining the palaeo ice flow direction over the study areas. To do this, several pieces of evidence were used. Firstly, the orientation of the ribbed moraine ridges in each field were used as a proxy for working out the line of glacial flow across each region. Because ribbed moraine ridges form transverse to ice flow, the regional ice motion must have been perpendicular to their alignment. Secondly, the inferred direction could also be checked by studying the orientation of any nearby drumlins. Finally, for the study sites in Canada and Sweden, the direction was verified by checking the regional ice flow patterns shown on the Glacial Map of Canada (Prest *et al.*, 1968) and the map of Glacial Geomorphology of Central and Northern Sweden (Hättestrand, 1997a). Once the flowlines were drawn across the area, transects spaced at regular intervals could then be superimposed in the correct orientation for sampling the wavelength (Fig. 4.3).

The use of several scales of imagery in this thesis required the transects to be varied slightly to suit each locality. In relatively small-scale study areas, such as Lake Rogen in Sweden, the ribbed moraine is contiguous and the flow pattern recorded is uniform across the study site. This made it quite easy to draw evenly spaced transects across the entire region. However, viewing sites at a larger scale using satellite imagery revealed more complex distributional patterns whereby the ribbed moraine tended to cluster into fields that were often separated over large distances. Viewing at this scale also exposed flow regimes that were more complex than in the smaller study areas (see Figure 4.4). Both these factors made it extremely difficult to cover large areas with evenly spaced sampling lines. Therefore, individual fields of ribbed moraine were isolated by digitising a boundary around them and then using the principles outlined above, evenly spaced transects were digitised across each field (Fig. 4.5).

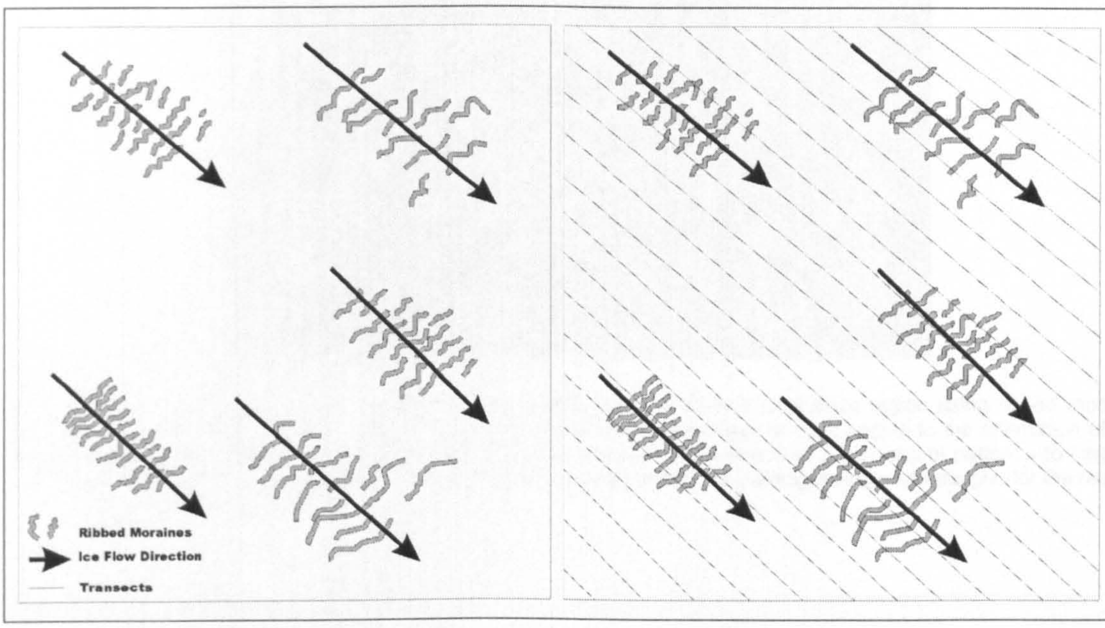

Figure 4.3. Demonstration of how systematically drawn sampling lines were constructed across a ribbed moraine region. Note how the transects are oriented in the same direction as the regional ice flow direction. When a sample line crosses a series of ribbed moraine ridges, the wavelength is measured in the manner specified in Figure 4.1.

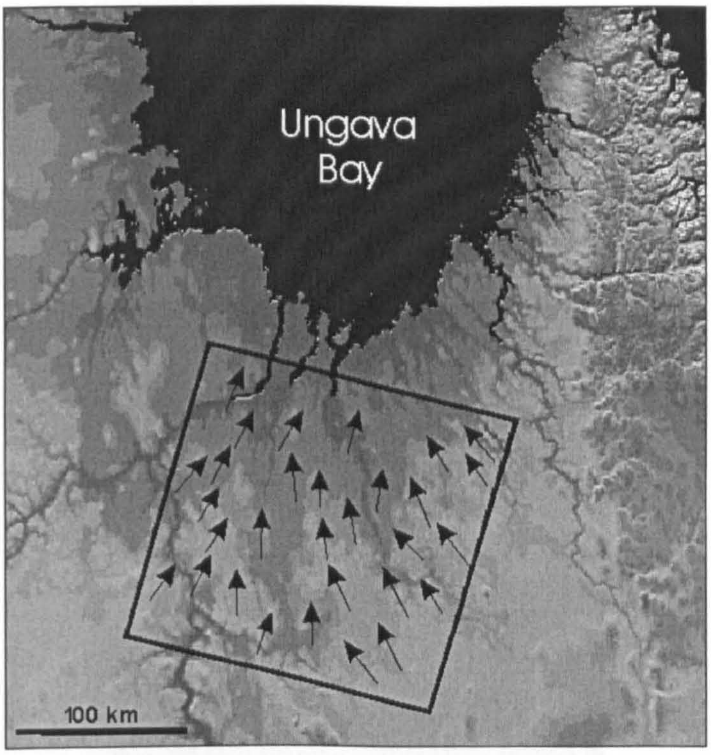

Figure 4.4. A reconstruction of the palaeo ice flow direction in the River Kaniapiskau region using ribbed moraine orientation as an ice flow indicator. Arrows pointing downstream were drawn at right angles to the orientation of the ridges in each ribbed moraine field. The pattern of arrows shows that ice flowed in a convergent pattern into Ungava Bay. Flow patterns such as this proved too complicated to act as a base for building a single sample grid for the region.

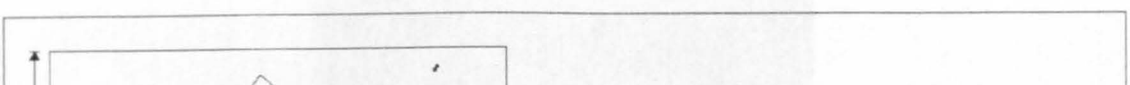

Figure 4.5. An example of how sampling lines were constructed for areas viewed at the scale of satellite imagery. The diagram on the left shows a selection of mapped ribbed moraine ridges in the River Kaniapiskau region. Each separate field has been isolated by digitising a boundary around its perimeter. The diagram on the right demonstrates how the sampling grids were then constructed inside each field. Lines spaced approximately 1.5 km to 3 km apart were then digitised across each field in the direction of regional ice flow.

4.3.4. Stereo aerial photographs

The first place chosen to map ribbed moraine and acquire ribbed moraine wavelength data from was the Lake Rogen area, in southwest Härjedalen, central Sweden (Fig. 4.6). This region is the type locality for Rogen moraine and was therefore an obvious choice as a study site.

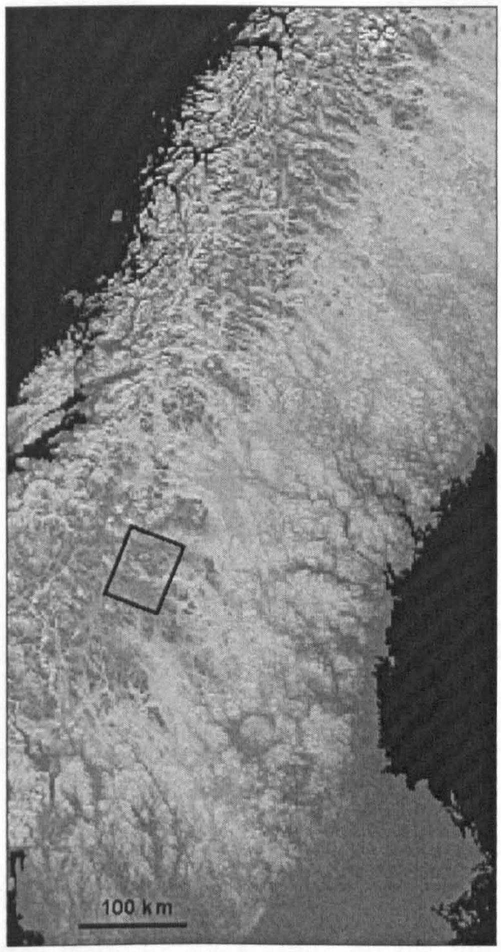

Figure 4.6. Location map of the study site in the Lake Rogen area in Sweden in southwest Härjedelan, central Sweden. The box shows the area covered by the aerial photographs used to study the ribbed moraine ridges in this locality.

To comprehensively map this area, 1:60,000 aerial photographs covering approximately 3600 km^2 were acquired. Transparent A4 acetate sheets were placed on top of the aerial photographs and the ridge crest of the ribbed moraine ridges were traced onto these overlays. This procedure was followed until the all the ribbed moraine ridges identified in the region were mapped. Any mountains and lakes in the area were also mapped to record their position. This was necessary to avoid the mistake of measuring the distance between any ribbed moraine ridges separated by these features, as this measurement would not represent a true ribbed moraine wavelength (Fig. 4.7).

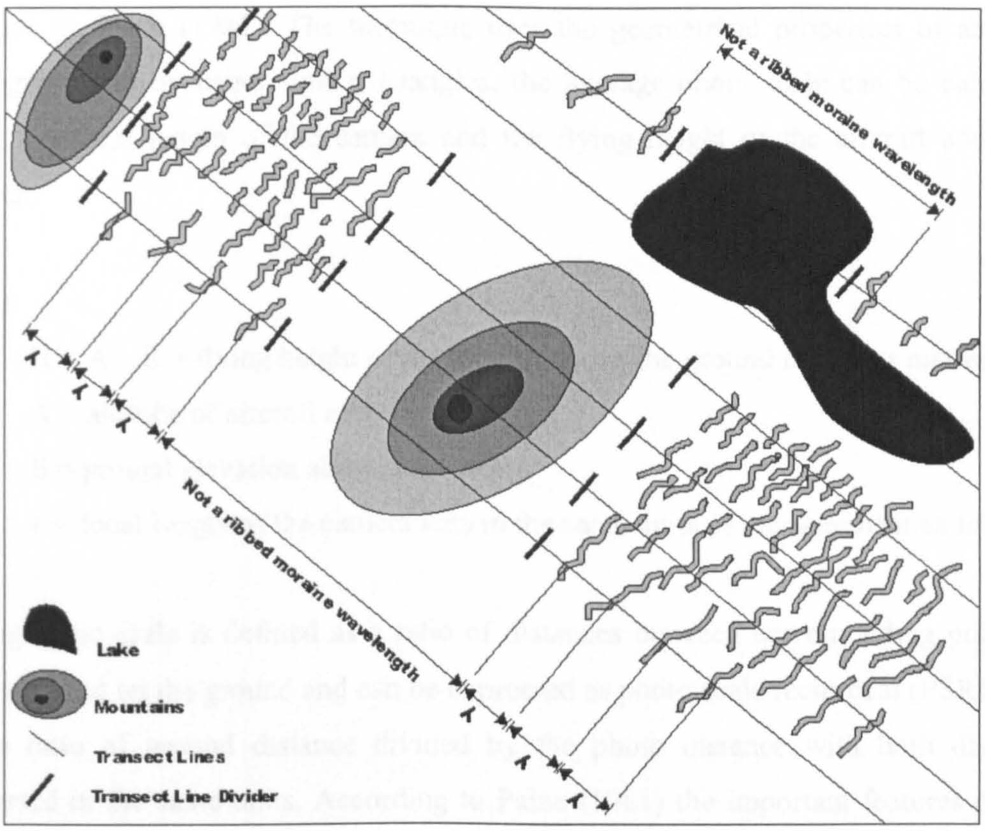

Figure 4.7. In Sweden, the absence of ribbed moraine on steep mountain slopes indicates that the mountains in this region acted as barriers that interrupted the ribbed moraine forming process. Because of this, ribbed moraine fields separated by mountains are unrelated and as the diagram indicates, the first and last ridge of such fields is not a ribbed moraine wavelength. Wavelength measurements were not taken across lakes because in most cases large water bodies conceal submerged ribbed moraine and the series is broken. As the diagram shows, ribbed moraine ridges at either ends of a lake were not used to measure wavelength.

The transparent overlays were then fitted together to form a mosaic. From this, one large map of the area was made by transposing all the information recorded on the overlays onto a large sheet of tracing paper. Following the principles laid out in Section 4.3.2, transects approximately 1 km apart were then drawn over the entire Lake Rogen area. Mountain and lake barriers were filtered out of the sampling strategy to eliminate erroneous measurements. This was done by simply dividing any transect lines that crossed over these features (see Figure 4.7). In total, the study area had 56 sampling lines and from this 2666 individual wavelength measurements were obtained.

The initial measurements were made using a ruler to measure the wavelength to the nearest millimetre. The next stage was concerned with converting these measurements to metres. Before this could be done, however the scale of the aerial photographs had to be determined. This was achieved by using basic scale equations formulated for use on vertical aerial photographs. For the purpose of this study, the procedure followed those laid out by Paine (1981). The technique uses the geometrical properties of an aerial photograph and by using similar triangles, the average photo scale can be calculated using the focal length of the camera and the flying height of the aircraft above the ground.

Where

$H = A - E$ = flying height of the aircraft above the ground in feet or metres

A = altitude of aircraft above sea level

E = ground elevation above sea level

f = focal length of the camera lens in the same units of measurement as for H

Photographic scale is defined as a ratio of distances between corresponding points on the photo and on the ground and can be expressed as photo scale reciprocal (PSR). PSR is the ratio of ground distance divided by the photo distance with both distances expressed in the same units. According to Paine (1981) the important features of PSR are that it is unitless and smaller numerical values of PSR represent a larger scale, i.e. a PSR of 10,000 is greater than a PSR of 40, 000. This means if the PSR is small, it is closer to the actual size of the object being measured than if the PSR is large. PSR is also the number that the photo size of an object must be multiplied by to obtain its actual size. This study used PSR to convert the wavelength measurements from millimetres to metres, as the information required to solve the scale equations was easy to obtain and the equations are easily solved. To work out the average PSR for a photo or an entire flight line the following equation needs to be solved:

$$PSR = \frac{A - E}{f} \text{ or } \frac{H}{f}$$

A good working example is provided by Paine (1981 pg, 72). Lets suppose the average nominal PSR scale that the flight mission was chartered for was 14,000, the attempted flying height above mean sea level was 8000 feet and the focal length of the camera is 6 inches. From a topographic map the average ground elevation covered by the photo was 800 ft. From these figures the average photo PSR is:

$$PSR_{800} = \frac{A - E}{f} = \frac{8000\text{ ft} - 800\text{ ft}}{0.5\text{ ft}} \quad \text{or}$$

$$PSR_{800} = \frac{H}{f} = \frac{7200\text{ ft}}{0.5\text{ ft}} = 14,400$$

The Lake Rogen study site is situated in quite mountainous terrain and as such elevation changes across the area. This meant that the PSR would also change depending on the elevation of the terrain, because the ground elevation above sea level (*E* in the formula) is not constant across the site. This factor was taken into account when calculating the PSR in this area and to improve accuracy, average relief data derived by Lundqvist (1953) was used to estimate the average elevation across various parts of the site. This showed the area should be divided into three general elevation zones. The first was the area to the north of Lake Rogen, which has an average elevation of 306 m. The second was at Lake Rogen itself, where the average elevation was estimated to be 37.5 m. The final zone is situated to the south of Lake Rogen and has an average elevation of 250 m. Therefore, three PSR formulae had to be used, PSR_{306}, $PSR_{37.5}$ and PSR_{250}. The solutions for each are shown below:

$$PSR_{306} = \frac{A - E}{f} = \frac{9200\text{ m} - 306\text{ m}}{0.15248} = PSR\ 58696$$

$$PSR_{37.5} = \frac{A - E}{f} = \frac{9200\text{ m} - 37.5\text{ m}}{0.15248} = PSR\ 60089$$

$$PSR_{250} = \frac{A - E}{f} = \frac{9200\text{ m} - 250\text{ m}}{0.15248} = PSR\ 58328$$

PSR_{306} was used to convert the measurements from millimetres to metres on flow lines 1 through to 28, $PSR_{37.5}$ was used on flow lines 29 through to 43 and PSR_{250} was used on flow lines 44 through to 56. The results of the Swedish wavelength measurements are discussed in Chapter 9.

For the purpose of producing a digital map of the ribbed moraine in this region, one ASTER image was displayed and manipulated using ERDAS Imagine 8.5. Any ribbed moraine ridges that were identified were digitised on screen by drawing a line along the crest of the ridge and the data were stored as an ARC coverage. When mapping was completed, approximately 5500 ribbed moraine ridges were recorded in the region. The results of the analysis conducted using this map are discussed in Chapter 8.

4.3.5. Digital Elevation Model

To obtain wavelength information on ribbed moraine in Ireland, a 25 m resolution DEM of the northeast midlands region was acquired, which covered an area approximately 9000 km^2 (Fig. 4.8).

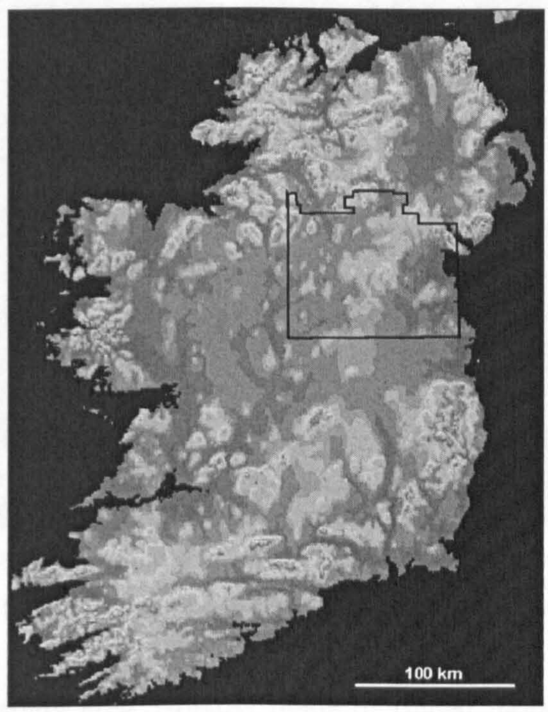

Figure 4.8. Location map of the Irish ribbed moraine field. The coverage of the DEM used to map the ribbed moraine ridges in Ireland is marked by a black outline.

To acquire the data, the DEM was displayed and manipulated on a PC using the remote sensing package ERDAS Imagine 8.5. Because Clark and Meehan (2001) had previously digitised the ribbed moraine ridges in this region using the same DEM, it was not necessary to re-map the area, as the author was given access to their original ARC coverage. Where possible, Clark and Meehan mapped the outline of each ribbed moraine ridge by digitising the break of slope. However, on the smaller ridges, they simply digitised the ridge crest. The ARC coverage was loaded into ERDAS Imagine and acted as a guide for building the sampling lines across this study site, which were drawn approximately every 1.5 km to 2 km apart across the image (Fig. 4.9).

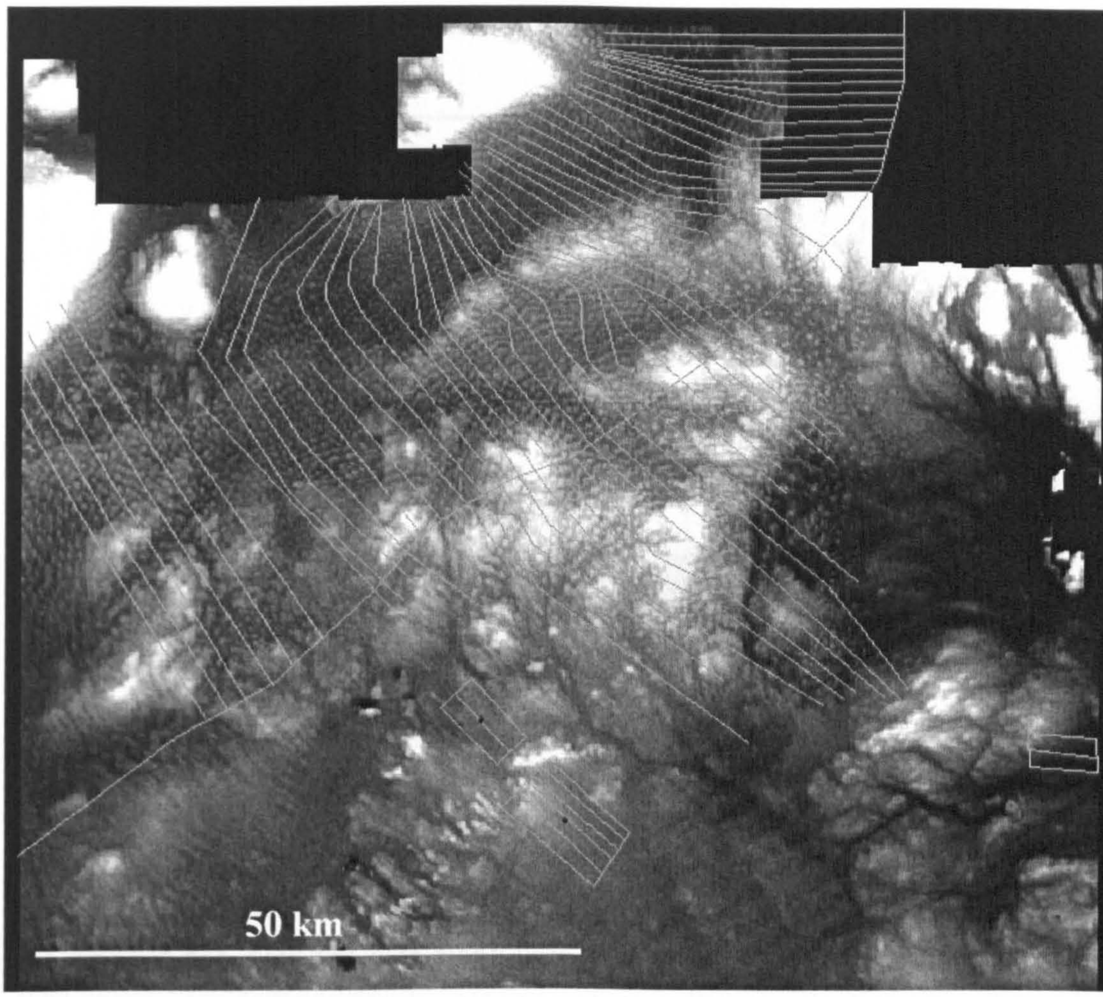

Figure 4.9. Showing the DEM of the Irish ribbed moraine region displayed as a grey scale elevation image with sampling lines placed on top. In this region it was found that the ribbed moraine ignored topographic barriers and are found superimposed on top of hills in the region (see Chapter 8). This eliminated the need for segmenting the transect lines.

In some parts of the study area, isolated fields of ribbed moraine where also found. Where this was the case, the fields were enclosed by digitising a boundary around the perimeter of the field and the transects drawn inside the boundary (see Figure 4.5). In this part of Ireland, it was observed that the ribbed moraine largely ignored the influence of topography and are actually superimposed on many of the hills in the area (see Chapter 7). This strongly indicated that hills did not impede the ribbed moraine forming process and because of this, the sampling lines were not segmented in the same manner thought necessary in Sweden (see Figure 4.7). To obtain the wavelength data from the DEM, a manual method of measurement was chosen. The large ribbed moraine ridges in Ireland were so easily resolved using the DEM that measuring their wavelength manually proved a relatively simple task. To obtain the wavelength data the following procedures were employed. Using the sampling lines as a guide, transects were taken across the DEM to obtain topographic profiles of the terrain (Fig. 4.10).

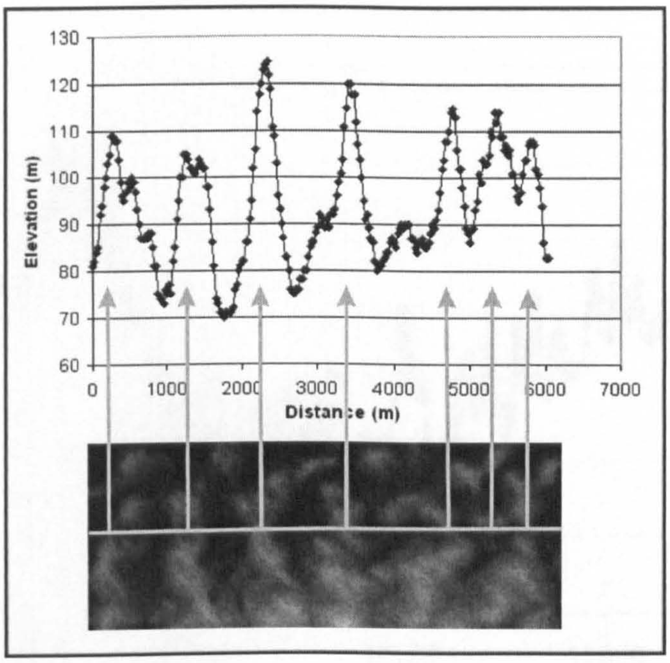

Figure 4.10. Demonstration of a topographic profile obtained by taking a transect across the DEM. Note how the peaks on the graph record the undulating topography caused by the presence of ribbed moraine. The DEM was displayed as a grey scale elevation image, which shows the ribbed moraine ridges as light grey, the surrounding terrain is dark grey to black in colour.

The distance and elevation data along with the map coordinates of each transect were then exported into the spreadsheet package Microsoft Excel. Using the distance and elevation data, scatter plots were constructed to show the profile in graphical form (Fig. 4.11). By viewing the graphs on-screen and pointing the mouse cursor at the highest point of each peak, it was possible to obtain a reading that showed how far along each transect the ridge crest was situated. Beginning with the first peak and continuing across the graph, the distance along the transect at which the highest point of each peak occurred was recorded. To verify that all the peaks were caused by the occurrence of ribbed moraine and not other topographic features, e.g. drumlins, it was necessary to check the DEM. The map coordinates that were exported along with the other profile data, show the exact location of every elevation and distance value on the DEM. Using this information it was possible to view the feature on the DEM that caused the peak. If it was not caused by a ribbed moraine, the peak was rejected and its recorded position eliminated from the data series. Consistently checking the data in this manner reduced errors and helped keep the data set accurate. The remaining values were then put into the spreadsheet and the wavelength was calculated by simply calculating the difference between successive values in the data series (Fig. 4.12). The results of the Irish wavelength measurements are discussed in Chapter 7

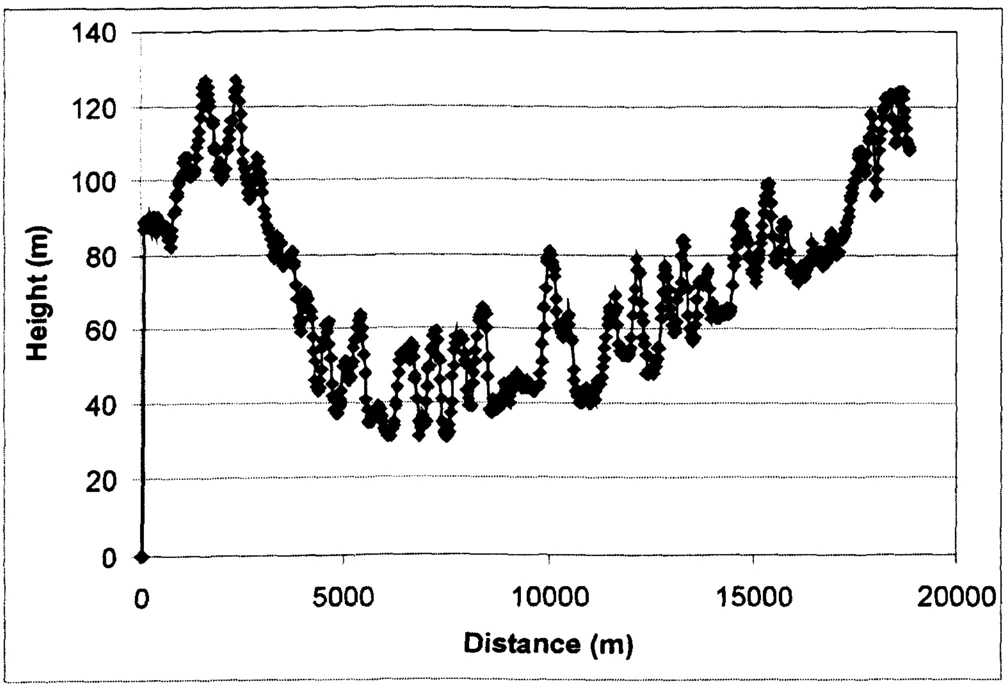

Figure 4.11. An example of a scatter plot produced in Excel using the elevation and distance data exported from the DEM.

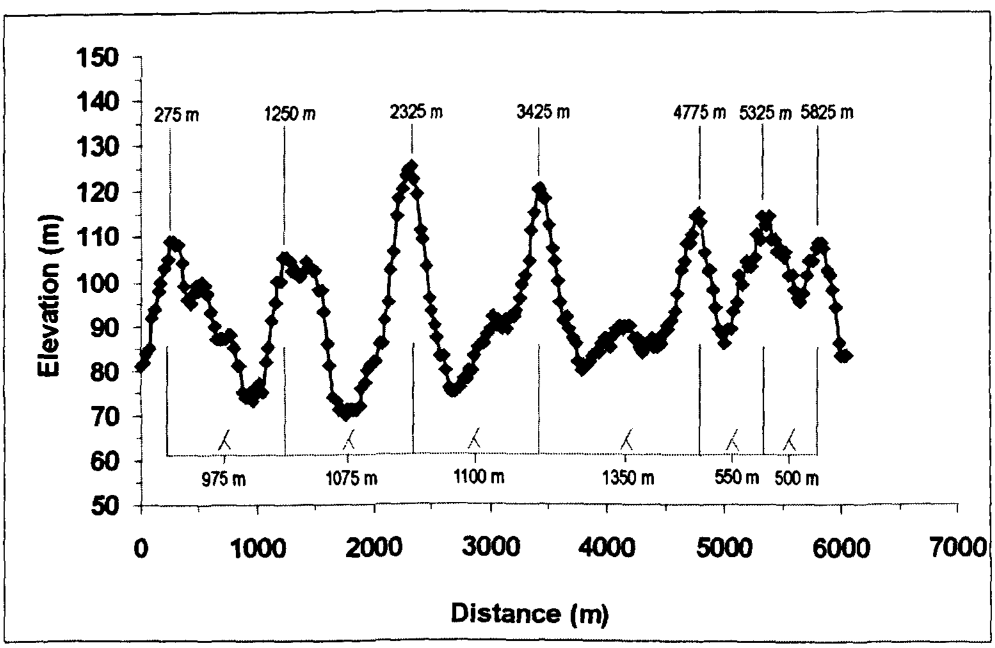

Figure 4.12. A working example of the manual wavelength measurement technique used on the DEM. The distance that each ridge crest is located along the transect is shown above each peak. The wavelength is calculated by taking the difference between each of these values. In this example, the calculated wavelengths are shown beneath the graph.

4.3.6. Satellite imagery

To map and obtain wavelength information from ribbed moraine areas in Québec, Canada, two satellite images were acquired. The first was a Landsat MSS image, which covered the Lac Naococane region of Central Québec. The second image acquired, was a single band Panchromatic Landsat ETM+ image of the River Kaniapiskau region, which is situated just south of Ungava Bay in Northern Québec. The location of both study areas is shown in Figure 4.13. Each image was displayed and manipulated using ERDAS Imagine 8.5. Any ribbed moraine ridges that were identified were digitised on screen by drawing a line along the crest of the ridge and the data were stored as Arc coverages. When mapping was completed, approximately 12,800 ribbed moraine ridges were recorded in the Lac Naococane region, and in the Kaniapiskau area, approximately 12,000 were mapped. In order to sample the wavelength of these ribbed moraine ridges, transects were digitised across each ribbed moraine field in the manner specified in Section 4.3.3. The wavelength data were obtained using a mathematical procedure known as spectral analysis. The rational for choosing this method and the procedures followed for conduction spectral analysis is outlined in the following sections.

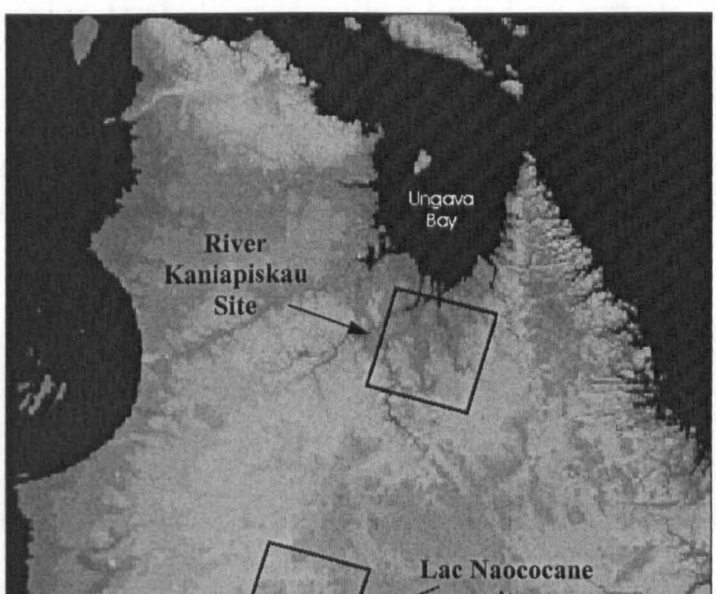

Figure 4.13. Map showing the location of the two study sites in Québec. The boxes show the coverage of the satellite imagery used to map the ribbed moraine ridges in both localities.

4.3.6.1. Spectral analysis; the rational

As was stated earlier in Section 4.3.2 large sample sizes were a requirement for this thesis. However, due to the volume of data that was generated by mapping areas at this scale, it was clear that measuring the wavelength manually would be too time-consuming. Alternatively, it was found that by using the reflective properties of an image, a mathematical technique known as spectral analysis could be used to obtain the wavelength automatically. When a satellite image is viewed, it is possible to identify landforms such as ribbed moraine from other features on the surface because they have different spectral characteristics than the surrounding area. In other words, they reflect light differently from the other objects in the vicinity. It is possible to see this variation in reflectance by taking a transect across a portion of an image. Figure 4.14, shows a reflectance profile obtained from a series of ribbed moraine ridges sampled from a Landsat ETM+ image.

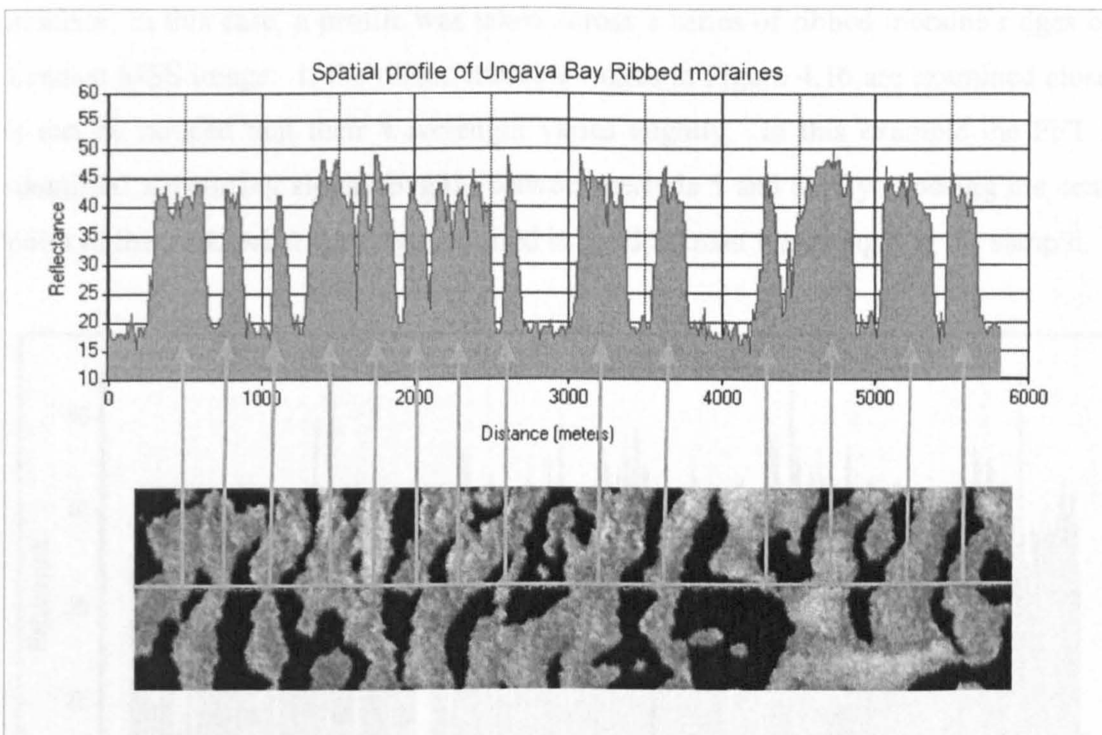

Figure 4.14. Demonstration that a spatial series of reflectance (i.e. a transect) taken across an image reliably records ribbed moraine. Note how in this case that peaks correspond to the ribbed moraine ridges. The transect was taken across a Landsat ETM+ image using the panchromatic band.

In this case, the ridges have higher reflectance values compared to the water between each ridge, and large peaks on the graph indicate their presence. As the connecting arrows indicate, the transect of reflectance values has the ability to record ribbed moraine ridges accurately. By taking transects in this manner the reflectance data is being viewed in the spatial domain, and although this is useful in that it shows the wavelength of the ribbed moraine ridges, it would be time consuming trying to decipher each ribbed moraine wavelength visually from the graph. This would be particularly true if very long transects were taken across an image (Fig. 4.15). However, by using a mathematical algorithm called the Fast Fourier Transform (FFT), spectral analysis makes the signal more meaningful by producing the frequency domain signal from the spatial domain signal. The FFT does this by assuming the spatial domain signal is composed of sinusoids of various frequencies. The algorithm computes the amplitude and wavelength of these sinusoids and the result is plotted as magnitude versus frequency. The resulting periodogram displays a frequency spectrum showing all the frequency components (spectral components) of the series. From this, it is possible to determine the wavelength of ribbed moraine ridges in the series and also the most dominant wavelength in the series. Figure 4.16 is an example of spectral analysis in practice. In this case, a profile was taken across a series of ribbed moraine ridges on a Landsat MSS image. If the ribbed moraine ridges in Figure 4.16 are examined closely, it can be noticed that their wavelength varies slightly. In this example the FFT has identified a recurring signal roughly between periods 5 and 8. By choosing the central point of the peak, what is being measured is the dominant wavelength in the sample.

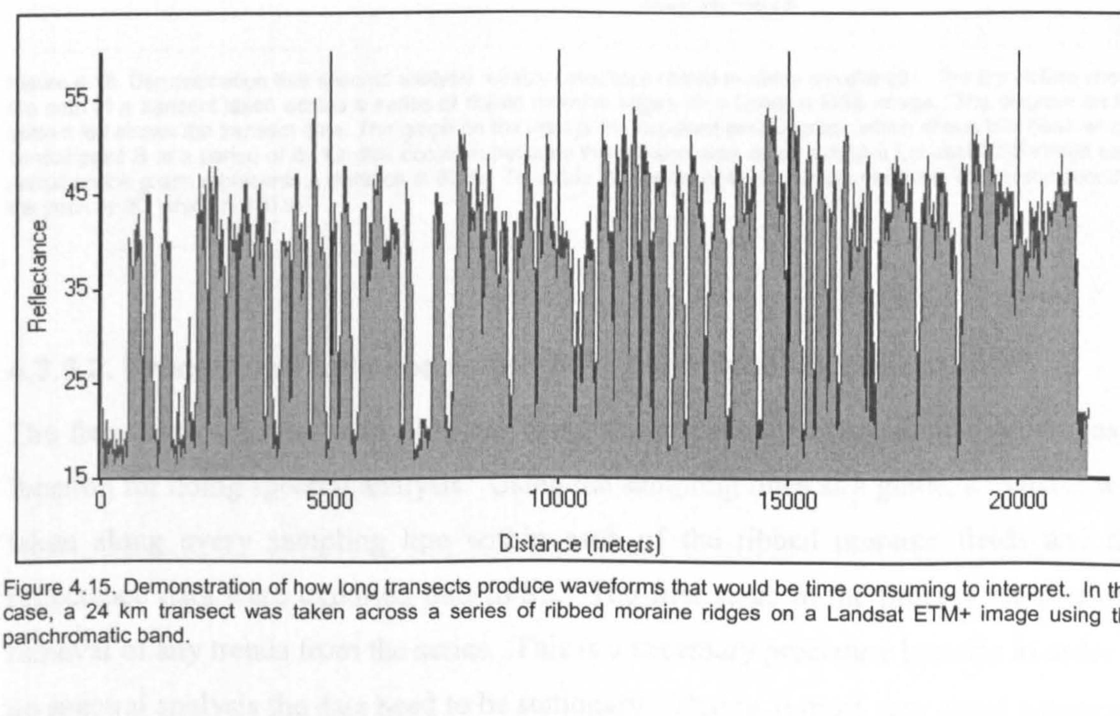

Figure 4.15. Demonstration of how long transects produce waveforms that would be time consuming to interpret. In this case, a 24 km transect was taken across a series of ribbed moraine ridges on a Landsat ETM+ image using the panchromatic band.

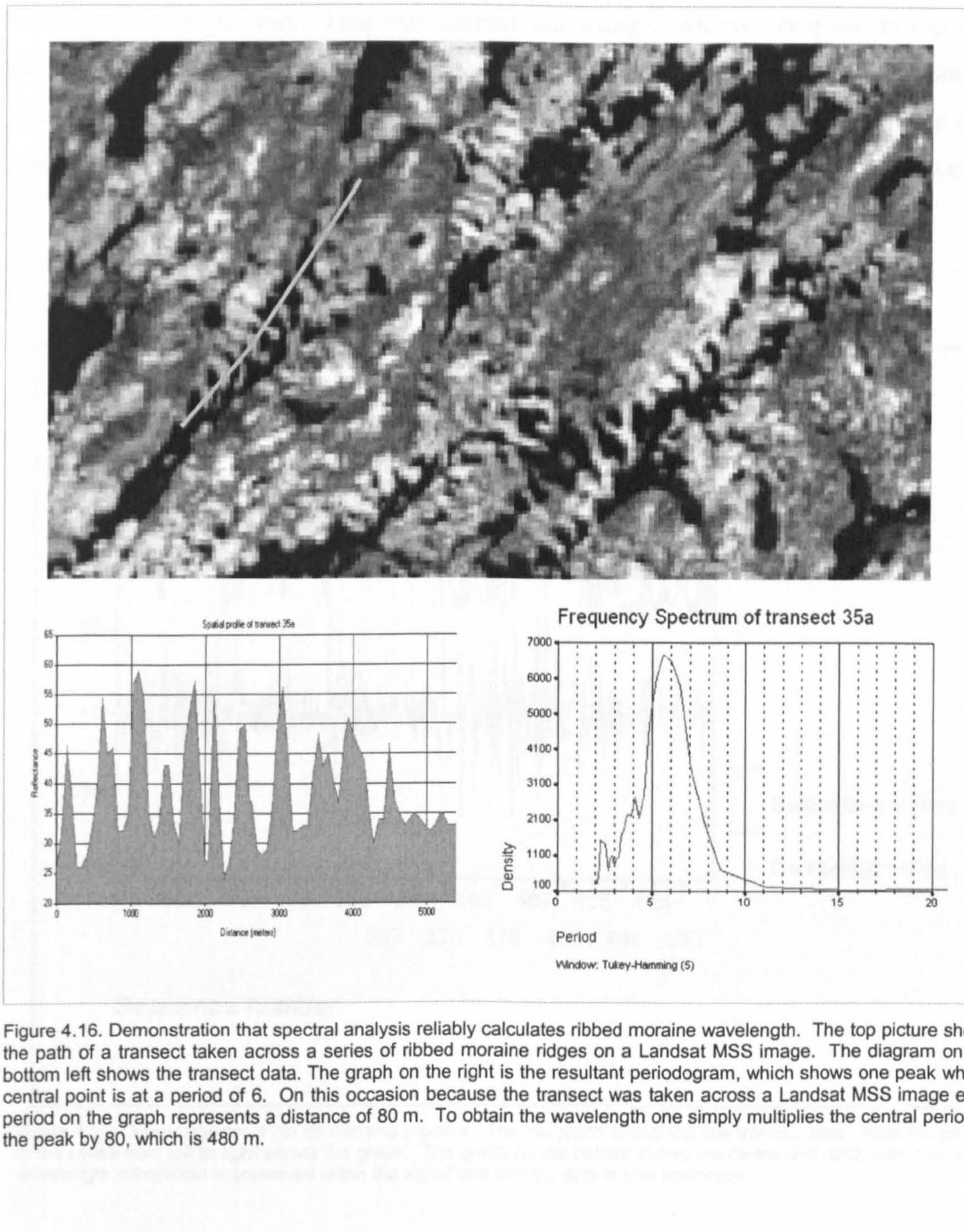

Figure 4.16. Demonstration that spectral analysis reliably calculates ribbed moraine wavelength. The top picture shows the path of a transect taken across a series of ribbed moraine ridges on a Landsat MSS image. The diagram on the bottom left shows the transect data. The graph on the right is the resultant periodogram, which shows one peak whose central point is at a period of 6. On this occasion because the transect was taken across a Landsat MSS image each period on the graph represents a distance of 80 m. To obtain the wavelength one simply multiplies the central period of the peak by 80, which is 480 m.

4.3.6.2. Procedures followed to produce the frequency spectrum

The frequency spectrum was obtained using the statistics package SPSS, which has a function for doing spectral analysis. Using the sampling lines as a guide, a transect was taken along every sampling line within each of the ribbed moraine fields and the reflectance data were exported into SPSS. The first stage in the process required the removal of any trends from the series. This is a necessary procedure because in order to do spectral analysis the data need to be stationary. That is, it must vary about a constant value i.e. a straight line. This was carried out using a widely accepted de-trending process called a difference transformation on the pixel value column, which created a new spatial series by calculating the difference between successive values in the data series. As is shown in Figure 4.17, the data now varies along a straight line; however, the important wavelength information is still preserved within the signal.

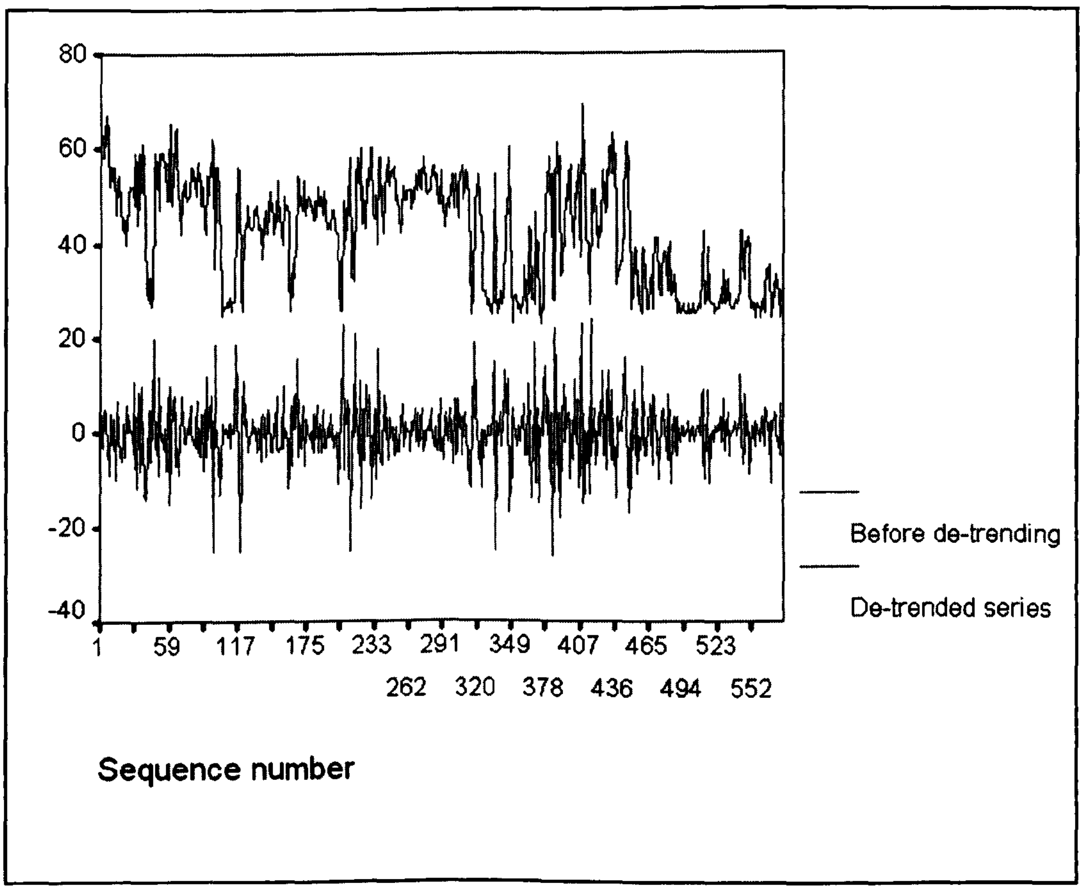

Figure 4.17. Demonstration of the de-trending process. The top graph shows the raw transect data. Note the trend in the series from left to right across the graph. The graph on the bottom shows the de-trended data, note how the wavelength information is preserved within the signal and that the data is now stationary.

The final stage was to perform the FFT on the de-trended series to produce a periodogram, which would display the frequency spectrum. In SPSS this in done by choosing the option to create a Spectral Plot, which allows the user to specify how the frequency spectrum is plotted. In SPSS there are two methods of plotting the frequency spectrum. The user can choose between either a periodogram, which is an unsmoothed plot of spectral amplitude, or a spectral density plot, which is a periodogram that has been smoothed to remove irregular variation from the spectrum. By smoothing a periodogram, the signal is made less noisy and is therefore easier to interpret, and for this reason all the data were plotted as spectral density plots. The process of smoothing requires a spectral window to be selected. This simply specifies the manner in which the periodogram will be smoothed to obtain the spectral density plot. In SPSS the user is given five spectral windows to choose from and after experimenting with all five, it was decided that the Tukey-Hamming window would be chosen as it produced the clearest peaks.

4.3.6.3. Interpretation of the frequency spectrum

In the example shown in Figure 4.16 the frequency spectrum was very easy to interpret as only one peak was obtained. This was expected, because all the ribbed moraine ridges had a similar wavelength. However, when it came to sampling larger ribbed moraine fields the spectral density plots were more complex (Fig. 4.18). This happens because long transects are more likely to cross regions where there is a mixture of ribbed moraine wavelengths, which meant a range of frequencies would be shown on the plot. In addition to this, because spectral analysis will search for any recurring periodicities in a spatial series, it will not discriminate between ribbed moraine and other features that have a recurring periodicity. For example, the frequency of large-scale topographic features such as undulating terrain on which the ribbed moraine is superimposed will also be identified. Because of this, it was important to have a robust method of discerning between peaks that reflected ribbed moraine wavelength and peaks that did not. A straightforward method of filtering out any large-scale spectral signals was to simply plot the period axis to show wavelengths of only a few kilometres. This was appropriate, because it is the typical ribbed moraine wavelength scale. Peaks at longer periods are caused by some other phenomenon and were of no interest for estimating ribbed moraine wavelength.

The final stage was to determine which of the remaining peaks were ribbed moraine signals. As Figure 4.19 shows, there are several prominent peaks at periods of 7.5, 10 and 15, which correspond to wavelengths of 600 m, 800 m and 1200 m respectively. There is also a series of smaller peaks between periods 2 and 6. The most effective method for selecting appropriate peaks was to first calculate the wavelength for each of the peaks and then go back to the image and check whether there were ribbed moraine

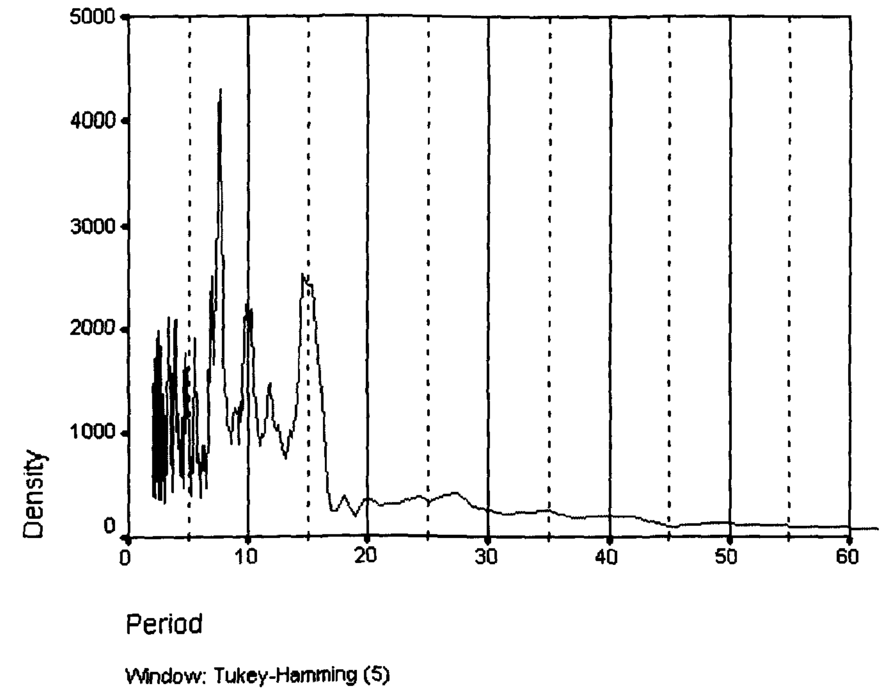

Figure 4.18. A spectral density plot of a transect that was taken across ribbed moraine terrain on an MSS image in the Lac Naococane region of Québec. In this case the transect was 53 km in length and crossed several series of ribbed moraine fields of different wavelengths, resulting in a plot more complex than the one shown in Figure 4.16.

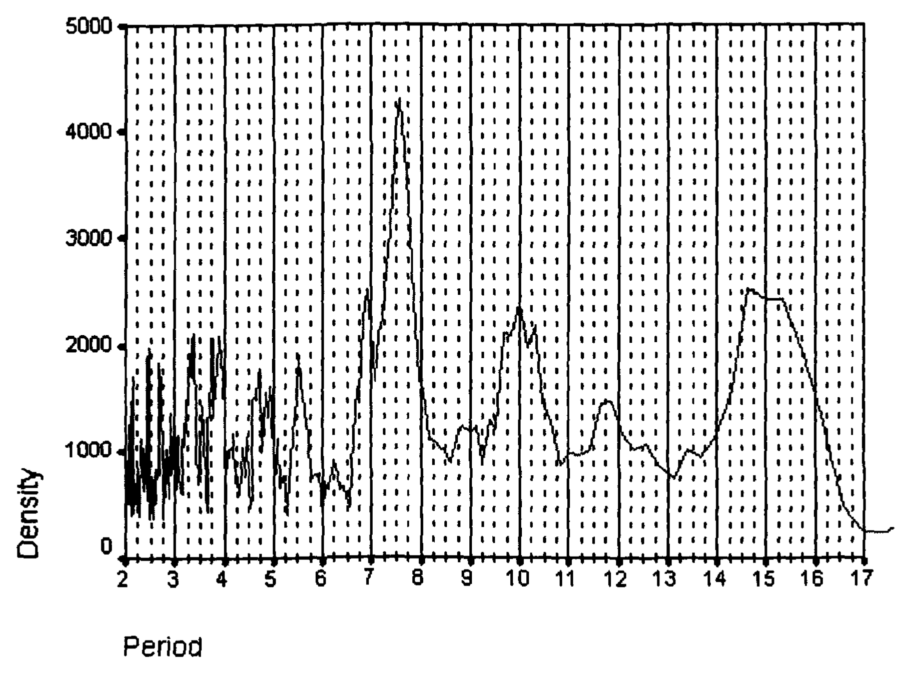

Figure 4.19. This is the same density plot shown in Figure 4.18, the only difference being the large scale spectral signals have been excluded. Note how it is much easier to interpret the peaks. In this case, several prominent peaks occur at periods of 7.5, 10, 15, and a series of smaller peaks occur between periods 2 to 6.

ridges of that wavelength along the transect. This was done easily in ERDAS Imagine using the Measurement Tool, which is a feature used for making measurements across an image. Using this tool, it was possible to take accurate measurements of ribbed moraine wavelength manually from the image, which could then be compared to the wavelengths predicted by the spectral analysis. The peaks that corresponded to the manual measurements were accepted and the rest were rejected. In Figure 4.19 the peaks that occurred between periods 2 to 6 were all rejected, as no ribbed moraine ridges were found along the transect at this scale. Consistently checking the data in this manner helped reduce the amount of errors in the data set. The results of the Québec wavelength measurements are discussed in Chapter 5 and 6.

4.4. Summary

The use of remote sensing in this study provided an effective method of mapping ribbed moraine ridges from various locations. The imagery used in this thesis was particularly advantageous because its wide spatial coverage allowed large areas of ribbed moraine to be mapped accurately. This in turn ensured the study captured a large sample of ribbed moraine ridges, which was necessary to ensure the data would be representative. The Landsat MSS imagery proved adequate for mapping ribbed moraine terrain, however its relatively low spatial resolution meant it could not capture very small scale ribbed moraine ridges. This was overcome by using Landsat ETM+ imagery in conjunction with the aerial photographs and the DEM, and ensured the study captured the true scale range of ribbed moraine.

The various types of imagery used in this thesis meant a variety of methods were needed to extract the ribbed moraine wavelength measurements. Measuring wavelength from the map produced from aerial photographs and from transect data taken from the DEM, proved relatively straightforward and the manual methods used provided accurate measurements. Mapping ribbed moraine landscapes using satellite imagery generated large amounts of data and it was clear that measuring the wavelength manually would be too time-consuming. Instead, spectral analysis was used as it provided a fast and more objective method of obtaining the wavelength information from digital satellite imagery.

The following four chapters investigate the characteristics of ribbed moraine in the four chosen areas and report the results of the wavelength data obtained using the methodology outlined above.

Chapter 5: The Characteristics of Ribbed Moraine in the Lac Naococane Region, Central Québec

5.1. The study site

Lac Naococane is a large lake in central Québec situated at latitude 52° 50 N and Longitude 70° 40 W. The lake itself and surrounding landscape are covered liberally with large tracts of ribbed moraine, which made it a good area to choose as a study site (Fig. 5.1).

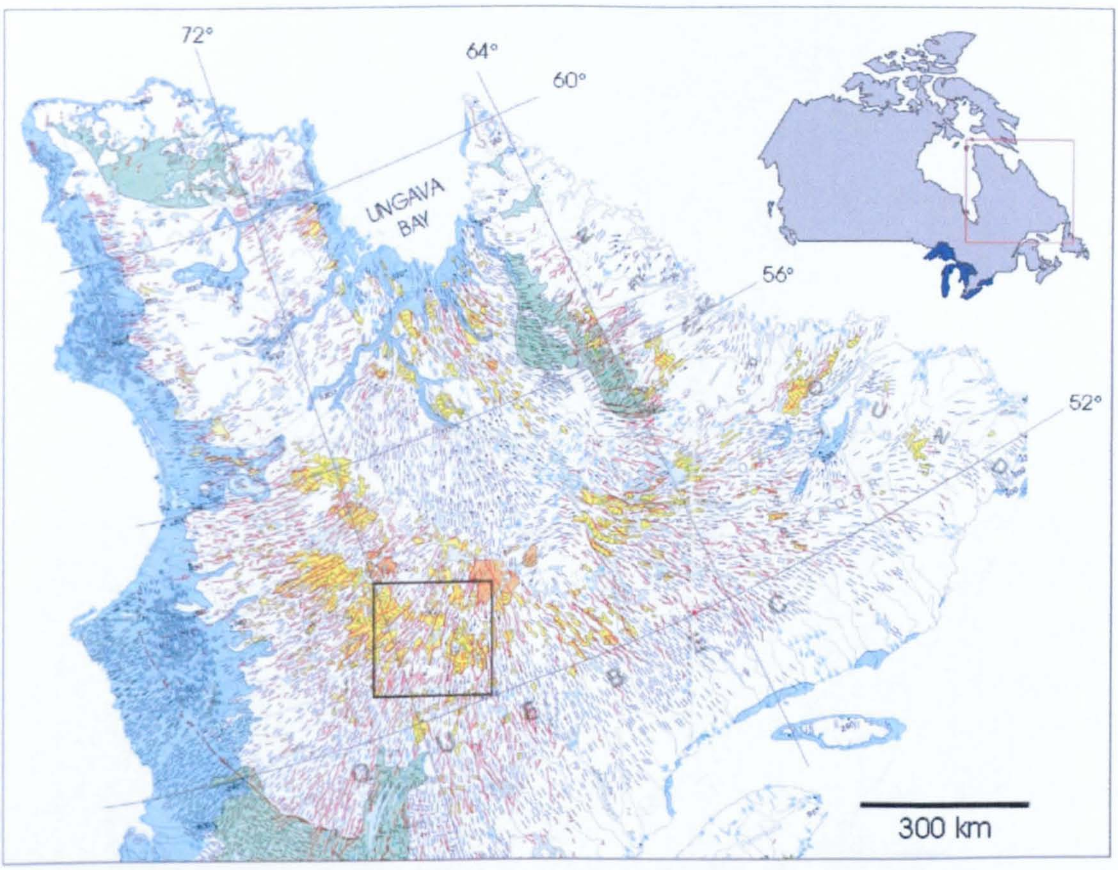

Figure 5.1. Location map showing the study site at Lac Naococane. The box indicates the coverage of the Landsat MSS and ASTER imagery used to study the ribbed moraine in this region. The figure is adapted from the Glacial Map of Canada (Prest *et al.*, 1968) where areas of ribbed moraine are marked as yellow patches.

Figure 5.2 shows the estimated position of the Nouveau- Québec Ice Divide during the last glaciation. The study site is marked on the map and is located approximately 150 to 250 km south of the main Nouveau-Québec Ice Divide around an area defined as the Caniapiscau Divide.

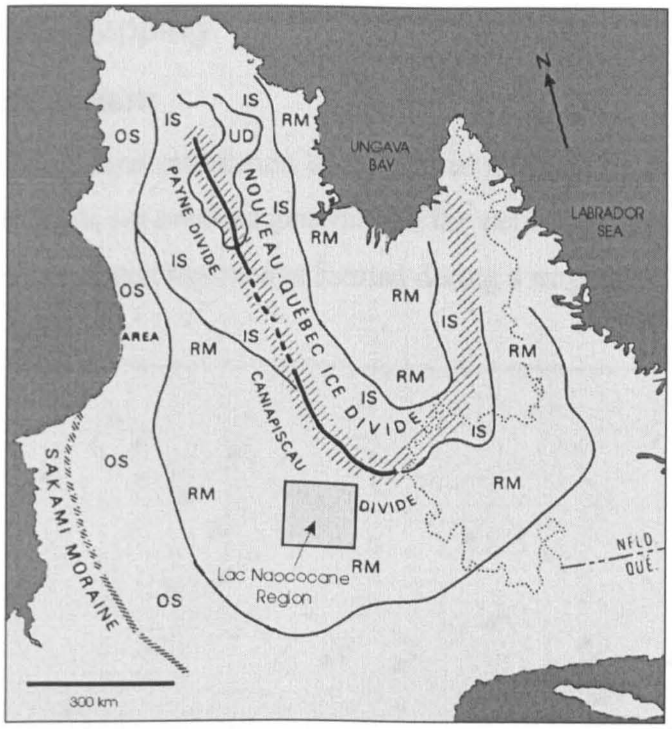

Figure 5.2. The position of the Nouveau-Québec Ice Divide adapted from Bouchard (1989). The Lac Naococane study site can be seen on the map marked by a box. The centre of the region is located approximately 150 km south of the main divide.

5.2. Data sources and methodology

To map and study the ribbed moraine ridges in the Lac Naococane region, one digital Landsat MSS scene (80 m, 185 × 185 km) and several Advanced Spaceborne Thermal Emission and Reflectance Radiometer (ASTER) scenes (15 m, 60 × 60 km) were acquired and geocoded. To obtain an indication of the general topography of the study site a 30-arc second (ca 0.5-1 km) Digital Elevation Model (DEM) was obtained. This allowed visualisation of the general topography of the study site and was used to investigate relationships between topography and ribbed moraine distribution in the region. To carry out detailed topographical analysis, ten 30 m resolution ASTER DEMs were acquired. All the ribbed moraine ridges that could be identified from the imagery were mapped. This was accomplished by visual interpretation of the landforms and on-screen digitising directly into Erdas Imagine (see Section 4.3.6). Once mapped, the wavelength of the ribbed moraine ridges at Lac Naococane was determined using spectral analysis following the procedures outlined in Chapter 4 (see Sections 4.3.6.1 to 4.3.6.3). The following sections reports on the results of the mapping and morphometric analysis of the landforms.

5.3. Results from mapping

5.3.1. Large-scale pattern

Figure 5.3 shows the general orientation of the ribbed moraine fields across the region. The fact that all the fields are oriented generally in the same direction, strongly indicates that the ribbed moraine in this region was formed during a single ice flow event.

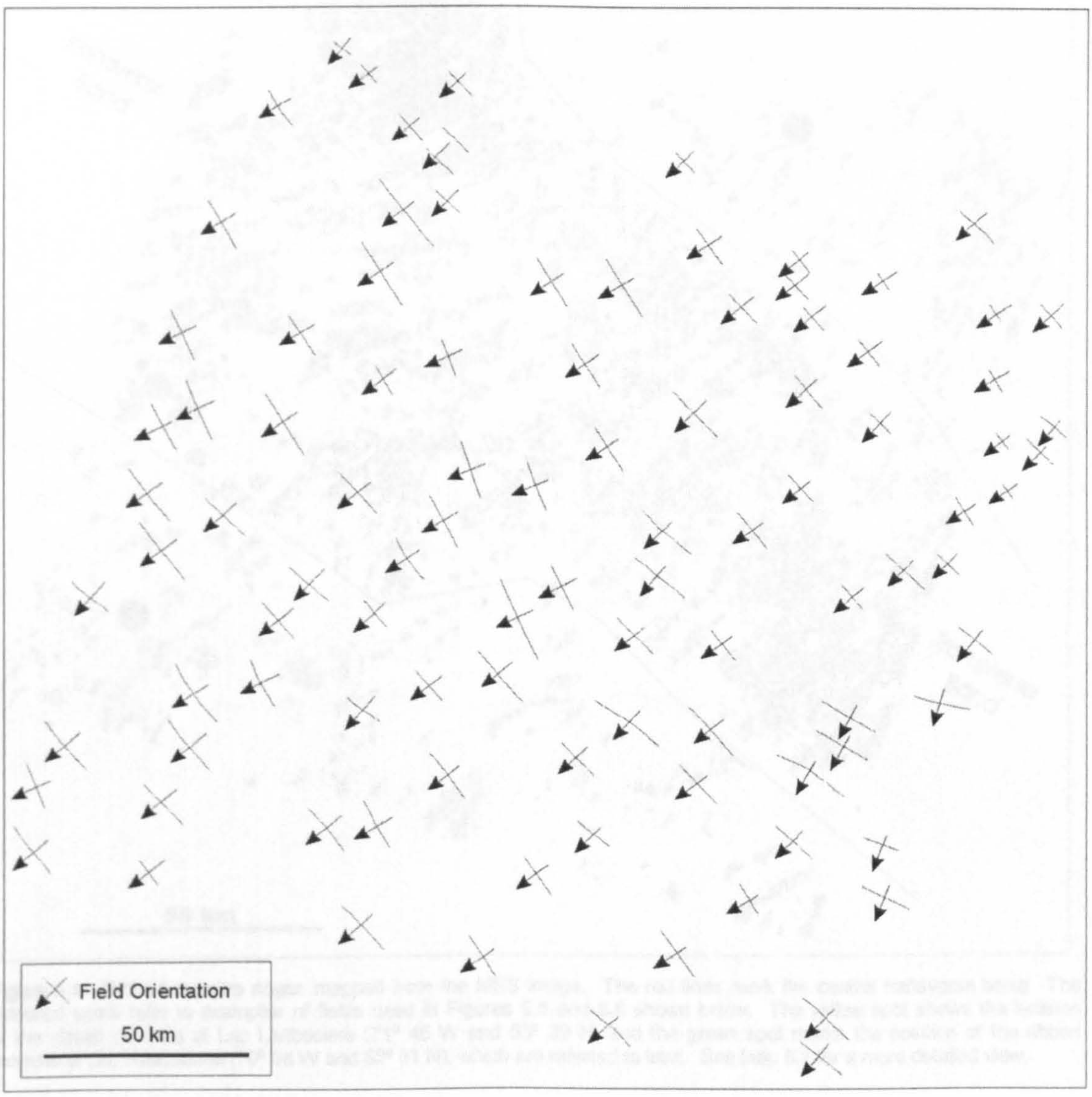

Figure 5.3. Orientation of ribbed moraine fields in relation to the regional ice flow pattern. The lines shows the general orientation the ribbed moraine ridges of each field and the arrows the related ice flow direction. Note the conformity of field orientation across the region, which strongly indicates that the ribbed moraine in this region was formed during the same ice flow event.

In total, 12851 ribbed moraine ridges were mapped from the MSS image and the resulting ARC coverage is shown in Figure 5.4 and Map 5.1. The most obvious pattern is a large swathe of ribbed moraine concentrated in a broad transverse band across the centre of the study site. The band measures approximately 200 km from east to west and is generally between 80 km to 100 km wide in a downstream direction (Fig. 5.4).

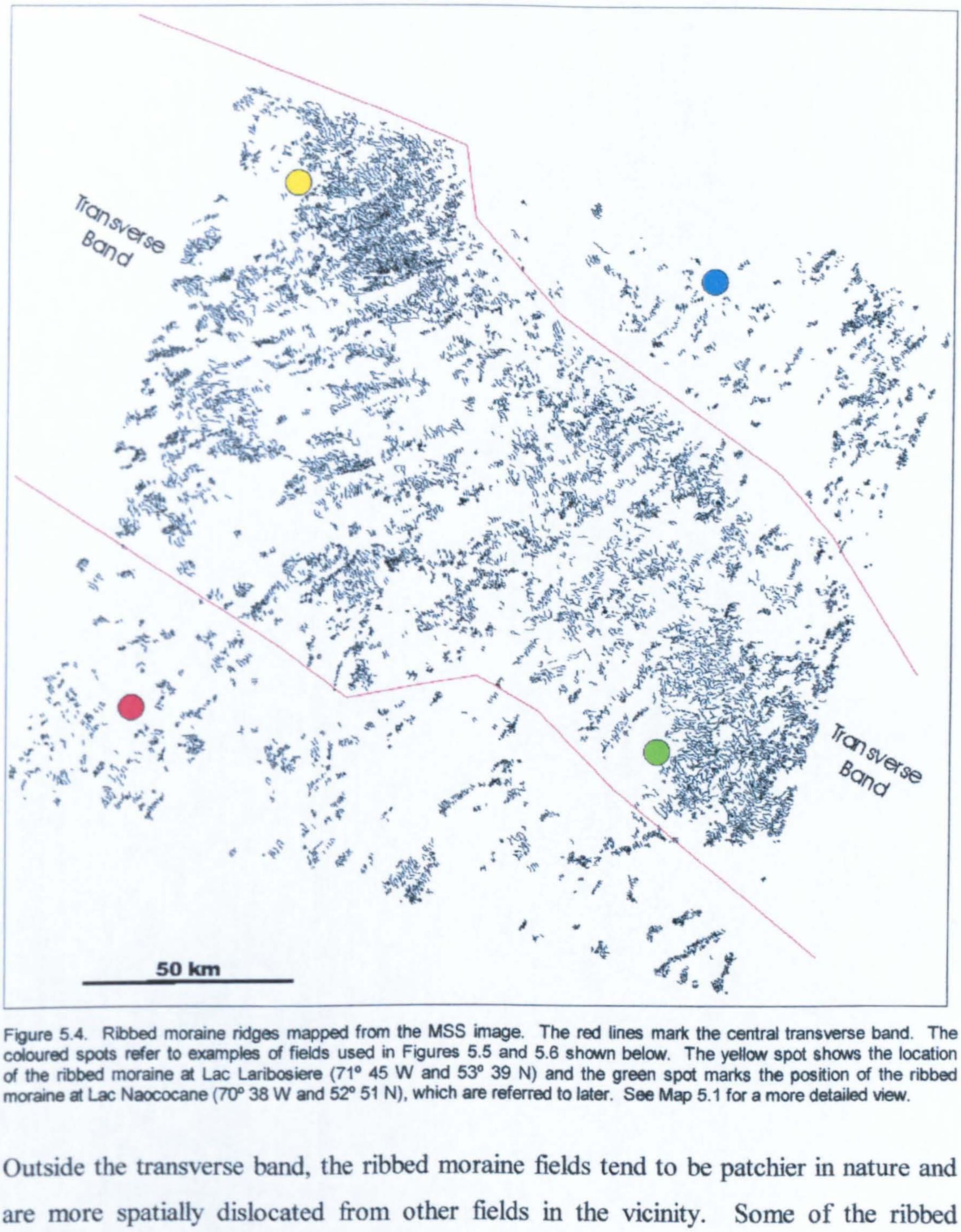

Figure 5.4. Ribbed moraine ridges mapped from the MSS image. The red lines mark the central transverse band. The coloured spots refer to examples of fields used in Figures 5.5 and 5.6 shown below. The yellow spot shows the location of the ribbed moraine at Lac Laribosiere (71° 45 W and 53° 39 N) and the green spot marks the position of the ribbed moraine at Lac Naococane (70° 38 W and 52° 51 N), which are referred to later. See Map 5.1 for a more detailed view.

Outside the transverse band, the ribbed moraine fields tend to be patchier in nature and are more spatially dislocated from other fields in the vicinity. Some of the ribbed moraine fields within the transverse band are quite large and the two biggest fields are marked by the yellow and green spots in Figure 5.4. Both these fields are shown in greater detail in Figure 5.5.

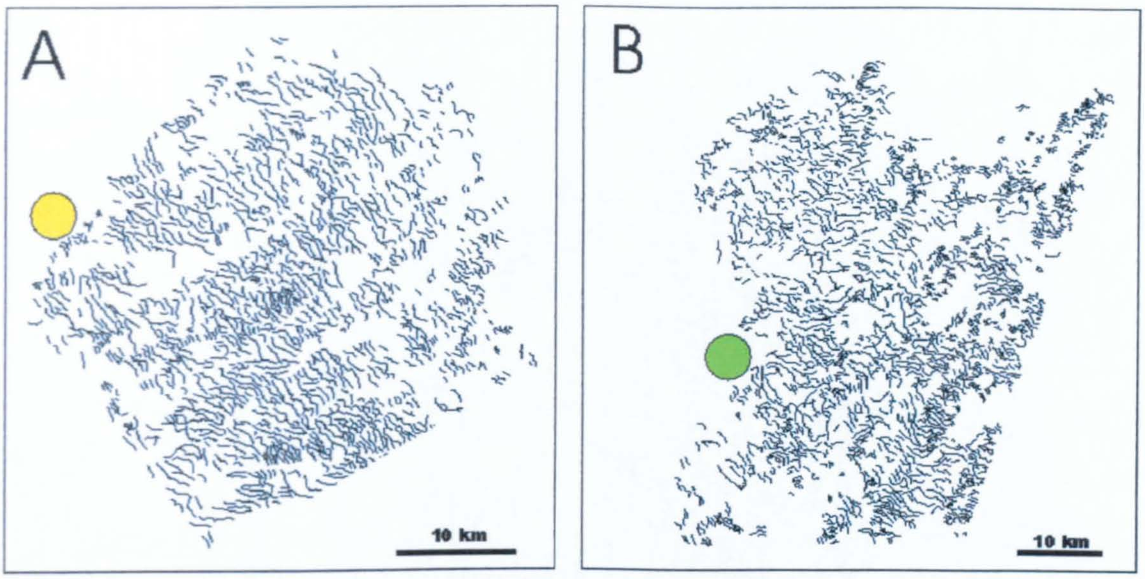

Figure 5.5. Two large ribbed moraine fields located within the transverse band. Figure 5.5a shows a larger ribbed moraine field at Lac Laribosiere. Figure 5.5b shows the ribbed moraine at Lac Naococane.

Figure 5.5a illustrates a large field of uninterrupted ribbed moraine just north of Lac Laribosiere and measures approximately 36 km long and 33 km wide. The field in Figure 5.5b shows the ribbed moraine mapped at Lac Naococane itself and is slightly larger than the field shown in Figure 5.5a. At its widest point, this field measures 45 km and is 53 km in length. Generally, the ribbed moraine fields outside the band to the north east and south west, tend to be much smaller when compared to those that make up the central band. Figure 5.6a and 5.6b show some examples of these smaller ribbed moraine fields whose locations in the study site are marked by the red and blue spots in Figure 5.4.

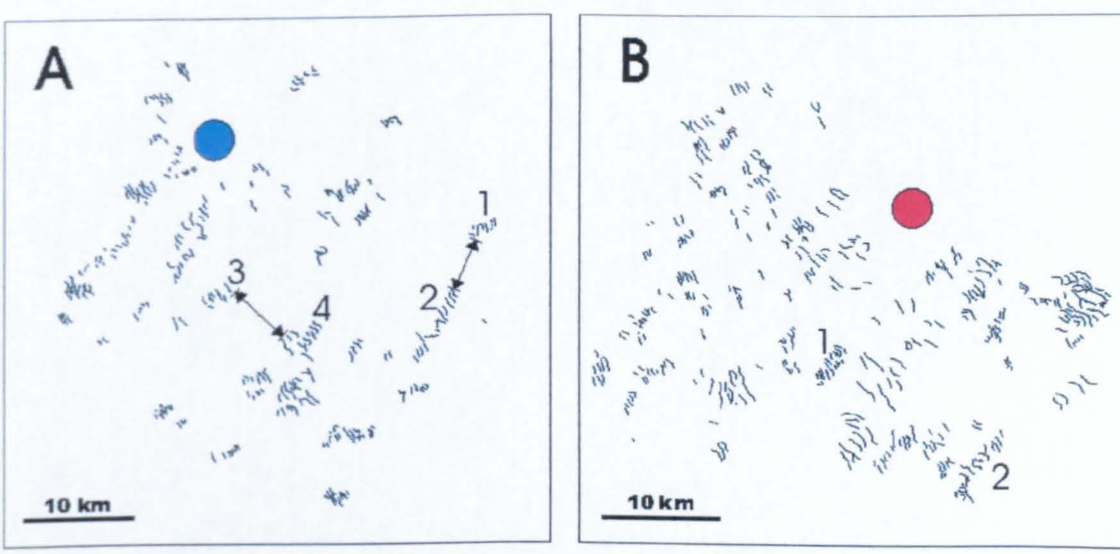

Figure 5.6. The characteristics of the ribbed moraine fields located outside the transverse band. Note how the fields are smaller and more spread out in nature.

Figure 5.6a shows the spatial distribution of the ribbed moraine marked by the blue spot. The fields marked 1 to 4 give an impression of their scale, which range between 2.5 to 7 km in length and 800 m to 1.5 km wide. As Figure 5.6a demonstrates, the fields are also more spatially dislocated than those located within the central band. This is true of both downstream and lateral spacing and in some cases, the fields are separated over quite large distances. For example, the distance downstream between fields 1 and 2 is 5 km, and the lateral separation between the fields marked 3 and 4 is 6 km. The ribbed moraine fields shown in Figure 5.6b are located in the region marked by the orange spot in Figure 5.4. These fields have similar properties as those shown in Figure 5.6a. Their field dimensions are fairly similar and their spatial distribution is also quite patchy. For example, field number 1 is 4 km long and 1.3 km wide and field number 2 is 7.1 km in length and 1.4 km wide.

If the distributional pattern of ribbed moraine in the area is viewed in closer detail it is possible to place the fields into the following general categories:

1. Elongate ribbons and narrow tracks
2. Clusters
3. Isolated fields.

5.3.2. Elongate ribbons and narrow tracks

Figure 5.7 shows some examples of large ribbon like ribbed moraine fields that run across the study area. As is shown, these ribbons exist at several scales across the region and range from extremely long ribbons marked at position B, C and D which are all between 40 km and 45 km in length to relatively small ribbons measuring between 12 km the 18 km in length (fields E, F and G). The ribbed moraine ribbons also vary considerably in width. In the examples shown here, the widest ribbons, A and B, measure 7 km, whilst the thinnest field, F is only 700 m wide.

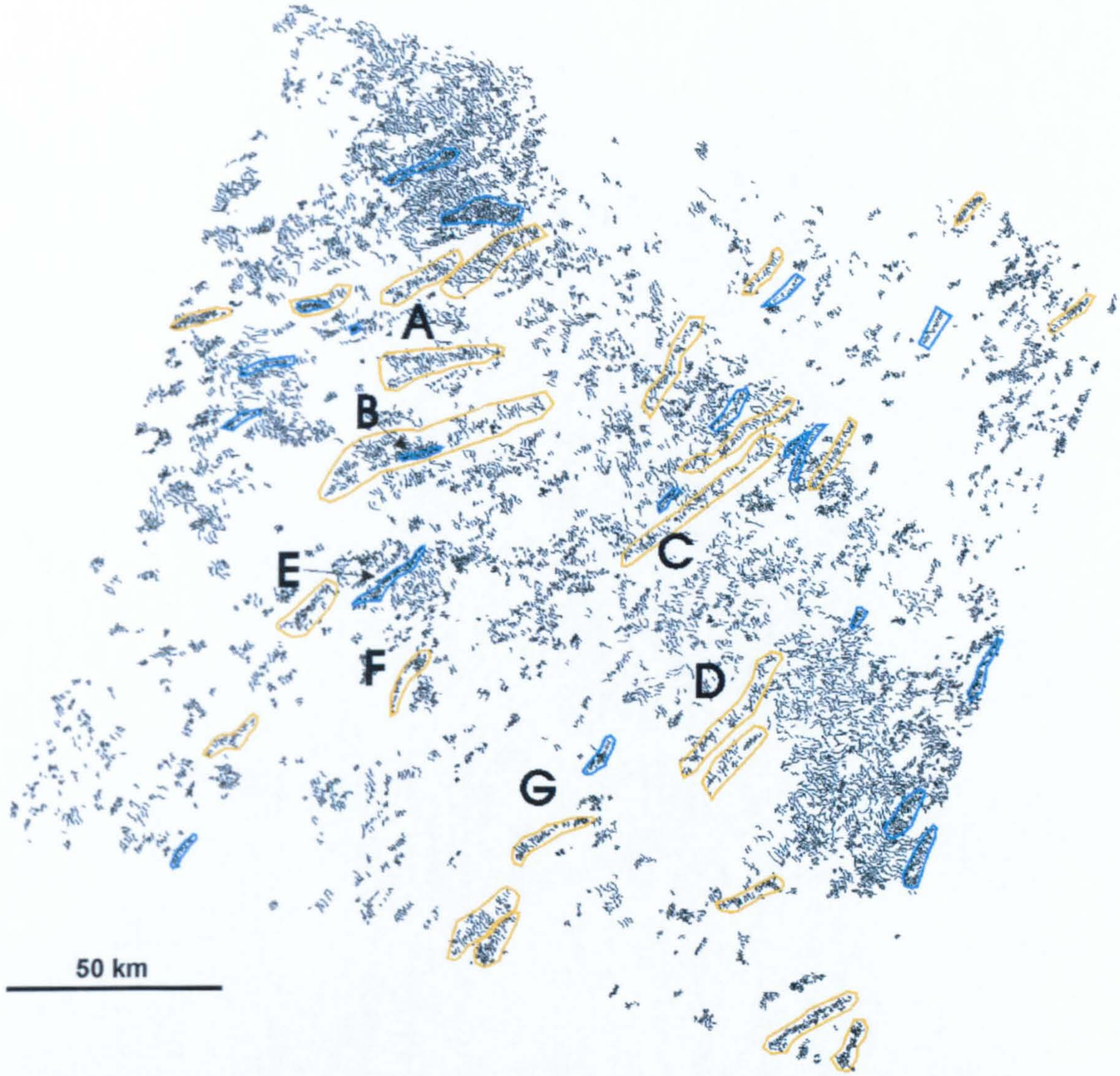

Figure 5.7. Showing examples of ribbons and tracks of ribbed moraine in the study area. Ribbons are bounded by a yellow perimeter and the narrow tracks are enclosed in blue.

As well as there being relatively independent ribbed moraine ribbons in the region it is also possible to identify very narrow tracks of ribbed moraine which run through the study site. A defining feature of the ribbed moraine ridges that make up these tracks is their size and spacing. They tend to be more closely spaced and are much smaller than the ribbed moraine ridges that surround them. Figure 5.8 shows two examples of this type of field, which are marked by the arrows at point B and E in Figure 5.7. The ribbed moraine track at location B is at the edge of a large ribbon 47 km in length. The average wavelength of the ribbed moraine ridges inside the blue perimeter is 307 m, whilst the surrounding ridges have an average wavelength of 467 m. This is an interesting observation because it indicates that the ribbed moraine forming process is capable of producing ridges at different scales in close proximity.

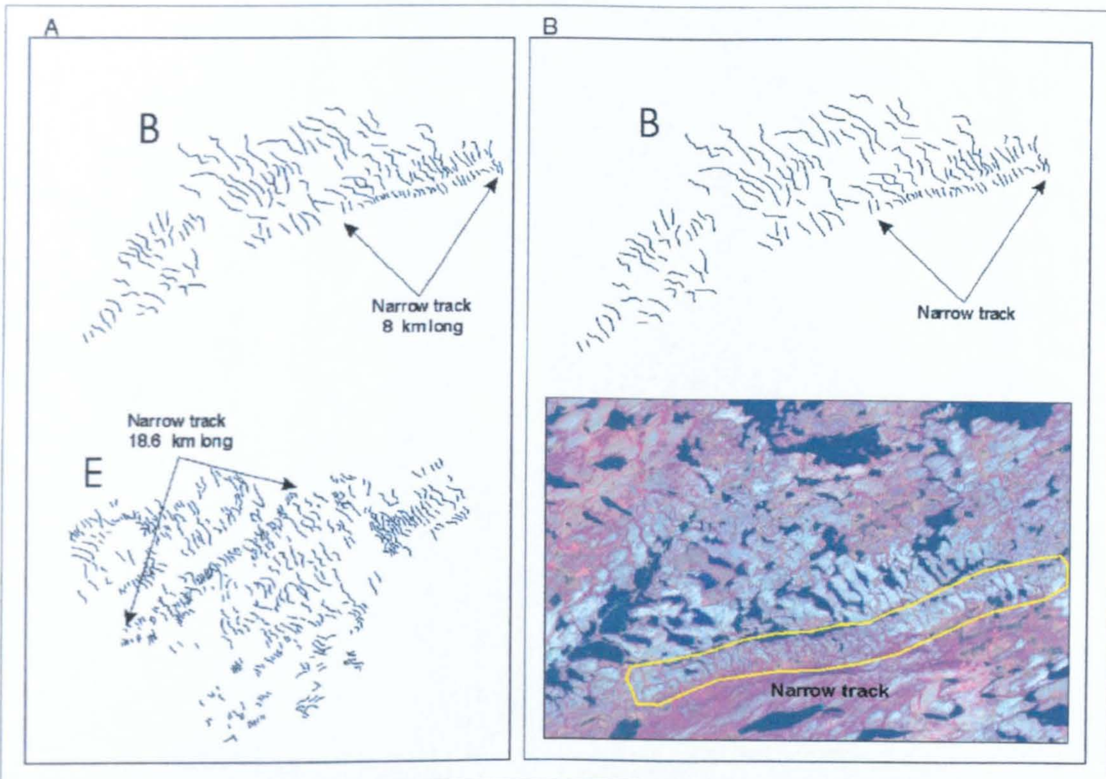

Figure 5.8. Two examples of ribbed moraine tracks in the Lac Naococane region. The track at the top of Figure 5.8a is situated on the outside of a ribbon type field shown in greater detail in Figure 5.8b. The picture is taken from an ASTER satellite image and the track is enclosed by a yellow boundary. Note how the ribbed moraine ridges of the track are much smaller in scale and are more closely spaced compared to the adjacent ridges. The track at the bottom of Figure 5.8a is an example of a narrow track running through a cluster of larger scale ribbed moraine.

5.3.3. Clusters

Another pattern that emerged is that the ribbed moraine in the area also tended to form in large clusters. These clusters are either highly concentrated, whereby the ribbed moraine ridges are densely packed together within the bounds of the cluster or are more dispersed in nature and form a less coherent group of fields. Figure 5.9 shows examples of both types of ribbed moraine cluster. It can be seen that the most densely packed clusters occur within the transverse band. The largest and most coherent of these are located at Lac Naococane (marked green) and at Lac Laribosiere (marked yellow). In both of these places, the ribbed moraine ridges are more or less uninterrupted and are very densely packed compared to other areas across the region. It is possible to find other clusters with ribbed moraine ridges as densely crowded as the aforementioned fields, however, they tend to be of a much smaller spatial extent. For example, the cluster marked by the blue spot is an assemblage of ribbed moraine ridges with similar spacing as those found at Lac Naococane and Lac Laribosiere. This cluster however is much smaller with an area of only 60 km^2 compared to that of Lac Naococane, which is 230 km^2. The two fields marked by the red and black spots are an example of clusters where the ribbed moraine ridges are not so highly concentrated. In both of these examples, there are large gaps of several kilometres between each ribbed moraine field, which gives the cluster a more patchy appearance. The very loose scattering of ribbed moraine ridges in the bottom left hand corner of Figure 5.9 (marked by the orange spot) is an example of this type of dispersed cluster. In this instance, the cluster is composed of loose sequences of ridges that are interspersed with large spaces, these are broken only by the occurrence of one or two isolated ribbed moraine ridges.

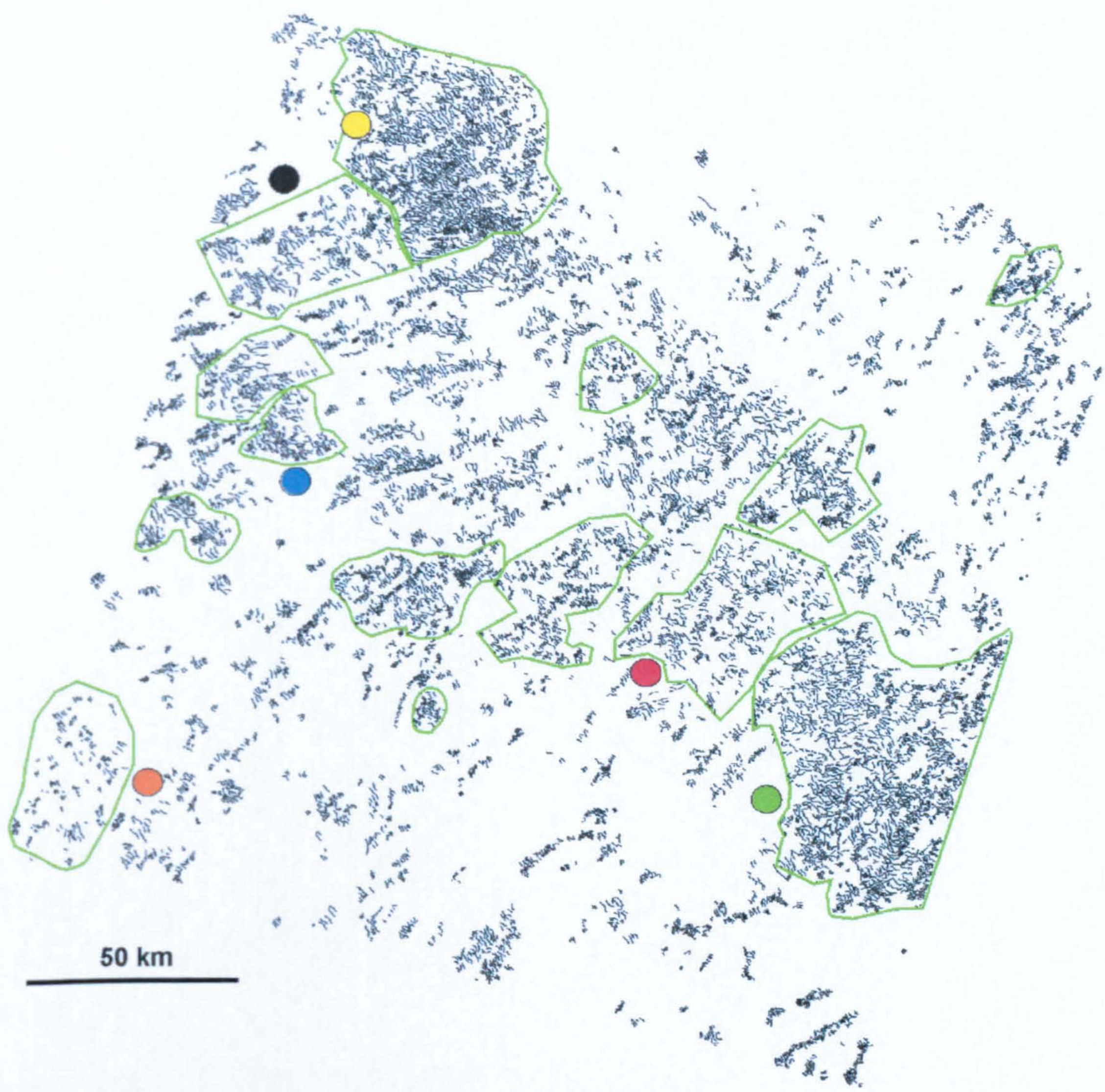

Figure 5.9. Some examples of cluster type ribbed moraine field of various scales.

5.3.4. Isolated fields

Elsewhere across the region the landscape is dotted with a smattering of small isolated fields that fill in the gaps (Fig. 5.10). These fields are much smaller than those described above and contain fewer ribbed moraine ridges. For example, all the fields enclosed in red in Figure 5.10, range between, 1.5 km to 7 km in length. It can be noticed that the majority of these fields tend to have been formed north and south of the transverse band, however it is possible to identify fields within the band itself that are comparatively independent of other ribbed moraine fields. The field marked by the red spot in Figure 5.10 is such an example. In this case the fields nearest neighbours are over 3 km either side of it and 7 km to the south.

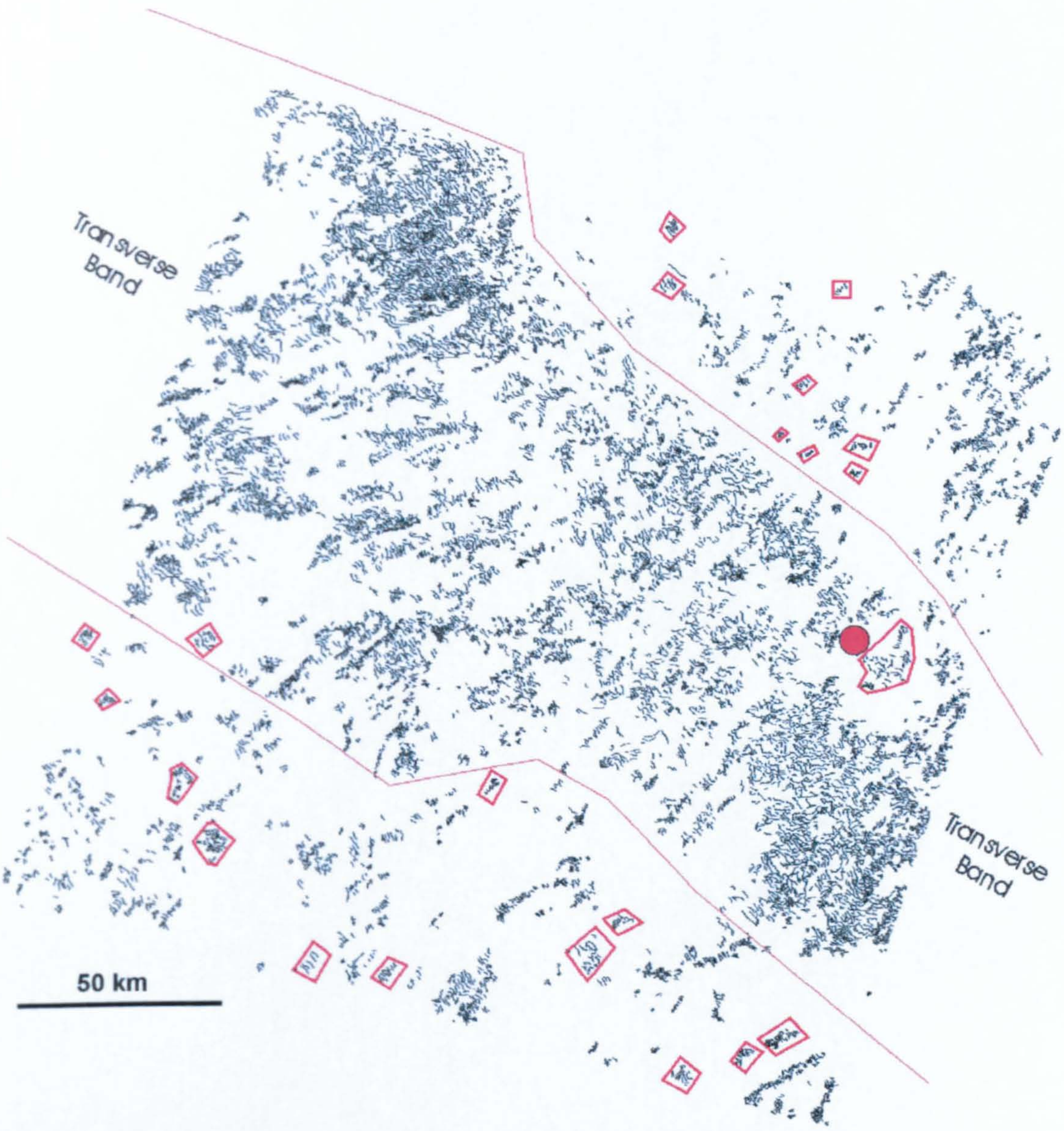

Figure 5.10. Showing examples of isolated ribbed moraine fields dotted around the study area. Note how much smaller they are compared to the other types of ribbed moraine fields reported above.

5.4. Morphological characteristics of ribbed moraine in the Lac Naococane region

5.4.1. Plan view morphology

In the Lac Naococane region it is possible to see many ribbed moraines that fit the classic morphological description, i.e. large areas of well developed, closely spaced ridges that are generally oriented transverse to ice flow and which tend to curve in the down ice direction (Hättestrand, 1997b). Many of the ribbed moraine ridges shown in Figure 5.11 could be classified as belonging to this "classic" category as the ridges appear to fit the above definition. However, close inspection of all the ridges in Figure 5.11 reveals there to be variety of forms more complex in shape than that described above.

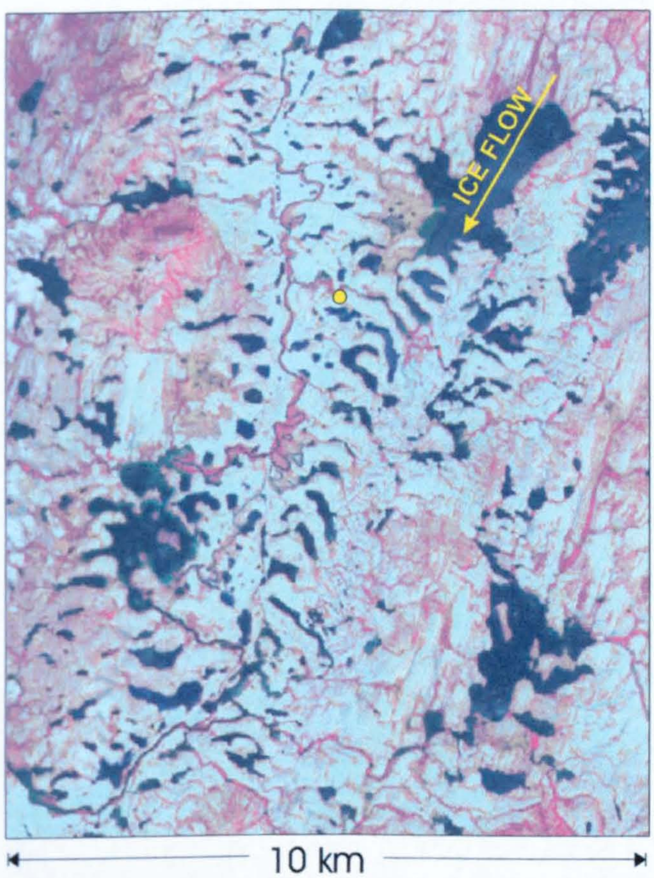

Figure 5.11. ASTER satellite image showing a field of "classical" ribbed moraine ridges. Notice how they are regularly spaced and that many of the ridges are arcuate and concave in the down ice direction. The ribbed moraine ridge marked by a yellow dot and is 1700 m long and 305 m wide. The regional ice flow direction is indicated by the yellow arrow.

Figure 5.12 is an enlarged view of a field just south of Lac Naococane. In combination with the classic ridge type, it is possible to identify a range of ribbed moraine morphologies within this field. These include barchan shaped ridges, which are much shorter in length than the other ridges in the field, and a variety of very broad ribbed moraine ridges that show no curvature. Of the ridges that are curved, it is also possible to identify several that are arcuate in the opposite direction to the regional ice flow pattern, and in plan form their concave side faces in the up ice direction (See blue arrows in Figure 5.12). Some of the ridges have horns at their ends that point downstream and some are anastomosing. Both of these characteristics are considered by Hättestrand (1997b) as being classic ribbed moraine features, however, they are absent in the vast majority of ridges in this field. Figure 5.13 shows another ribbed moraine field situated 28 km east of Lac Naococane. This field also contains ribbed moraine ridges that are quite diverse in shape. As well as having classic type ridges, it is possible to identify rectangular ridges, which have sharp flow parallel ends rather than the more typical tapering ends, and several examples of vague, poorly formed ribbed moraine ridges can be seen throughout the field. At the bottom of the image, some ridges appear to have been modified and broken into drumlinized mounds that have a smeared appearance with the original structure of the ridge barely visible.

Both these examples serve to illustrate that ridge morphology within a single ribbed moraine field is usually quite diverse; a fact that seems true of ribbed moraine in general. For example, Figure 5.14 shows a ribbed moraine field situated at the top left hand corner of the study site, (71° 54 W and 53° 56 N). In plan form, the ridges look quite different from the more classical type shown in Figure 5.11. Here, the ridges have many straight edges and lack the curved, sinuous outlines of classical type ribbed moraine ridges. The backdrop of the lake enhances the straight edges and most ridges appear more angular or blocky than curvy and it can be noticed that virtually none of the ridges are concave in the down ice direction. These ridges are also liberally covered with drumlinized mounds and narrow flutings superimposed on the ridge. In most cases, the flutings tend to run the full width of the ridge with their long axis oriented in the direction of the regional ice flow. The flutings pointed out in Figure 5.14 range between 400 m and 800 m in length and are relatively narrow, being approximately 50 m wide. The drumlinoid elements are slightly larger topographic features that vary generally between 300 m to 400 m in width and 500 m to 600 m in length and have long axes aligned with the regional ice flow direction.

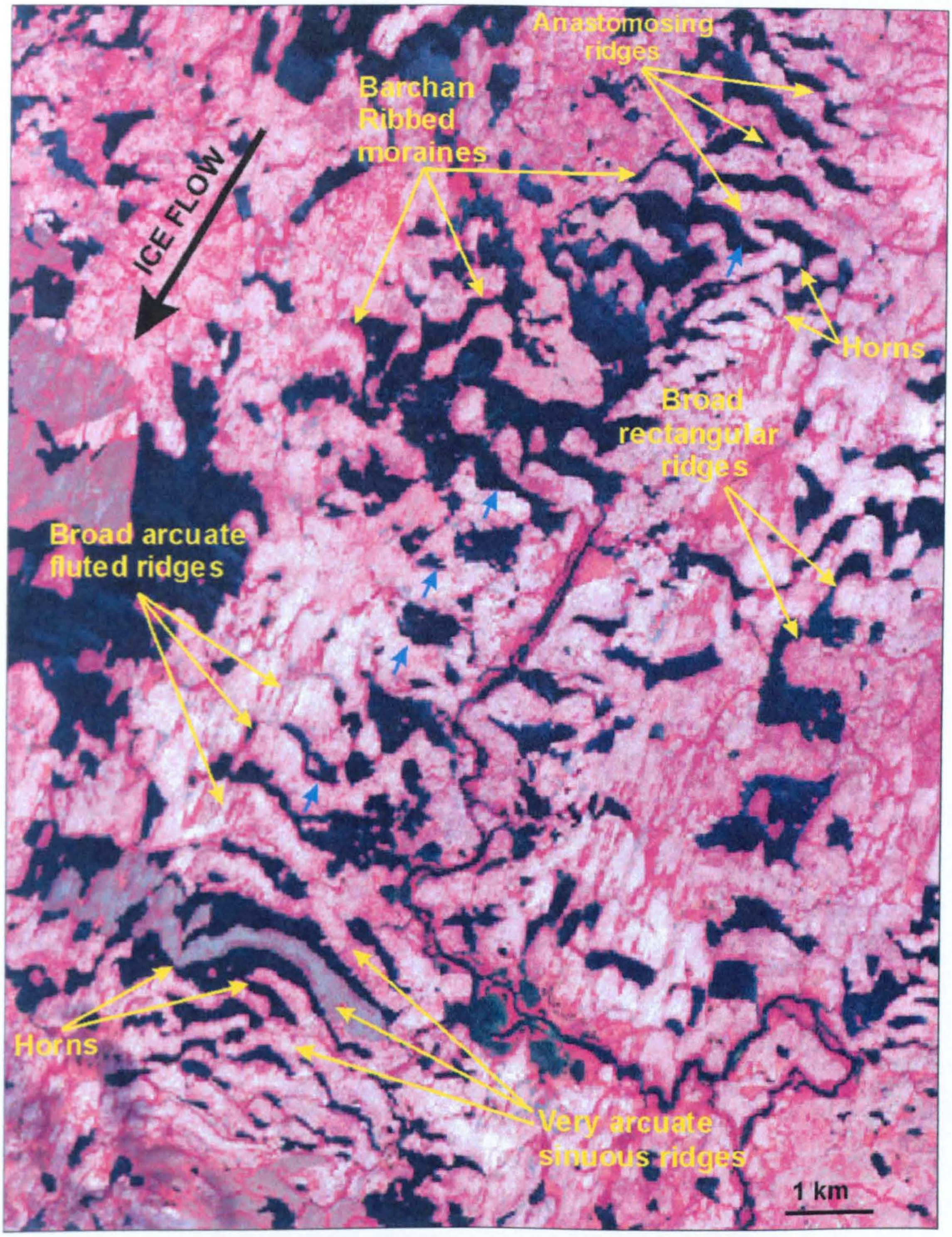

Figure 5.12. An enlarged view of an ASTER satellite image clearly showing the detailed anatomy of a ribbed moraine field at Lac Naococane. Notice the variety of ribbed moraine ridge morphology within this single field. Some of the ridges are concave in the down ice direction, however, there are at least five in this field (marked by blue arrows) that curve in the opposite way and several that are not curved at all.

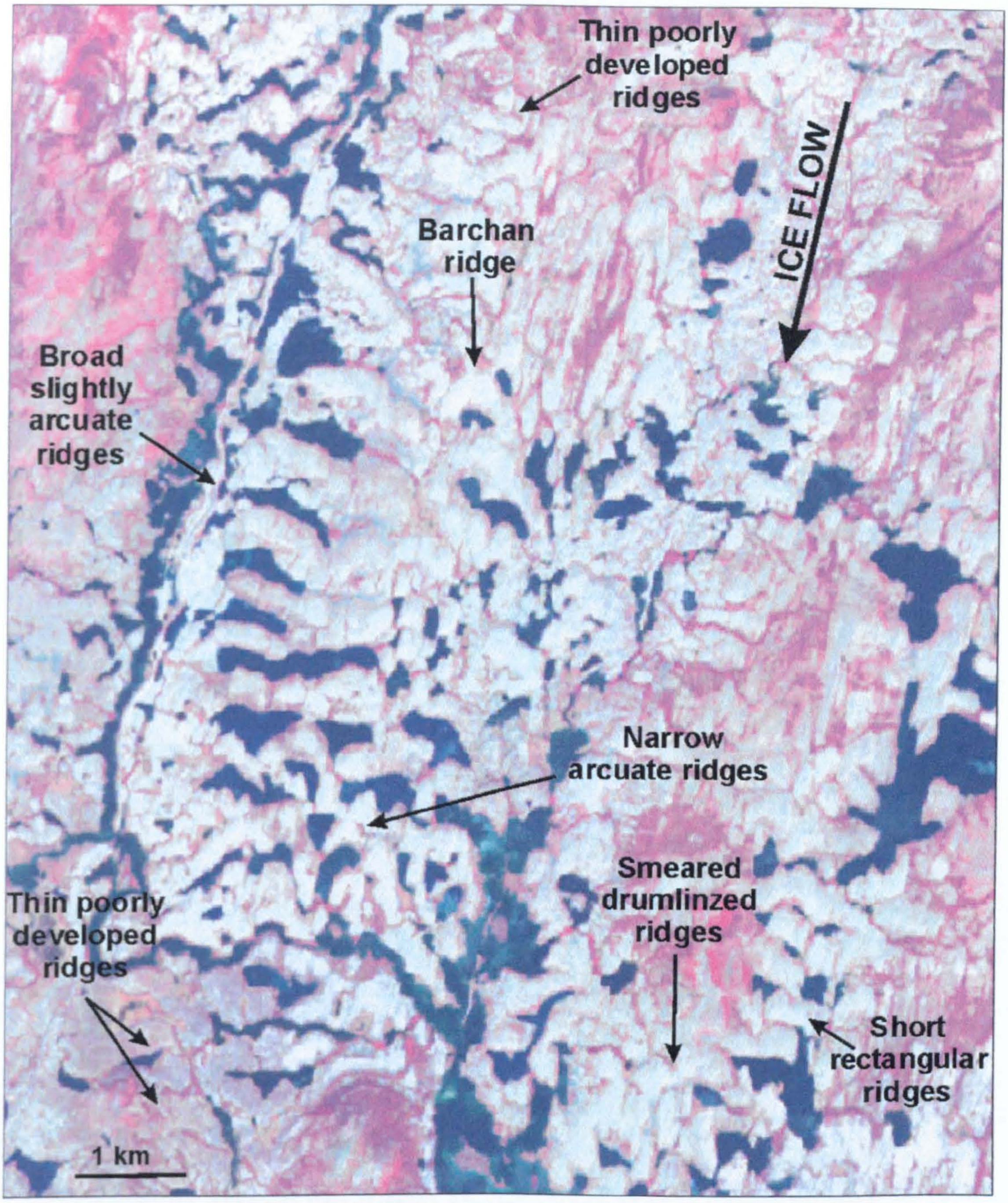

Figure 5.13. Another example of a well-developed ribbed moraine field viewed on an ASTER satellite image just east of Lac Naococane at 69° 59 W and 52° 43 N. Note the variety of forms ranging from classic ribbed moraine ridges to very poorly developed ridges.

In this region, drumlinization of the ribbed moraine is a typical characteristic and the vast majority of ridges display some degree of modification. This characteristic however, is not confined to this area and many other ribbed moraine ridges right across the study site display some form of drumlinization (Fig. 5.15).

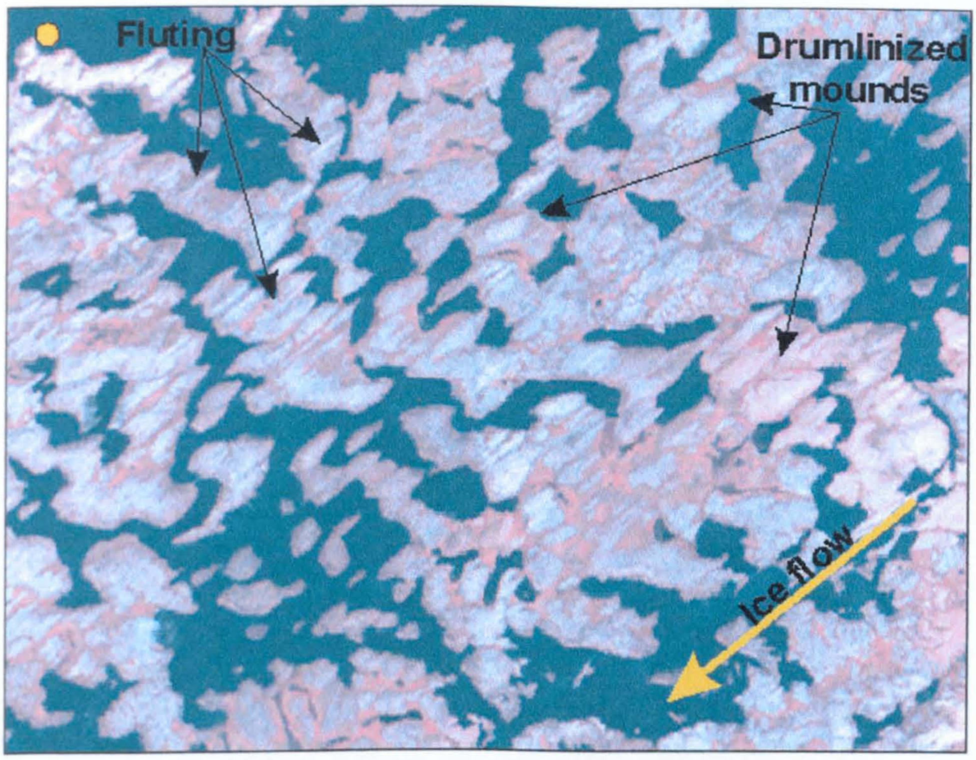

Figure 5.14. ASTER satellite image showing ribbed moraine to the north west of Lac Laribosiere (71° 54 W & 53° 56 N). The ribbed moraine ridges have many straight edges and lack the curved, sinuous outlines associated with more classical forms. The backdrop of the lake enhances the straight edges and most ridges appear more angular or blocky then curvy and sinuous. Notice how the vast majority of the ridges have been fluted and drumlinized to various degrees by the overriding ice sheet. For scale the ribbed moraine ridge marked by the yellow dot in the top left corner is 1388 m long and 230 m at its mid point. Image taken from ASTER satellite image.

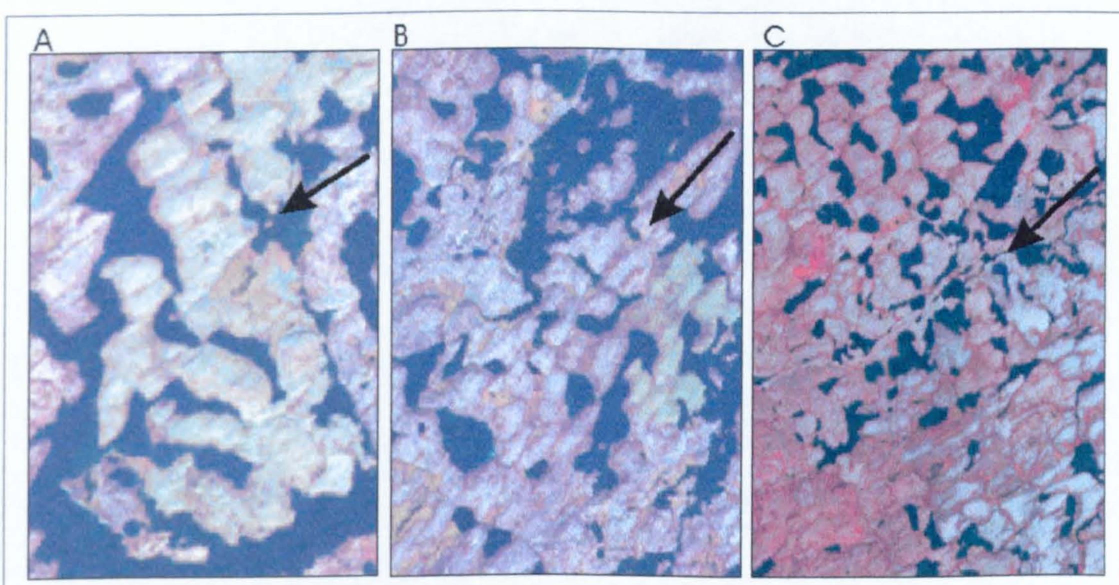

Figure 5.15. Examples of drumlinized and fluted ribbed moraine at various locations across the study site. Figure 5.15a are ribbed moraine ridges located at 71° 36 W and 53° 39 N that show various degrees of drumlinization. Figure 5.15b shows some ribbed moraine ridges situated at Lac Nichicun 71° W and 53° 10 N, drumlinized mounds are clearly evident on the central ridges. Figure 5.15c are some ribbed moraine ridges situated near the Caniapiscau Reservoir at 72° 53 W and 54° 27 N which have been heavily drumlinized. Note how in all cases the drumlinization and flutings are at right angles to the ribbed moraine ridges and can thus be associated with an ice-flow direction similar to the ribbed moraine formation. Arrows indicate regional ice flow direction. Images taken from ASTER satellite imagery.

Other ribbed moraine ridges that differ in morphology from those described above are shown in Figures 5.16. The outline shape of these ridges appears to be more jagged or rugged compared to the classic type shown in Figure 5.11 which tend to have a trimmed, smooth looking outline. This difference is very apparent if both types are compared directly as is demonstrated in Figure 5.17. This shape of ribbed moraine is common across the entire region and it is possible to locate many examples. They can be found either as large clustered groups, isolated fields or mixed together with the more classic type ridges. Figure 5.16a shows a large expanse of ribbed moraine approximately 160 km^2 at 71° 21 W and 53° 03 N. Although some smoother ridges can be seen, the overwhelming majority have a jagged outline appearance. In Figure 5.16b, it is possible to see a mixture of jagged ridges and more classic looking forms.

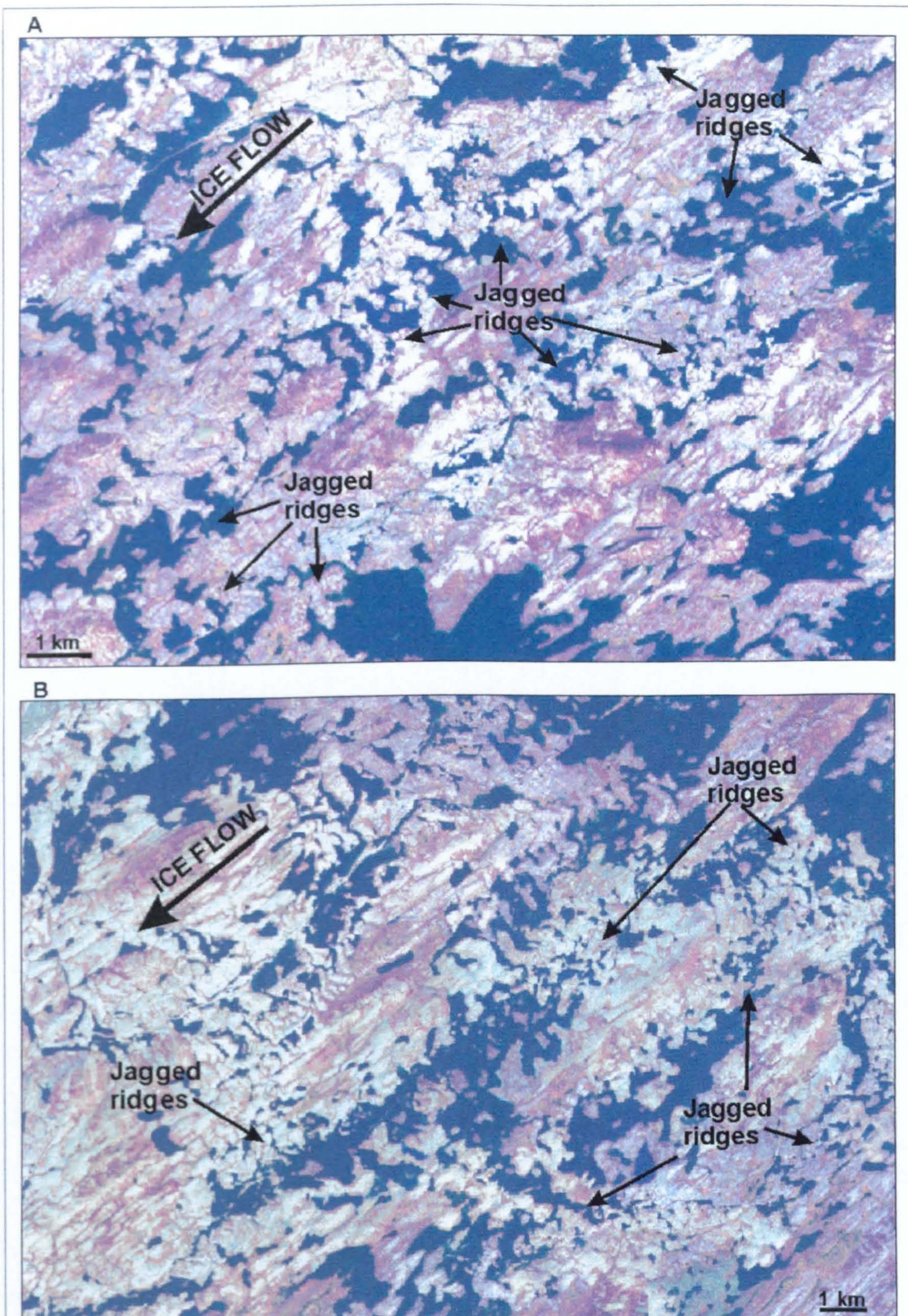

Figure 5.16. ASTER satellite images showing two areas beside Lac Nichicun where jagged shaped ribbed moraine ridges can be found. Figure 5.16a is located 15 km south east of Lac Nichicun at 71° 27 W and 53° 03 N and is an area liberally covered with this type of ridge. Figure 5.16b, is situated at 71° 02 W and 53° 22 N and contains a mixture of morphological types, including ribbed moraine ridges of various scale.

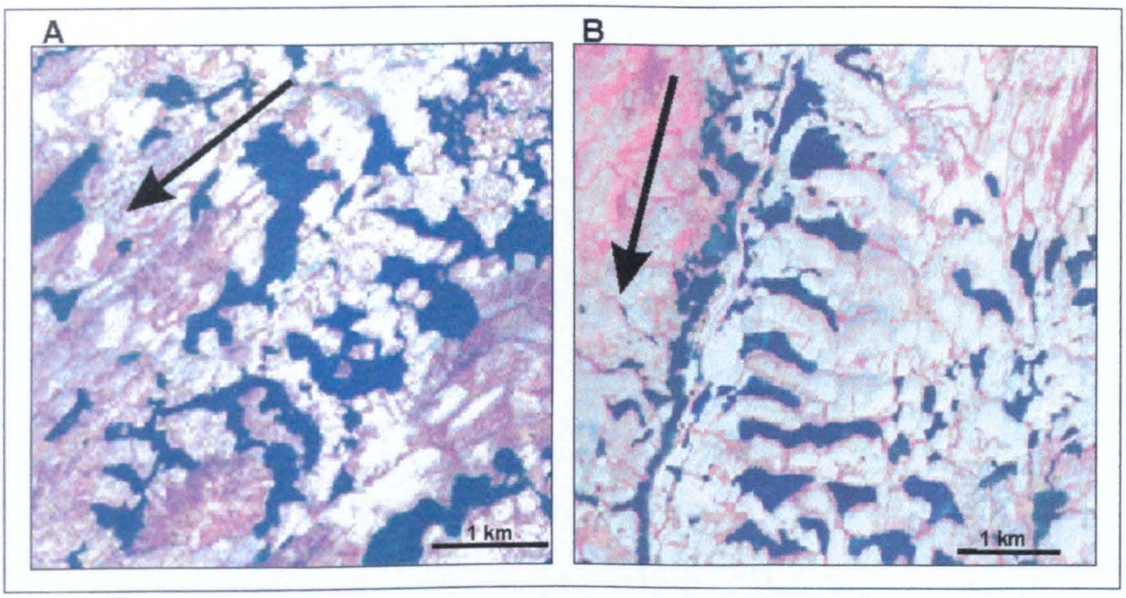

Figure 5.17. ASTER satellite images showing a side-by-side comparison of some jagged ribbed moraine ridges, Figure 5.17a and some classical ridges, Figure. 5.17b.

As well as hosting a variety of well-developed ribbed moraine, the Lac Naococane region also contains a plethora of more subtle ridges (Fig. 5.18). This type of ribbed moraine does not have a distinct morphology and is difficult to categorise as the shape varies considerably from place to place. Nonetheless, they are clearly related to ribbed moraine because they are always found in ribbed moraine terrain and are often positioned next to well-developed fields. Figure 5.18a shows a cluster of poorly formed ridges situated 80 km north of Lac Naococane at 69° 49 W and 53° 30 N. Nearby, it is possible to see several ribbon type ribbed moraine fields between 9 km and 10 km in length made up of well-formed ridges. Here however, with the exception of a few small minor ribbed moraine ridges 500 m in length, the ridges are not clearly defined, and in places it is difficult to see where one ridge ends and another begins. Nonetheless, it is possible to make out transverse ridge structures that are morphologically akin to well-developed ribbed moraine ridges. The narrow corridor of ribbed moraine in Figure 5.18b is situated 27 km east of Lac Nichicun in an area covered liberally with both well developed and poorly formed ridges. In this case, a variety of morphologies can be identified ranging from broad bulbous looking ridges to short thinner forms with up stream pointing horns. The ridges in Figure 5.18c appear to be formed in very thin till and are quite angular in appearance. They are transverse to the regional ice flow pattern and are aligned in such a way as to give a mosaic appearance to the landscape. The ridges presented in Figure 5.18d are situated 8 km north east of Lac Dalmas, and is a region with an abundance of ribbed moraine. In this location, a few broad ridges have been formed that are aligned oblique to the ice flow direction. It is also possible to identify what appears to be very faint looking ribbed moraine structures at the top right hand side of the image. Elsewhere, large mounds have been aligned transversely forming broken lumpy ridges.

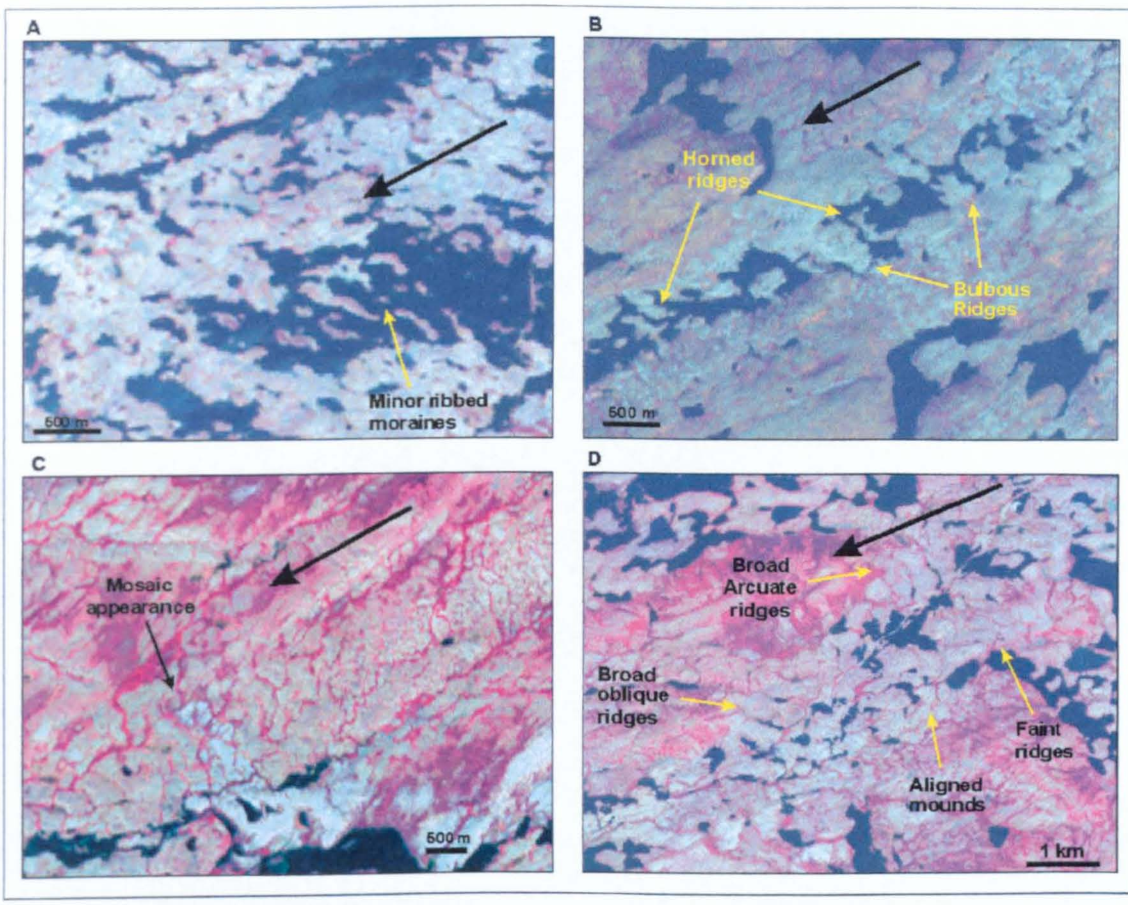

Figure 5.18. Showing several examples of more subtle types of ribbed moraine found at a variety of sites across the study area. Figure 5.18a shows some subtle type ribbed moraine north of Lac Naococane at 69° 49 W and 53° 30 N. Figure 5.18b shows a narrow corridor of poorly developed ridges near Lac Nichicun at 71° 25 W and 53° 18 N. Figure 5.18c shows some thin angular looking ribbed moraine ridges 26 km south of Lac Dalmas at 71° 53 W and 53° 12 N that have a mosaic appearance. Figure 5.18d shows a variety of poorly defined ridges 8 km from Lac Dalmas at 71° 32 W and 53° 30 N. The regional flow pattern is shown by the large black arrows. Images made from ASTER satellite imagery.

In addition to ribbed moraine fields containing ridges of various shapes, it is also common for the ridges to vary in scale. In this region, this phenomenon is quite widespread and most of the fields contain ribbed moraine ridges of various sizes. Figure 5.19 shows an area where this characteristic is clearly evident. The smaller ribbed moraine ridges are very similar in plan form to the larger ridges and within a single field, it is possible to identify small ridges that are sinuous, arcuate and also straight. Like the larger arcuate ridges, the smaller versions can also be curved in both the up ice and down ice direction. In some cases, the difference in scale between ribbed moraine ridges in the same field can be extreme. For example, in field number 2 in Figure 5.19 the small ridges situated immediately left of the yellow dot are minor ribbed moraine ridges and are only 500 m long and 50 m wide, whilst some of the bigger forms at the top of the field are just under 3 km in length and 300 m wide. This change in scale is also evident if adjacent fields of ribbed moraine are compared and in many parts of the study site it is also possible to see independent fields in close proximity containing ribbed moraine ridges of completely different sizes. Some examples of this can be seen clearly in Figures 5.19 and 5.20.

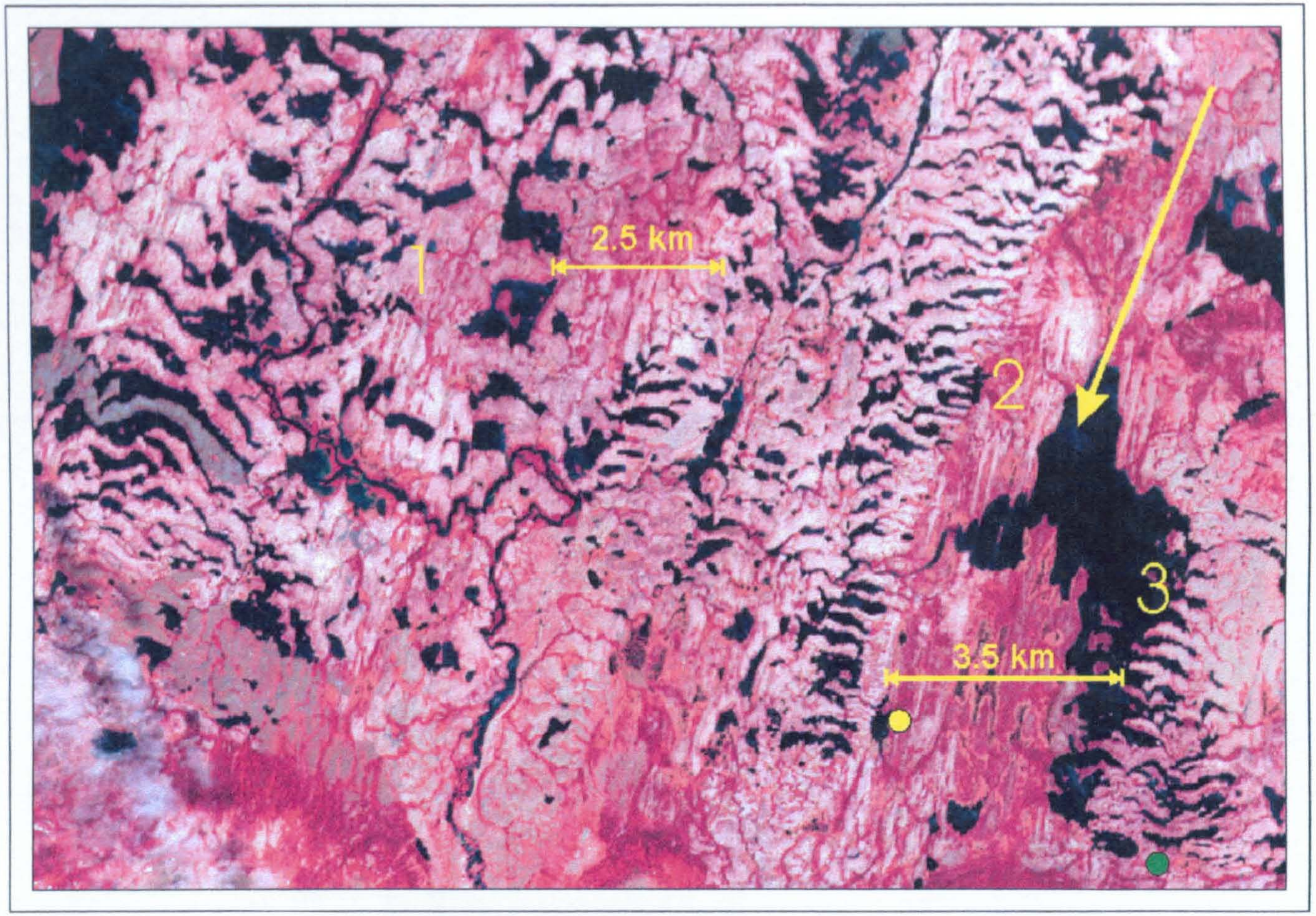

Figure 5.19. ASTER satellite image showing three ribbed moraine fields in close proximity in the Lac Naococane region (70° 19 W & 52° 32 N). Note the change in scale of the ribbed moraine over relatively short distances. For example, the ribbed moraine ridges in field number 1 are much larger than those in field number 2 even though they are separated by a short distance of just 2.5 km. This change in scale can also occur within the same ribbed moraine field and examples of this are clearly evident in field number 2. Here, smaller scale ribbed moraine ridges are sandwiched between larger ridges. Also, the ridges situated immediately to the left of the yellow dot are extremely small compared to the other ridges in the field being just over 500m long and 50 m wide. Field number 3 also demonstrates these characteristics. Note how the ribbed moraine ridges to the right of the green dot are much thinner and smaller than the ridges at the start of the field. The yellow arrow indicates regional ice flow direction.

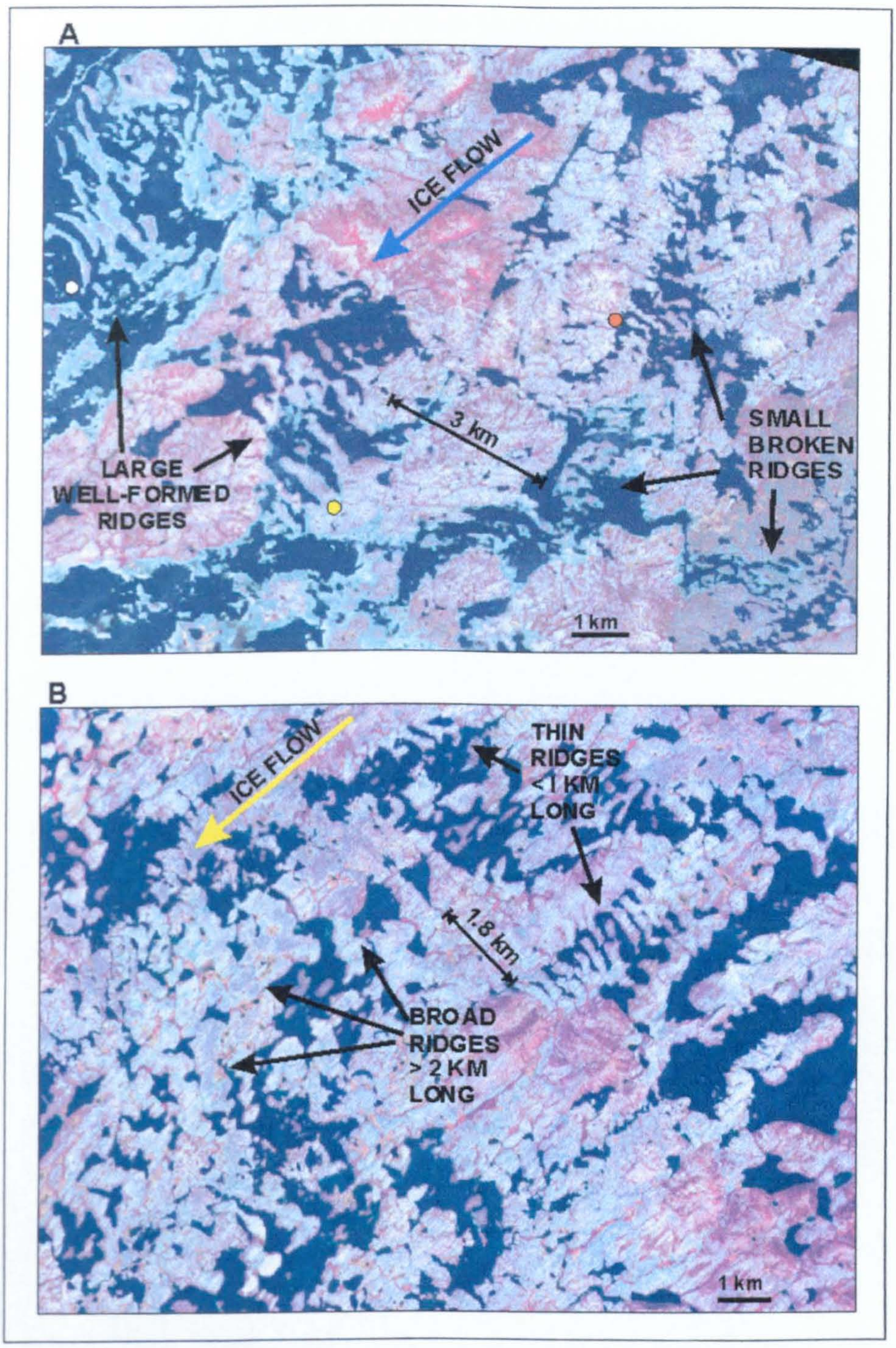

Figure 5.20. ASTER satellite images of two ribbed moraine fields exhibiting different scales. The fields in Figure 5.20a are situated near a large lake 152 km north of Lac Naococane at 69° 39 W and 54° 10 N. In this area, fields of large well-formed ridges are found next to fields of small ridges. To demonstrate the change in scale, 3 ribbed moraine ridges have been marked by spots. The two large ridges marked by the white and yellow spots are both 1400 m in length whilst the small ribbed moraine ridge marked by the orange spot is only 514 m in length. Figure 5.20b shows different scales of ribbed moraine near lake Nichicun at 71° 45 W and 53° 05 N. In this case, a ribbon of thinner ribbed moraine ridges is surrounded by very broad forms twice their length.

5.4.2. Individual ridge morphology

Using high resolution ASTER DEM's it was possible to build a picture of the topographic morphology of the ribbed moraine ridges in the Lac Naococane region. This was done by taking cross sections over entire ribbed moraine fields (Fig. 5.21) and longitudinal profiles along the length of individual ribbed moraine ridges (Fig. 5.22).

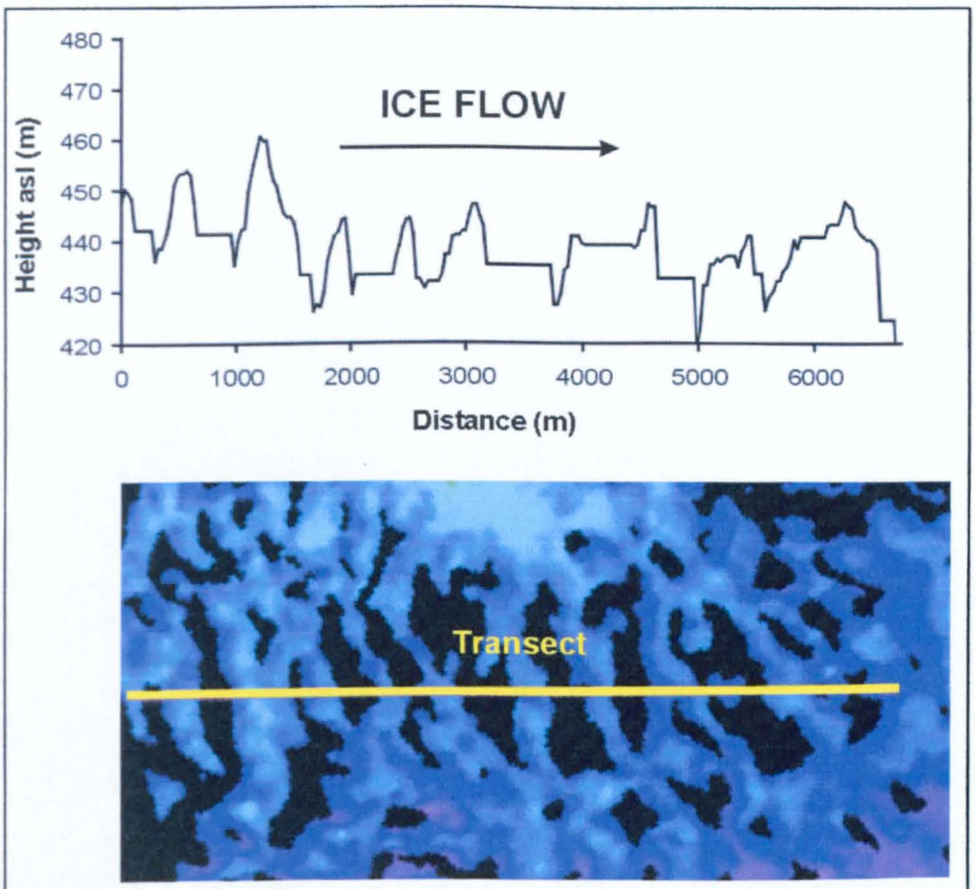

Figure 5.21. A transect of elevation taken across a ribbed moraine field on an ASTER DEM which is displayed as a Pseudo Colour image. The graph on the top shows the topography across the field. The yellow line shows the transect path which was taken from left to right across the DEM.

It has been reported by several authors that in cross section, ribbed moraine ridges are generally asymmetric with the distal (down-ice) slope being much steeper than the proximal slope (Shilts *et al.*, 1987; Aylsworth and Shilts, 1989; Bouchard, 1989; Hättestrand and Kleman, 1999). To investigate whether these were typical characteristics at Lac Naococane, transects totalling 280 km in length were taken across a random sample of ribbed moraine fields. Each profile was then visually assessed to determine the symmetry of the ridges and to investigate whether the distal or proximal side had the steepest slope. In total, 91% of the ribbed moraine ridges sampled had an asymmetric cross profile with 51% having a steeper distal slope and 40% a steeper proximal slope.

The longitudinal profiles (i.e. along ridge crests) showed that all the ridges sampled had undulating crests, which appeared to be a typical characteristic of the ribbed moraine ridges in the region (Fig. 5.22). Generally, the undulations are several metres in height however; it is common to find large bumps on many of the ridges ranging between 20 m to 30 m high. These undulations are very apparent when the ridges are viewed in 3-D and an example of this can be seen in Figure 5.23, which shows a 3-D surface plot of some large ribbed moraine ridges near Lac Dalmas.

The ASTER DEM's were also used to investigate the assertion made by Bouchard (1989) Menzies and Shilts (1996) and Hättestrand and Kleman (1999) that the "accordant summit" or crest height of ribbed moraine ridges within a single field is very consistent. This opinion is supported by very little data and Bouchard (1989) is the only author to have produced any empirical evidence in support of this claim. In his study, Bouchard demonstrated that the measured profile of the crest height across a single ribbed moraine field in Québec had a variability of less than 3 m over a distance of 1 km. In this thesis, access to high-resolution elevation data meant that this claim could be critally evaluated.

Transects totalling 340 km in length were taken across a random sample of 20 ribbed moraine fields. The elevation data were exported into a spreadsheet and graphs showing each transect profile were constructed. Each of the graphs was then used to determine the X and Y coordinates of each ribbed moraine summit along a particular transect and this information was recorded on the spreadsheet. Scatter plots were then made using these data and regression analysis applied on the points to derive the R Squared value (Fig. 5.24). If the hypothesis/assertion that ribbed moraine ridges tend to have accordant summits is true, then the data points should all fit closely along a straight line and the R Squared value would tend towards 1. However, as Table 5.1 shows, only 3 of the fields in the sample have what might be considered relatively high R Squared values (greater than 0.7) which means that in 85 % of the fields sampled, the ridge summits are not accordant. These findings contradict those of Bouchard (1989) and throws doubt on the assertions made by both Bouchard (1989) and Hättestrand and Kleman (1999) that ribbed moraine fields have accordant summits. It may simply be the case that

Bouchard's findings were site specific and therefore not applicable to ribbed moraine in general.

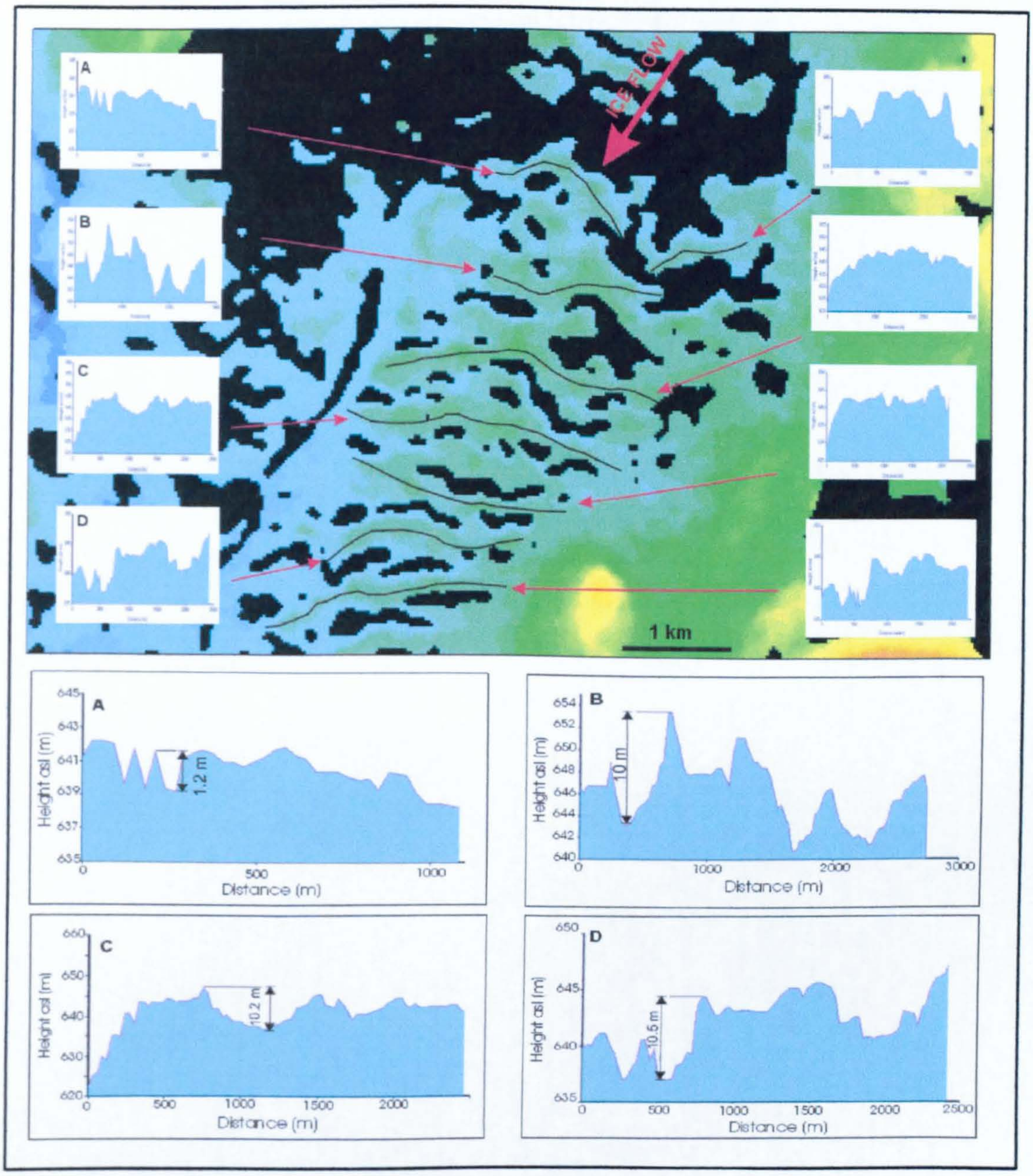

Figure 5.22. Examples of the longitudinal profiles taken along ridges on the DEM. The DEM is displayed as a Pseudo Colour image in which the highest elevations are yellow, then green and down to blue which are the lowest areas. The black regions are lakes between the ribbed moraine ridges. In the above examples the black lines running across the ridges mark the path of each profile and the corresponding graph can be seen at the side. Note how all the ridges undulate. The graphs marked A to D are enlarged at the bottom to give an indication of the height range of the undulations, which in the cases presented range between 1.2 m and 10.5 m. These are quite large when the estimated thickness of the ridge is taken into consideration, for example in the graph marked B the total thickness of the ridge is approximately 12 m, however the largest bump on the ridge measures 10 m high.

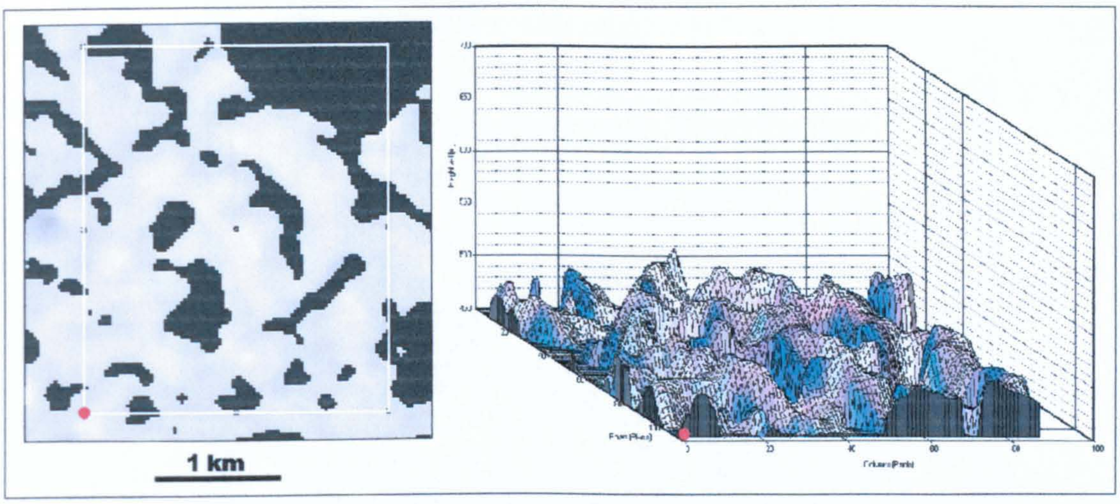

Figure 5.23. An example of a three dimensional surface plot constructed using a 30 m ASTER DEM. The image on the left shows some ribbed moraine ridges on the DEM, which is displayed as a grey scale elevation model. The graph on the right is the 3-D surface plot of the area marked by the white box on the DEM. The red dot marks the viewing position across the area. Note the undulating nature of the ridges.

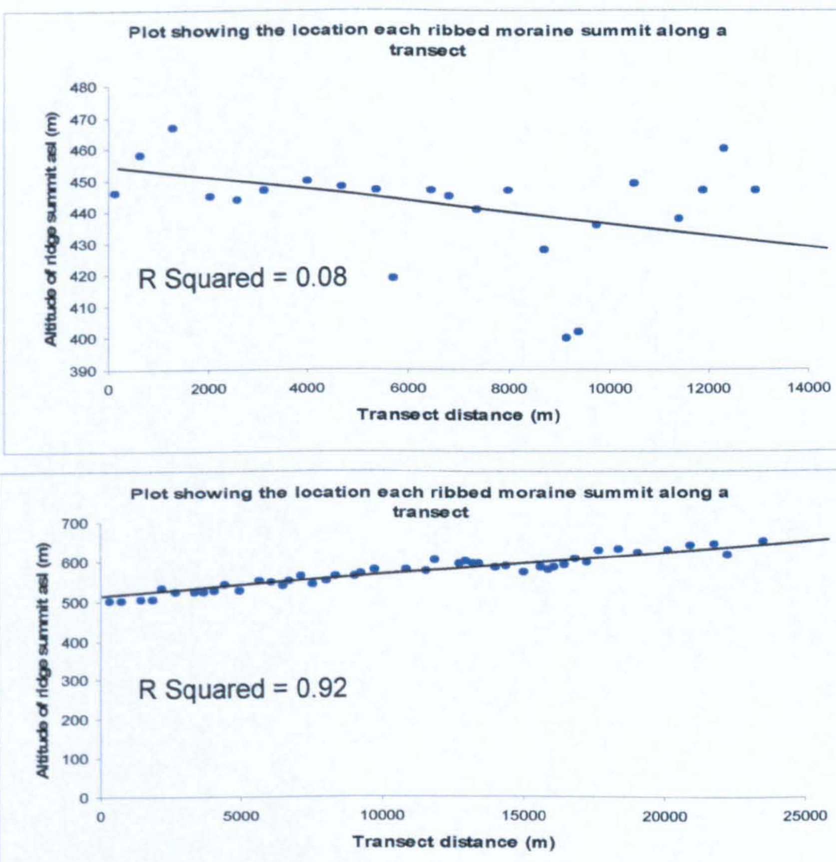

Figure 5.24. Showing two examples of regression analysis conducted on the summit positions of two ribbed moraine fields in the region. The top example shows a case where the summits are not accordant. Note how the summit points diverge greatly from the best-fit line, which is reflected in the low R Squared value that was obtained by conduction regression analysis on the data points. The bottom example shows a case where all of the summit points are very close to the best-fit line and this is reflected by the high R Squared value of 0.92.

Table 5.1. R Squared values for transect data of 20 ribbed moraine fields totalling 340 km in length. Note that only three of the fields in the sample have high R Squared Values, which means the majority ribbed moraine ridges in these fields do not have accordant summits

R Squared	R Squared	R Squared	R Squared
0.56	0.07	0.36	0.08
0.11	0.04	0.66	0.19
0.28	0.15	0.53	**0.92**
0.36	0.48	0.52	0.57
0.53	0.04	**0.77**	**0.80**

5.4.3. Detailed matching of ribbed moraine ridges

Lundqvist (1969), Bouchard (1989), Hättestrand (1997b) have all observed that ribbed moraine ridges fit together like a jigsaw puzzle. Whilst Bouchard and Lundqvist place little emphasis on this observation, the whole idea underpins Hättestrand's theory of ribbed moraine formation. For him, the apparent close matching of the ridges is evidence that they were once joined together forming a single coherent till sheet. This till, he claims was subsequently pulled apart by basal shear stresses imparted by the ice, producing sequences of transverse ridges. To test this hypothesis, Hättestrand matched some ridge outlines that he traced from aerial photographs. The matching process involved sliding each of the traced ridges back along the regional ice flow path until they join. To obtain a neater fit, several ridges were also rotated into place. Figure 5.25 shows the example of ridge matching presented by Hättestrand and Kleman (1999). The apparent close fit, they state, is evidence that these ridges were once joined, and in this example, they believe the ice sheet has pulled apart and extended two slabs of till by 35 % and 60 %.

To explore the extent to which jigsaw matching is a common characteristic at this site three cases were randomly selected. Two representing well-expressed "classical" ribbed moraine ridges (Fig. 5.26) and one case of hummocky type ribbed moraine (Fig. 5.27). Heavily drumlinized ribbed moraine ridges were avoided as post formational modification may have disturbed the pattern too much. In all cases, the end result was less convincing than that presented by Hättestrand and Kleman (1999). When matching the classic type ridges it was possible to match some of the ridges reasonably well. However, in general, there were more gaps and miss matches than clear joins and the overall result failed to produce anything that resembled a single coherent sheet of till (Fig. 5.26). This failure is even more apparent when attempts were made to match the hummocky ridges (Fig. 5.27). In this example, none of the ridges fitted neatly together and the apparent gaps and poor matches make it difficult to envisage how they ever could have been joined together as a single slab of till.

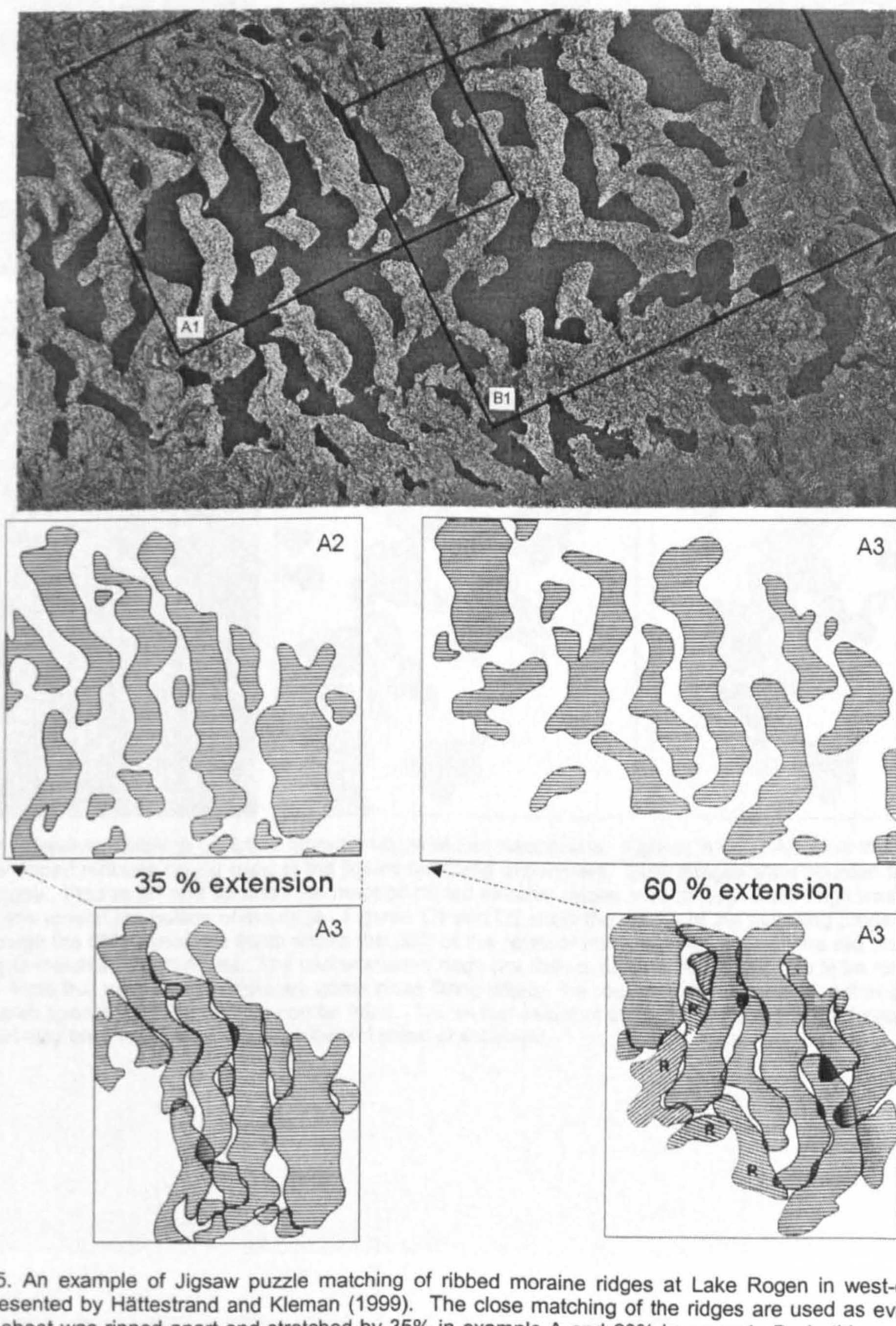

Figure 5.25. An example of Jigsaw puzzle matching of ribbed moraine ridges at Lake Rogen in west-central Sweden presented by Hättestrand and Kleman (1999). The close matching of the ridges are used as evidence that the till sheet was ripped apart and stretched by 35% in example A and 60% in example B. In this case, the obvious overlaps in the "jigsaw" are confined to the ridge horns. Hättestrand believes these overlaps are not part of the original ridge that was formed at the time of the initial separation. They are simply by-products of drumlinization, which subsequently distorted the original morphology and hence offers an explanation for the poor fit. However, note that even with some overlapping allowed, there are still many gaps between the matched ridges.

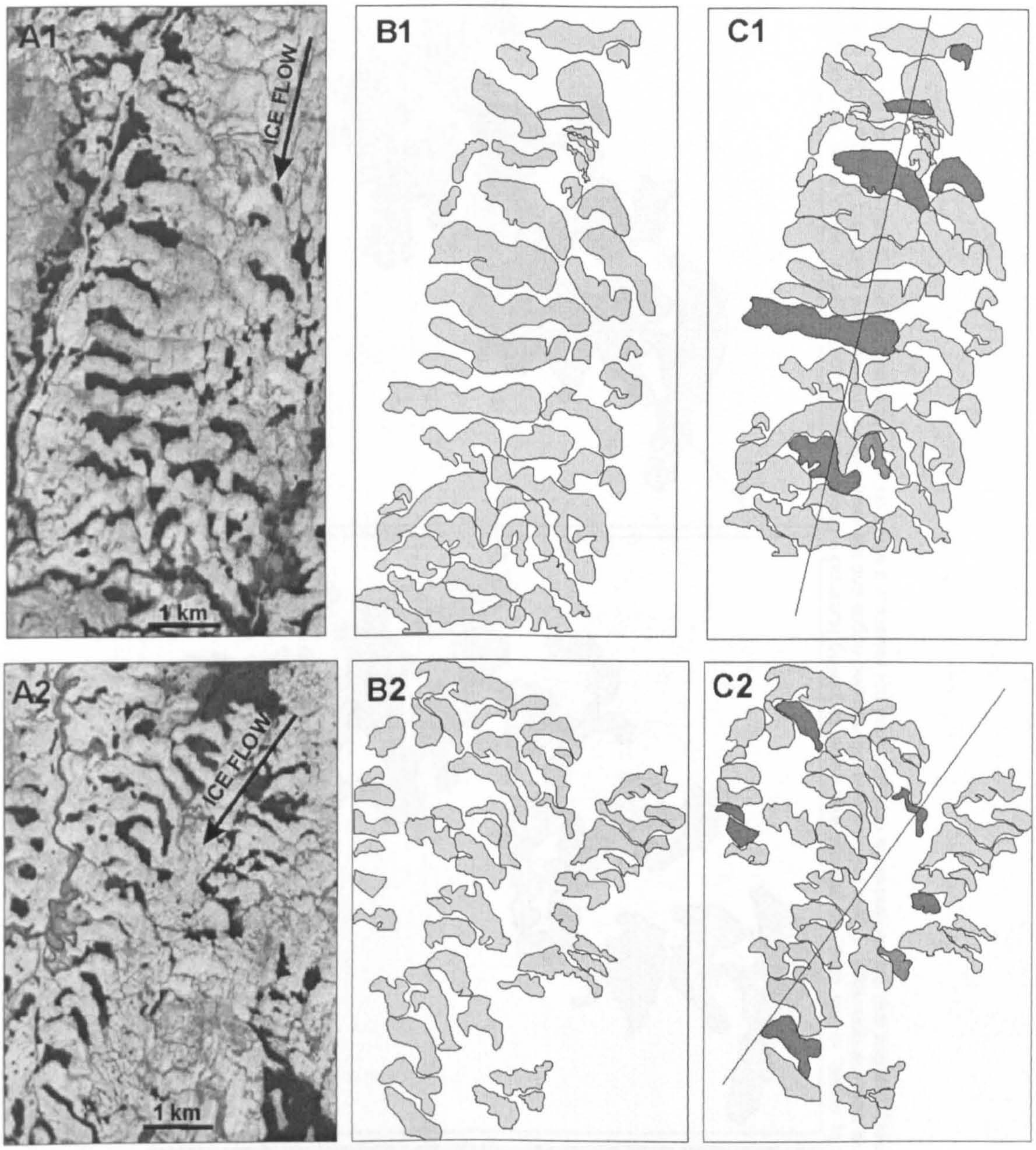

Figure 5.26. Detailed matching of ribbed moraine ridges at Lac Naococane. Figures A1 and A2 show the two fields of classic type ribbed moraine ridges used in the jigsaw matching experiment. Both images were sourced from ASTER satellite images. Figures B1 and B2 show the mapped ribbed moraine ridges in each field. Each ridge was mapped by digitising a line around the outline of the ridge. Figures C1 and C2 show the results of the matching process. The line running through the ribbed moraine fields shows the path of the regional ice flow. The ridges were slid along this axis when trying to match adjacent ridges. The darker shaded ridge are ribbed moraine ridges that had to be rotated to give a better fit. Note that even though there are some close fitting ridges, the vast majority fit poorly or not at all and there are many open spaces in which nothing can be fitted. The overall result of this matching experiment failed to produce anything that may once have resembled a coherent sheet of sediment.

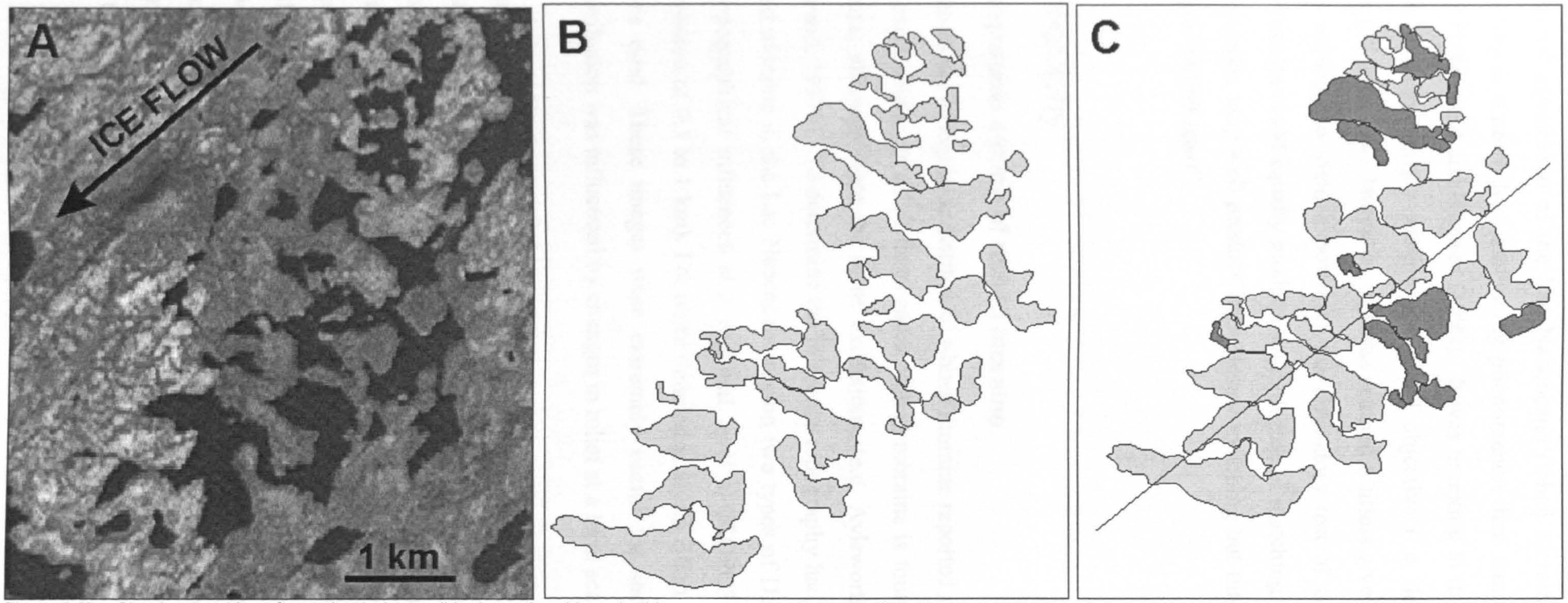

Figure 5.27. Showing matching of non-classical type ribbed moraine ridges. In this case, an attempt was made at joining hummocky ribbed moraine ridges together, which have been classified by Hättestrand (1997) as being a more poorly developed form of the more classical type ridge. Figure 5.27b shows the mapped ridges and the results of the matching are presented in figure 5.27c. Note how in this instance the end result is very poor as none of the ridges fit neatly together and the conglomerate of ridges does not resemble a single coherent till sheet. Figure 27a taken from an ASTER satellite image.

From this initial exploration of the Lac Naococane ribbed moraines, it is clear that jigsaw matching is a much less convincing phenomenon than thought by Hättestrand (1997b) and Hättestrand and Kleman (1999). It was tempting to develop this analysis into a more thorough (larger sample sizes) and objective (i.e. develop quantitative measures of fit) procedure. However, this was deemed fruitless given that the degree of matching is unlikely to yield a powerful discriminatory test of competing theories. Different processes could equally produce some degree of matching. Sand ripples on a beach for example, may well produce high jigsaw matching but this does not indicate that they were "pulled apart".

5.5. Topography

5.5.1. Topographic setting of ribbed moraine

Table 5.2 shows the topographic settings of ribbed moraine reported in various localities in Sweden and Canada. In all of these cases, ribbed moraine is found mostly in basins or depressions, although there are some exceptions, (e.g. Aylsworth and Shilts, 1989 and Hättestrand, 1997b). To determine the influence topography had on the distribution of the ribbed moraine in the Lac Naococane region two types of DEM were acquired. To study topographical influences at a regional level a GTOPO30 DEM was used (spatial resolution of 0.5 to 1 km). For more detailed analysis, 30 m resolution ASTER DEM's were used. These images were extremely useful for showing how ribbed moraine distribution was influenced by changes in relief at a local scale.

The topography of the study site is portrayed in Figure 5.28. The area sits approximately 340 m to 1100 m above sea level and is bordered on its northern side by a broad plateau like feature which arcs around the site encompassing its eastern and southeastern flank. The plateaux itself is incised by several narrow valleys and some broader depressions and is dotted occasionally with several high points along its length. To the southeast lies the Mount Ottish mountain chain, which for the most part, bounds the south-western (bottom) part of the study site. Inside the perimeter, several large basins are clearly evident. These are broken periodically in the central regions of the study site by small conical hills, and an area of high ground situated in front of a broad arc of hills that sweep eastwards from the bottom left hand corner.

Table 5.2 Location and topographic setting of ribbed moraine in Sweden and Canada.

Country	Locality	Topographic setting	Reference
Sweden	Lake Rogen	Mostly restricted to concave ground in the direction of ice flow	Lundqvist (1989)
Canada	General observations of ribbed moraine in Canada	Found in broad swales and lowland basins and in the broad floors of shallow depressions in upland areas	Mollard and James (1984)
Canada	Central and Northern Québec	Commonly found in topographic lows. However, closely spaced (20 m) Rogen-like features less than 2m high can be found superimposed on large drumlinoid ridges in interfluvial areas.	Bouchard (1989)
Canada	Keewatin	Distributed largely independent of topography close to the ice divide. Further away from the divide they are found preferentially in depressions that trend parallel to ice flow.	Aylsworth and Shilts (1989)
Sweden	West of Strömsund in the areas south of Henningskällen and southwest of Flykällen in the Öjån and Storån Valleys.	Found in depressions and areas in which a relatively deep narrow valley opens into flatter terrain.	Shaw (1979)
Sweden	Västerbotten County	Found mostly in basins of dissected landscapes. Also in rather flat terrains and on upslope and downslope positions.	Markgren and Lassila (1980)
Sweden	General observations of ribbed moraine in Sweden	On local scale ribbed moraine is commonly confined to plains, basins and wide upland plateaux. Some examples forming islands in the sea suggest they must be situated on convex parts of the sea floor, protruding above the present sea surface.	Hättestrand (1997b)

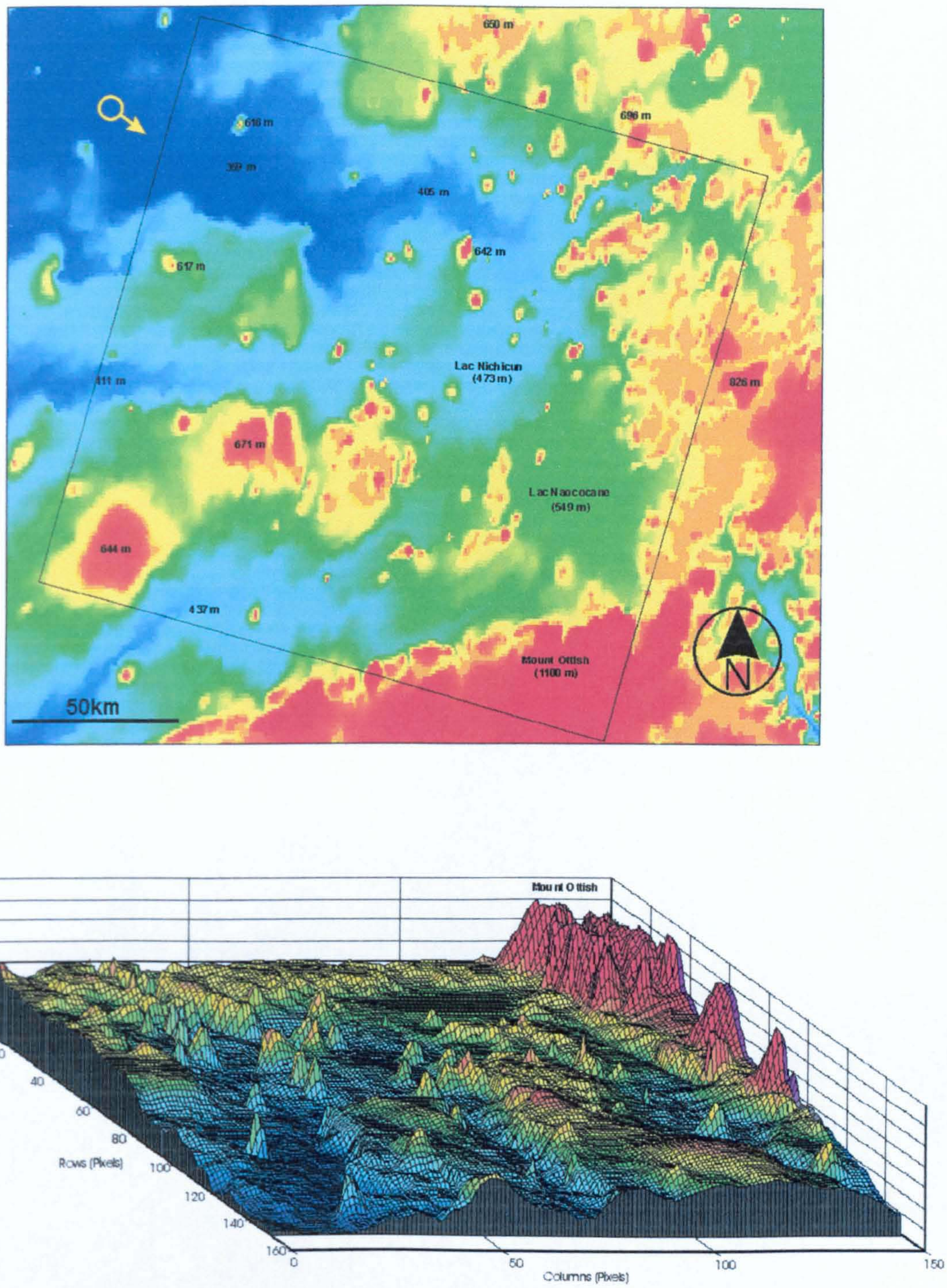

Figure 5.28. The figure on top is a GTOPO30 DEM of the Lac Naococane region displayed as a Pseudo colour image. Elevation is coded to show the highest elevations as red, grading down to orange, yellow, green, blue to purple, which represents the lowest lying regions. The 3-D surface plot at the bottom was produced using the DEM and gives a good impression of the general topography. The yellow arrow on the DEM marks the point at which the surface plot is viewed from looking across the long depression towards Mount Ottish.

To investigate the topographic setting of the ribbed moraine fields at this site, the ARC coverage of the mapped ribbed moraine crests was laid on top of the DEM (Fig. 5.29). Viewed in this manner, it is possible to see that approximately 75 % of the ribbed moraine ridges are located in and on the slopes of the large basin that runs east to west through the centre of the study site. The vast majority of these belong to the large transverse band of ribbed moraine discussed previously in Section 5.3.1. The large basin directly in front of the Ottish mountain chain and the valleys in the north eastern plateau make up the other large depressions in the study site and they too contain fields of ribbed moraine, although not as many as the central basin. Together these three locations contain approximately 80 % of the entire ribbed moraine population. The rest can be found on slopes leading both in and out of the major basins (e.g. A, B, C and D), on some hilltops (e.g. E and F), on relatively open, upland ground (e.g. G and H) and along some narrow valleys in the Mount Ottish chain, which are marked I.

To explore whether smaller scale differences in topography influenced ribbed moraine distribution some higher resolution imagery was needed and for this purpose several ASTER DEM'S were acquired. The DEM's were used to make relief images, which gave a detailed 3-D perspective of the terrain. When viewed at this scale, it was possible to determine that the ribbed moraine ridges occupied a variety of topographical settings. Mostly, the more classical type ridges tended to be found in the swales and lower lying regions (Fig. 5.30a, 5.30b and Figure 5.31). However, this was not an exclusive relationship as they were also observed on the slopes of some small hills in the area (e.g. Fig. 5.30c). Generally, the higher ground tended to contain ridges that were shorter in length and less sinuous in form and many of these could be seen superimposed on both the proximal and distal slopes of all the small hills in the area (Fig. 5.30). The summits of these hills tended to be free of ribbed moraine ridges however, one case was observed were the ridges traversed the entire hill and some shorter forms could be seen situated on the actual summit (see Figure 5.30a).

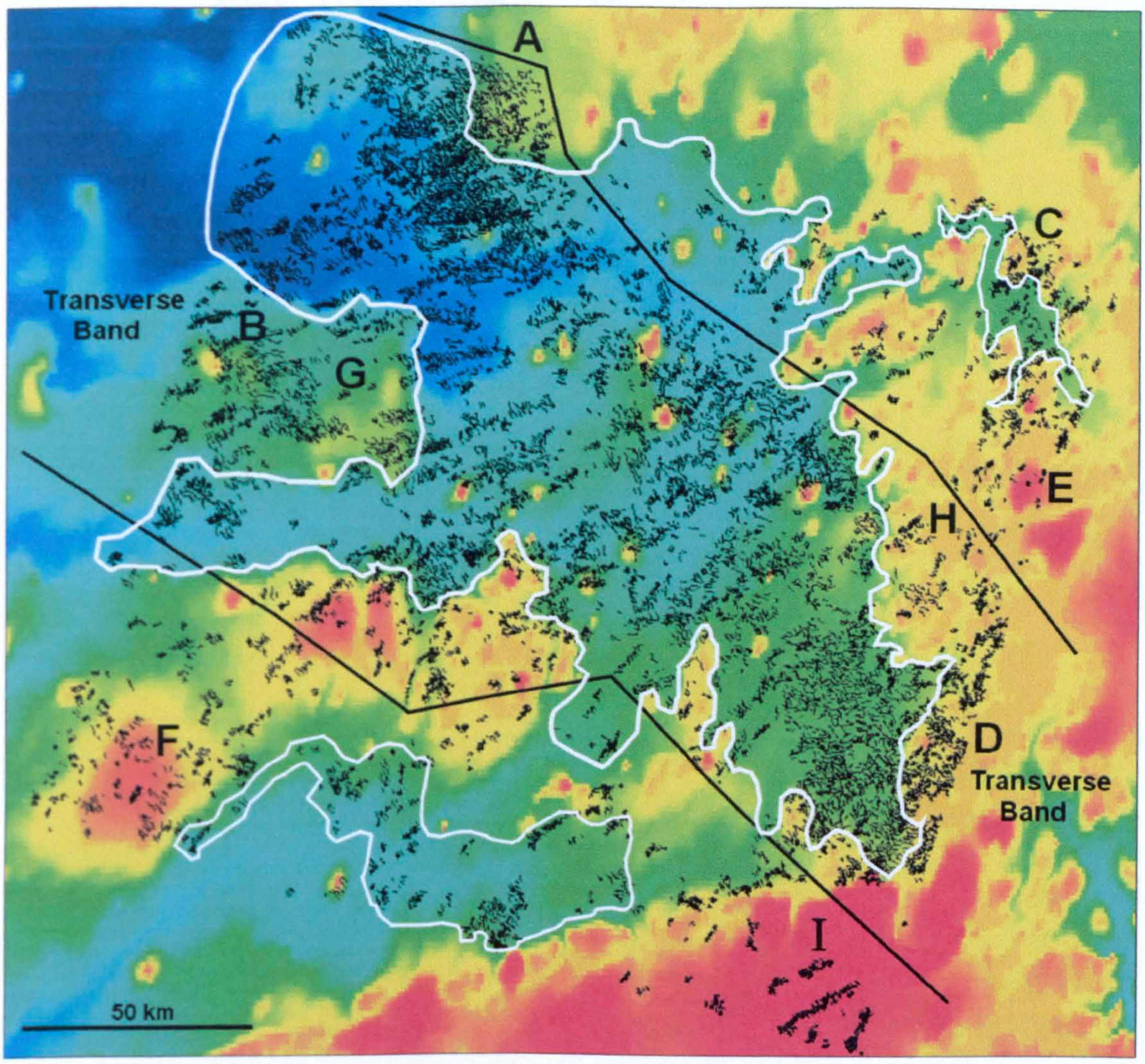

Figure 5.29. DEM of the region with the ARC coverage of the ribbed moraine crests superimposed on top. The white polygon encloses those ribbed moraine ridges situated in the major basins and valleys in the region. Note how the transverse band that runs through the centre of the study site, is made largely of ribbed moraine located in the central basin. It is estimated that approximately 75% to 80% of the ridges were formed in depressions. The remaining ridges can be found on slopes running into and out of these basins, on top of some hills and in places, open upland ground.

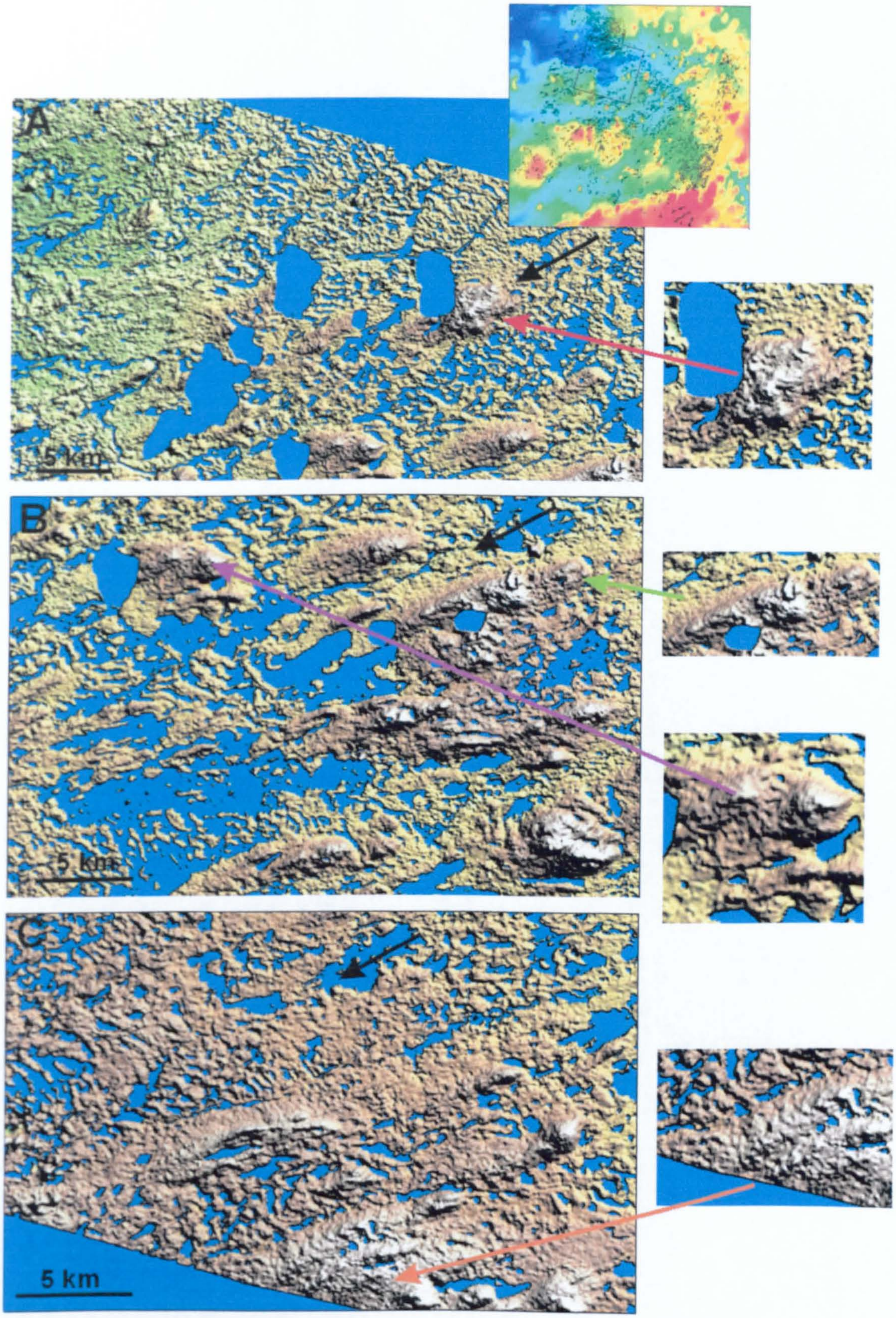

Figure 5.30. A relief image made using an ASTER DEM. These images aid investigations of topography as they give the viewer a detailed 3-D perspective of the ribbed moraine terrain. The top right hand image is a thumbnail view of the GTOPO30 DEM of the Lac Naococane area and the box shows the ASTER DEM's coverage. The images to the right of the main diagram are enlarged views of the relief image showing areas on interest in greater detail. The black arrows indicate the regional ice flow direction. Note how the more classical type ridge is largely found in the low lying areas and that the higher slopes contain shorter less sinuous ridges. Note also that ribbed moraine ridges can be seen to cover an entire hill, including the summit (Fig. 5.30a) and are also found running through narrow cols (Fig. 5.30b).

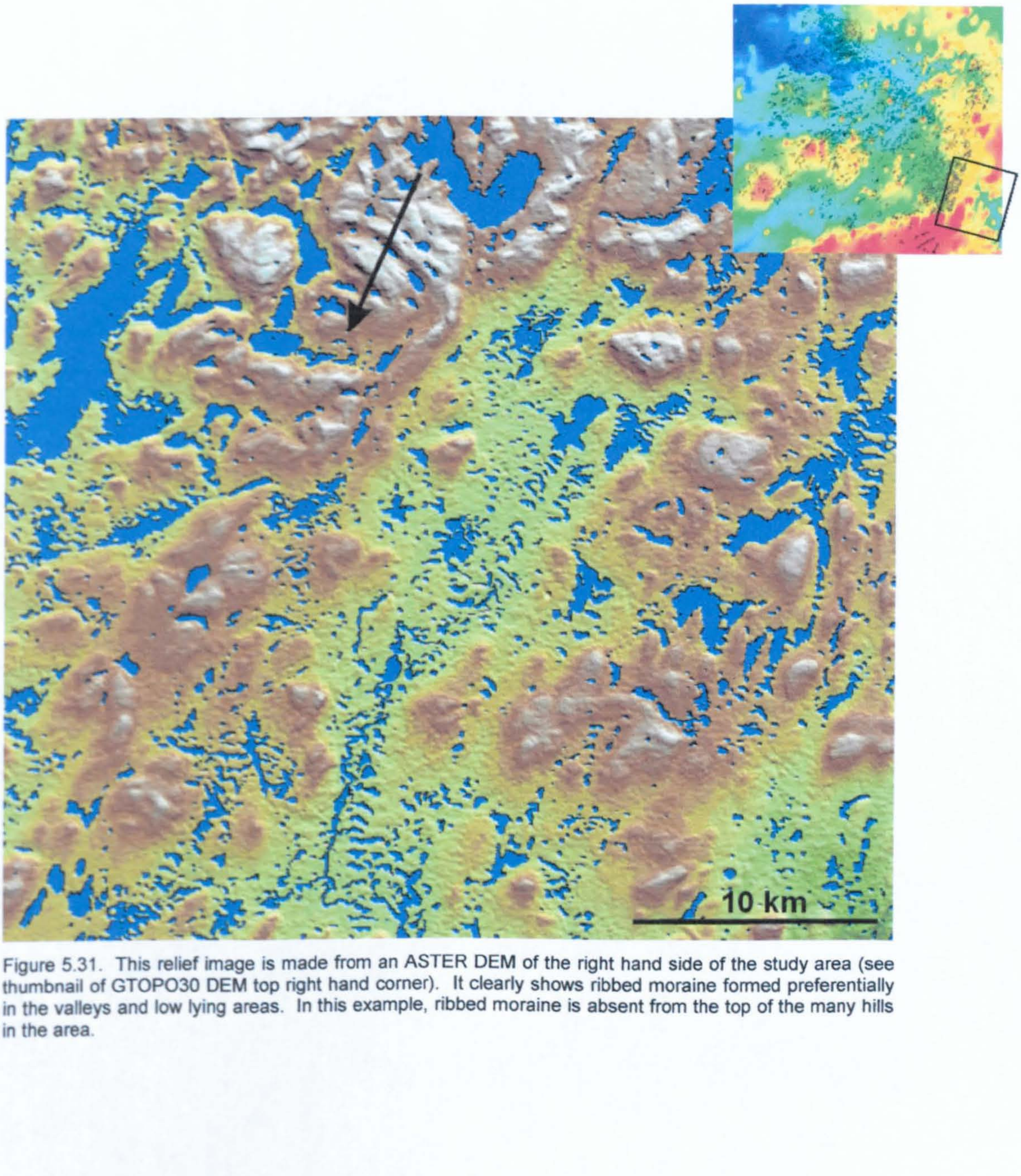

Figure 5.31. This relief image is made from an ASTER DEM of the right hand side of the study area (see thumbnail of GTOPO30 DEM top right hand corner). It clearly shows ribbed moraine formed preferentially in the valleys and low lying areas. In this example, ribbed moraine is absent from the top of the many hills in the area.

5.5.2. Relationships to slope aspect

In the Lac Naococane area, ice flowed generally from the northeast in a southwest direction across the study site. This meant that slopes facing the northeast would have experienced compressive stresses as the ice sheet flowed against them and slopes facing the southwest would have been regions of extending glacial flow as the ice flowed over them (Fig. 5.32).

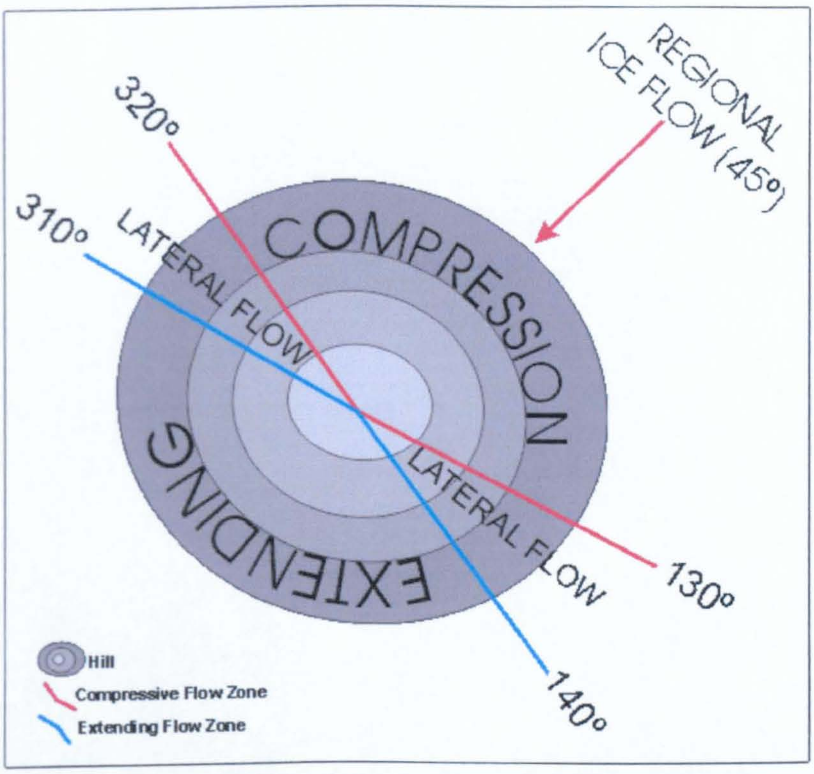

Figure 5.32. In the Lac Naococane study site ice moved across the region from a northeasterly direction. This meant that slopes facing this way would have acted as areas of compression to the oncoming ice sheet whilst slopes facing the southeast would have been areas of extending glacial flow.

To investigate whether the different stress regimes influenced ribbed moraine distribution some detailed analysis was conducted using a GIS. The first stage in this analysis involved making an aspect image of the study site using the GTOPO30 DEM. This image showed the compass direction, or aspect, of each slope in the region and colour coded the different slopes for easier visual interpretation. By defining compressive slopes as those facing 320° to 130° and extensional slopes as those facing 140° to 310° (Fig. 5.32) the GIS was utilised to map the area of both categories (Fig.

5.33) and assess the relative proportion of ribbed moraine in each category (Figures. 5.34 & 5.35).

The results of the compressive slope test showed that 43 % of the ribbed moraine population formed on slopes that experience compressive ice flow (Fig. 5.34) and areas of extending flow had 51 % of the ribbed moraine population (Fig. 5.35). Contrary to some published reports (e.g. Bouchard, 1980,1989; Minel, 1980; Sollid & Sørbel, 1984) no preferential relationship between ribbed moraine occurrence and compressive slopes was found for this sample of 12851 ribbed moraine ridges.

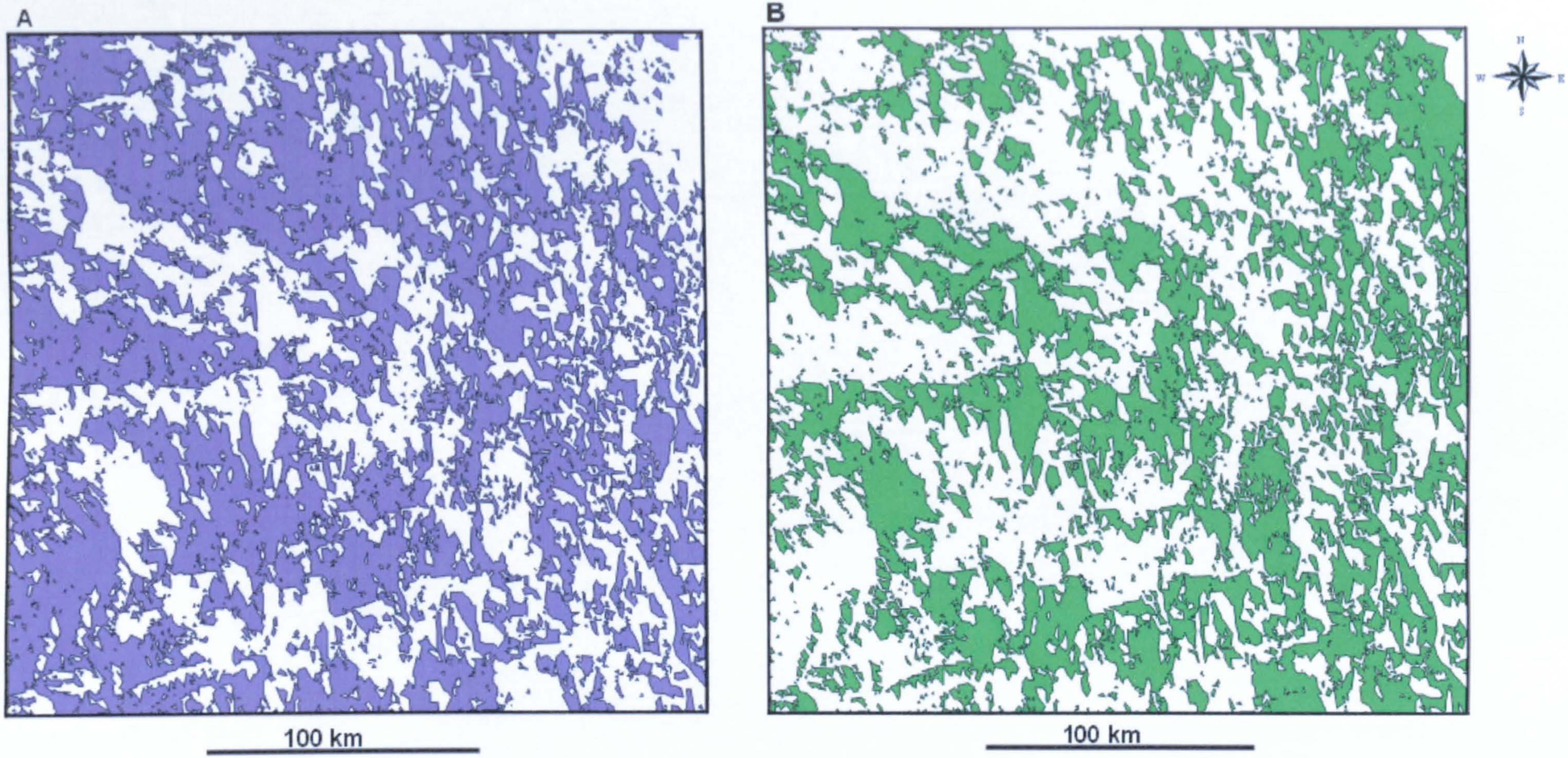

Figure 5.33. The polygon layers created in ArcView GIS, which show the total area of slopes that would have experienced extending glacial flow (A) and compressive glacial flow (B).

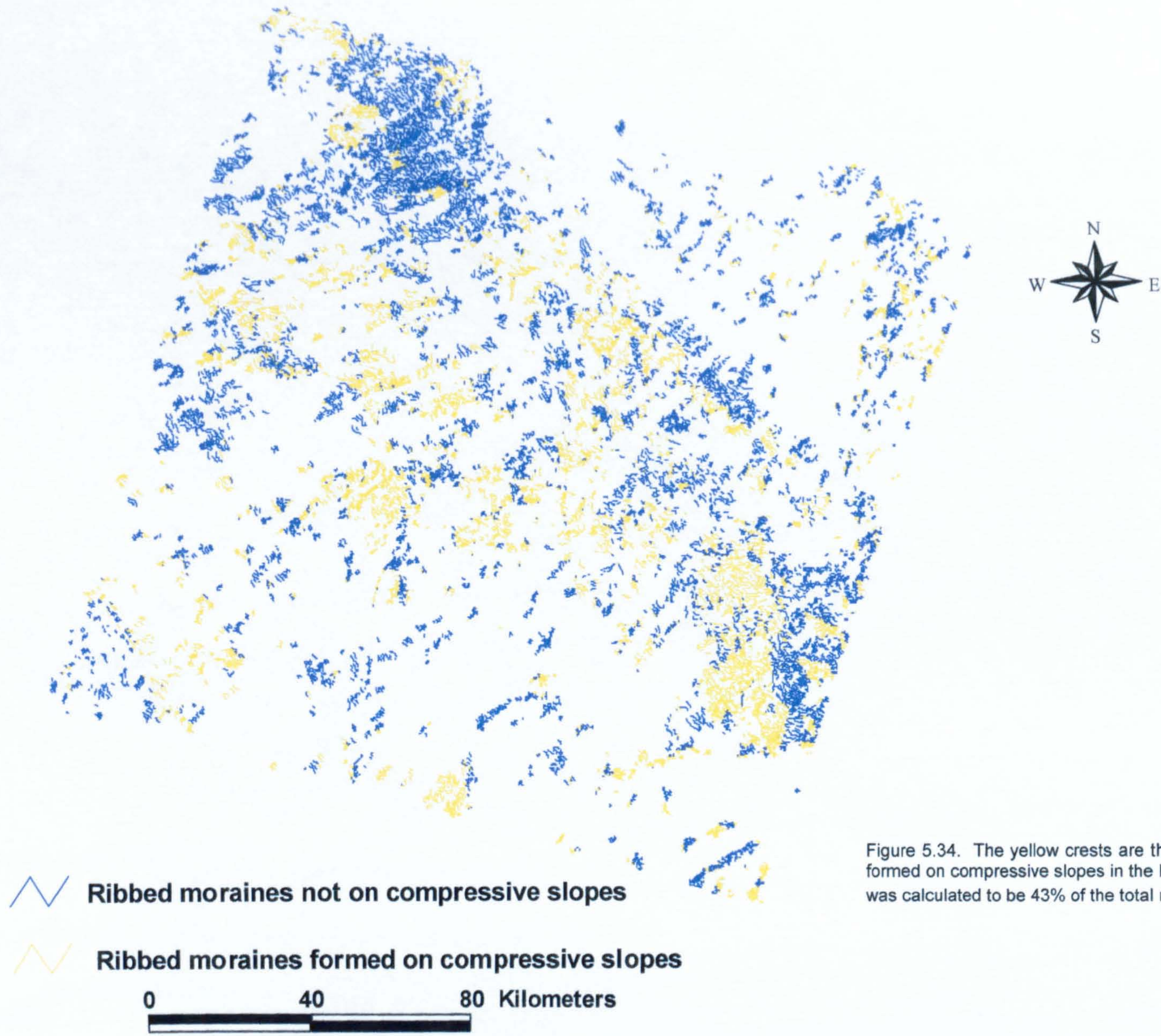

Figure 5.34. The yellow crests are the ribbed moraine ridges that formed on compressive slopes in the Lac Naococane region, which was calculated to be 43% of the total ribbed moraine population.

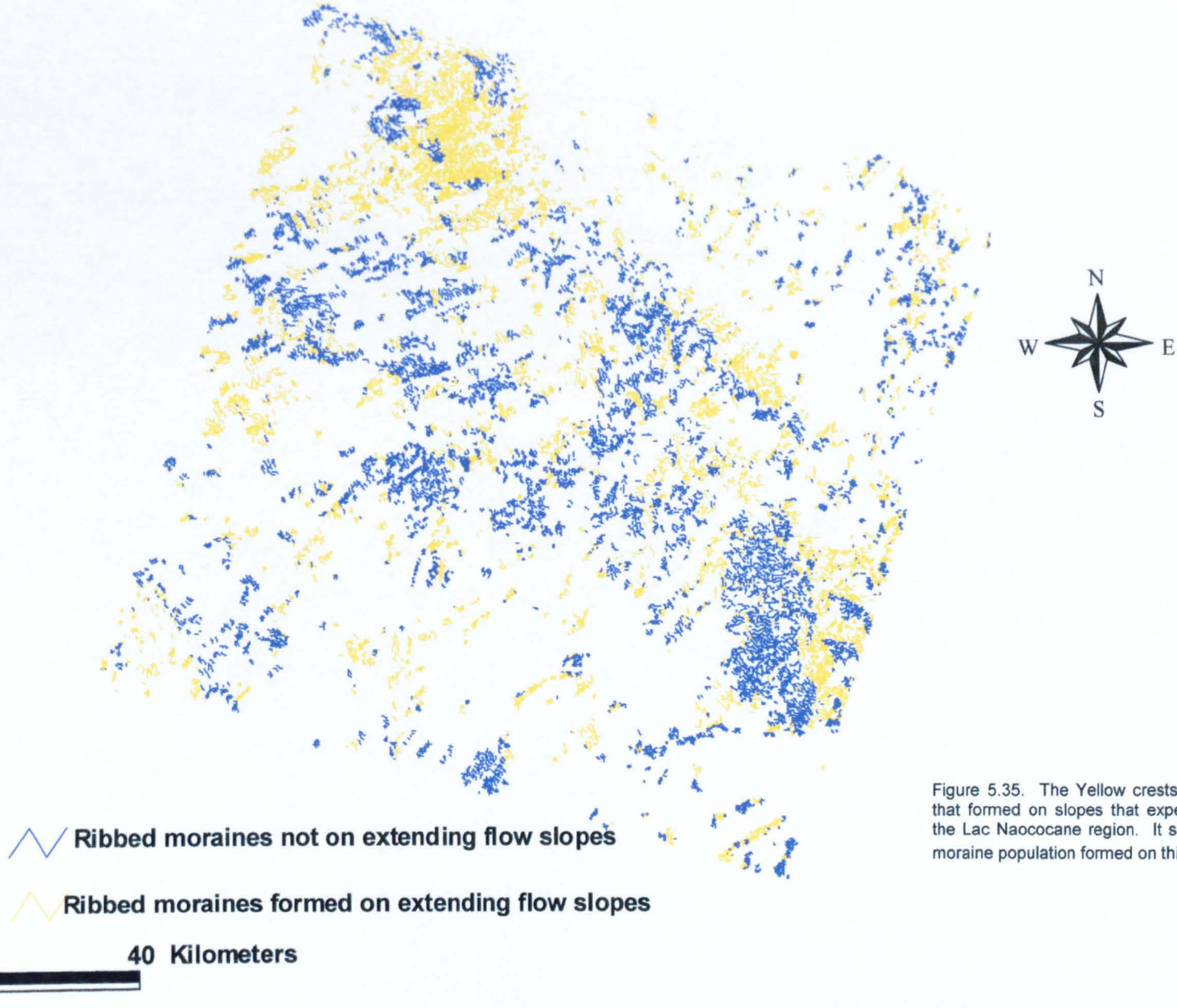

Figure 5.35. The Yellow crests are those ribbed moraine ridges that formed on slopes that experienced extending glacial flow in the Lac Naococane region. It shows that 51% of the total ribbed moraine population formed on this type of slope.

5.6. Morphometric measurements

To build a quantitative database of ribbed moraine characteristics in this region, measurements were conducted on four aspects of ribbed moraine morphometry. These were ridge height, ridge width, ridge length and ribbed moraine wavelength, which is defined as the distance between the crest of consecutive ribbed moraine ridges in the down ice direction (see Figure 4.1). The following sections report the findings for this study site.

5.6.1. Ribbed moraine wavelength

The wavelength of the ribbed moraine ridges in the Lac Naococane region was calculated using spectral analysis (see Sections 4.3.6.1 to 4.3.6.3). This involved taking transects across each ribbed moraine field in the region, exporting these data into SPSS and then conducting spectral analysis to produce periodograms which showed the frequency spectrum of each transect. The frequency spectrum was then used to determine the wavelength of the ribbed moraine ridges along each transect. In this locality, data from transects totalling 10852 km in length were used to obtain the wavelength data. These data were then used to make a histogram to show the wavelength distribution of the ribbed moraine at this locality (Fig. 5.36). The majority of ribbed moraine ridges in the region have wavelengths ranging between 250 m and 1000 m, which represents 96.8% of the total sample. The other 3.2% of ridges have wavelengths between 1050 m and 1800 m. The smallest wavelength measured was 172 m, the largest was 1800 m, the average wavelength was 498 m and the most frequently occurring wavelength, the mode, was 320 m.

To examine the spatial distribution of ribbed moraine wavelength some analysis was conducted using a GIS to produce density maps. High density represents short wavelengths and vice versa, therefore, mapping the density acted as a surrogate for mapping ribbed moraine wavelength. A sampling grid of 180 km by 180 km covering the region was constructed in the GIS, placed on top of the ribbed moraine Arc coverage and all the ribbed moraine ridges inside each grid cell were counted (Fig. 5.37). However, there were two problems using this approach. The first was choosing a suitable grid cell size, but as 98% of the ribbed moraine ridges in this area were found to be less than 2500 m long (see Section 5.6.2 below) a grid cell size of 2500 m was chosen. This at least ensured a greater chance that the cells would contain entire ridge crests rather than many segments, which would be the case if a cell size smaller than this were chosen. Even so, when draping a grid on top of any set of lines segmentation is unavoidable and some overlap has to be expected. The other problem was that in some instances a cell might only contain a few ribbed moraine ridges, which may be very closely spaced, so, a small count does not necessarily indicate ribbed moraine ridges with long wavelengths. Nonetheless, the results provide a good indication of how ribbed moraine density (and wavelength) varies across the region.

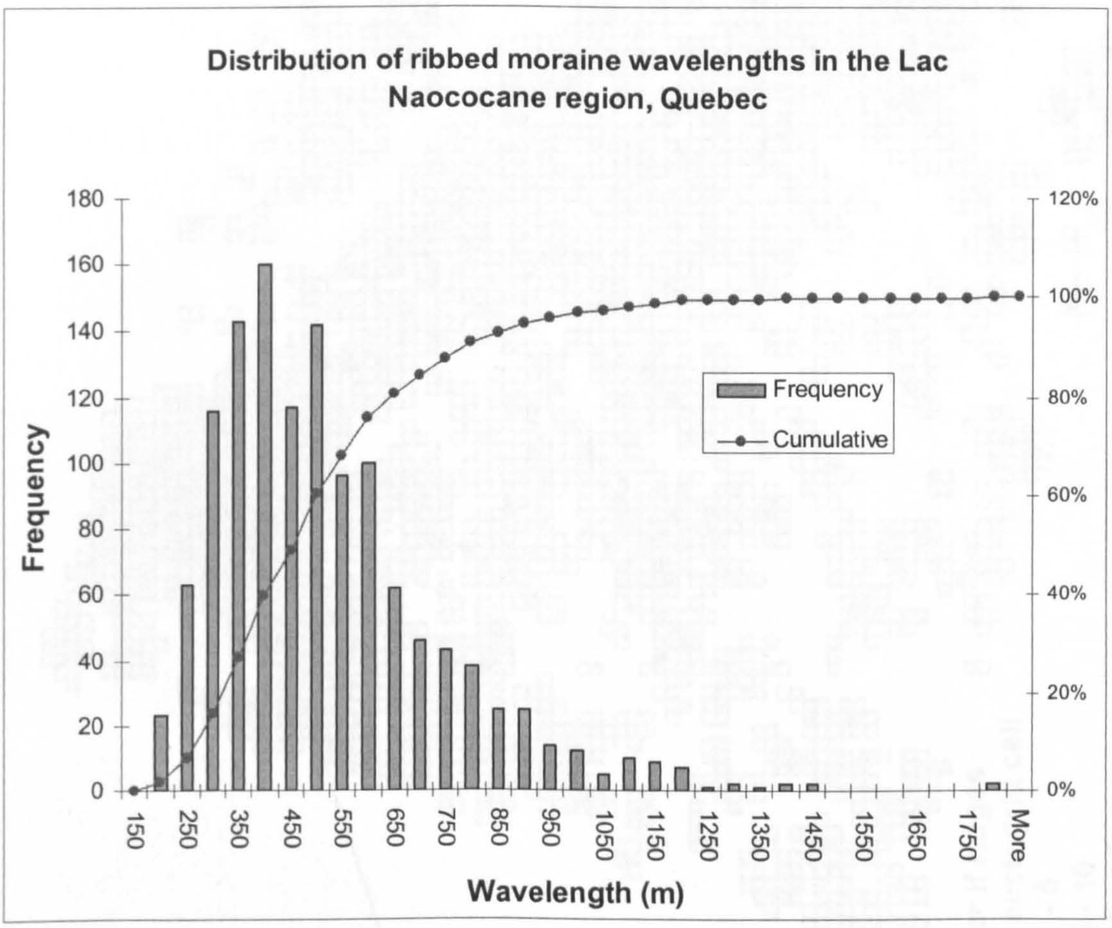

Figure 5.36. Distribution of ribbed moraine wavelengths determined by spectral analysis from transects totalling 10852 km.

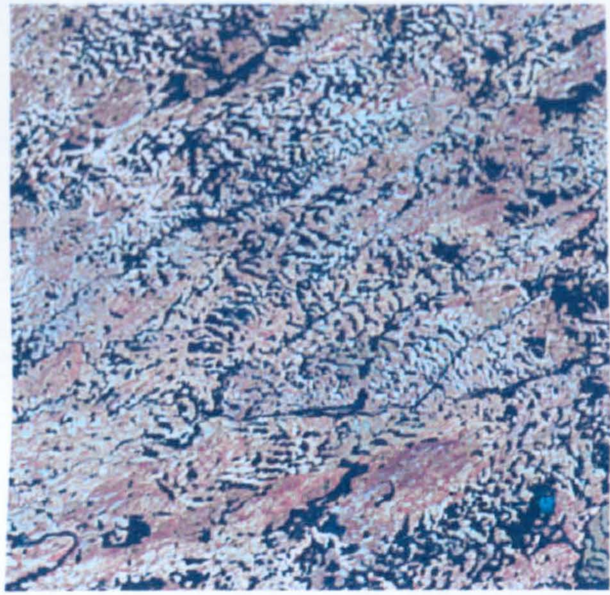

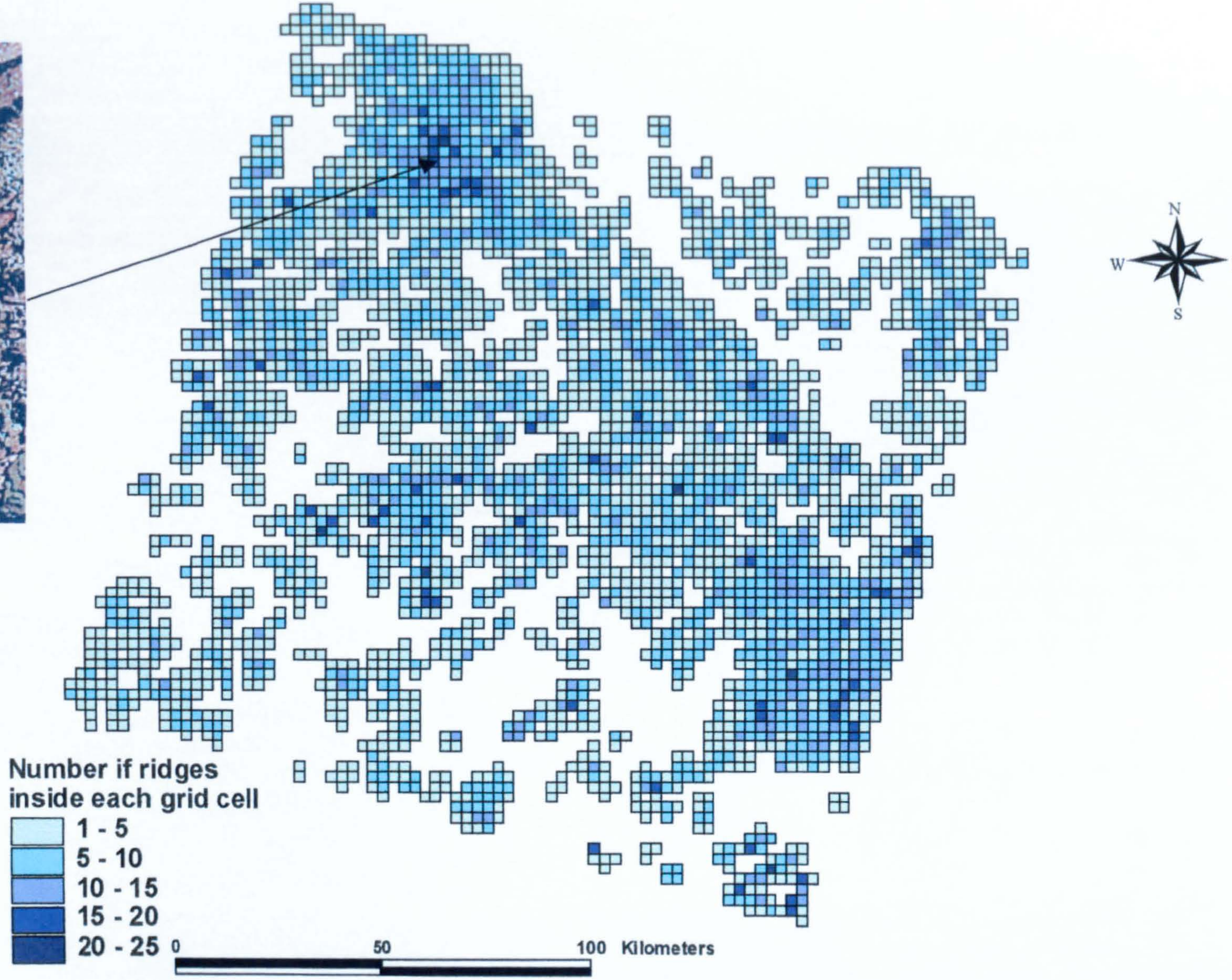

Figure 5.37. An impression of where ribbed moraine ridges with short / long wavelengths are situated in the region can be obtained from this map of ribbed moraine density. The darker the shade of blue, the more densely packed the ridges are and the shorter the spacing, or wavelength between the ridges. The picture above was taken from a Landsat MSS image of the area of very densely packed ridges situated at the top left of the map. Note how a cluster of densely packed ribbed moraines are surrounded by less densely packed ridges. Visual inspection of the map and the satellite image showed a tendency for more classic type ridges like those shown here to have a shorter wavelength than more poorly formed ridges.

Most parts of the study site have regions of ribbed moraine with mixed wavelength (Fig. 5.37). However, the largest concentration of ribbed moraine with shorter wavelengths are found in the area of the transverse band. The band itself has the two largest clusters of closely spaced ridges, which on close inspection showed them to be made of well-formed classic type ridges (see Figure 5.37). Visual inspection of the imagery found this observation to be generally true of most places containing ribbed moraine of short wavelengths. The opposite appeared to be the case with regions containing ribbed moraine of longer wavelengths, which tended to be comprised of poorly formed type ridges.

To investigate whether topography influenced ribbed moraine wavelength, the intersected grid was laid on top of the GTOPO30 DEM (Fig. 5.38) to visually examine for any obvious patterns. This showed that there was no single topographic setting where one could find a ribbed moraine of a certain wavelength. For example, ribbed moraine ridges with short wavelengths could be found on slopes leading into basins (A), within the main axis of large central basin (B) and on the tops of hills (C). However, the majority of ridges with shorter wavelengths tended to be on gentle slopes rather than in the basins or hilltops. Ribbed moraine ridges with longer wavelengths were also found in various topographic settings, and could be located in both basins (D) and on top of hills (E). No systematic relationship was found between wavelength and topographic setting.

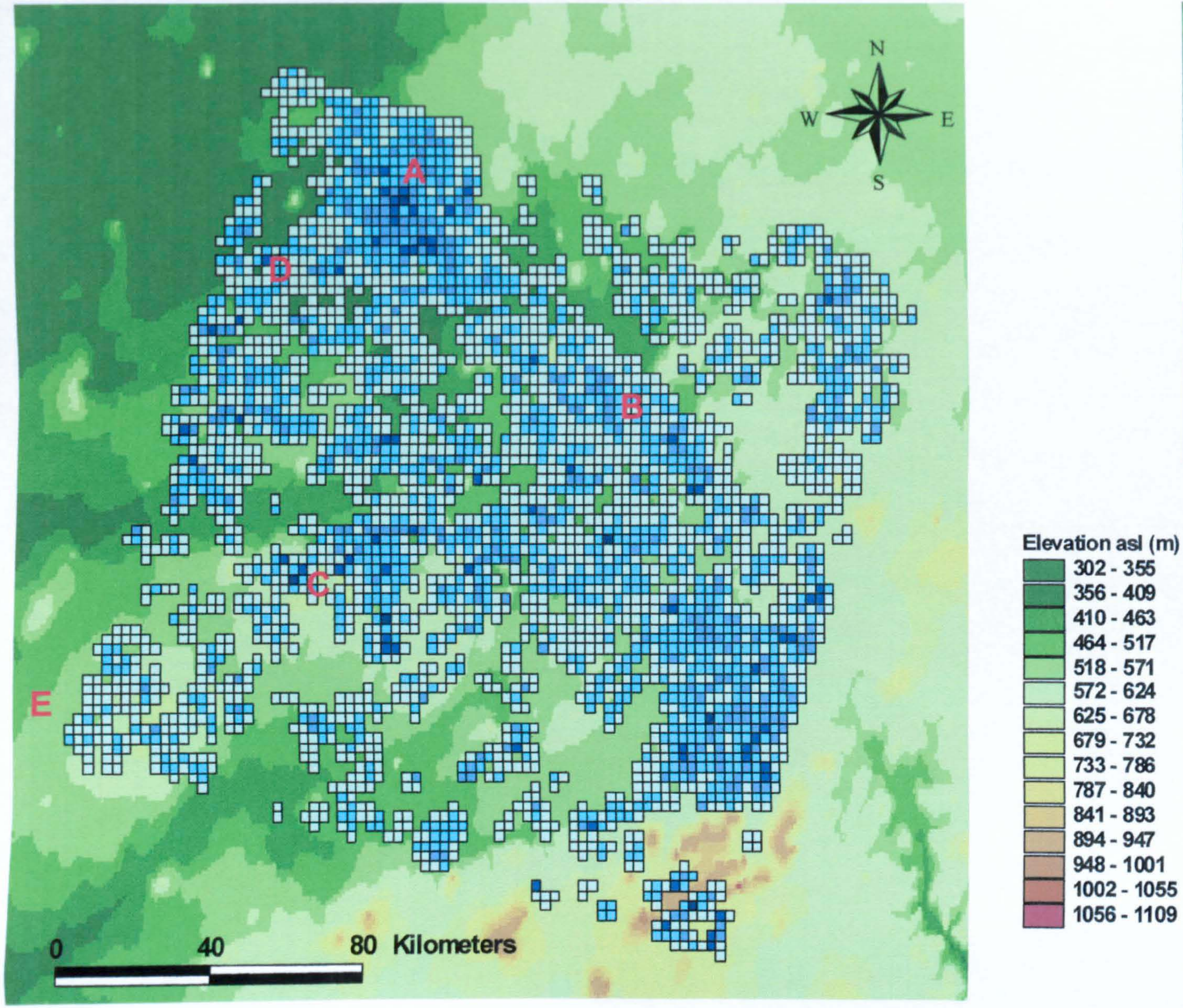

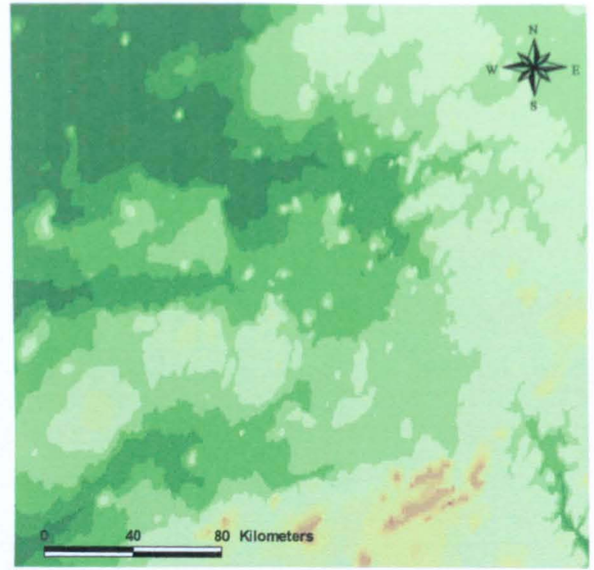

Figure 5.38. By draping the ribbed moraine density map on top of a DEM of the study site a visual assessment could be carried out to determine whether topography influenced ribbed moraine wavelength. The fact that there was no single topographic setting were ribbed moraine ridges of a particular wavelength could be found suggested that topography does not influence ribbed moraine wavelength. For example, note how ribbed moraines with both short and long wavelengths are located in a variety of topographic situations.

5.6.2. Ribbed moraine ridge length

Information on the length of the ridges in the study site was obtained by accessing the attribute table of the mapped ribbed moraine ridges contained in the ARC coverage. This table contains the recorded length of each digitised line (ridge crest) and was used to plot a histogram showing the distribution of ridge length (Fig. 5.39). In the study area, 98% of ridges are between 200 m and 2500 m in length. The minimum ridge length was found to be 180 m, the maximum 5967 m and the mean ridge length 918 m. It should be noted that there is a possibility of there being smaller ridges in this locality; however, the 80 m pixel resolution of the MSS image limited the abilities to discern below this resolution.

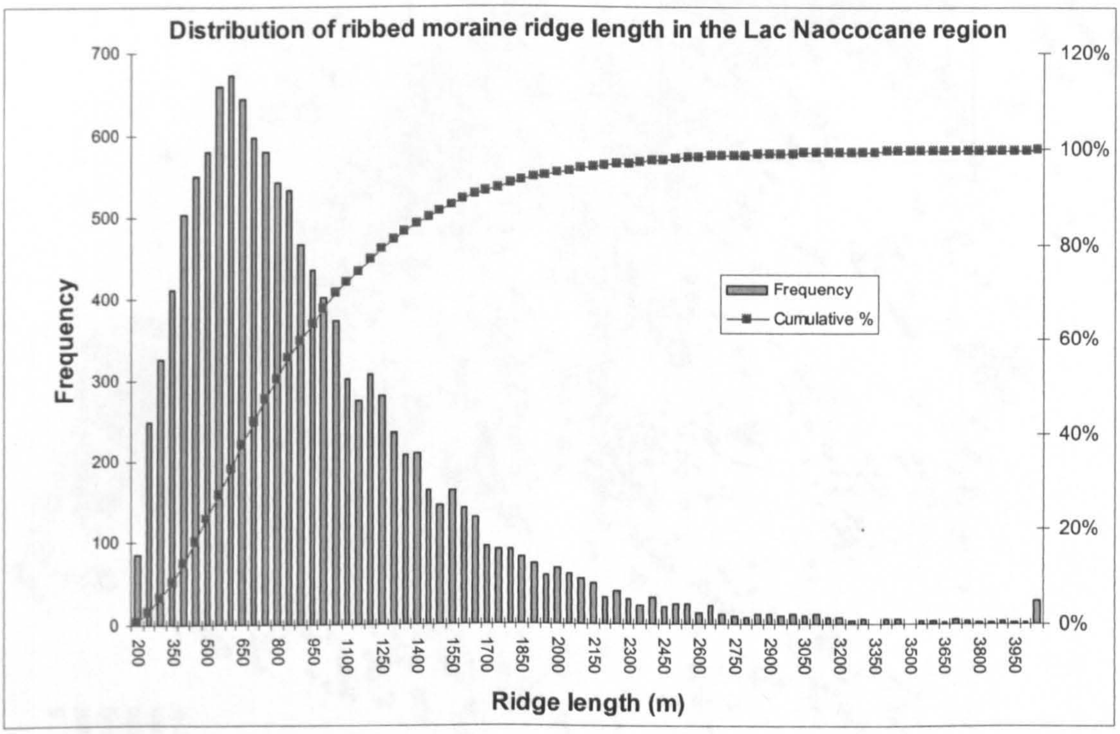

Figure 5.39. Distribution of ribbed moraine ridge length from a sample of over 12000 mapped ridges in the Lac Naococane region. 90% of the ribbed moraine ridges range in length from 200m to 2000 m, with the maxima at 600 m.

To visually explore these length data, the ribbed moraine crests were classified into groups of various lengths (Fig. 5.40). Two obvious patterns emerged from this study. Firstly it showed that all of the longer ridges in the region were located in the area referred to as the Transverse Band. Outside this, the vast majority of ridges were less than 1000 m long. Secondly it overwhelmingly demonstrates that the ribbed moraine fields in the Lac Naococane region are made up of ridges of various lengths (Fig. 5.41), without any consistent clustering of fields of a certain length.

Figure 5.40. Ribbed moraine crests classified into 5 separate groups based on ridge length. Note how the vast majority of the longer ridges, i.e. those above 1000 m long are located largely in the area referred to as the transverse band. Note also how most ribbed moraine fields contain ridges of mixed length. The area marked by the box is enlarged in figure 5.41 to illustrate this more clearly.

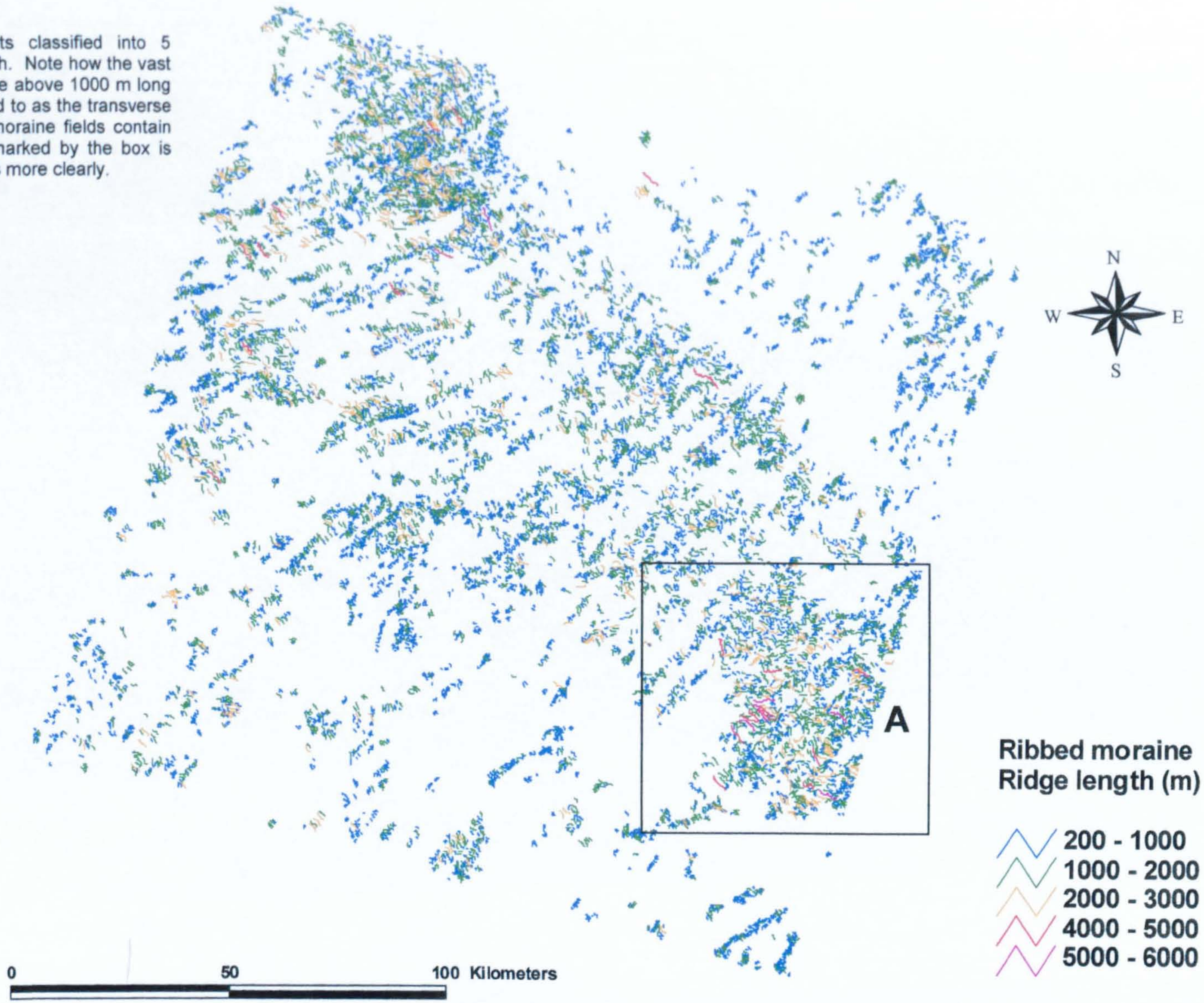

Figure 5.41. Enlarged view of the ribbed moraine field marked by the box in figure 5.40. Note how the field is made up of ridges that vary quite dramatically in length.

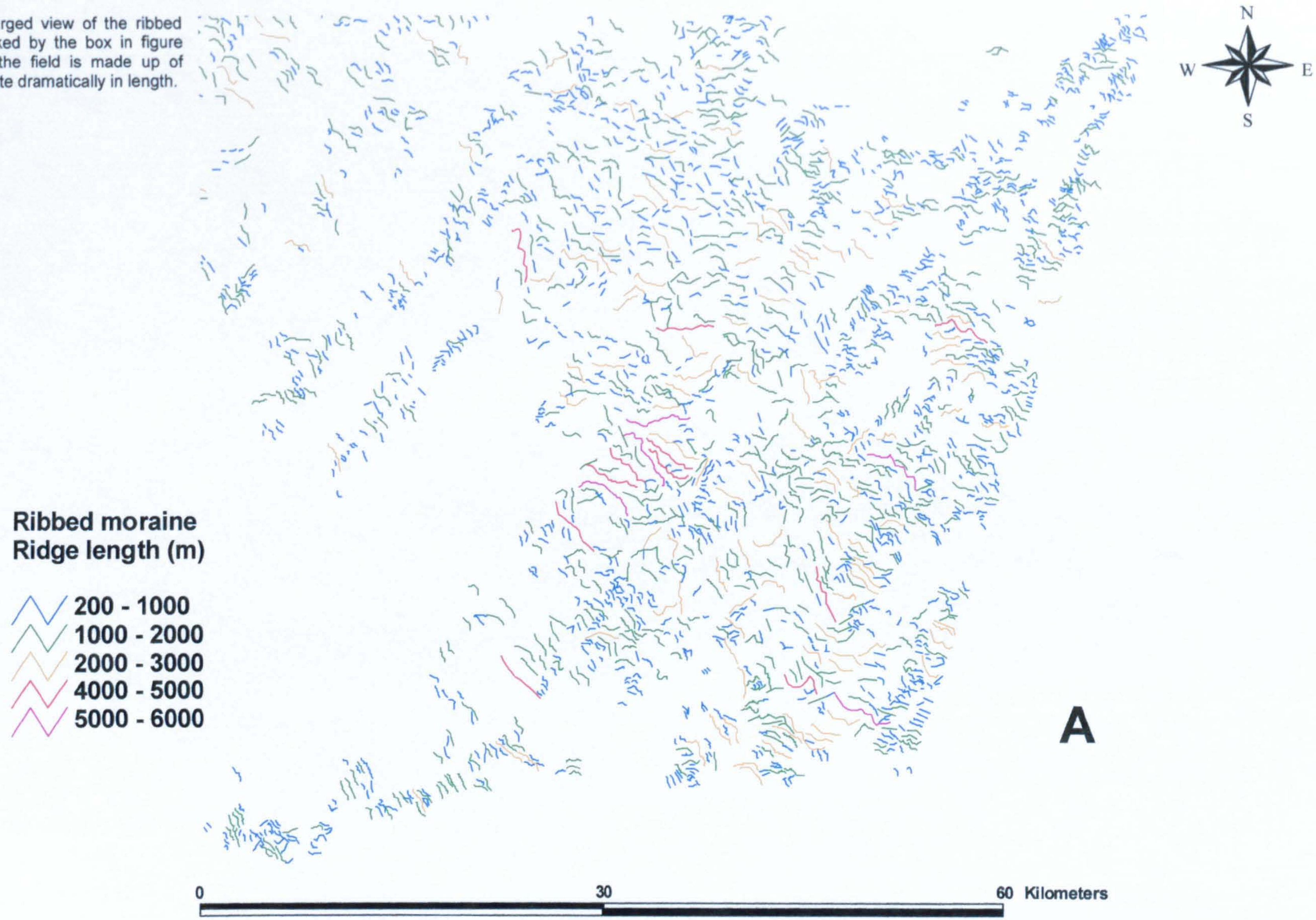

5.6.3. Ribbed moraine ridge height

Information on the heights of the ribbed moraine ridges was obtained using the ASTER DEM's. Transects were taken across 500 randomly sampled ridges and the distance and elevation data, along with the map coordinates of each transect, were exported into a spreadsheet package. Using the distance and elevation data, scatter plots were constructed to show the profile in graphical form. By viewing the graphs on-screen and pointing the cursor at the bottom and top of each peak elevation readings were obtained which were then used to work out the height of the ridge (Fig. 5.42). To verify that all the peaks were caused by the occurrence of ribbed moraine and not other topographic features it was necessary to check the DEM. The map coordinates that were exported along with the other profile data show the exact location of every elevation and distance value on the DEM. Using this information it was possible to view the feature on the DEM that caused the peak. If a ribbed moraine did not cause it, it was rejected and its height was not recorded. Consistently checking the data in this manner reduced errors and helped keep the data set accurate.

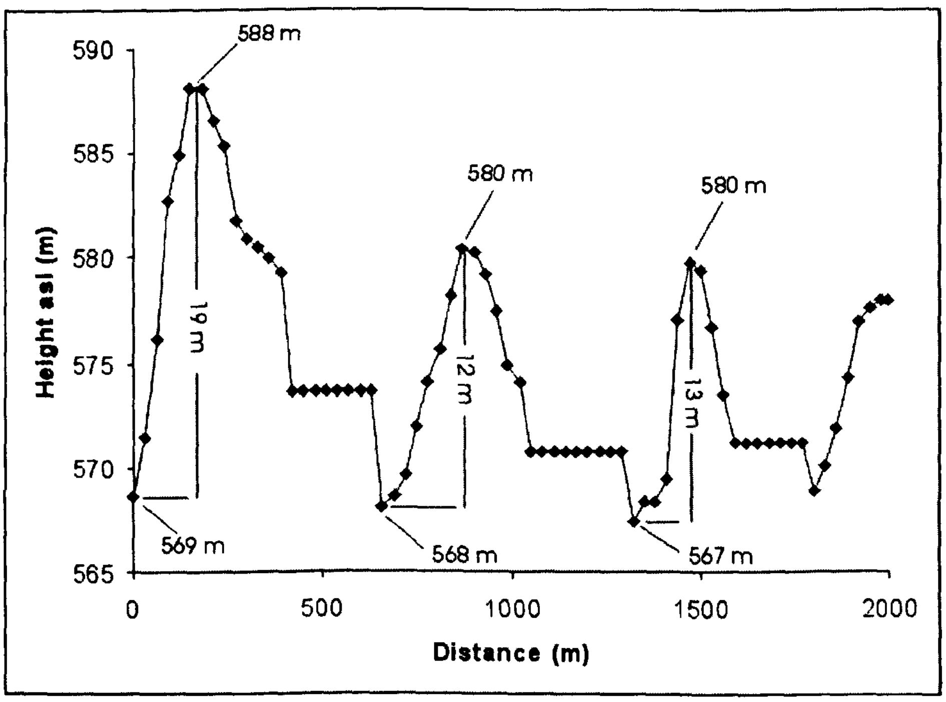

Figure 5.42. A working example of how the ribbed moraine ridge height was measured. The elevation at the base of the ridge is recorded along with the highest point on the ridge. The height is calculated by taking the difference between the two values. In the example shown above the ridges are 19 m, 12 m, and 13 m respectively.

The height distribution of the sampled ridges can be seen in Figure 5.43, which shows the majority of ridges have heights ranging between 1 m and 22 m. However, a reasonable number of ridges are much higher than this and over 8% of the ribbed moraine ridges sampled had heights ranging between 22 m and 40 m high with the remainder being between 40 m and 64 m in height.

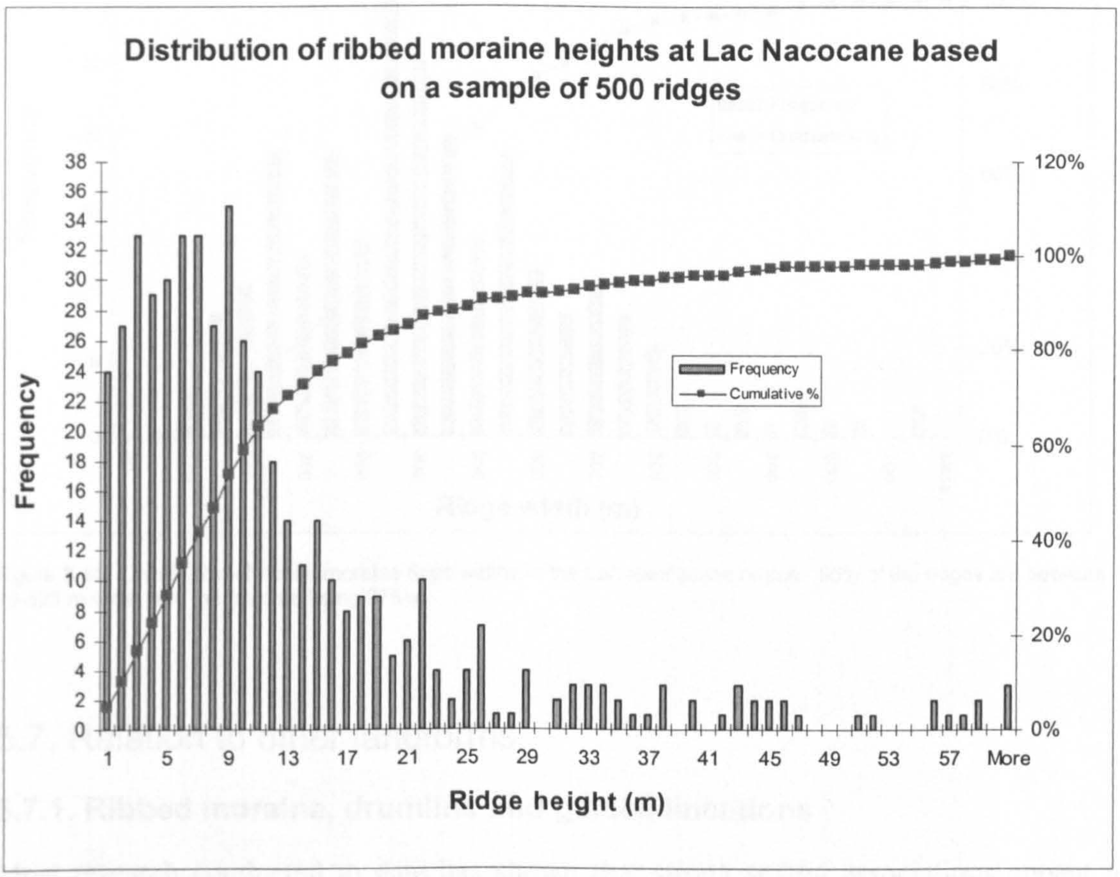

Figure 5.43. The distribution of ridge heights from a sample of 500 ribbed moraine ridges in the Lac Naococane region. 87% of the ridges sampled ranged between 1 m and 22 m in height. However, a large number of ridges were found to be much higher with the maximum height recorded being 64 m.

5.6.4. Ribbed moraine ridge width

To investigate the width of the ribbed moraine ridges in this region a sample of 250 ridges were chosen randomly from various locations across the site. Using a GIS, lines were digitised across the width of each ridge and then data were obtained via the attribute table regarding their width which were exported into a spreadsheet. A histogram was plotted using these data to show the distribution of ridge width in this region (Fig. 5.44). In this sample, 95% of ridges are between 70 m and 550 m wide.

The minimum ridge width was found to be 76 m, the maximum 715 m and the mean ridge length 298 m.

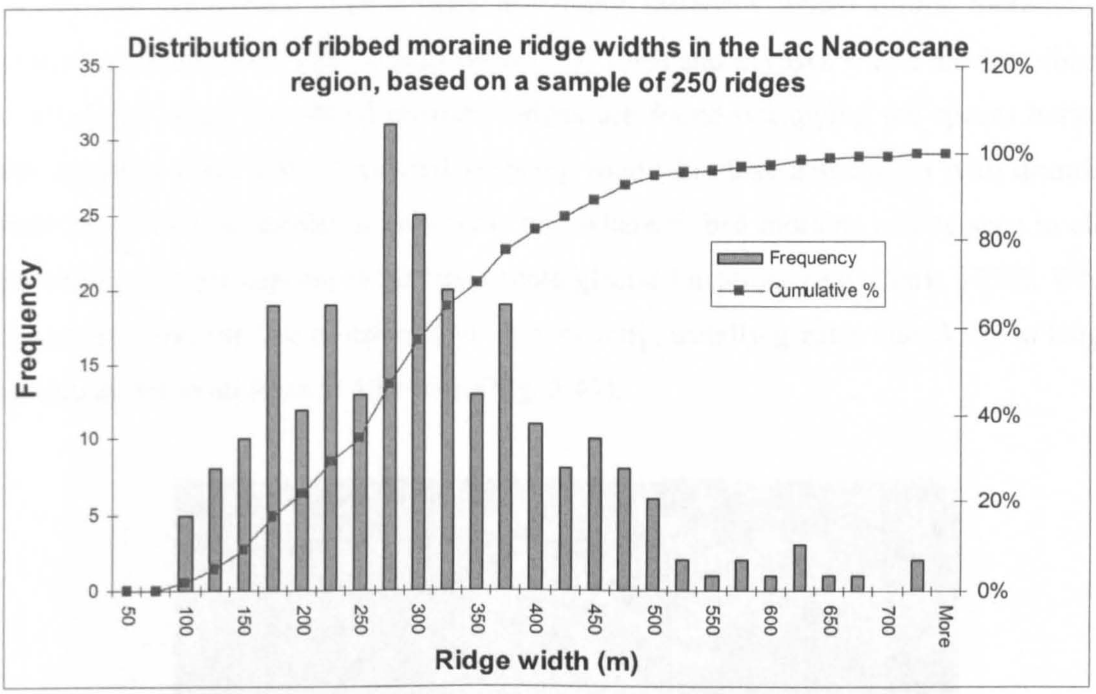

Figure 5.44. Distribution of ribbed moraine ridge widths in the Lac Naococane region. 95% of the ridges are between 70-525 m wide, with the maxima being 275 m.

5.7. Relation to other landforms

5.7.1. Ribbed moraine, drumlins and glacial lineations

Most research conducted to date has shown that strong spatial associations appear to exist between ribbed moraine and drumlins. Both landforms have been found in a variety of settings and it has been noted how ribbed moraine in basins commonly passes into drumlins on topographic highs (Markgren and Lassila, 1980; Lundqvist, 1969, 1989) yet are found together on flat ground (Aylsworth and Shilts, 1989; Lundqvist 1989).

Close examination of the ribbed moraine in the Lac Naococane region found that drumlinization and fluting on the ridges was a rather common feature (see Section 5.4 above). In most cases the drumlinization is at right angles to the ridges and can thus be associated with an ice-flow direction similar to the ribbed moraine formation. In some areas, the original structure of the ridge had been altered so much by drumlinization that the ridges might be best thought of as drumlinized ribbed moraine (see Figures 5.14 & 5.15). It may well be the case that these types of ridges represent a transitional stage between a true ribbed moraine ridge and a drumlin.

In the Lac Naococane region there are many instances where ribbed moraine and drumlins can be found next to each other (Fig. 5.45) and in cases where the drumlins are particularly large, the ribbed moraine ridges are found occupying the spaces between the drumlins (Fig. 5.46). As well as being found in close association with drumlins, there are several examples in this study site where ribbed moraine can be seen in close proximity to what appears to be mega-scale glacial lineations (e.g. Clark, 1993). Where this is the case, the lineations tend to be very long, usually greater than 3 km in length, and range between 50 m to 150 wide (Fig. 5.47).

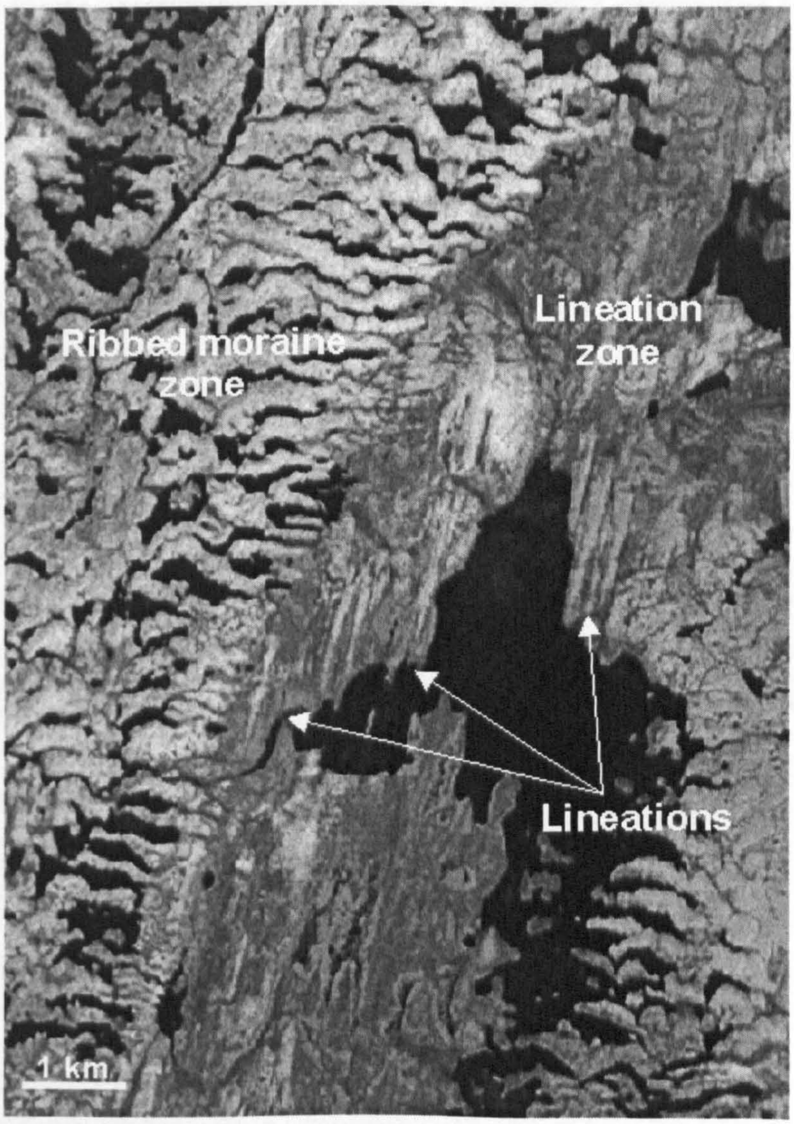

Figure 5.45. ASTER image illustrating an abrupt lateral transition between ribbed moraine and glacial lineations. Note that in this case there appears to be no overprinting of the ribbed moraine ridges and there is exclusivity of landforms.

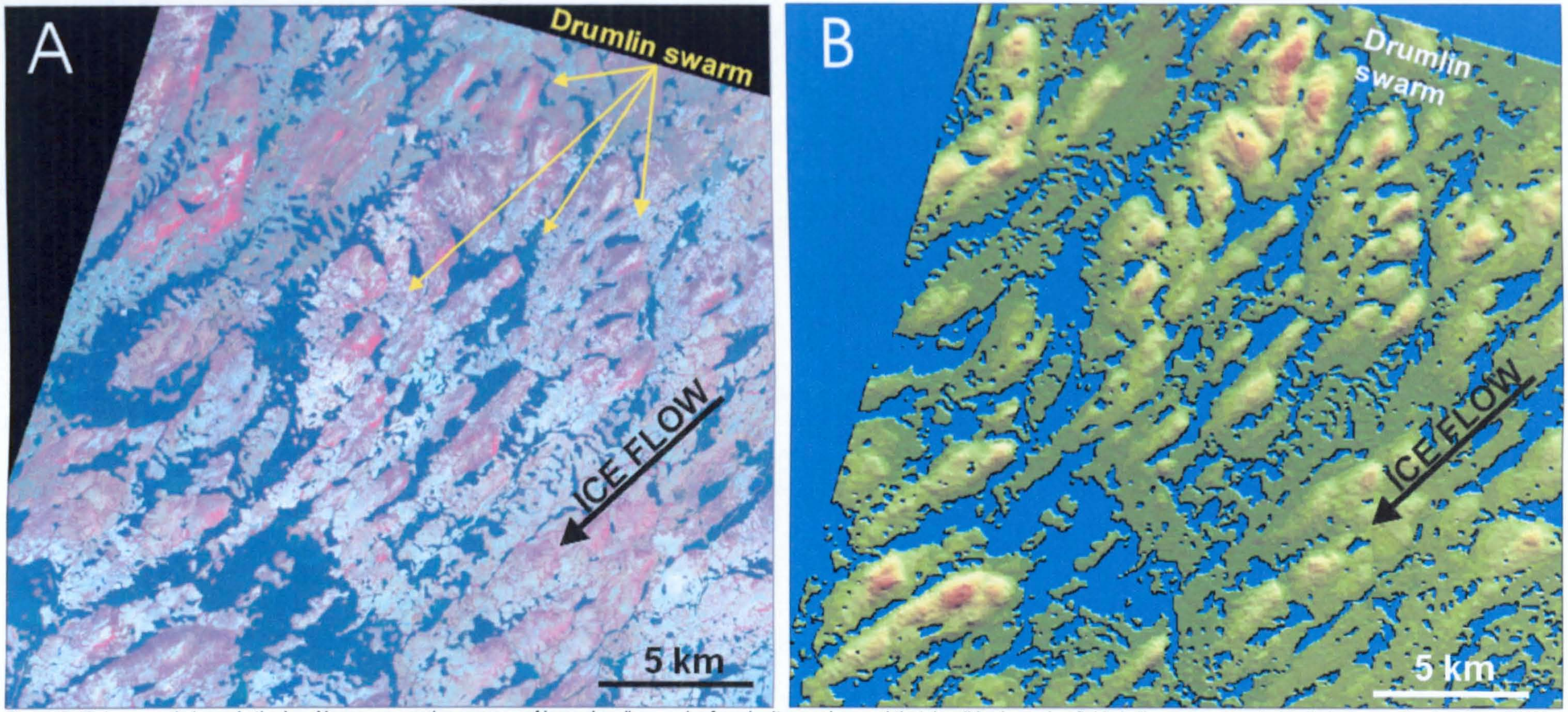

Figure 5.46. In several places in the Lac Naococane region swarms of large drumlins can be found. It was observed that the ribbed moraine fields in these areas tended to lie between the drumlins. This is shown clearly in the above images, which were taken from an ASTER satellite image (Figure 5.46a) and a relief image of the same area that was made from an ASTER DEM (Fig. 5.46b).

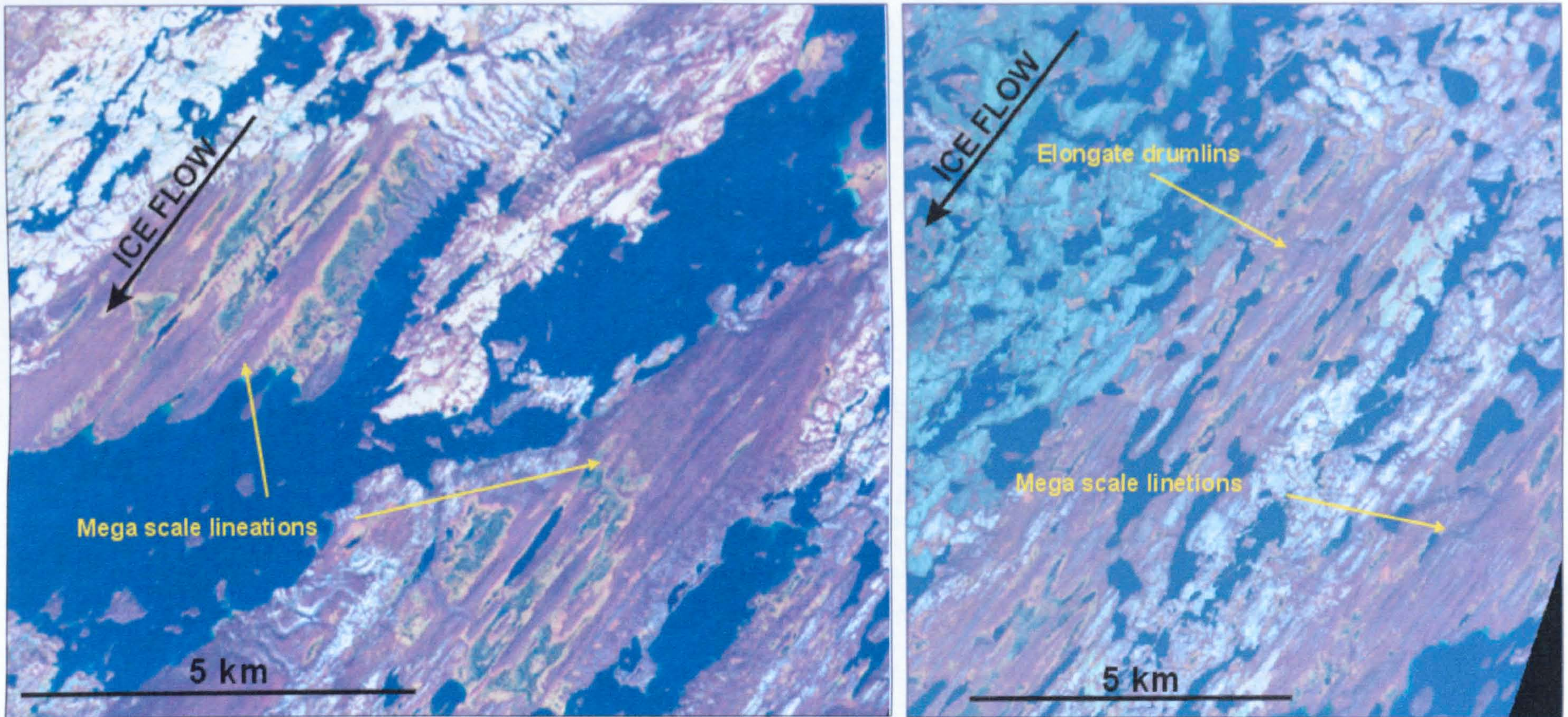

Figure 5.47. ASTER satellite images showing two ribbed moraine fields in close proximity to drumlins and mega-scale glacial lineations. The figure on the left shows a field of classic type ribbed moraine ridges of varying scales. The ridges show no obvious signs of drumlinization yet immediately downstream and to the right elongate spindle drumlins and mega-scale lineations are clearly present. The figure on the right shows a ribbed moraine field with some spindle type drumlins and mega-scale lineations situated immediately down-stream from the ribbed moraines. Note the appearance of the ribbed moraine ridges which show signs of drumlinization, and that this has occurred immediately upstream from the lineations. It may be the case that this area marks a transition zone where the ribbed moraines were transformed by the overriding ice sheet into drumlins and mega-scale glacial lineations.

5.7.2. Ribbed moraine and eskers

Many eskers are clearly evident snaking their way through the Lac Naococane region (Fig. 5.48). They were always observed to be draped on top of the ridges and can be seen in a variety of settings with ribbed moraine. They are found at the edge of ribbed moraine fields, weaving across entire fields at various angles to the alignment of the ridges and running through meltwater cuts in the ridges. Nowhere was it observed that eskers were associated with a particular size or shape of ribbed moraine ridge and in many places they cross over areas where ribbed moraine is absent. The fact that all the eskers observed in the region were draped on top of the ridges is evidence that they post-date ribbed moraine formation and were laid down during final deglaciation.

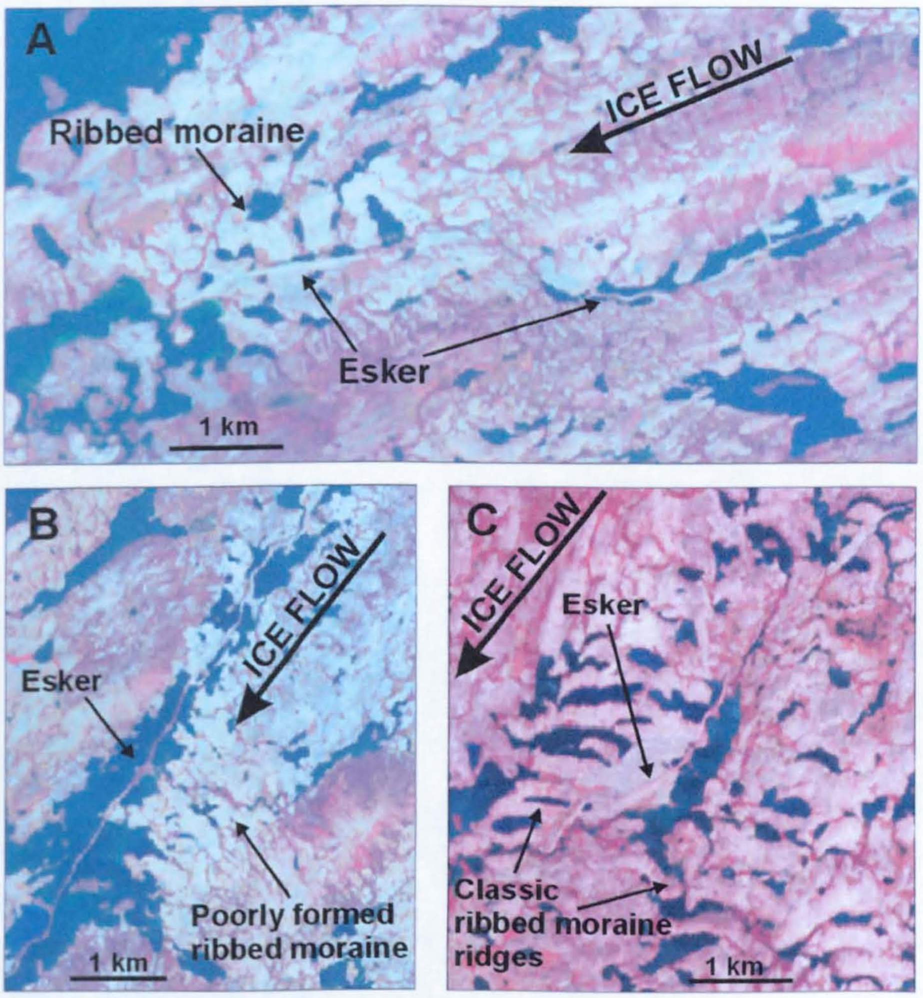

Figure 5.48. Many eskers meander their way through the Lac Naococane region and are found in a variety of settings together with ribbed moraine. They can be seen running across ribbed moraine fields at various angles to the ridges (Fig. 5.48a & 5.48b) and can be seen positioned next to ribbed moraine fields (Fig. 5.48c). Note the variety of ridge forms and also that the eskers are always superimposed on top of the ribbed moraine ridges. Nowhere in the study site was it observed that ribbed moraine formed on top of eskers and is evidence that eskers came after the ribbed moraine ridges were formed. Images made from ASTER satellite imagery.

5.8. Summary and conclusions

Using satellite imagery to map large areas of ribbed moraine in the Lac Naococane region established that the ribbed moraine was produced approximately synchronously and most likely belonged to the same ice flow event. The large-scale distributional pattern revealed that the majority of ribbed moraine ridges in the region were concentrated in a large swathe across the study area, known as the transverse band (see Figure 5.4). This band contained many large ribbed moraine fields that were up to 45 km wide and over 50 km long. Outside the band, the ribbed moraine fields tended to be smaller and more spatially dislocated. The overall impression given was that conditions for ribbed moraine formation were more favourable within the area of the transverse band.

Close inspection of the site revealed that ribbed moraine was distributed in various patterns that were summarised into 4 general categories. These were, elongate ribbons, narrow tracks, clusters and isolated fields. Each field type was not restricted to a particular area within the study site and examples of each could be found at various locations across the region. Surprisingly it was also possible to find one field type within the confines of another and Figure 5.8, which shows some narrow tracks running through ribbed moraine clusters and ribbons illustrates this point clearly. This is an important observation because it highlights the fact that the ribbed moraine forming process can operate at different scales within a confined area.

Large-scale visual observations of ribbed moraine ridges in this region revealed a diverse range of morphology. These have been summarised in Figure 5.49, which gives a good indication of the complexity in form between the various types. What became evident from mapping the fields was that many ridges were morphologically different from the more classic type that is often described in the literature and that most fields contained ridges of mixed morphology (see Figures 5.12 & 5.13). This was an interesting observation and has implications for formative theories because for any theory to be credible it must be able to explain the various forms.

Using DEM's to investigate the topographic setting of the ribbed moraine in the study area revealed that most ribbed moraine fields were situated in basins and depressions (see Figure 5.29), which is consistent with other observations cited in the literature. Nonetheless, approximately 20% of the ribbed moraine ridges were observed on high

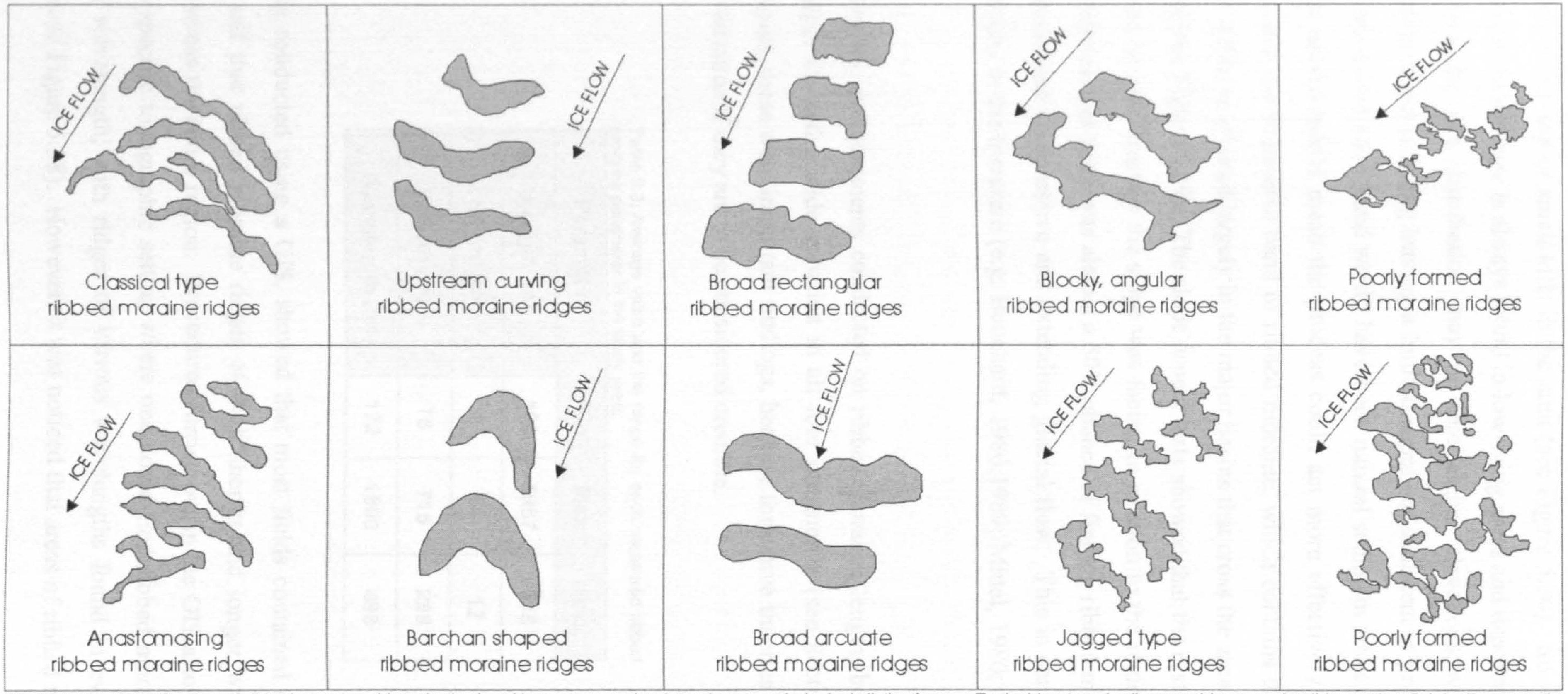

Figure 5.49. Classification of ribbed moraine ridges in the Lac Naococane region based on morphological distinctions. Each ridge type is discussed in more detail in section 5.4.1. Because the poorly formed type ridges do not have a distinct morphology two examples were included to illustrate their diversity of form (see also figure 5.18).

ground and the ASTER DEM's showed several cases where ribbed moraine ridges were superimposed on top of small hills in the area (see Figure 5.30). So it is not a simple case that ribbed moraine is always found in low-lying areas and depressions. A credible explanation for this distribution may be that higher elevations would have been subjected to aerial scouring leaving a limited supply of sediment to produce the ridges. The basins on the other hand would have been natural sediment sinks and an abundant sediment source would mean the process could act more effectively in these places. The fact that the transverse band of ribbed moraine, which contains the largest ribbed moraine fields, is situated largely in the major basins that cross the area lends support to this idea (see Figure 5.29). The slope aspect tests showed that the distribution was not influenced by the direction the slope was facing in relation to the regional ice flow. It was concluded that there was almost a 50% chance of finding ribbed moraine on slopes that experienced compressive and extending glacial flow. This is contrary to existing observations in the literature (e.g. Bouchard, 1980,1989; Minel, 1980; Sollid & Sørbel, 1984).

Morphometric measurements conducted on ribbed moraine, length, height, width and wavelength showed a wide variation in all four parameters (see Section 5.6 & Table 5.3). Again, these were important findings, because formative theories need to account for this variation if they are to be considered credible.

Table 5.3. Average value and the range for each measured ribbed moraine parameter in the study area.

Parameter	Min	Max	Mean
Length (m)	180	5967	918
Height (m)	1	64	12
Width (m)	76	715	298
Wavelength (m)	172	1800	498

Analysis conducted using a GIS, showed that most fields contained ridges of mixed length and that ribbed moraine ridges of both shorter and longer wavelengths were spread across the entire region. Procedures carried out in the GIS also concluded there was no specific topographic setting where one could find ribbed moraine of a certain type of wavelength, with ridges of various wavelengths found in every topographic setting (see Figure 5.38). However, it was noticed that areas of ribbed moraine with the short wavelengths tended to be clustered on many of the transitional slopes throughout the study site, rather than in basins or hilltops.

Finally, the relationships between ribbed moraine and other glacial landforms were investigated. It was noted that many eskers meander through the study site and that they are always found draped on top of the ridges. This was seen as evidence that they post date ribbed moraine formation and that they were simply laid down during deglaciation. The fact that they are post formational features indicates they were unlikely to have influenced the ribbed moraine formational processes. In the Lac Naococane region, it was also found that ribbed moraine had strong spatial associations with drumlins and glacial lineations and these have been summarized in Figure 5.50. Both ribbed moraine and drumlins were observed together in a variety of settings and drumlinization of the ribbed moraine ridges was a common characteristic in this region (see Figures 5.14 and 5.15). In the literature, it is often noted that there are downstream transition zones whereby ribbed moraine appears to grade into drumlins. However, abrupt lateral transitions, were also observed in this area. Where these occur, the landforms can be either exclusive, whereby a field of lineations is situated next to a ribbed moraine field with no mixing of the landforms, or they can be mixed, whereby the ribbed moraine fields are overprinted with glacial lineations (see Figure 5.50). Elsewhere across the site, it was observed that heavily drumlinized ribbed moraine appeared to grade into drumlins (see Figure 5.47). This was an important observation because it lends support to the idea that drumlins and ribbed moraine are genetically linked and may form part of a bedform continuum.

✱✱✱

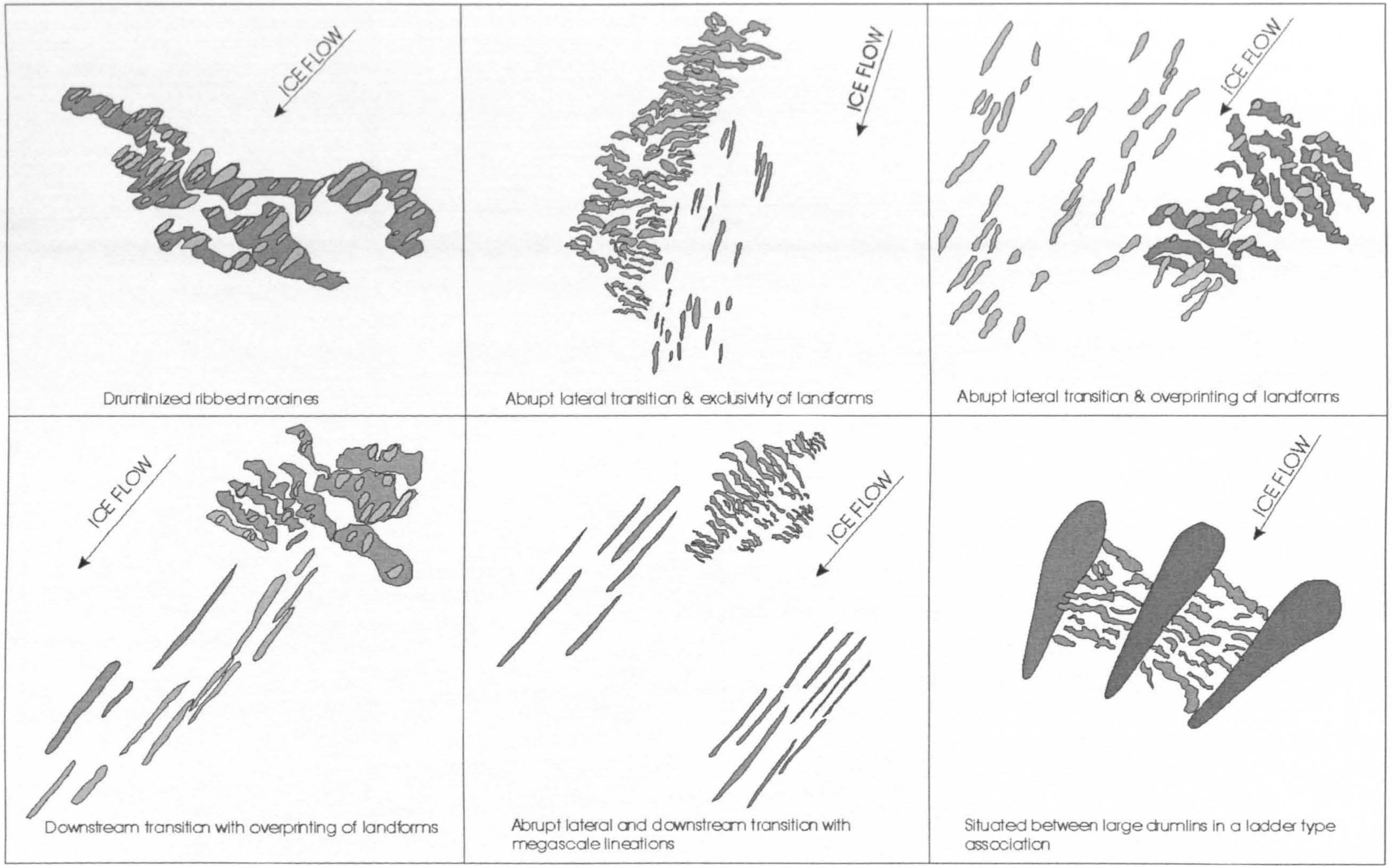

Figure 5.50. Schematic diagram illustrating the spatial relationships between ribbed moraine, drumlins and mega-scale glacial lineations discussed in section 5.7. Relationships range from simple drumlinization of the ridges, to more complex associations whereby ribbed moraine fields are found in lateral and downstream transition zones with drumlins and glacial lineations. In places where the drumlins are large enough, ribbed moraine has been observed occupying the space between the drumlins.

Map 5.1. Distribution of Ribbed Moraine, Lac Naococane, Quebec, Canada

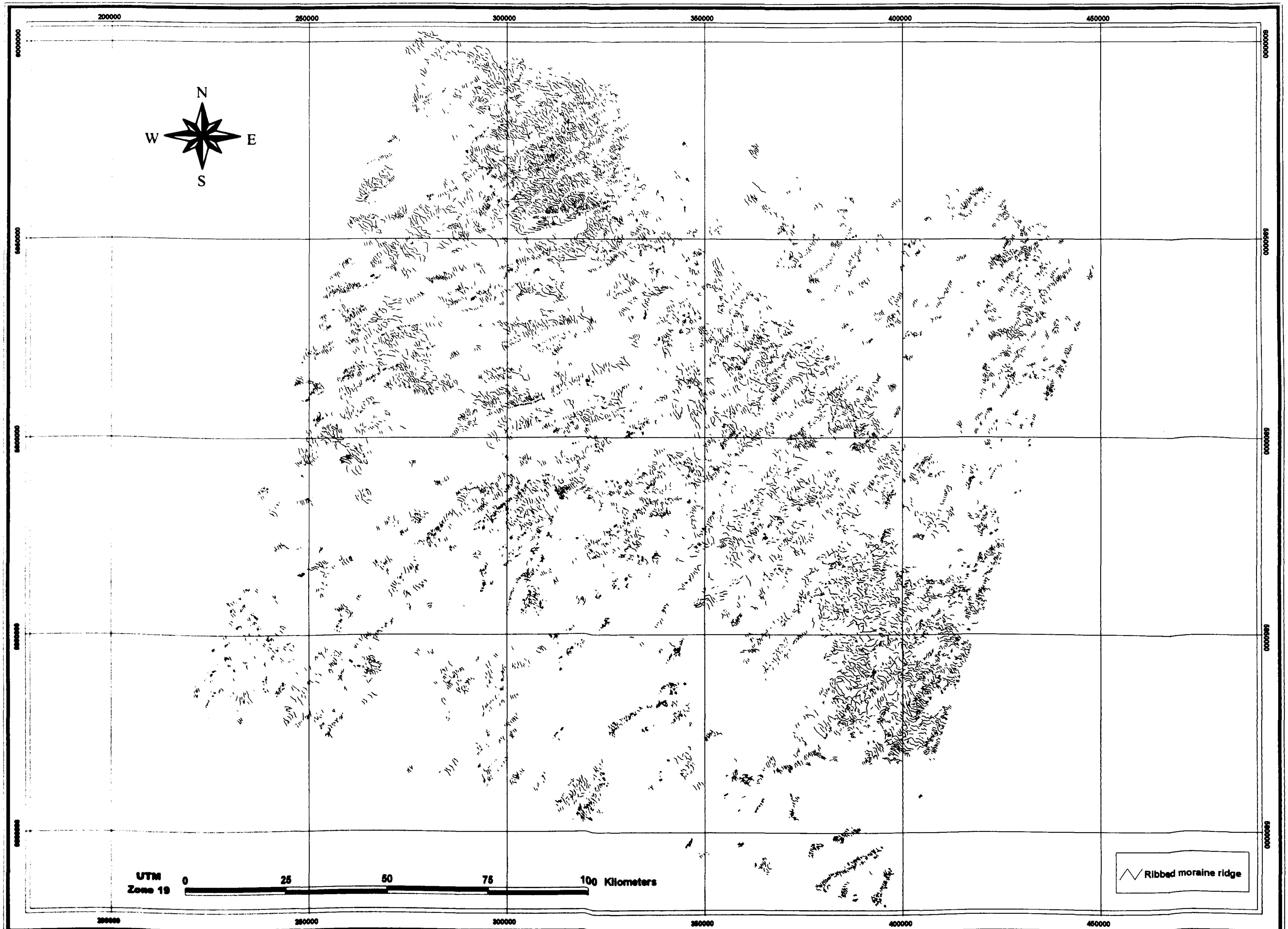

Chapter 6: The Characteristics of Ribbed Moraine in the River Kaniapiskau Region, Northern Québec

6.1. The study site

The River Kaniapiskau study site is situated just south of Ungava Bay in northern Quebec. The location of the site is marked by a box in Figure 6.1, which shows the coverage of the ETM+ image used to map the ribbed moraine ridges in this locality. As can be seen, the study site contains most of the ribbed moraine in the northern parts of Quebec. Figure 6.2 shows the sites position in relation to the Nouveau-Québec Ice Divide. The River Kaniapiskau site is situated on the opposite side of the divide to the Lac Naococane site.

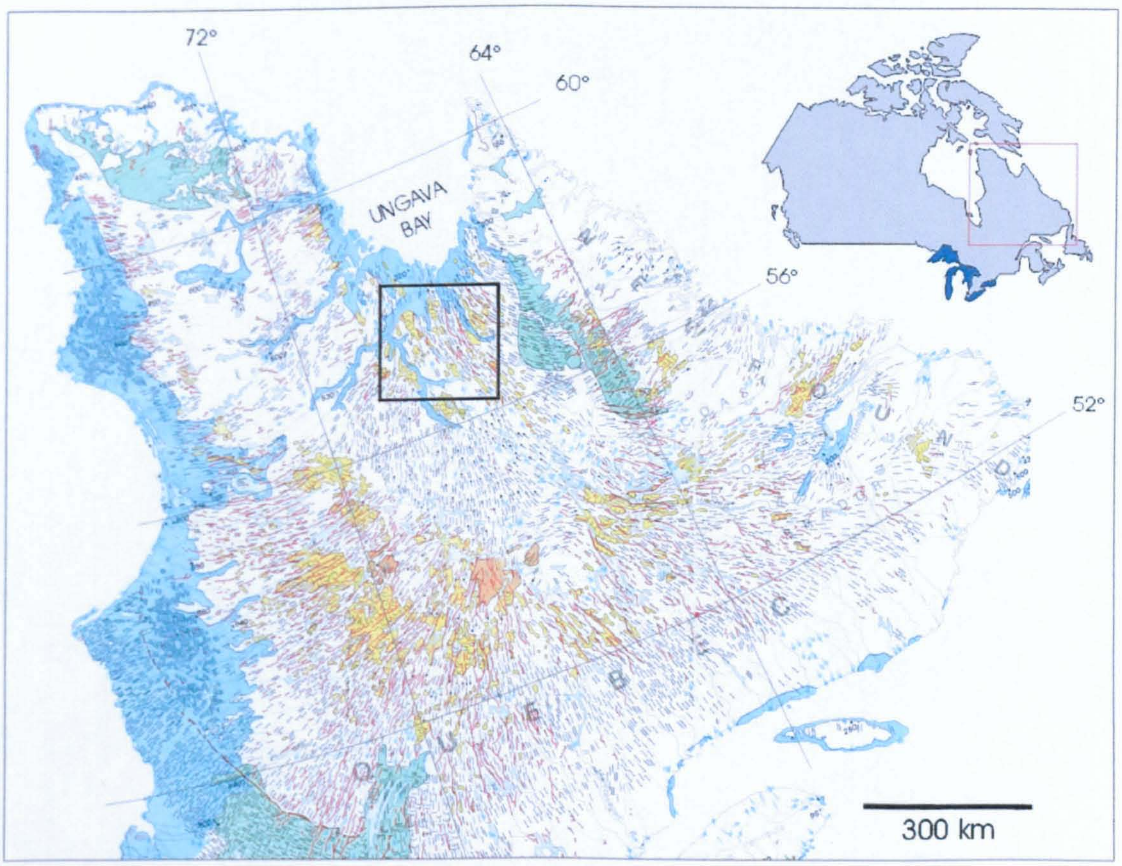

Figure 6.1. Location map showing the River Kaniapiskau study site to the south of Ungava Bay. The box indicates the coverage of the Landsat ETM+ image used to map the ribbed moraine ridges in this region. The figure is adapted from the Glacial Map of Canada (Prest *et al.*, 1968) where areas of ribbed moraine are marked as yellow patches.

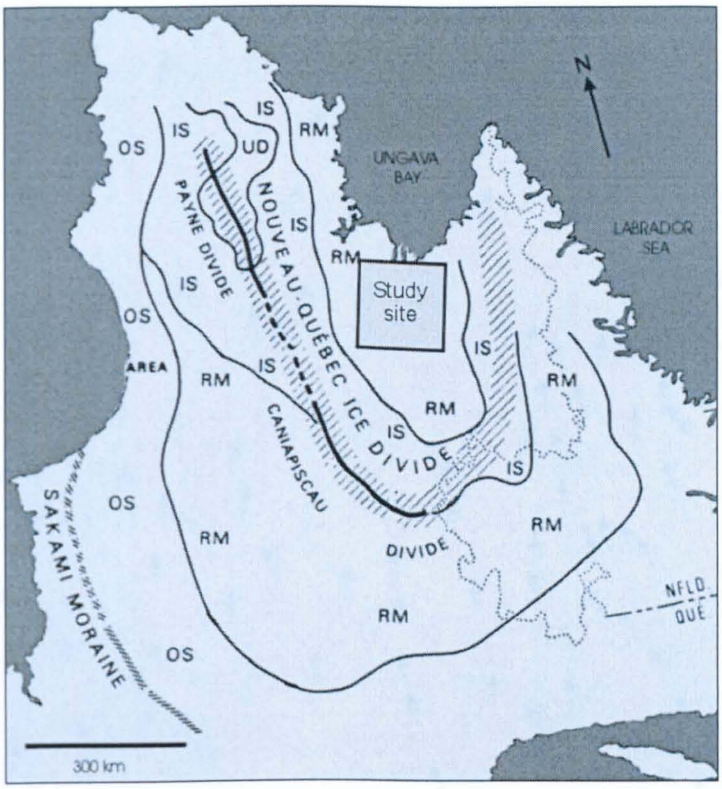

Figure 6.2. The position of the Nouveau-Québec Ice Divide adapted from Bouchard (1989). The River Kaniapiskau study site is enclosed on the map by a box. Note the ice divide surrounds the entire site.

6.2. Data sources and methodology

To map the ribbed moraine ridges in the River Kaniapiskau region, one digital Landsat ETM+ scene (Panchromatic band 15 m, 185 × 185 km) was acquired and geocoded. To obtain an indication of the general topography of the study site a 30-arc second (ca 0.5-1 km) Digital Elevation Model (DEM) was obtained. This was used to investigate relationships between topography and ribbed moraine distribution in the region. The ribbed moraine ridges were mapped and their wavelength determined following the procedures laid out in Chapter 4. The following sections reports on the results of the mapping and morphometric analysis of the landforms.

6.3. Results from mapping

6.3.1. Large-scale pattern

Figure 6.3 shows the general orientation of the ribbed moraine fields in the River Kaniapiskau area. The orientation of the fields shows a convergent ice flow pattern from the ice divide into Ungava Bay (see Figure 6.2).

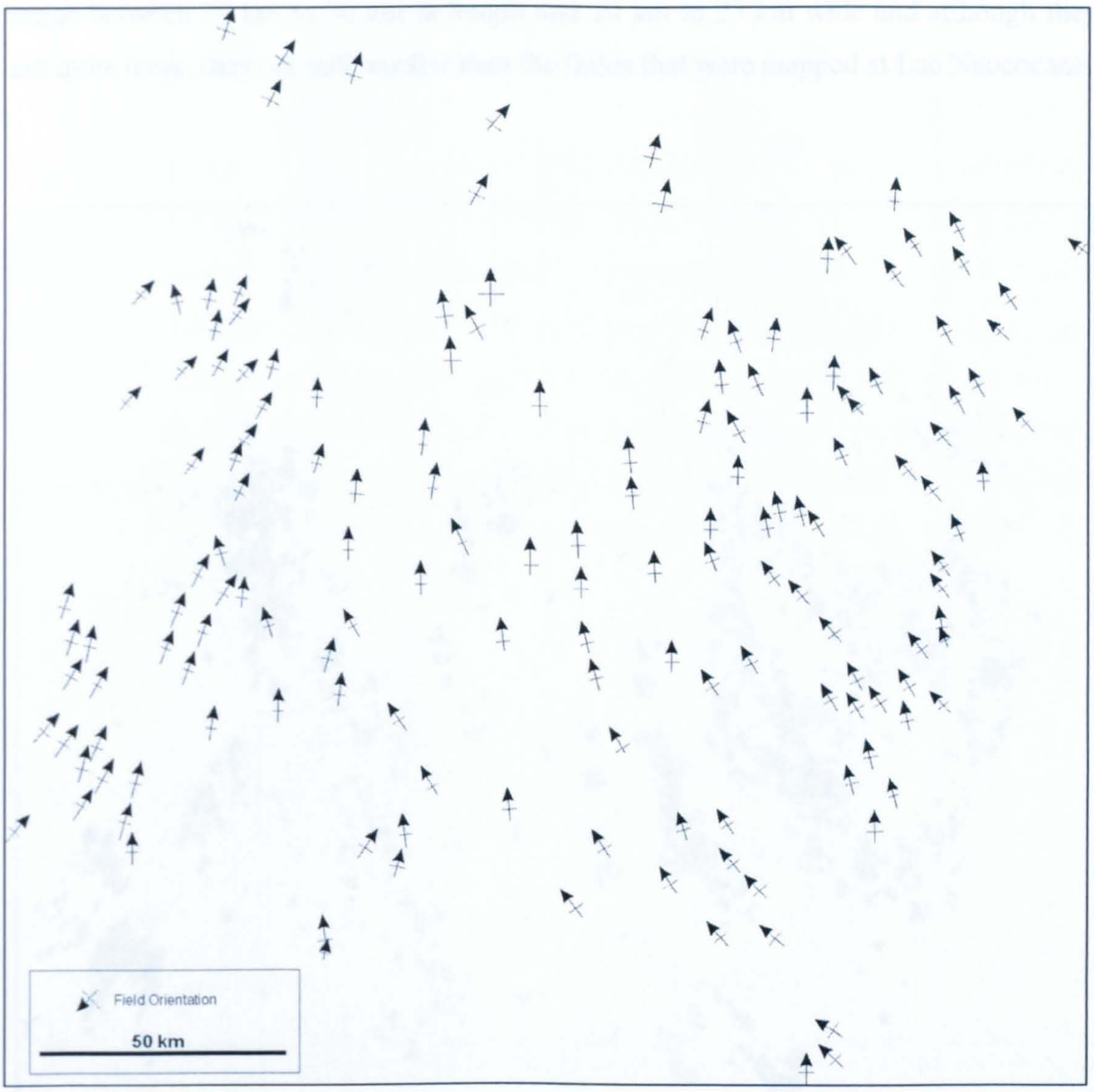

Figure 6.3. Ribbed moraine field orientation map in relation to the regional ice flow pattern. The red lines show the general orientation of the ribbed moraine ridges in each field and the arrows the direction of ice flow. Note the strongly convergent pattern indicating ice from the Nouveau-Québec Ice Divide converged into the area flowing north into the bay.

A total of 12231 ribbed moraine ridges were mapped from the ETM+ image and the resulting ARC coverage can be seen in Figure 6.4 and Map 6.1. In this study area, ribbed moraine was not as extensive as that found at Lac Naococane and the fields tended to be concentrated in the eastern and western parts of the site. The central regions did contain several patches of ribbed moraine, however the fields tended to be quite small and were spatially isolated from the other ribbed moraine fields in the area. For example, the ribbed moraine fields marked by the orange spot in Figure 6.4 are all between 3 km and 5 km long and are 34 km from the field to the west, marked by the green spot, and 40 km from the large area of ribbed moraine to the east. The area contains several quite large independent ribbed moraine fields, which have been marked by coloured dots in Figure 6.4 and are shown in more detail in Figure 6.5. All the fields range between 25 km to 30 km in length and 10 km to 23 km wide and although they are quite large, they are still smaller than the fields that were mapped at Lac Naococane.

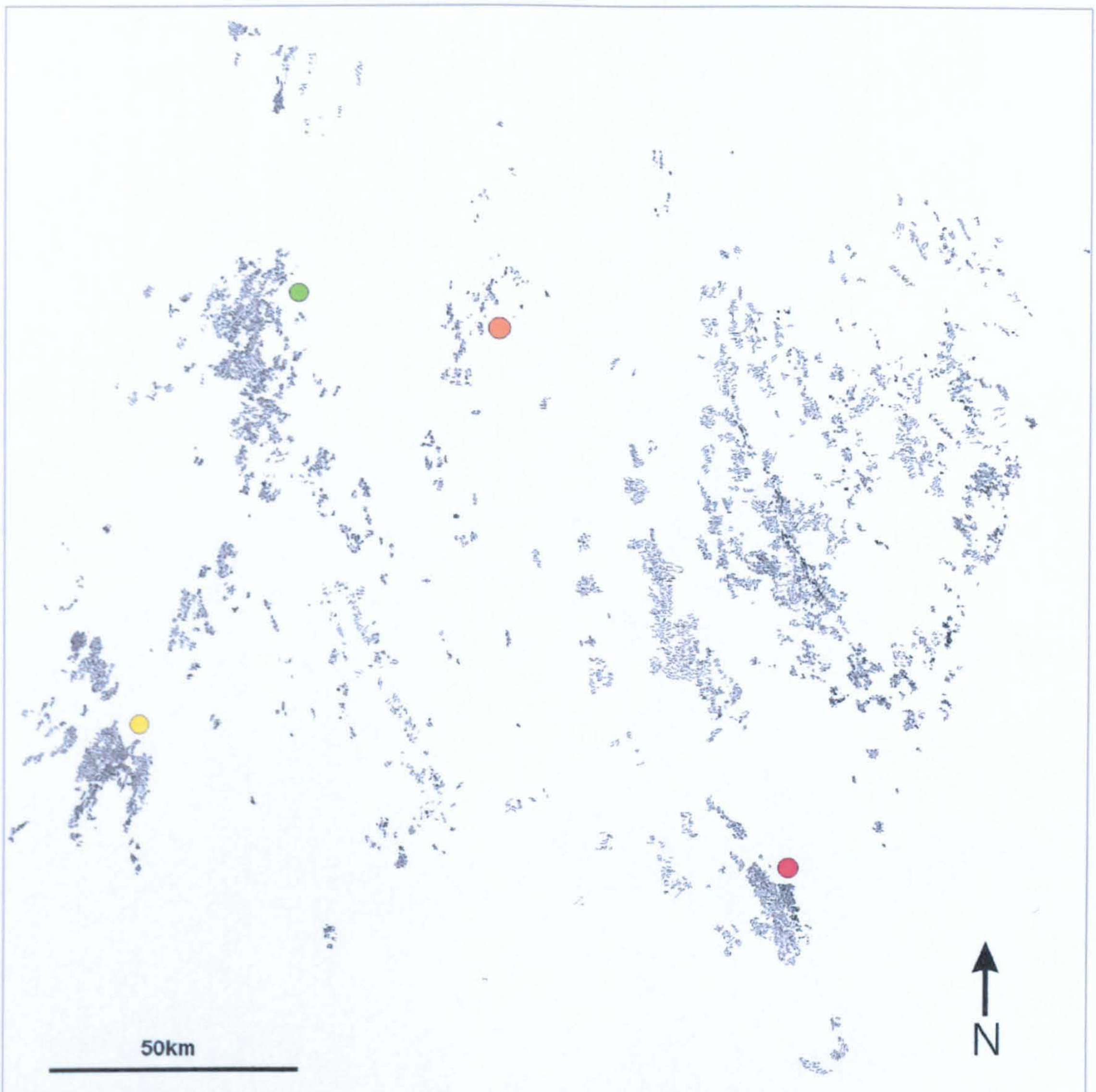

Figure 6.4. Ribbed moraine ridges mapped using the ETM+ image of the River Kaniapiskau study site. The coloured spots refer to examples of ribbed moraine fields enlarged in Figure 6.5 below. The ribbed moraine field marked by the green spot is just south of the river Koksoak (68° 48 W & 57° 45 N). The field marked by the yellow dot is Moraine Lake (69° 17 W & 56° 57 N). The orange spot marks some small ribbed moraine fields just east of Lake Garreau (68° 04 W & 57° 41N) and the red spot marks a large ribbed moraine field at Lake Secondon (67° 01 W & 56° 38 N). See Map 6.1 for a more detailed view.

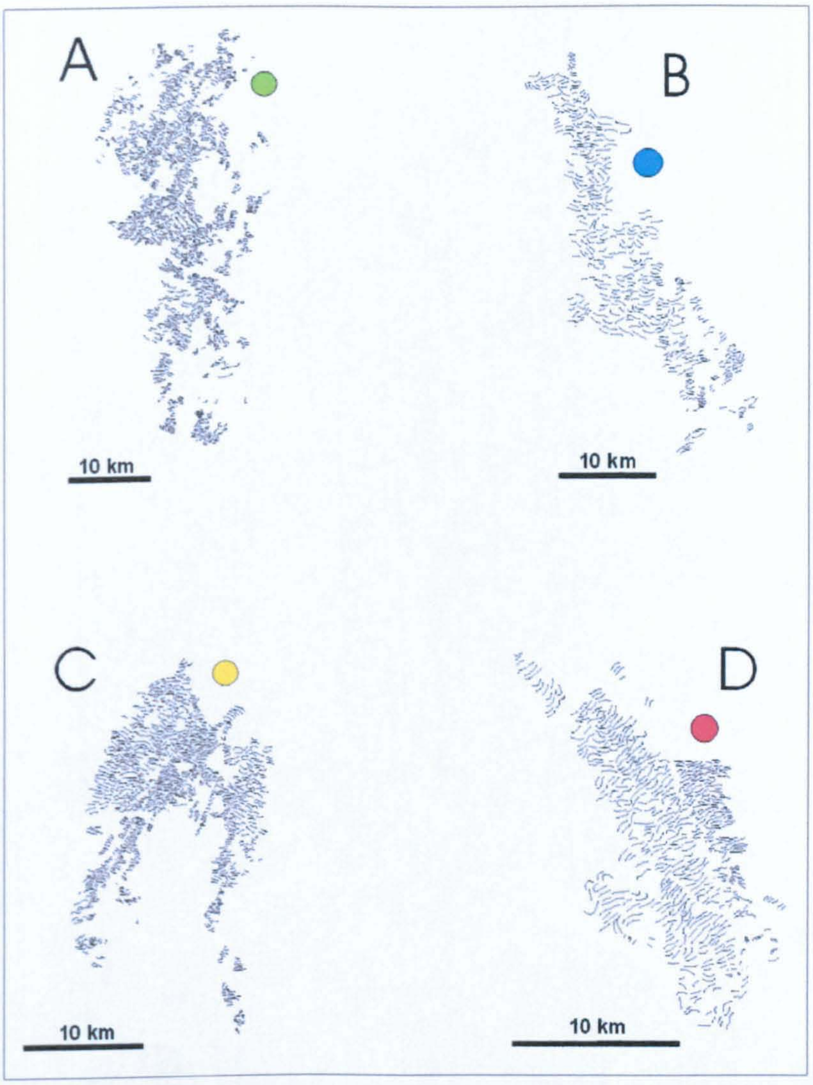

Figure 6.5. In the River Kaniapiskau area several large fields of uninterrupted ribbed moraine are evident. The examples above are the four largest found at the site. The colour dots mark their position in the study site (see Figure 6.4). At its longest point field A is 30 km long and 23 km wide, field B is 30 km long and 14 km wide, C is 26 km long and 16 km wide and D is 26 km in length by 10 km wide.

The distributional pattern of ribbed moraine in this location was classified into the following categories:

1. Elongate ribbons and narrow tracks
2. Clusters
3. Isolated fields

6.3.2. Ribbons and narrow tracks

In the River Kaniapiskau area, large ribbon type ribbed moraine fields were identified running through the site (Fig. 6.6). The ribbons have a range of morphologies and vary in scale across the region. The fields marked A, B and C in Figure 6.6 are examples of the more broader type ribbons in the area and are all between 27 km and 30 km in length and 5km to 8 km wide.

The narrower type ribbons, (e.g. fields D and E) are of similar length as the broader forms, however they are much narrower, being less that 1 km at their thinnest point. As well as containing relatively independent ribbed moraine type fields, many narrow tracks were also evident in the area. These are small-scale linear fields made of quite small-scale ribbed moraine ridges that are very closely spaced. The tracks can be relatively independent of other ribbed moraine fields, for example those marked G and H, or can be found running through fields of much larger scale ribbed moraine ridges, marked I. Figure 6.7 shows an enlarged view of the narrow track located at position I.

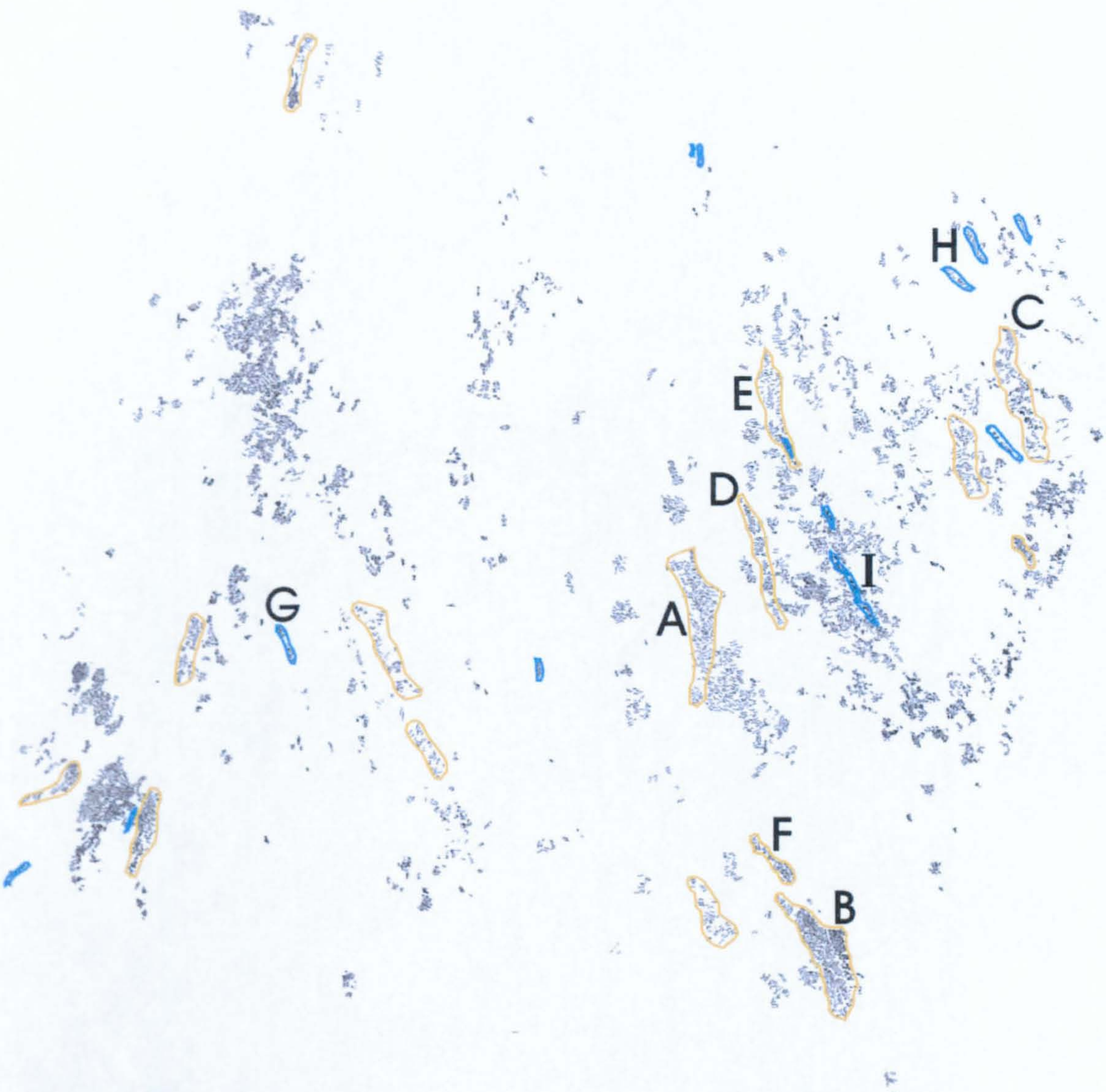

Figure 6.6. Some examples of ribbed moraine fields with ribbon and narrow track type field morphologies. Ribbons are enclosed in yellow and tracks in blue. The ribbon type fields are much larger linear patterns than the narrow tracks, which are made of small, closely spaced ribbed moraine ridges.

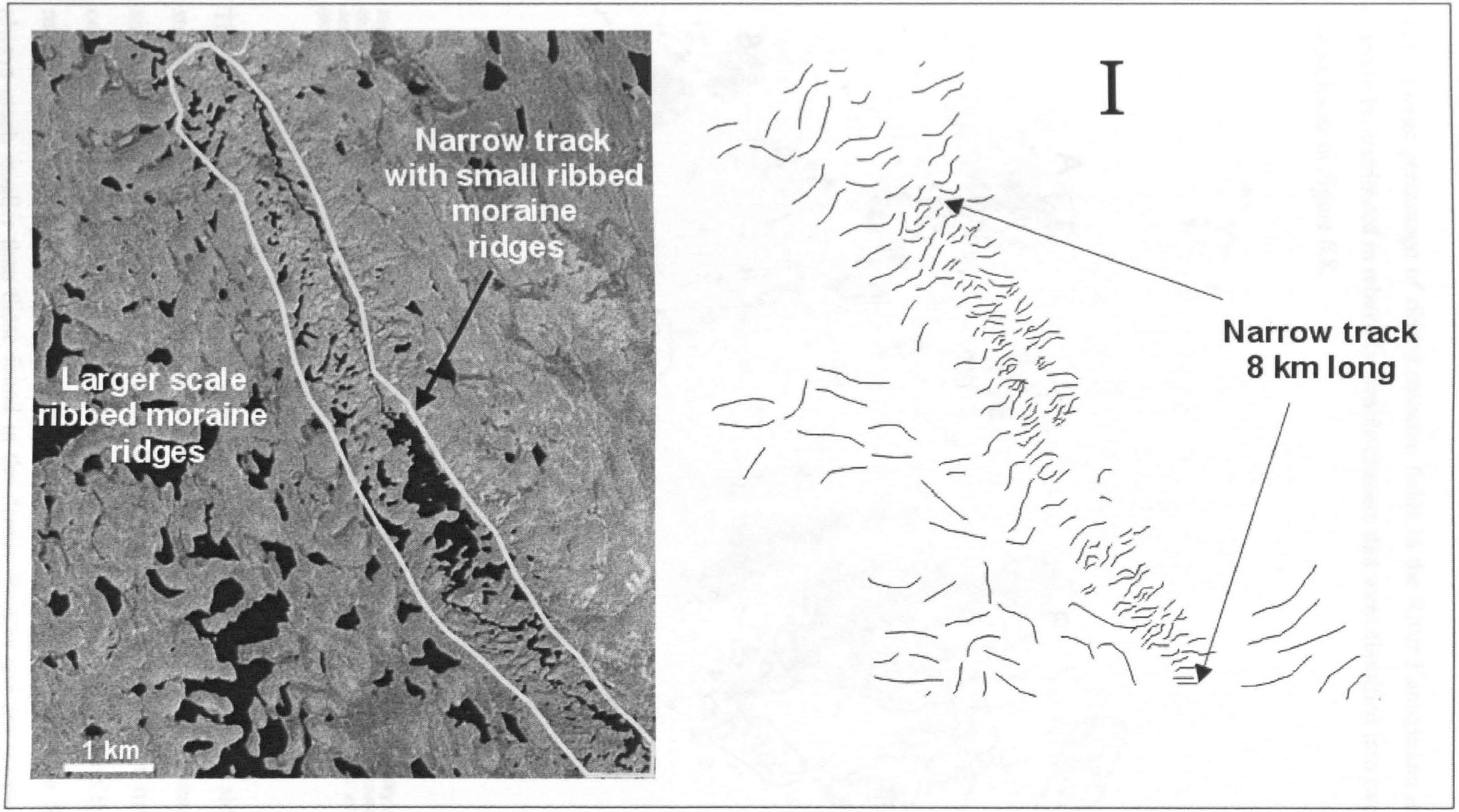

scale ribbed moraine fields. The example shown here is the narrow track marked I in figure 6.6. Note the obvious change in scale between the ridges in the track, enclosed in white, compared to the larger ridges to the left and that the ridges in the track have a much shorter wavelength than the surrounding ribbed moraines.

6.3.3. Clusters

Quite a large percentage of ribbed moraine fields in the River Kaniapiskau area were found to be distributed in relatively sizable clusters that were classified into two general categories as in Figure 6.8.

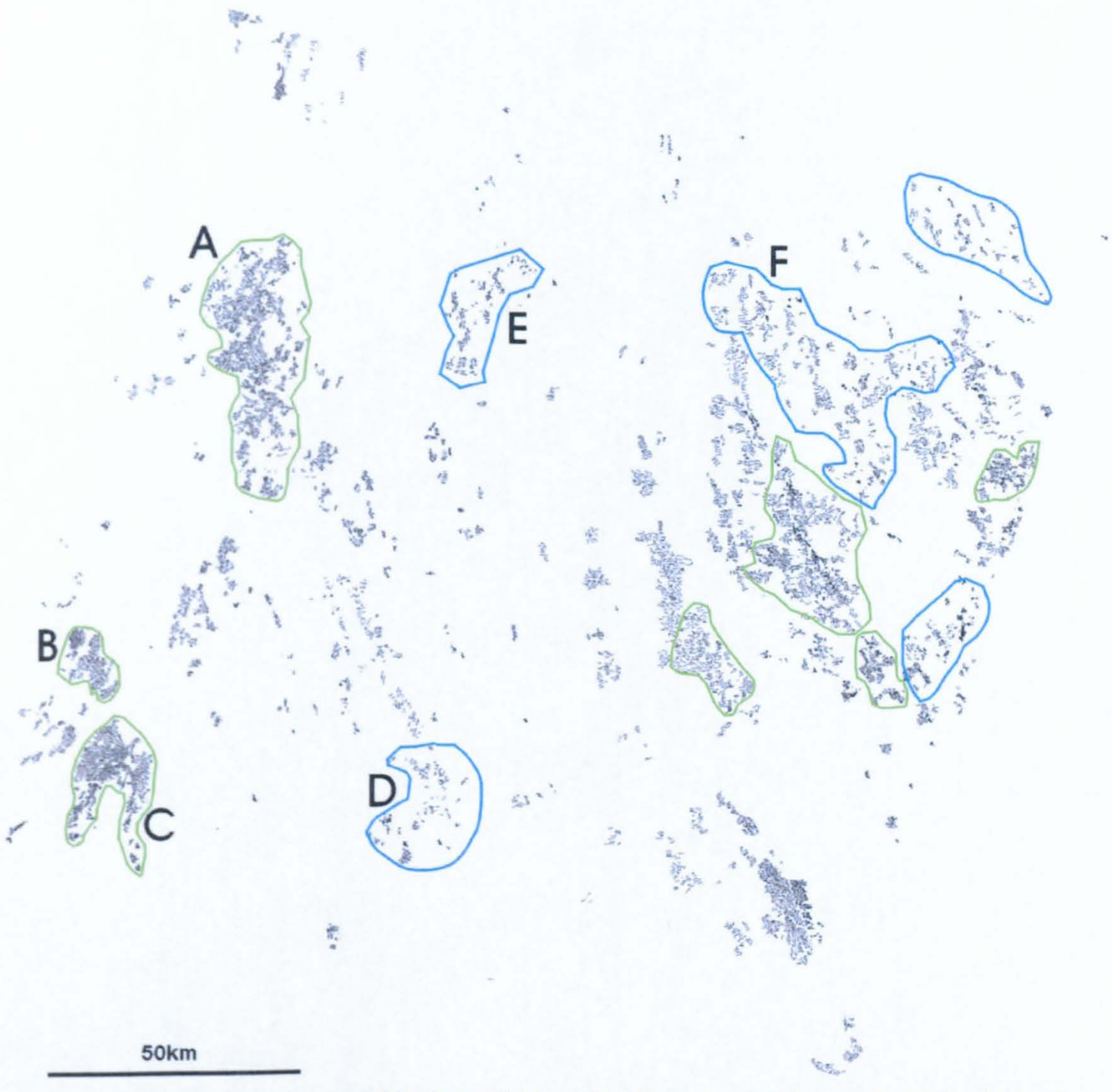

Figure 6.8. Examples of cluster type fields observed in the River Kaniapiskau study area. In this locality two types of cluster were apparent, Dense clusters, which were areas of densely packed ribbed moraine ridges (enclosed in green) and Dispersed clusters, which were made of small fields loosely gathered together in various places within the site (enclosed in blue).

The best examples of dense cluster type fields are located on the western side of the study site. In this area, the three large clusters, marked A, B and C represent quite sizable areas of ribbed moraine terrain. For example, the dense cluster marked A, covers an area of just over 300 km^2. The dispersed clusters are areas where the ribbed moraine fields are more loosely grouped together over wider areas. The fields are always much smaller than those found in the denser clusters and are separated from each other by distances of normally a few kilometres. For example, the dispersed cluster marked D in Figure 6.8 contains several small ribbed moraine fields that range from 1.5 km to 5 km in length and are separated over distances of up to 5 km.

6.3.4. Isolated fields

Elsewhere across the region, many isolated fields can be seen littering the study site. The ribbed moraine fields tend to be quite small-scale features and range between a few hundred metres to approximately 7 km in length and are distinctly separate from other ribbed moraine fields in their vicinity. The separation can be relatively small, usually less than 10 km, which is the case with the fields marked A in Figure 6.9. However, quite a number of fields are very isolated from the rest of the ribbed moraine population and their nearest neighbours can be tens of kilometres away. For example, the ribbed moraine field marked B in Figure 6.9 is situated 20 km from the dense cluster in the west and 22 km from the small ribbed moraine fields to the east.

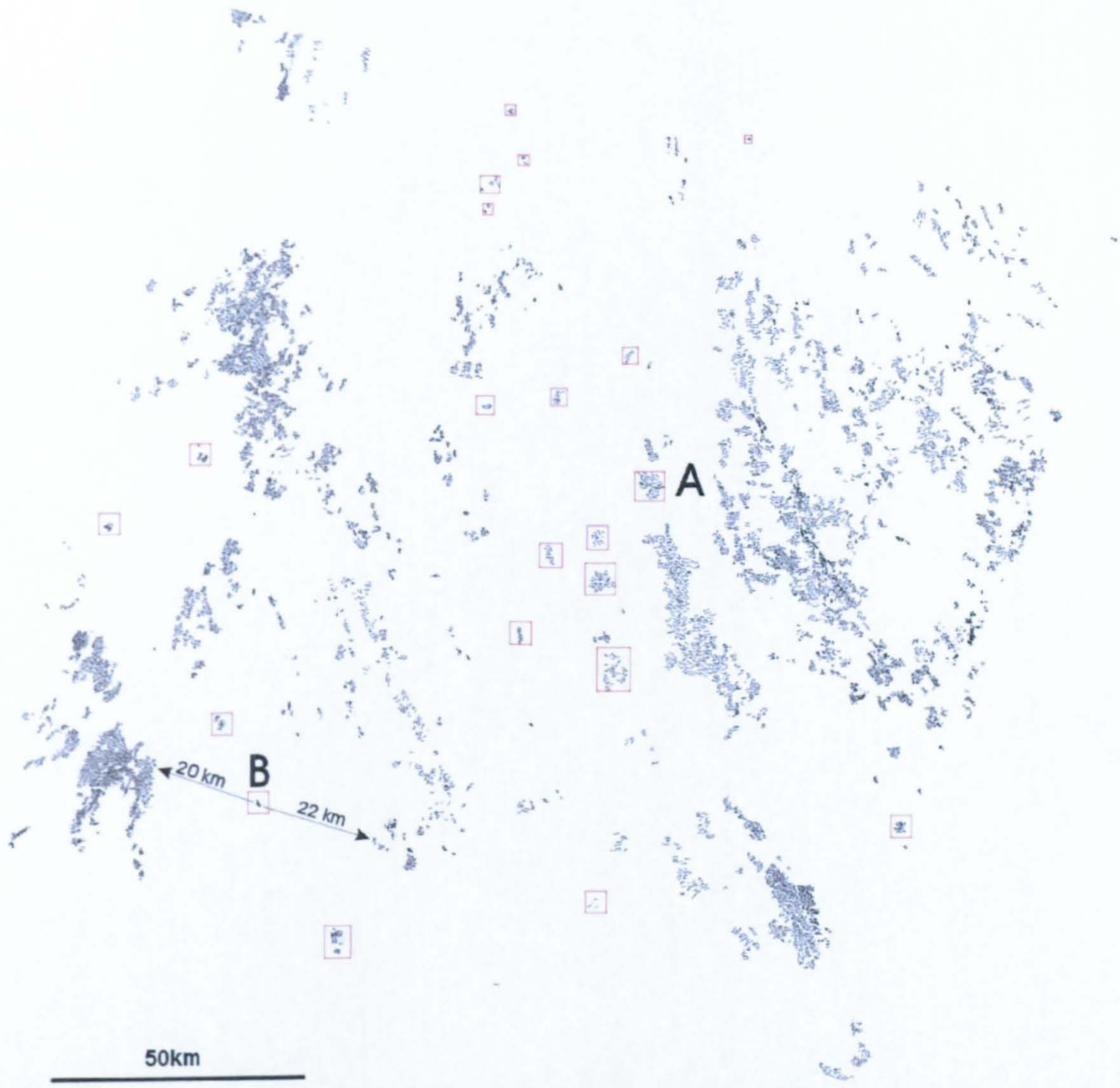

Figure 6.9. Some examples of isolated ribbed moraine fields in the River Kaniapiskau area. Note how they are usually quite small and are spatially distinct from other ribbed moraine fields. In some cases this separation can be quite large and in the order of tens of kilometres.

6.4. Morphological characteristics of the ribbed moraine in the River Kaniapiskau region

6.4.1. Plan view morphology

In the River Kaniapiskau area, it was possible to observe many ribbed moraine ridges that fitted the classic morphological description discussed in Section 5.4.1. However, as was the case in Lac Naococane, close inspection of the fields always revealed variations in form from the more classical type ridge (Figures 6.10 & 6.11).

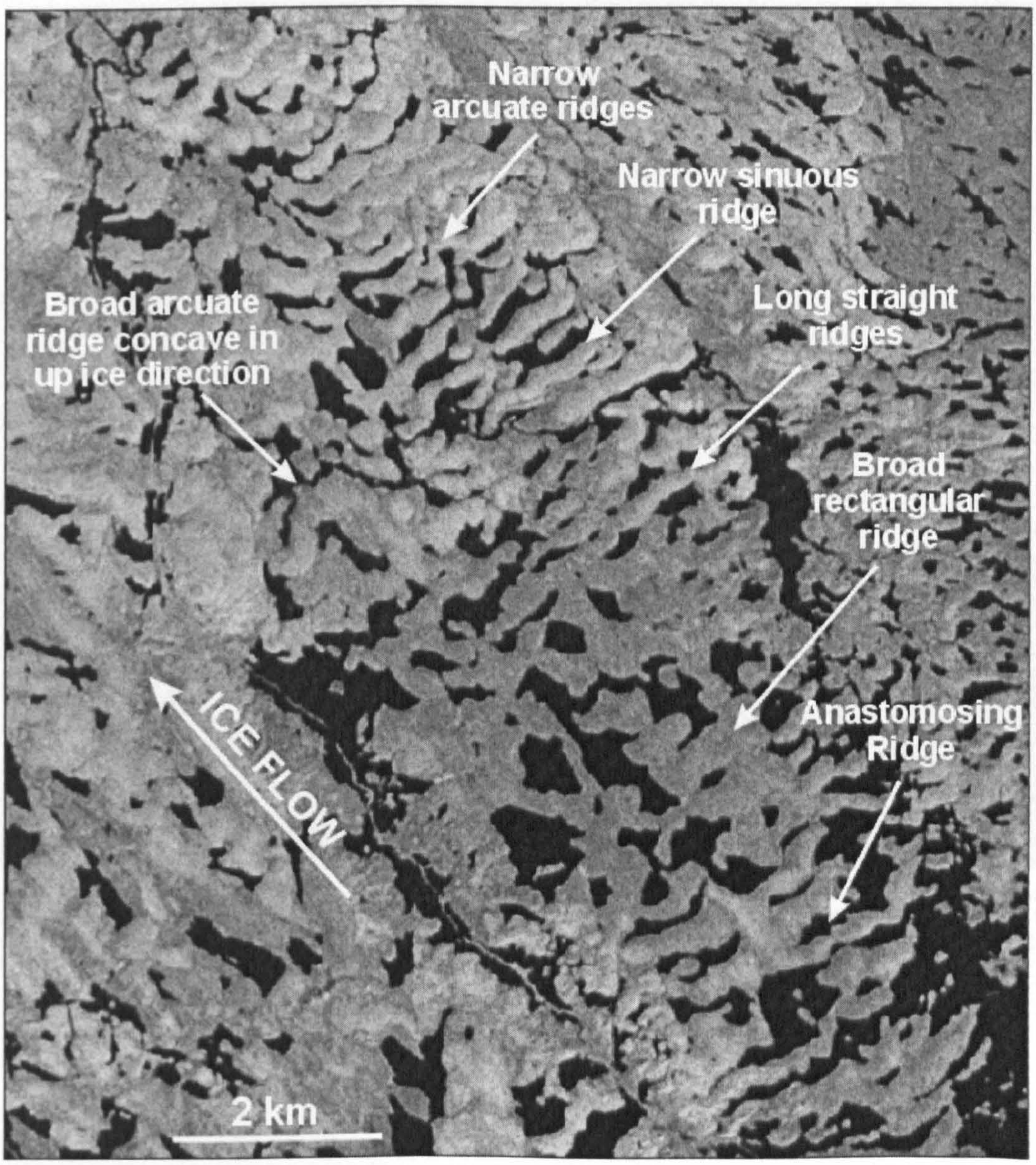

Figure 6.10. Showing an example of a ribbed moraine field containing ridges of mixed morphology. Note that many of the ridges sinuous, arcuate and concave in the down ice direction, which are typical characteristics of classical type ribbed moraine ridges. Note however the diversity in form of many of the ridges in the field. The field is situated at 67° 02 W & 56° 38 N. The picture was taken from Landsat ETM+ image.

In both these examples, a variety of ridge morphologies are present with the more classical forms and it is possible to identify long straight ridges, broad rectangular ridges, barchan shaped ridges and ridges that are arcuate and concave in the up ice direction within the same field. Some of the ridges in these fields are anastomosing, but it was not a common characteristic of the ribbed moraine in this region. However, as Figure 6.12 illustrates, there are cases in this area were anastomosing is a prevalent feature.

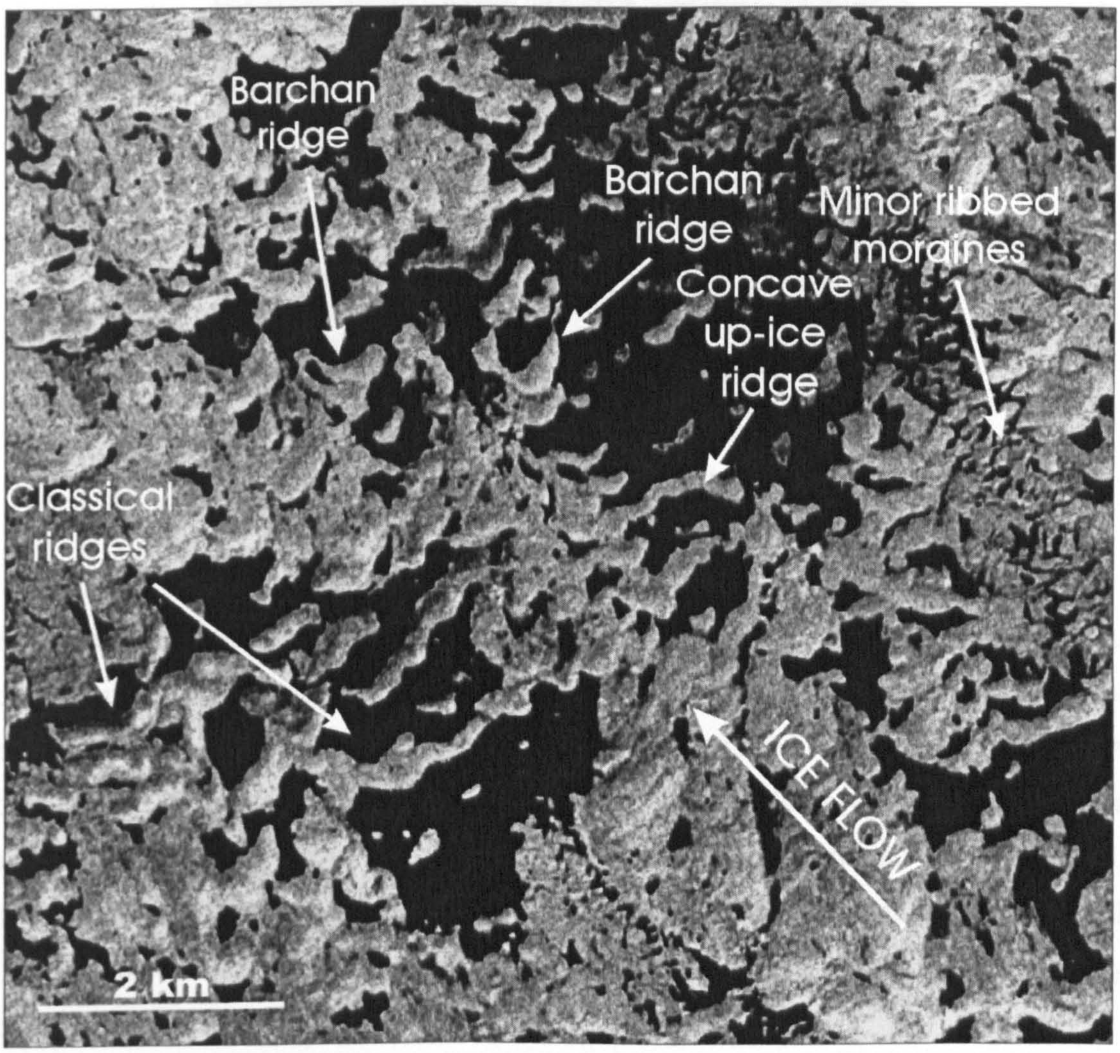

Figure 6.11. Showing another case where ribbed moraine ridges of mixed morphology are found together in the same field. In this example, classical type ridges are juxtaposed with barchan shaped ridges and arcuate forms that face upstream. Note also the change in scale in this field with minor ribbed moraine lying between the larger ridges. Picture taken from Landsat ETM+ Image.

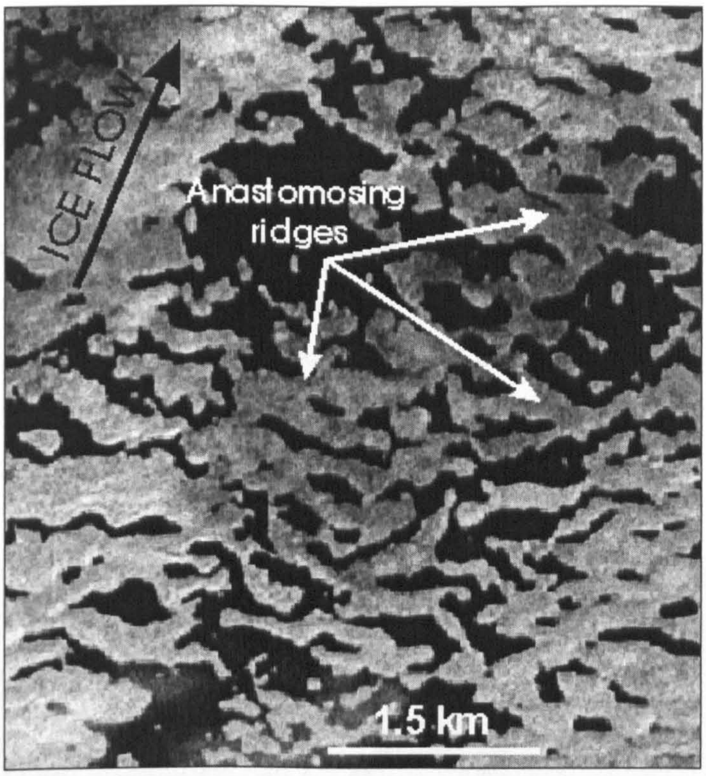

Figure 6.12. Anastomosing ridges are not overly common in the River Kaniapiskau site, however this field at Lake Moraine, situated a few kilometres west of the Kaniapiskau river at 69° 17 W & 56° 57 N is an exception. Note how common it is in this field and that quite a number of ridges are joined together in the field. Picture taken from Landsat ETM+ Image.

Both these examples illustrate the idea that ridge morphology within a single field is usually more complex and diverse than is described in the literature. Figure 6.13 shows part of the large ribbed moraine field at Moraine Lake situated in the south western part of the site. The ridges at the bottom of the field are quite large with bulging outlines and there is no clear separation between adjacent ridges. Downstream from this point, the ridges become more distinct looking and easier to define. However, most ridges still lack the curved sinuous outline associated with classical ridges and many have a lumpy outline appearance.

Elsewhere across the region, many of the more subtle forms of ribbed moraine ridge can be observed. In some cases, these ridges form quite large expanses of ribbed moraine terrain. For example, the ribbed moraine field shown in Figure 6.14 is the large field just south of the river Koksoak that was discussed in Section 6.3.1 (see field marked by the green spot in Figure 6.4 & 6.5). In this area, many transverse ridge structures are clearly present that are morphologically akin to well developed ribbed moraine ridges. However, no particular ridge structure dominates within the field and there are also ribbed moraine ridges of various scales within the confines of the field. What makes this field distinctive from other ribbed moraine fields is that most of the larger ridges have limbs that branch out and connect neighbouring ridges together and this gives the terrain a distinctive "lattice" type appearance which looks quite different from fields of classical type ridges.

In addition to ribbed moraine fields containing ridges of mixed morphology, it was also quite common to see ribbed moraine ridges of various scales in close proximity. In some cases, the scale change is quite dramatic and it is quite common to observe small-scaled minor ribbed moraine ridges juxtaposed with and located between much larger scale ridges (Fig. 6.15).

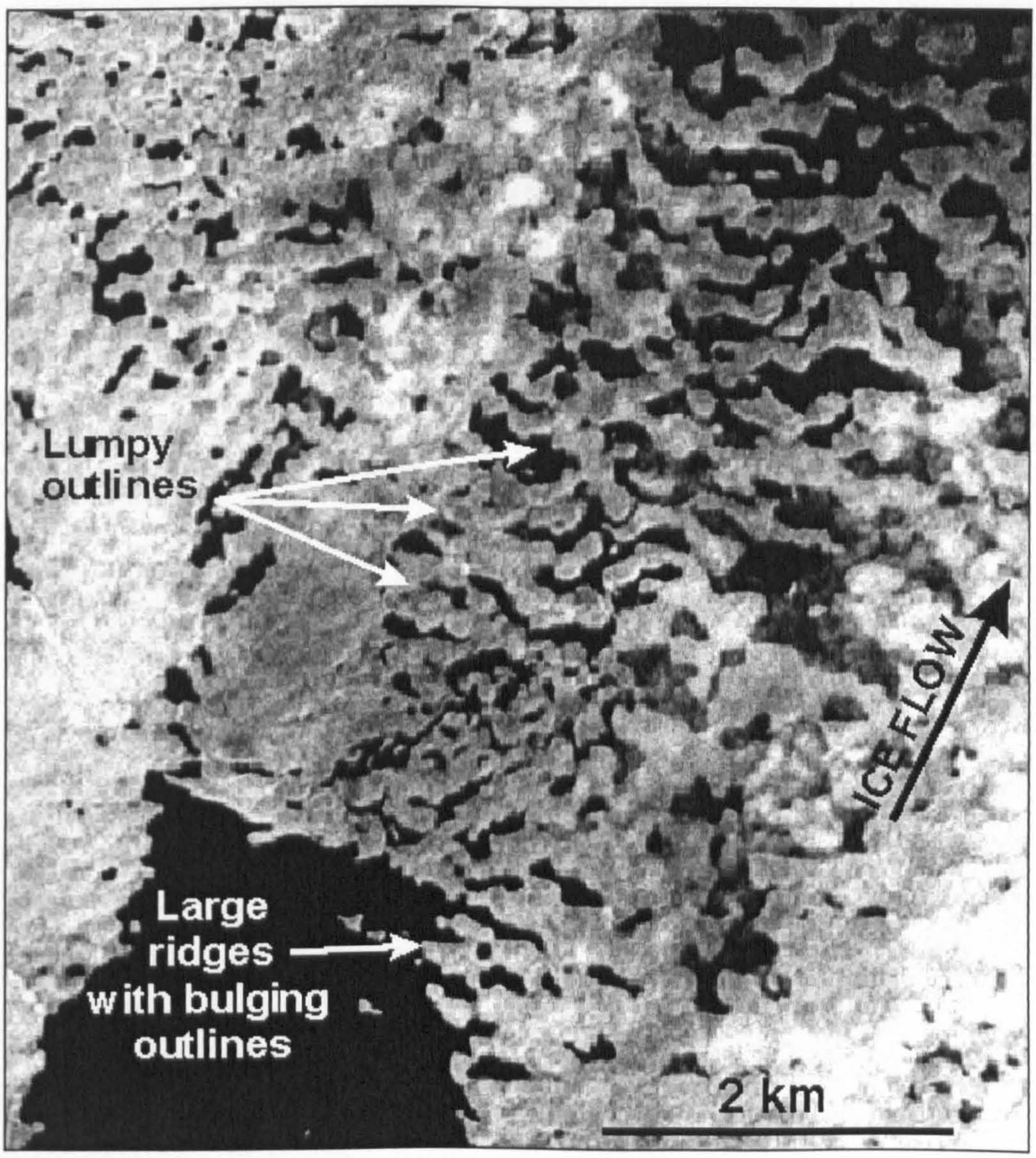

Figure 6.13. Part of the large ribbed moraine field at Moraine Lake (69° 17 W & 56° 57 N). Many of the ridges in this field have bulging outlines and have a lumpier outline appearance compared to the more curved, sinuous outlines of classical type ridges. Picture taken from Landsat ETM+ Image.

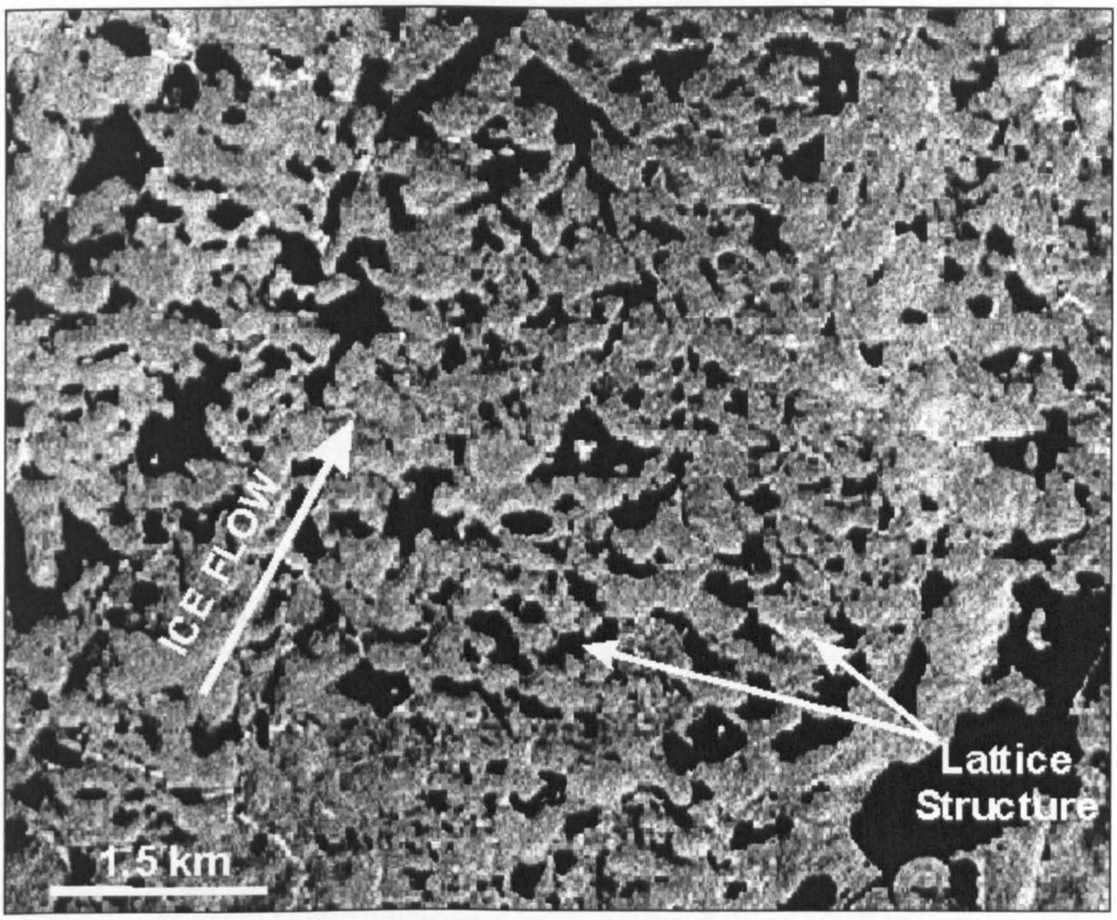

Figure 6.14. In various parts of the River Kaniapiskau site, large concentrations of more subtle type ribbed moraine can be observed. The example shown here is part of the large ribbed moraine field situated just south of the river Koksoak (68° 48 W & 57° 45 N). In this field, most of the ridges are interconnected by limbs that branch from the larger ridges and small scale ribbed moraine ridges, which this gives the terrain a distinctive "lattice" type appearance. Picture taken from Landsat ETM+ Image.

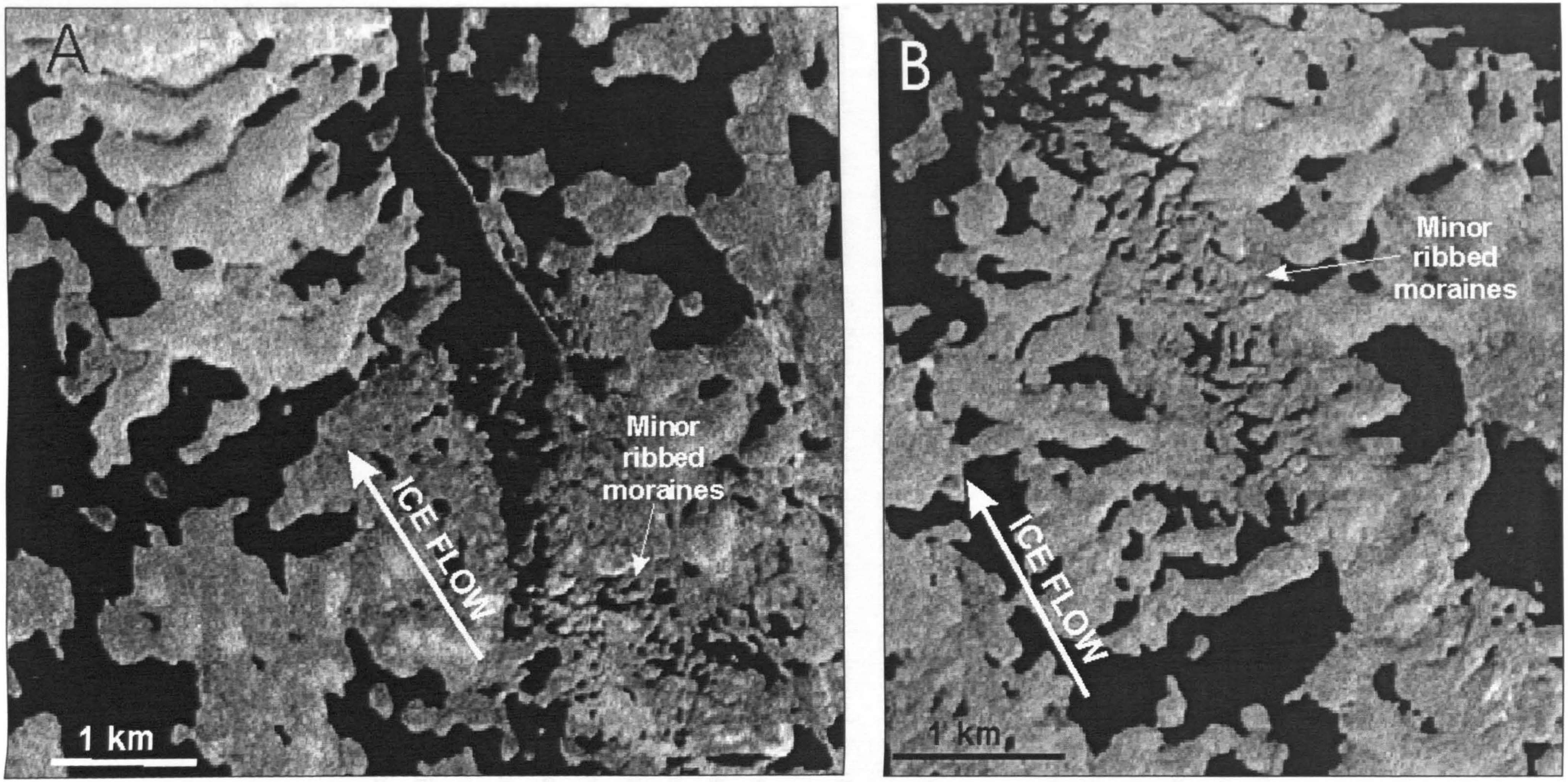

metres wide are located next to sequences of minor ribbed moraine ridges, which are the smallest scale ridges found. In Figure 6.15a the minor ribbed moraine ridges are located upstream from the larger forms and in figure 6.15b they are found located between the larger scale ridges. Picture taken from Landsat ETM+ Image.

6.5. Topography

6.5.1. Topographic setting of ribbed moraine

The general topography of the study site can be seen in Figure 6.16, which shows a GTOP30 DEM and a 3-D relief image of the site. Generally, the area is surrounded by a large broken plateau that arcs its way round the site on its eastern, southern and western flanks, and slopes gently towards the bay in the north, making the whole area resembles a large shallow amphitheatre. Several large rivers wind their way through the area. These have cut narrow channels through the landscape and the highlands that encompass the region are incised with many narrow valleys. Some larger depressions are also present in the area. The biggest of these contains Lake Erlandson, a large shallow basin that is approximately 100 km long and 50 km wide.

To investigate the topographic setting of the ribbed moraine in this area the ARC coverage of the mapped ribbed moraine ridges was laid on top of the DEM (Fig. 6.17). Interestingly, the majority of ribbed moraine ridges are not situated in the major depressions of the area, but rather, are concentrated in the narrow valleys and topographic lows of the large plateau that surrounds the site and on the slopes that run from this into the bay (e.g. A, B, C, D & E). White polygons mark these ribbed moraine fields and when viewed in this manner it is estimated that approximately 75 % of the ribbed moraine population are found in these regions. In comparison, the major basins contain much smaller numbers of ribbed moraine ridges (e.g. F). However, there is one exception, this being the large field just south of the river Koksoak (marked G), which contains approximately 15 % to 20 % of entire ribbed moraine population. Other smaller and more isolated pockets of ribbed moraine can be seen dotted about the landscape and these are situated in a variety of topographic settings and elevations. For example, the small fields marked H and I are situated on the shallow slopes near the bay and are at elevations ranging from 75 m to 150 m above sea level. In contrast, the small pocket of ribbed moraine marked J is located on the higher ground in the south at elevations around 350 m above sea level.

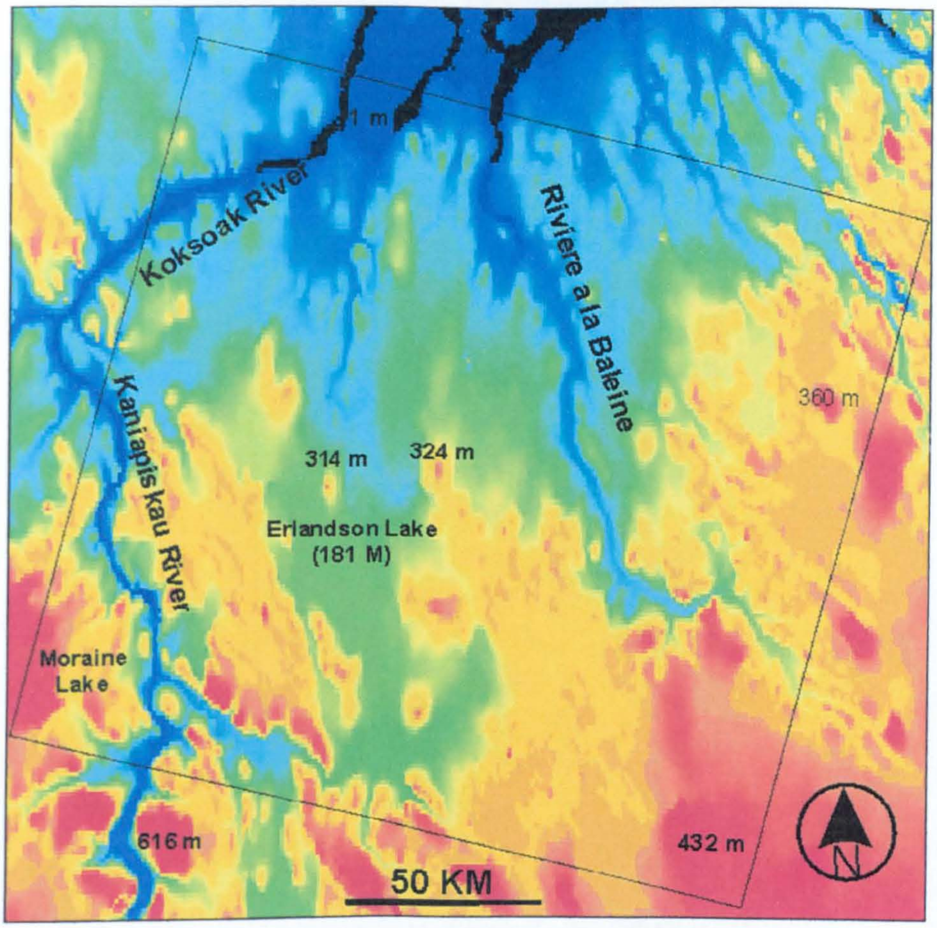

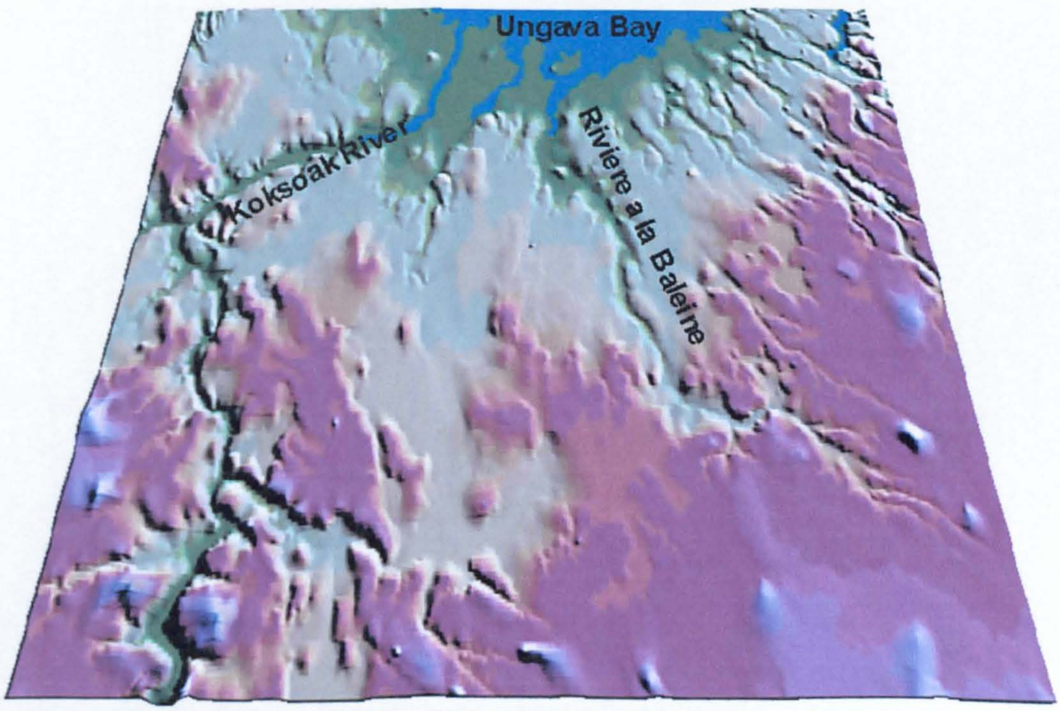

Figure 6.16. The figure on top is a GTOP30 DEM of the River Kaniapiskau study site displayed as a Pseudo colour image. Elevation is coded to show the highest elevations as red, grading down to orange, yellow, green, blue to purple, which represents the lowest regions. Black areas are at sea level. The relief image at the bottom was produced using the DEM and gives a 3-Dimensional impression of the general topography.

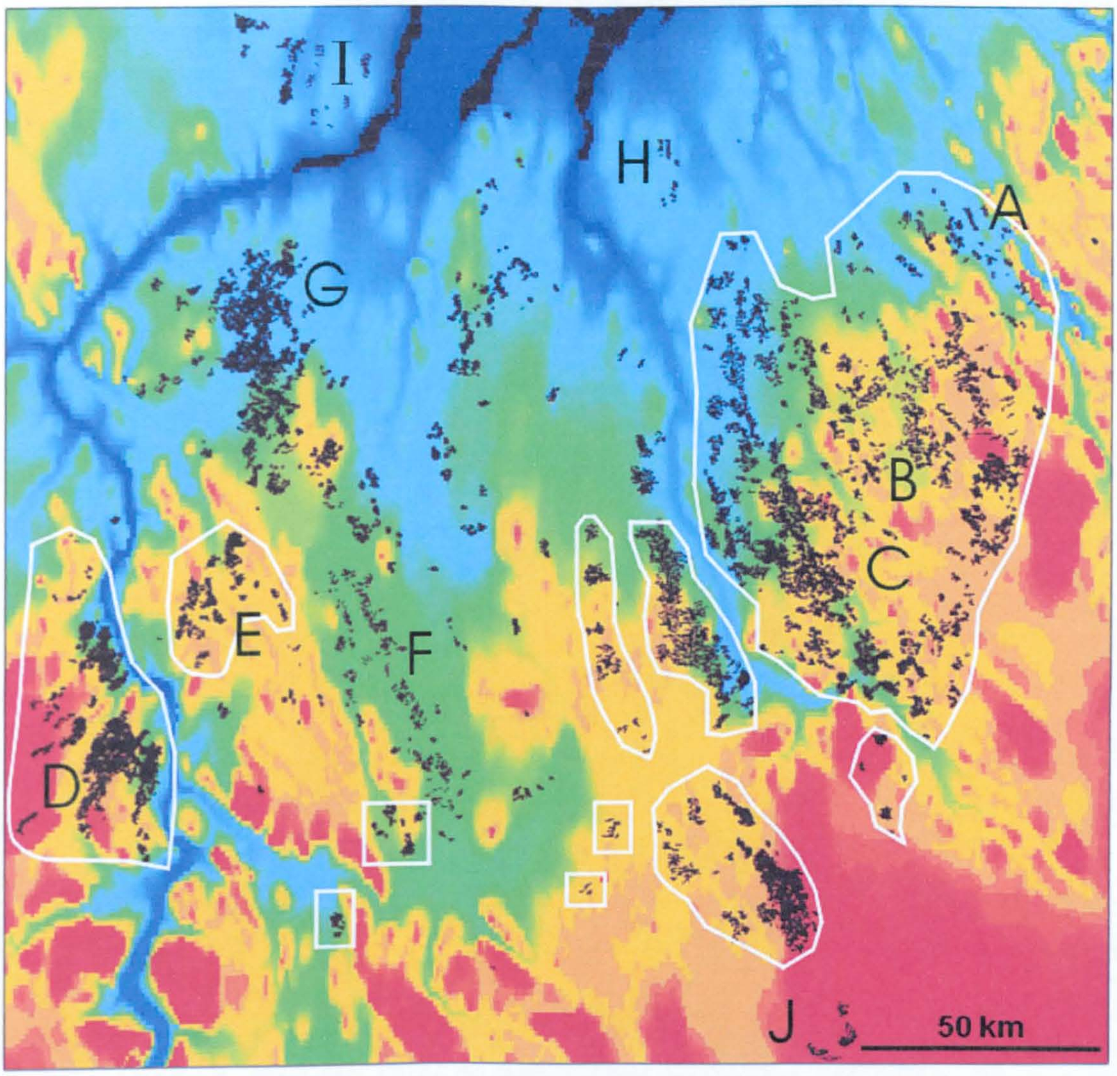

Figure 6.17. DEM of the region with the ARC coverage of the ribbed moraine crests superimposed on top. The white polygons enclose the ribbed moraine situated in the narrow valleys and topographic lows of the plateau and the slopes that run off this area towards the bay. It is estimated that approximately 75% of the ribbed moraine population lie within these regions.

6.5.2. Relationships to slope aspect

In the River Kaniapiskau region, ice converged into the bay from the Nouveau-Québec Ice Divide, which surrounded the study site during the last glaciation (Figures 6.2 & 6.3). This made the slope aspect tests slightly more complex than those conducted at Lac Naococane (see Section 5.5.2) because slopes of a particular aspect did not always experience the same stress regime. For example, slopes situated in the south western parts of the site with an south westerly aspect would have experienced compressive glacial stress, whilst slopes with the same aspect situated in the south east would have experienced extending glacial flow. Therefore to simplify matters, three sample areas where chosen, one from the east, one from the middle and the other in west and tests were then conducted on these regions.

In the eastern side of the River Kaniapiskau area ice flowed into the site from the southeast in a northwesterly direction across the area. Therefore, slopes facing the southeast would have experienced compressive stresses and slopes facing northwest extending glacial flow. By defining compressive slopes as those facing 320° to 130° and extensional slopes as those facing 140° to 310° the GIS was utilised to map the area of both categories and assess the relative proportion of ribbed moraine in each category (Figures 6.18 & 6.19). The results showed that 31 % of the ribbed moraine sampled formed on compressive slopes and 51 % formed on slopes that experienced extending glacial flow. In the central parts of the study site 58% of the ribbed moraine sampled were formed on compressive slopes and 28% on extending slopes (Fig. 6.20) and in the western sector, 31 % were formed on compressive slopes and 52% on extending slopes (Figures 6.21 & 6.22). Contrary to some published reports (e.g. Bouchard, 1980,1989; Minel, 1980; Sollid & Sørbel, 1984) no preferential relationship was found between ribbed moraine occurrence and compressive slopes in this area.

15 km

15 km

Figure 6.18. In the eastern part of the study area, ice flowed from the southeast in a nortl westerly direction, therefore, slopes facing between 55° to 215° would have been zone: of compression (A). From this sample, 31 % of the ribbed moraines sampled formed o compressive slopes (B).

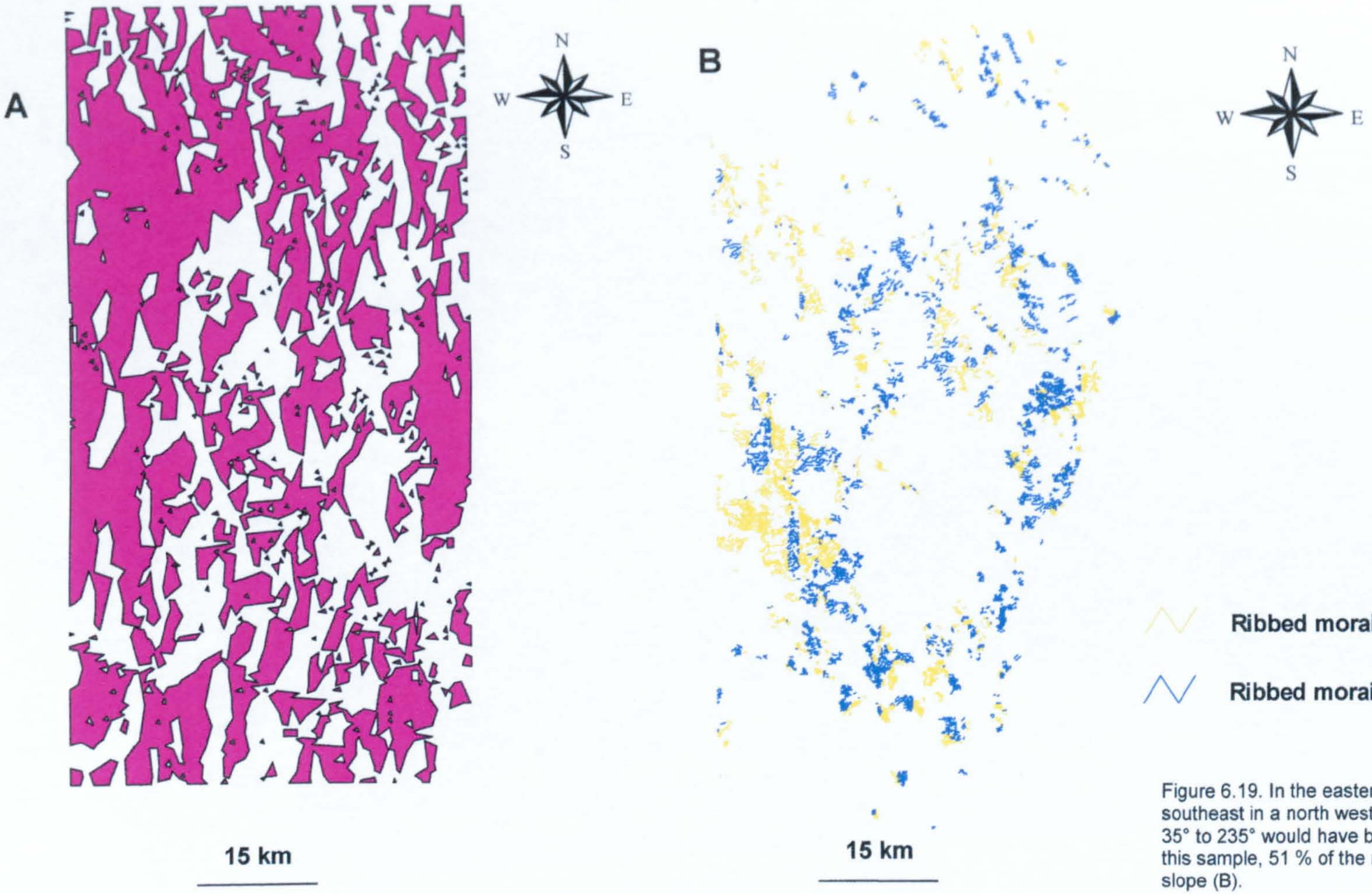

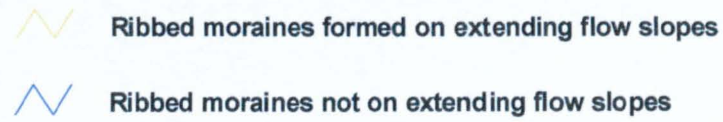

Figure 6.19. In the eastern part of the study area, ice flowed from the southeast in a north westerly direction, therefore, slopes facing between 35° to 235° would have been zones of extending glacial flow (A). From this sample, 51 % of the ribbed moraines sampled formed on this type of slope (B).

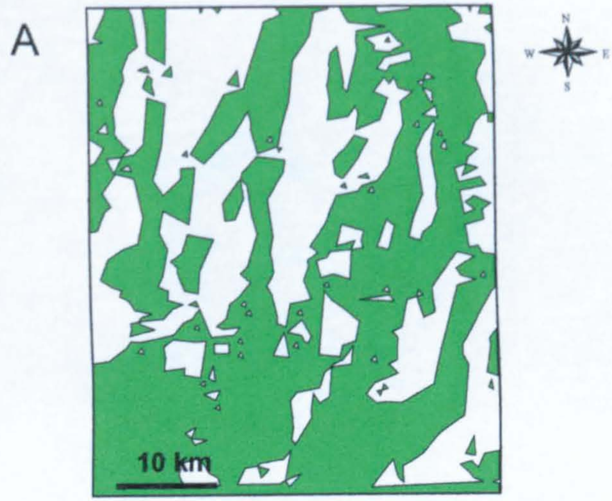

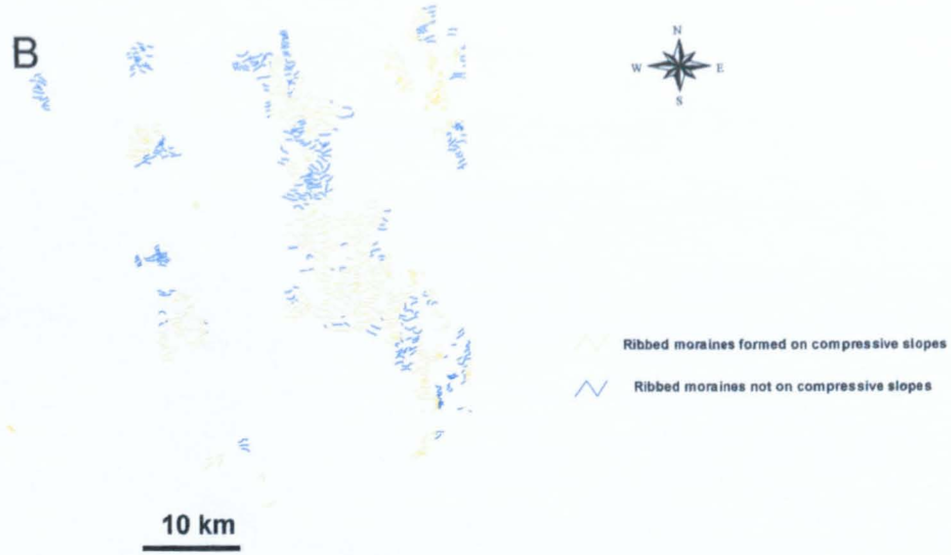

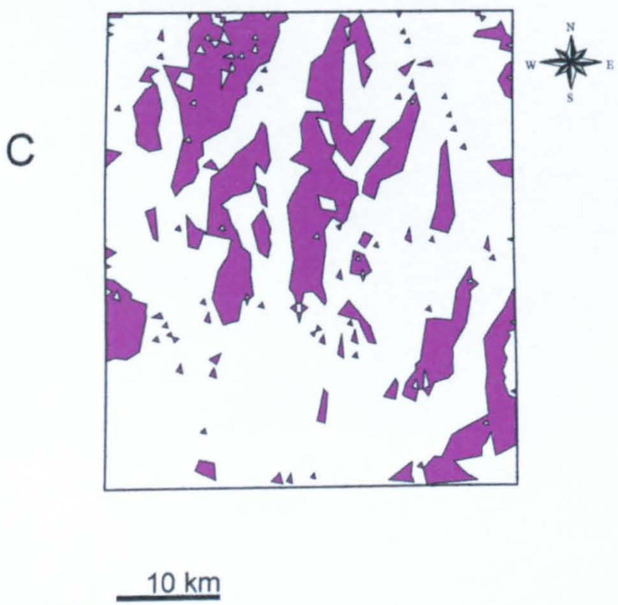

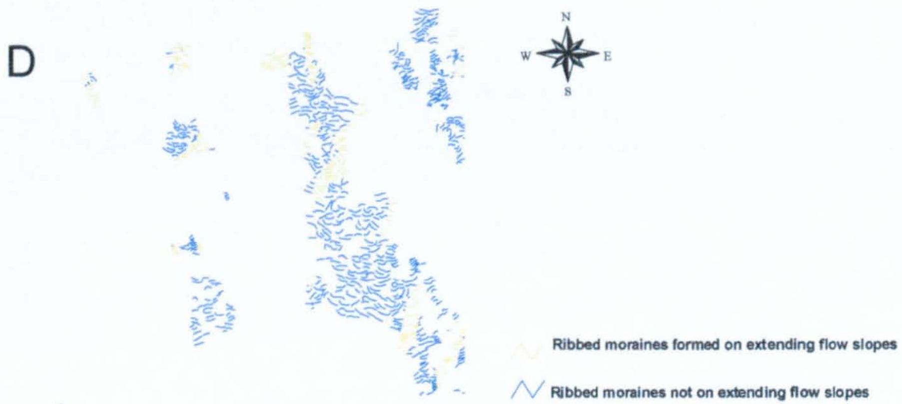

Figure 6.20. In the central parts of the study area ice flow from the south in a northerly direction, therefore, slop facing between 55° and 260° would have been zones compression (A) and 35° to 280° areas of extending glac flow (C). From this sample, 31 % of the ribbed morair sampled formed on compressive slopes (B) and 51 % forn on slopes that experienced extending glacial flow (D).

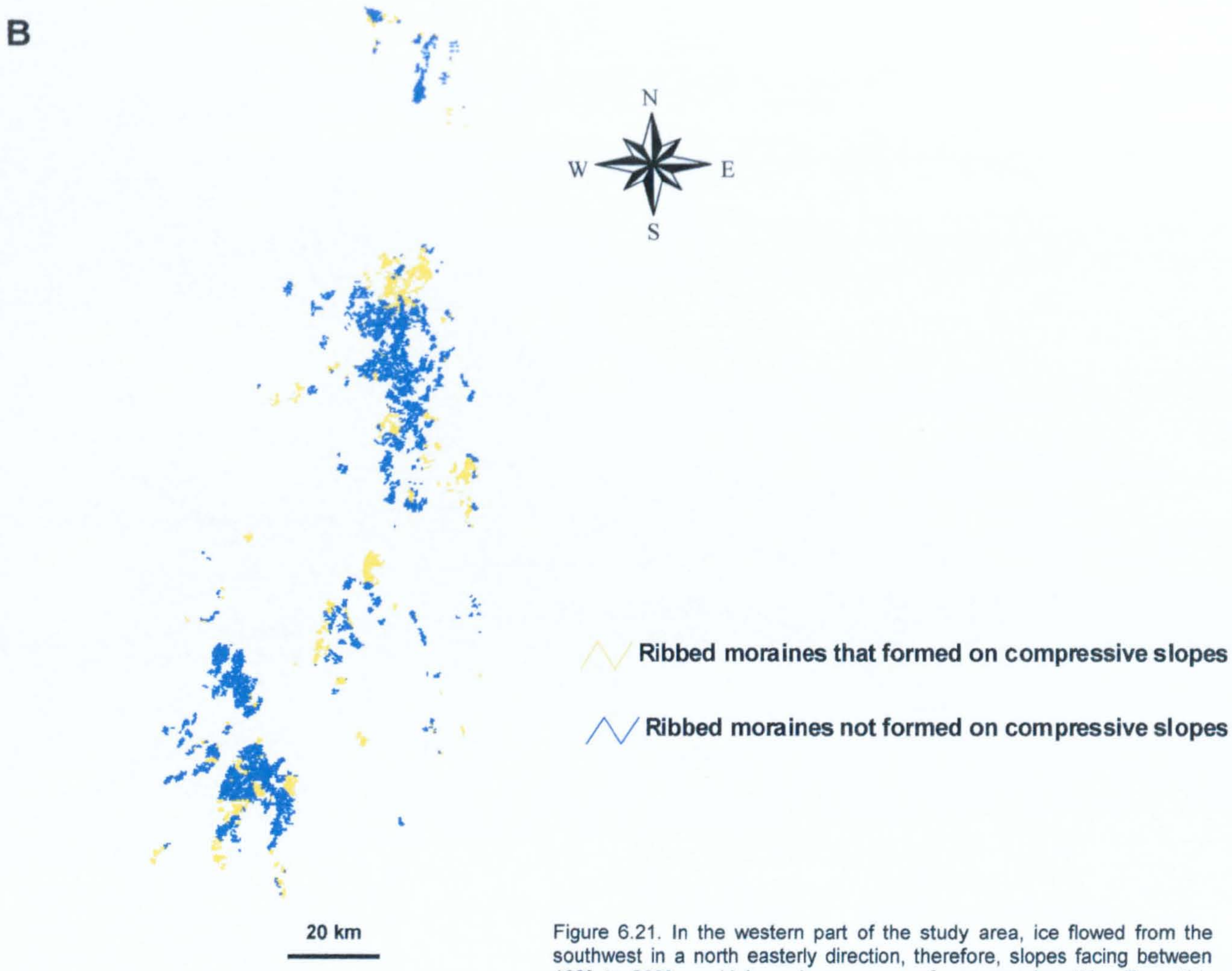

Figure 6.21. In the western part of the study area, ice flowed from the southwest in a north easterly direction, therefore, slopes facing between 122° to 282° would have been zones of compression (A). From this sample, 31 % of the ribbed moraines sampled formed on compressive slopes (B).

A

B

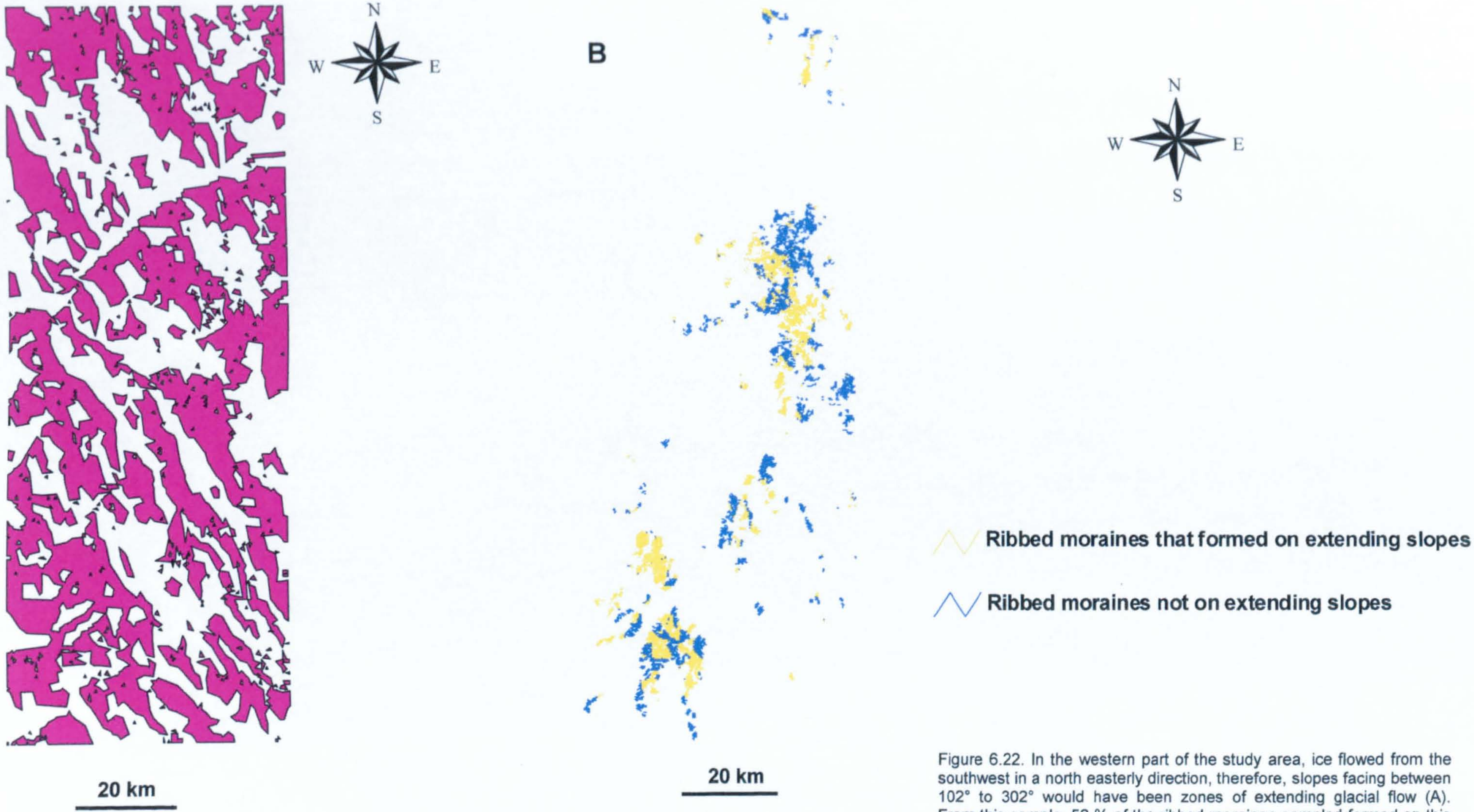

Figure 6.22. In the western part of the study area, ice flowed from the southwest in a north easterly direction, therefore, slopes facing between 102° to 302° would have been zones of extending glacial flow (A). From this sample, 52 % of the ribbed moraines sampled formed on this type of slope (B).

6.6. Morphometric measurements

To add to the quantitative database of ribbed moraine characteristics, measurements were conducted on three aspects of ribbed moraine morphometry. These were ridge length, ridge width and ribbed moraine wavelength. The following sections report the findings for this study site.

6.6.1. Ribbed moraine wavelength

The wavelengths of the ribbed moraine ridges in the Lac Naococane region were calculated using spectral analysis (see Sections 4.3.6.1 to 4.3.6.3). This involved taking transects across each ribbed moraine field in the region and conducting spectral analysis on these transect data to produce periodograms, which showed the frequency spectrum of each transect. The frequency spectrum was then used to determine the wavelength of the ribbed moraine ridges along each transect. In this locality, data from transects totalling 1243 km in length were used to obtain the wavelength data. These data were then used to make a histogram to show the wavelength distribution of the ribbed moraine ridges at this locality (Fig. 6.23).

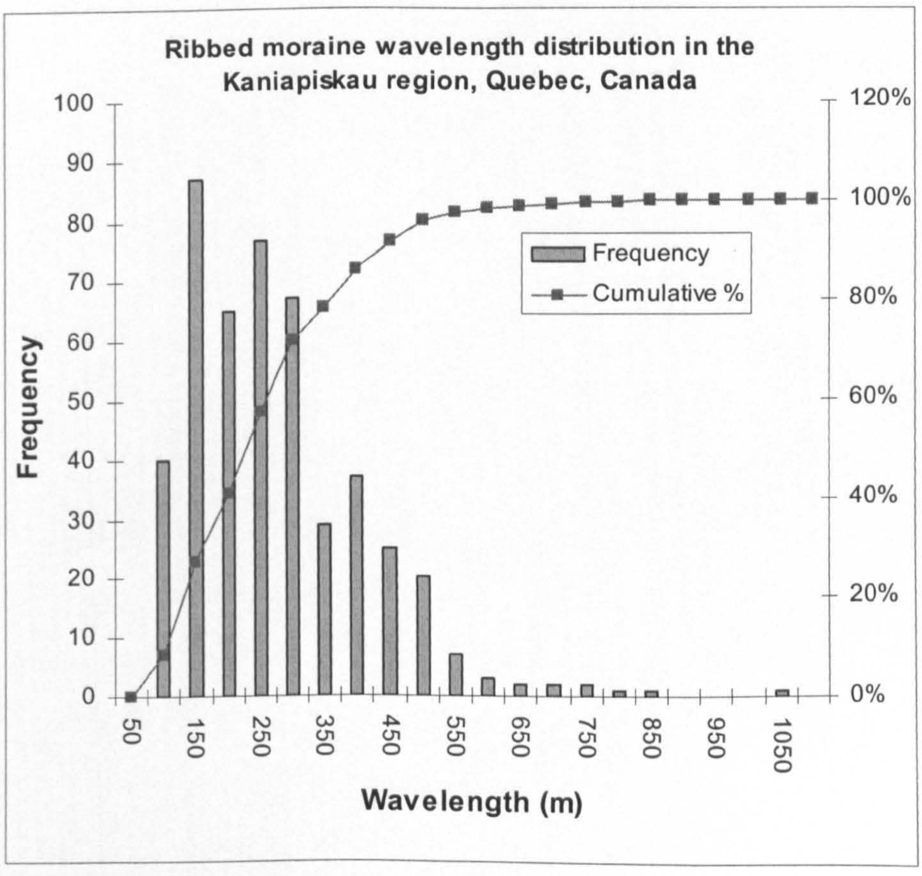

Figure 6.23. Distribution of ribbed moraine wavelengths determined by spectral analysis from transects totalling 1243 km.

The majority of ribbed moraine ridges in the region were found to have wavelengths ranging between 100 m and 550 m, which represents 97.4% of the total sample. The other 2.6% have wavelengths between 600 m and 1050 m. The smallest wavelength measured was 60 m, the largest was 1050 m, the average wavelength was 253 m and the most frequently occurring wavelength, the mode, was 150 m.

The spatial distribution of ribbed moraine wavelength was examined using a GIS. Following the same procedures used for the Lac Naococane site (see Section 5.6.1) a density map was produced which showed the locations of the various ribbed moraine wavelengths in the region (Fig. 6.24). In general, the area is largely covered with ribbed moraine of a similar wavelength, however there are some exceptions and fields containing ribbed moraine ridges of a shorter wavelength can be seen in the east, southeast, southwest and western regions of the site. To investigate whether topography influenced ribbed moraine wavelength, the density map was laid on top of the GTOPO30 DEM to visually examine for any obvious patterns (Fig. 6.24). This showed that there was no single topographic setting where one could find ribbed moraine ridges of a certain wavelength. For example, ribbed moraine ridges with long wavelengths could be seen at the highest (A) and lowest (B) elevations in the site, on the slopes running off the plateau into the bay (C) and in the centre of large depressions (D). A similar situation occurs with ribbed moraine of short wavelength, however, there was a tendency for these to be concentrated on higher ground (e.g. E & F).

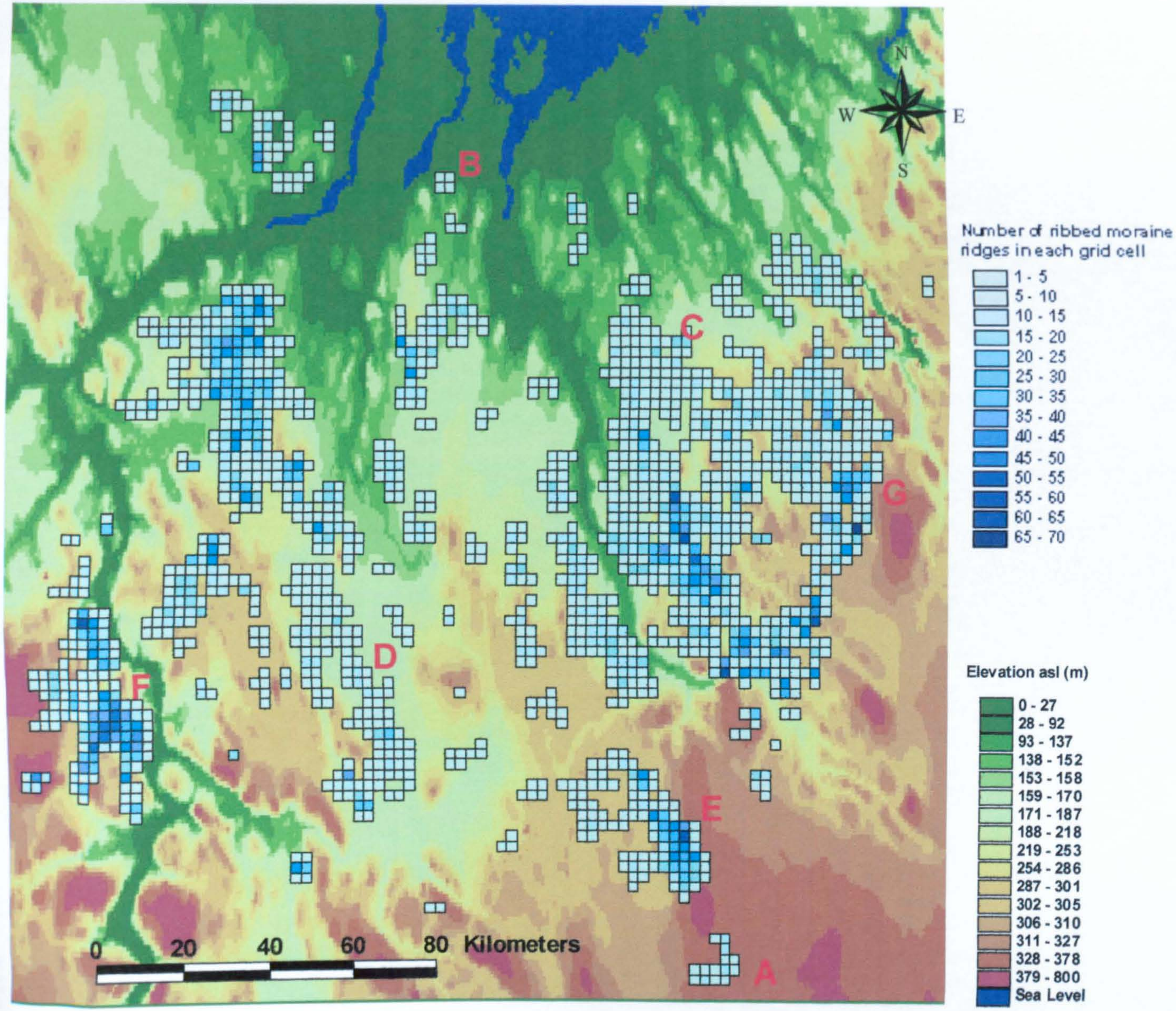

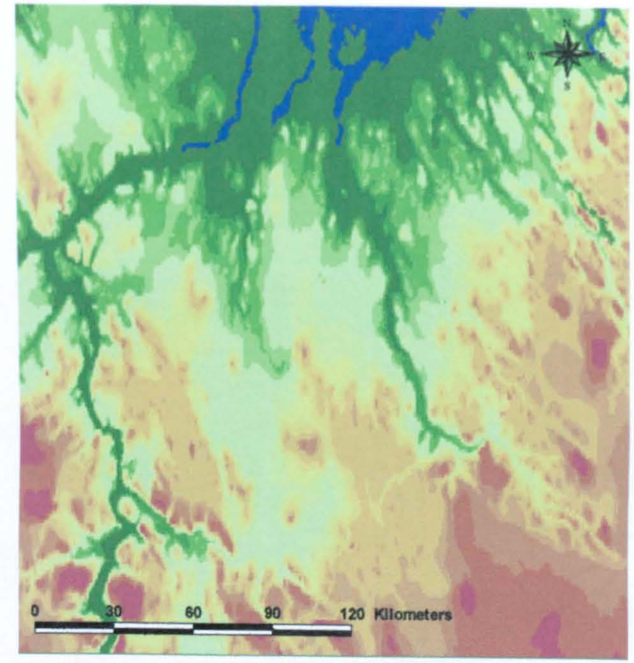

Figure 6.24. An impression of where ribbed moraine ridges with short & long wavelengths are situated in the region can be obtained from the ribbed moraine density map. The darker the shade of blue, the more densely packed the ridges are and the shorter the spacing, or wavelength between the ridges. By draping the density map on top of the GTOPO30 DEM a visual assessment could be carried out to determine whether regional topography influenced ribbed moraine wavelength. The fact that there was no single topographic setting were ribbed moraine ridges of a particular wavelength could be found suggested that topography does not influence ribbed moraine wavelength. For example, note how ribbed moraine ridges with long wavelengths are located in a variety of topographic situations.

6.6.2. Ribbed moraine ridge length

Information on the length of the ridges in the study site was obtained using the same methods described previously in Section 5.6.2. Figure 6.25 shows the resultant histogram and in this study area it can be seen that 98% of ridges are between 200 m and 2500 m in length. The minimum ridge length was found to be 32 m, the maximum 2993 m and the mean ridge length 561 m.

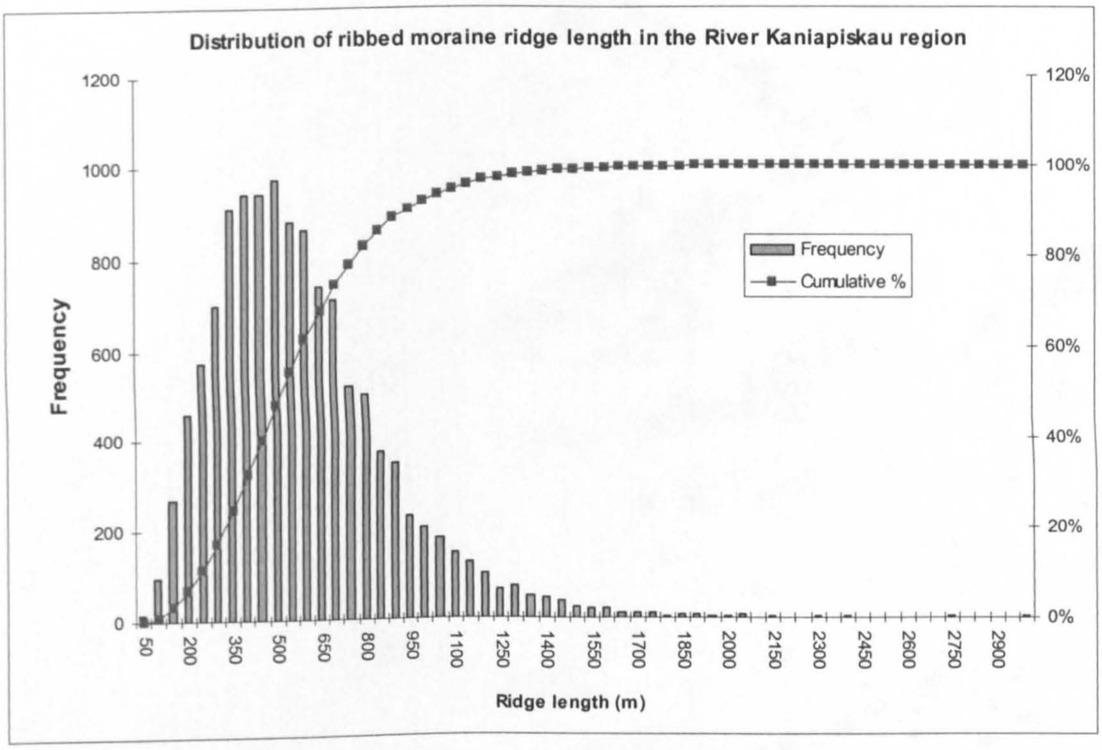

Figure 6.25. Distribution of ribbed moraine ridge length from a sample of over 12000 mapped ridges in the River Kaniapiskau region. 98 % of the ribbed moraine ridges have lengths ranging between 50 m and 1350 m, with the maxima at 500 m.

To visually explore these length data, the ribbed moraine crests were classified into groups of various lengths (Fig. 6.26). The most obvious pattern to emerge was that the ribbed moraine fields in the River Kaniapiskau region, like those of Lac Naococane, are made up of ridges of various lengths without any consistent clustering of fields of a certain length.

Figure 6.26. Ribbed moraine crests classified into 6 separate groups based on ridge length. Note that in general, the ribbed moraine fields are made of ridges that vary in length.

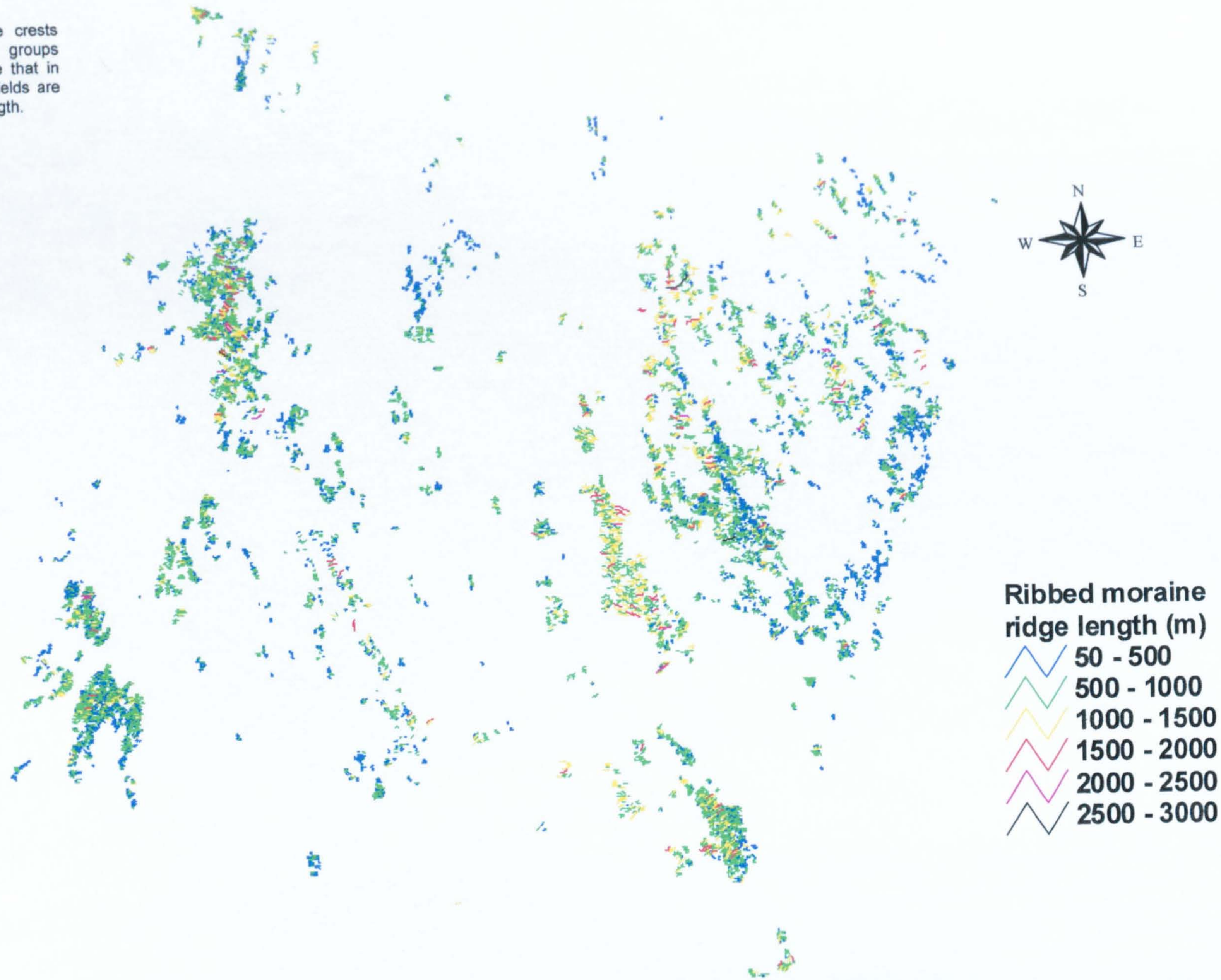

6.6.3. Ribbed moraine ridge width

To investigate the width of the ribbed moraine ridges in this locality, 250 ridges were randomly sampled from various locations across the site. The width of the ridge was determined following the procedures outlined in Section 5.6.4. Figure 6.27 shows the resultant histogram. In this sample, 98% of ridges are between 36 m and 500 m wide. The minimum ridge width was found to be 36 m, the maximum 803 m and the mean ridge length was 235 m.

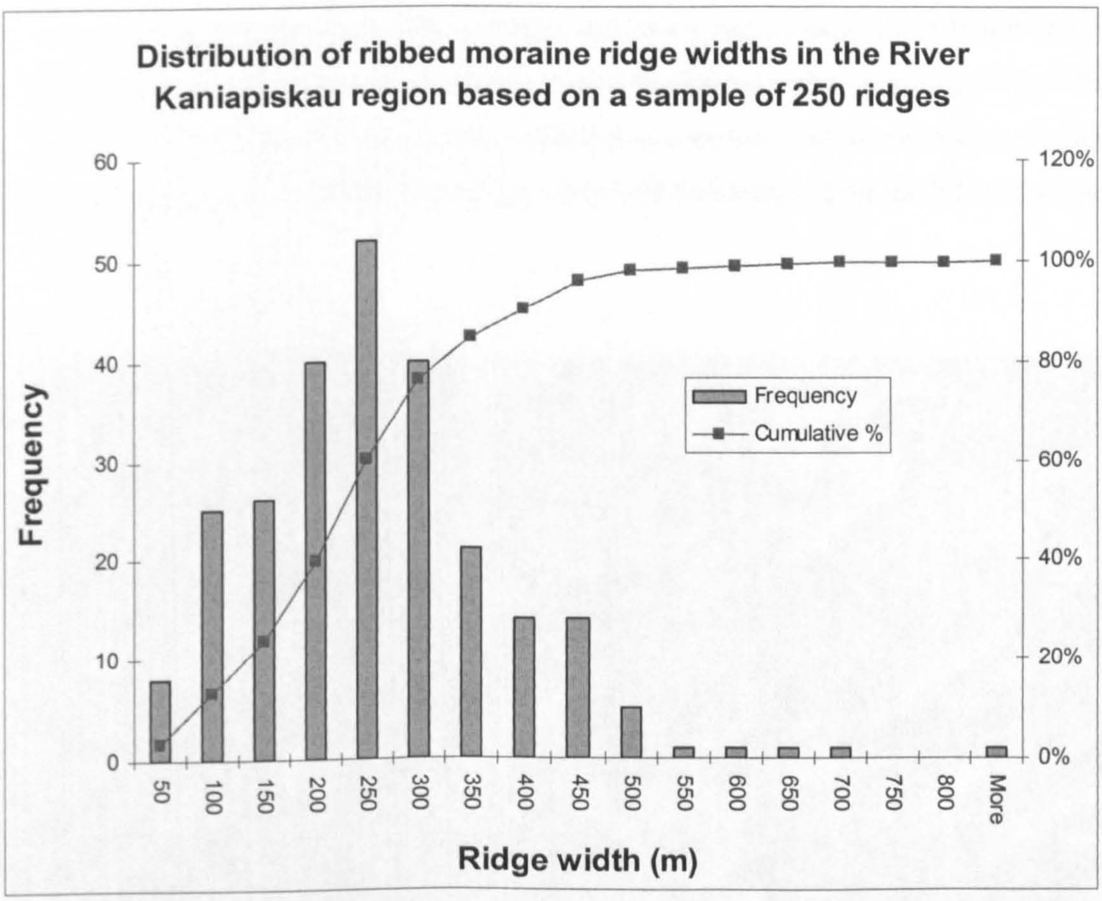

Figure 6.27. Distribution of ridge width in the Kaniapiskau region. 97% of the ridges in this area are between 40 and 500 m wide, with the maxima being 250 m.

6.7. Relation to other landforms

6.7.1. Ribbed moraine, drumlins and glacial lineations

As was demonstrated in Section 5.7, strong spatial associations exist between ribbed moraine, drumlins and mega-scale glacial lineations in Lac Naococane (see Figure 5.50). Large-scale observations in the River Kaniapiskau area concur with these findings and ribbed moraine fields were observed with drumlins and mega-scale glacial lineations in a variety of settings. The simplest association came in the form of drumlinization of the ridges (Fig. 6.28a). However, compared to the Lac Naococane region, this characteristic was less common and many ridges lacked this feature having a much smoother appearance in comparison to drumlinized ribbed moraine (Fig. 6.28b). To gain a better understanding of the relationship between ribbed moraine and glacial lineations in this site, all of the lineations that could be identified on the ETM+ image

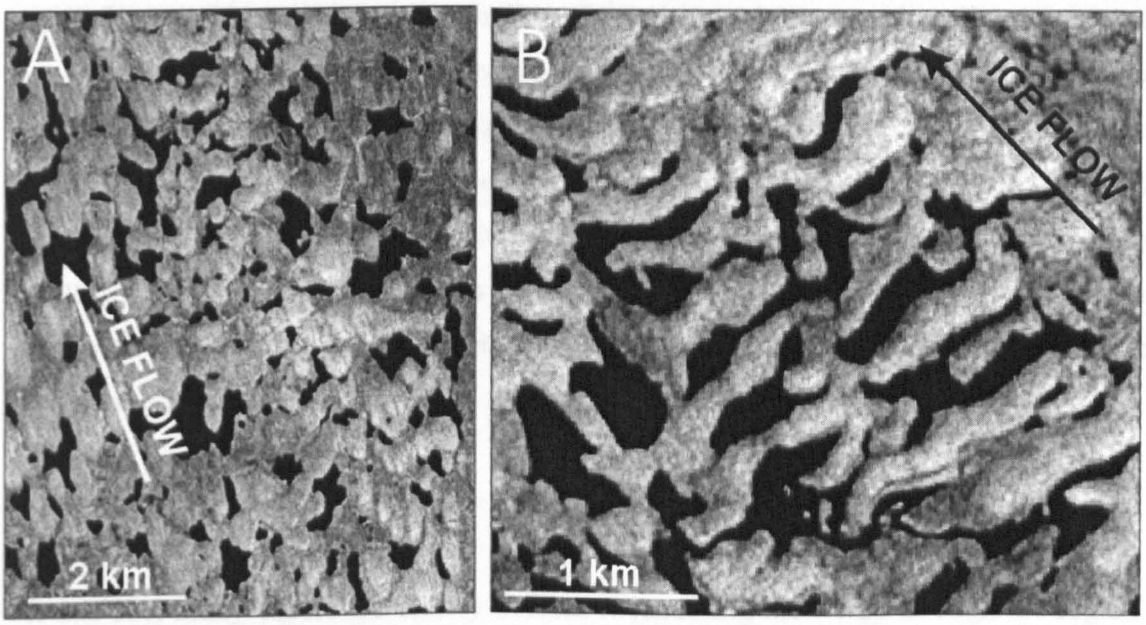

Figure 6.28. In the River Kaniapiskau area some ridges show signs of drumlinization and fluting on the surface of the ridges (A). However, it was not as prolific a feature as it was in Lac Naococane and many ridges observed at this site had a smoother surface (B).

were mapped within a GIS. The ARC coverage was then placed on top of the ribbed moraine ARC coverage, which gave an excellent visual overview of the spatial distribution of both landforms (Fig. 6.29). In total 2300 glacial lineations were mapped in the site, and although isolated swarms could be seen dotted about the area, the majority were found to be concentrated in a large sweep that cuts through the centre of the site. Given that the central swarm is 200 km long, up to 40 km wide and consists mostly of highly attenuated bedforms with elongation ratios greater than 10:1 (see inset picture in Figure 6.29) it is most likely the signature of a former ice stream track, as these elements fit the criteria for identifying palaeo-ice streams (Stokes and Clark, 1999). As is shown, the drift lineations are found in a variety of spatial associations with the ribbed moraine. As well as there being lateral transitions between ribbed moraine and drumlins (e.g. A), downstream transitions from ribbed moraine to lineations (e.g. B) and from lineations to ribbed moraine (e.g. C) are also evident, as is overprinting of the ribbed moraine by glacial lineations (e.g. D). Visual inspection of this site concluded that most of the lineations are superimposed on top of the ribbed moraine fields and therefore postdate these landforms. In the central regions, it looks as if entire ribbed moraine fields have been cannibalised by the ice stream. Where this has occurred, the ribbed moraine ridges have a heavily drumlinized appearance and superimposition of drumlins is a common feature (Fig. 6.30). It is possible that the pressures at the base of the ice stream largely destroyed pre-existing ribbed moraine ridges and this may explain the notable scarcity of ribbed moraine in the central depression (see Figure 6.17). Although it was more common to see lineations on top of the ribbed moraine, there were some instances where the reverse occurred. In these cases, mega-scale glacial lineations appeared to have small-scale minor ribbed moraine ridges superimposed on top and sandwiched between them. A more unusual case was also observed where the lineations appeared to have been broken up, or "ribbed" into small scale ribbed moraine ridges (Fig. 6.31); a relationship that is regarded as extremely rare but has been reported before in Keewatin, north of Dubawnt Lake (Aylsworth & Shilts, 1989).

6.7.2. Eskers

At this site, many eskers are clearly evident meandering their way through the region. They are found in similar settings as that described in Section 5.7.2 and were observed to be always draped on top of the ribbed moraine fields. The eskers were not found to be associated with a particular size or shape of ribbed moraine ridge and in many places they cross over areas where ribbed moraine is absent. The fact that all the eskers observed in the region were draped on top of the ridges is evidence they postdate ribbed moraine formation and were laid down during deglaciation.

Figure 6.29. Showing the ARC coverage's of the mapped glacial lineations and ribbed moraines in the River Kaniapiskau site. The inset picture is an ETM+ image of the area pointed out by the arrow and shows a high concentration of attenuated bedforms.

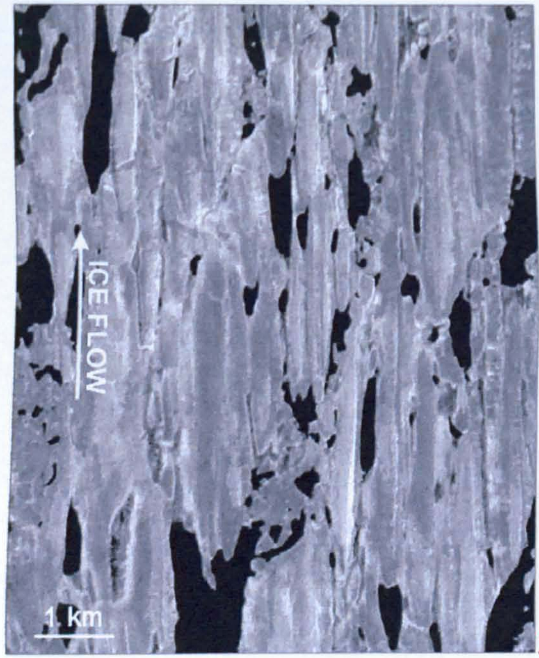

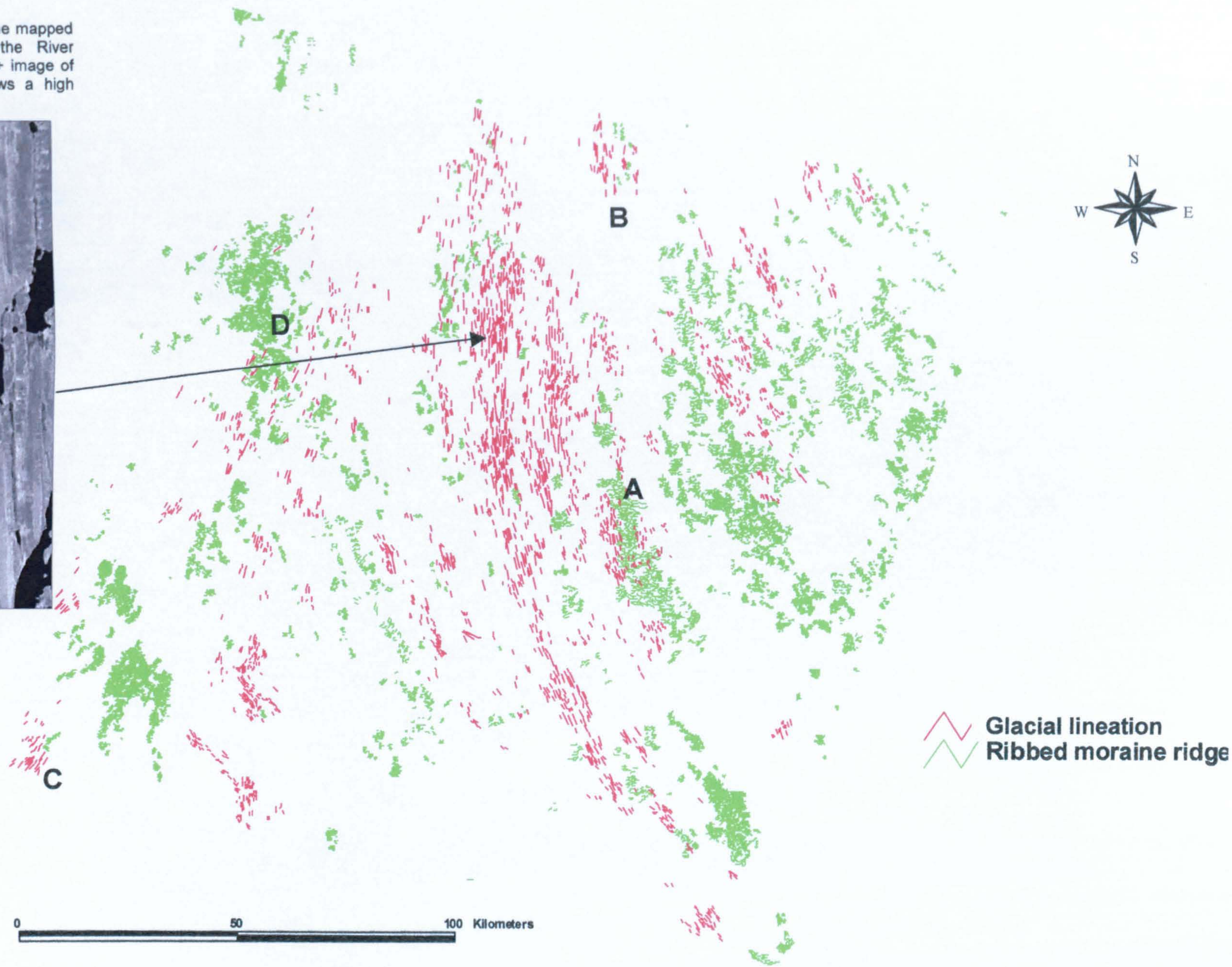

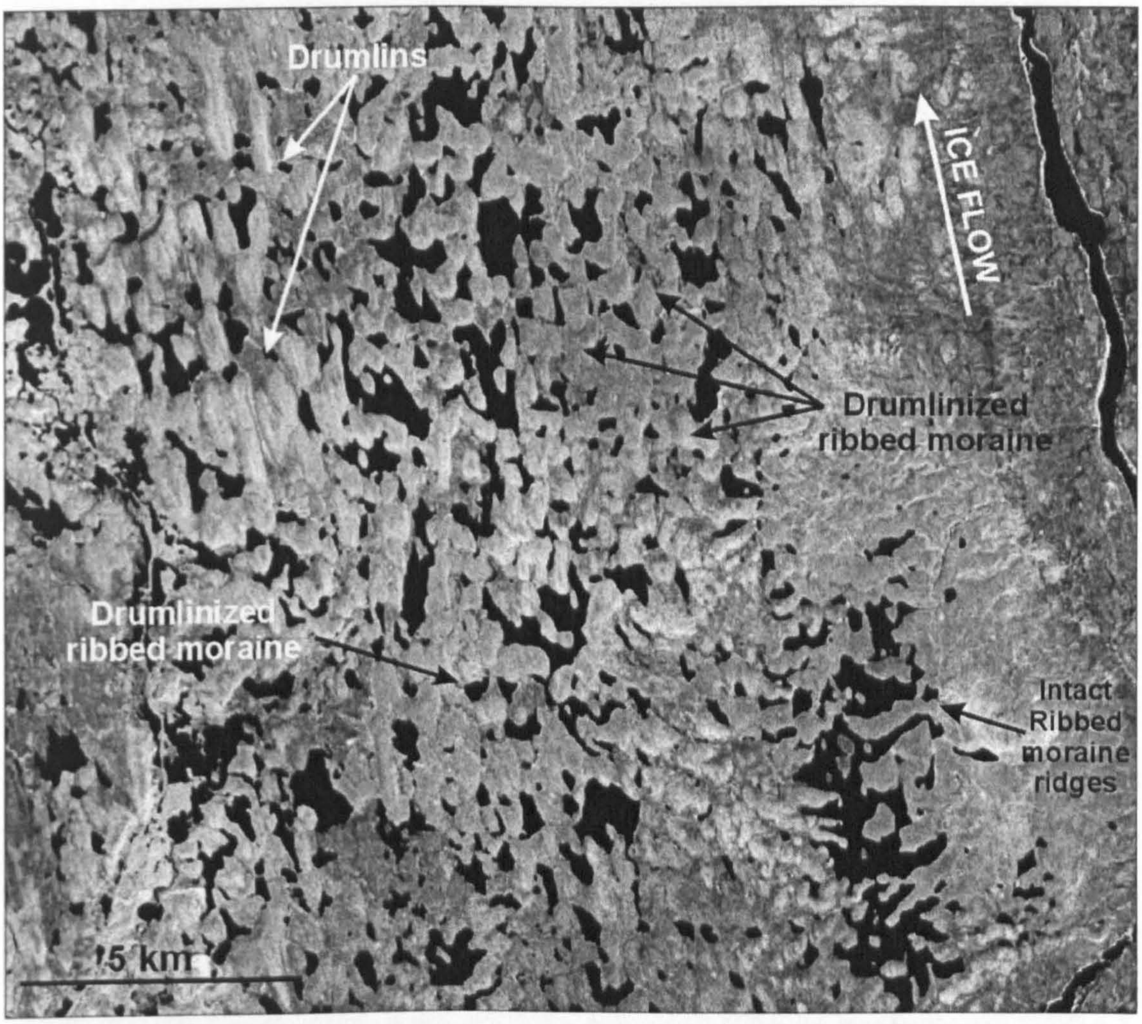

Figure 6.30. Showing an area of drumlinized ribbed moraine. Notice that there are intact ribbed moraine ridges in the bottom right and that ridge elements still survive in the central parts of the image even though they have been heavily drumlinized. Notice also, that many drumlins are clearly superimposed on top of the modified ridges in this area. The picture is of the area marked A in Figure 6.29 and was taken from the ETM+ image.

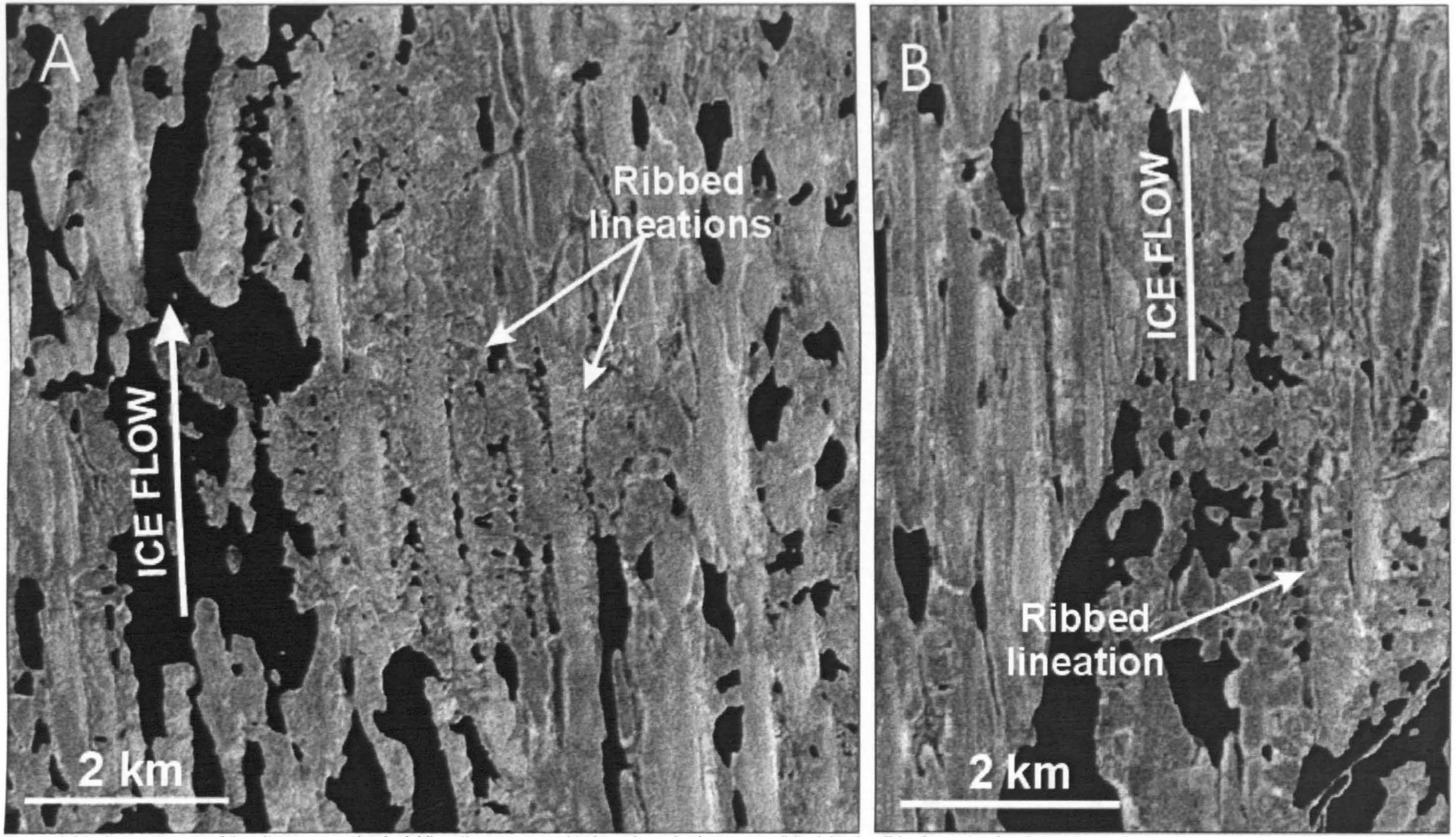

Figure 6.31. In some parts of the site mega-scale glacial lineations appeared to have been broken up, or ribbed, by the ribbed moraine forming process. In some cases it appears that small scale ribbed moraine ridges where superimposed on top of the lineations (A). However, there were examples where it looked as if the lineations have been reworked into ribbed moraines (B).

6.8. Summary and conclusions

Using satellite imagery to map large areas of ribbed moraine in the River Kaniapiskau region established that the ribbed moraine ridges were formed by ice converging into the bay. The large-scale distributional pattern revealed that the ribbed moraine in this region was not as extensive as that found at Lac Naococane and that the fields tended to be concentrated in the eastern and western parts of the site. The central regions lacked significant numbers of ribbed moraine ridges. However, it is hypothesised that an ice stream that went through this area may have reworked the ribbed moraine to such an extent that the ridges were no longer recognisable in their original state and only remnants of the former ridges and drumlinized ribbed moraine remain (see Section 6.7.1).

Close inspection of the site revealed that the ribbed moraine was distributed in the same patterns as those found across the ice divide in the Lac Naococane region. These were elongate ribbons, narrow tracks, clusters and isolated fields. Each field type was not restricted to a particular area within the study site, with examples of each found at various locations across the region. Similar to what was observed in Lac Naococane, it was also possible to find one field type within the confines of another and Figure 6.7, which shows a narrow track running through a large dense cluster of ribbed moraine illustrates this point clearly. This is an important observation because it highlights the fact that the ribbed moraine forming process can operate at different scales within a confined area.

Large-scale visual observations of ribbed moraine ridges in this region once again revealed a diverse range of morphology. As well as having most of the forms discussed in Section 5.4.1, two other kinds of ribbed moraine were also identified that looked morphologically distinct from other types of ridge illustrated in Figure 5.49. The first was classified as a lumpy ribbed moraine, as the characteristic bulging outline gave the ridges a rather lumpy appearance compared to the smooth outlines of classical type ridges (see Figure 6.13). The other was not an individual ridge, but rather a collection of ridges of mixed morphology and scale that were interconnected to form a distinctive "lattice" type ribbed moraine field (see Figure 6.14). Both are shown schematically in Figure 6.32.

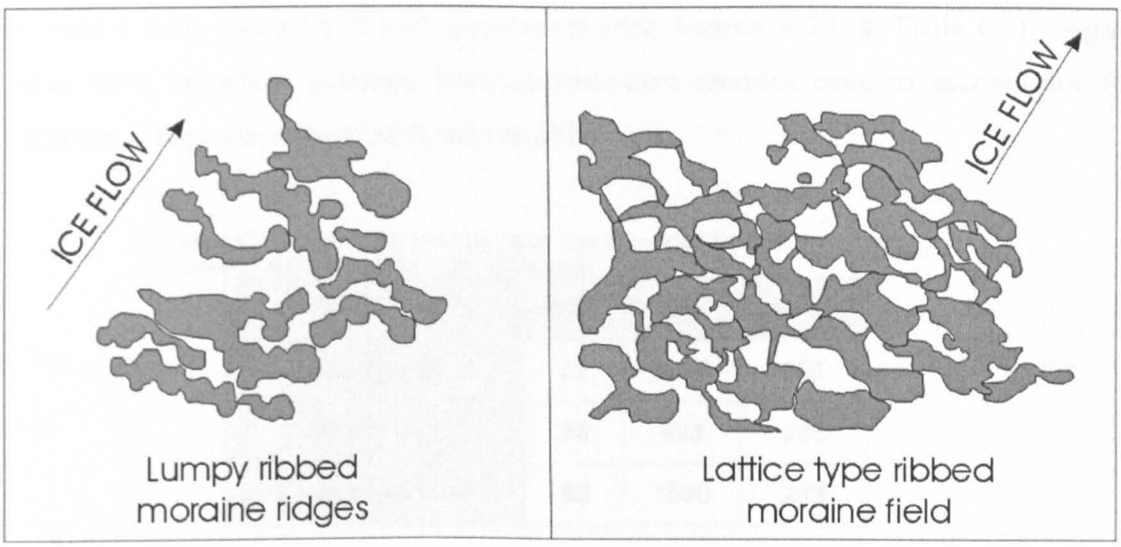

Figure 6.32. Showing the newly classified types of ribbed moraine observed in the River Kaniapiskau region.

Combined with the morphological types that were summarised in Figure 5.49, the complexity in form between the various types is clearly illustrated. What became evident from mapping the fields was that many ridges were morphologically different from the more classic type that is often described in the literature and that most fields contained ridges of mixed morphology (see Figures 6.10 & 6.11). This was an interesting observation and has implications for formative theories because for any theory to be credible it must be able to explain the various forms.

Using a DEM to investigate the topographic setting of the ribbed moraine in the study area revealed that the majority were concentrated in the narrow valleys and topographic lows of the large plateau that surrounds the site and also on the slopes that run from this into the bay (see Figure 6.17). Visual inspection of the mapped ribbed moraine ridges estimated that approximately 75% of the ribbed moraine population are located in these regions, rather than in the main central basin.

The slope aspect tests that were conducted showed that the distribution was not influenced by the direction the slope was facing in relation to the regional ice flow. The tests concluded that in the eastern region 31% of the ribbed moraine ridges sampled formed on compressive slopes, in the central parts 58% were formed on compressive slopes and in the western sector the figure was 31% (see Figures 6.18 & 6.22). Again, this is contrary to existing observations in the literature (e.g. Bouchard, 1980,1989; Minel, 1980; Sollid & Sørbel, 1984).

Morphometric measurements conducted on ribbed moraine length and wavelength showed a wide variation in both parameters (see Section 6.6.1 & Table 6.1). Again, these were important findings, because formative theories need to account for this variation if they are to be considered credible.

Table 6.1. Showing the average value and the range for each measured ribbed moraine parameter in the study area.

Parameter	Min	Max	Mean
Length (m)	32	2993	561
Width (m)	36	803	235
Wavelength (m)	60	1050	253

Analysis conducted using a GIS, showed that most fields contained ridges of mixed length and that ribbed moraine of both short and longer wavelengths was spread across the entire region. Procedures carried out in the GIS also concluded there was no specific topographic setting where one could find ribbed moraine ridges of a certain type of wavelength as ridges of various wavelengths could be found in every topographic setting (see Figure 6.24). However, it was noticed that areas of ribbed moraine with the short wavelengths tended to be clustered in the highest regions of the site.

Finally, the relationships between ribbed moraine and other glacial landforms was investigated. It was noted that many eskers meander through the study site and that they are always found draped on top of the ridges. This was seen as evidence that they post date ribbed moraine formation and that they were simply laid down during deglaciation.

Large-scale observations in the River Kaniapiskau region found that ribbed moraine in this region had strong spatial associations with drumlins and megascale glacial lineations. The simplest association was in the form of drumlinization of the ridges (Fig. 6.28a). However, compared to the Lac Naococane region, this characteristic was less prevalent and many ribbed moraine ridges lacked this feature (Fig 6.28b). Mapping the drumlins in this area showed that most were concentrated in a large sweep that runs through the centre of the site. It was hypothesised that this may be an ice stream track as the dimensions of the swarm and the morphological characteristics of the glacial lineations fit the criteria set out by Stokes and Clark, (1999) for identifying palaeo-ice streams. When the drumlin ARC coverage and the ribbed moraine ARC coverage were combined it established that there were lateral transitions between ribbed moraine and drumlins, downstream transitions from ribbed moraine to lineations and vis versa and that ribbed moraine was also overprinted by glacial lineations (see Figure 6.29). Visual inspection of this site concluded that most of the lineations are superimposed on top of the ribbed moraine fields and therefore postdate these landforms, and in the central regions, it looks as if entire ribbed moraine fields were cannibalised by the ice stream forming drumlinized ribbed moraine. Where this has occurred, the ribbed moraine ridges have a heavily drumlinized appearance and superimposition of drumlins was found to be a common feature (see Figure 6.30). Although it was more common to see drumlins on top of the ribbed moraine in this region, there were some cases where minor ribbed moraine ridges were found superimposed on top of megascale glacial lineations (see Figure 6.31a). A more unusual case was also observed where the lineations were broken up, or "ribbed" into small scale ribbed moraine ridges (Fig. 6.31b). Both of these have been summarised in Figure 6.33. This is an interesting observation because it indicates that there were multi-phases of ribbed moraine formation operating in this region.

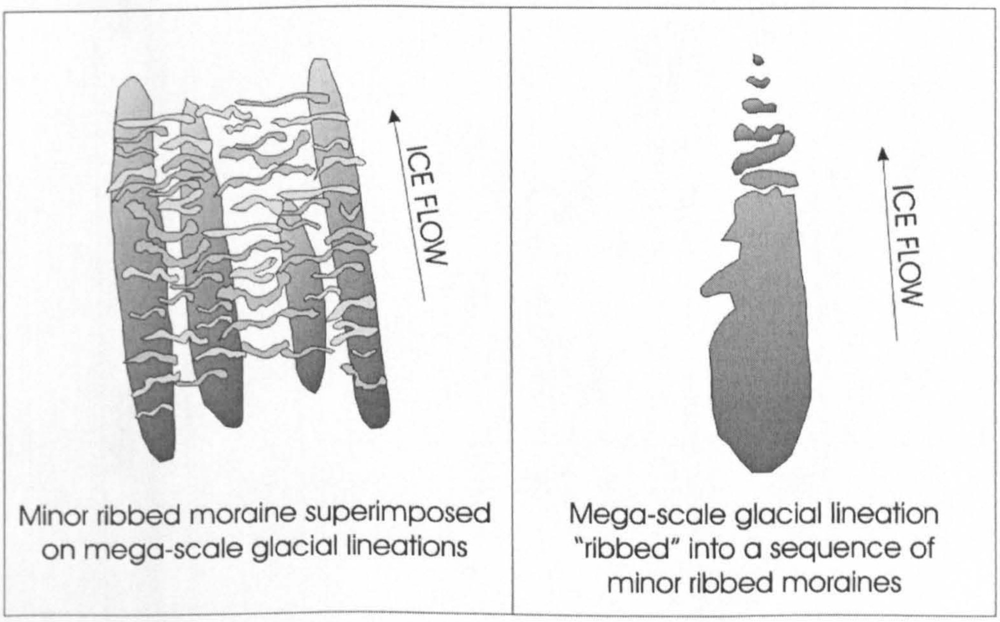

Figure 6.33. Schematic diagram illustrating two new spatial relationships observed between ribbed moraine and mega-scale glacial lineations discussed in Section 6.7.1.

***

Map 6.1. Distribution of Ribbed Moraine, Kaniapiskau River Region, Quebec, Canada

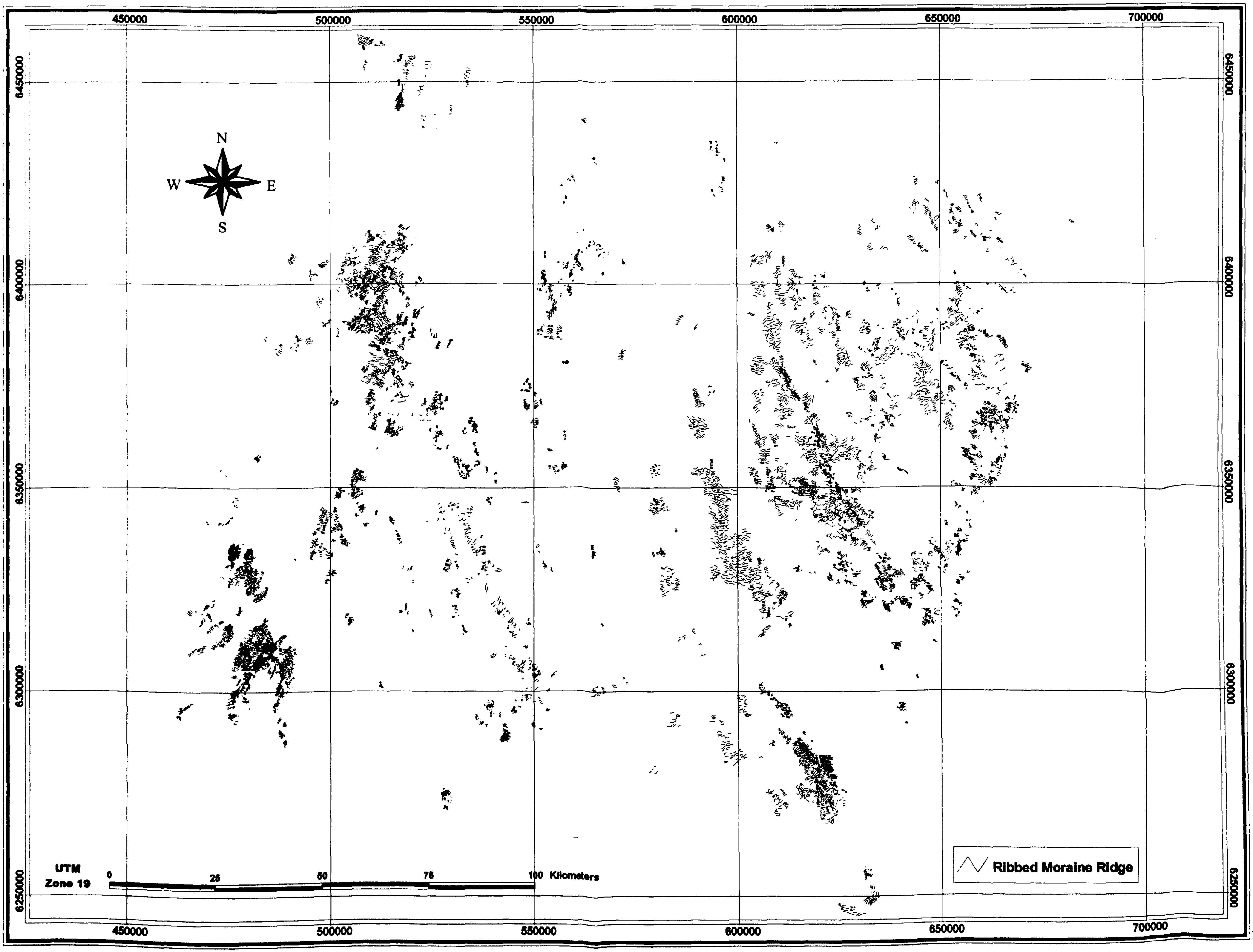

Chapter 7: The Characteristics of Ribbed Moraine in the Northeast Midlands of Ireland

7.1. The study site

The Irish ribbed moraine fields used in this study are situated in the northeast midlands and cover an area approximately 9000 km^2. The location of the site is shown in Figure 7.1 and the coverage of the DEM that was used is marked by the black boundary.

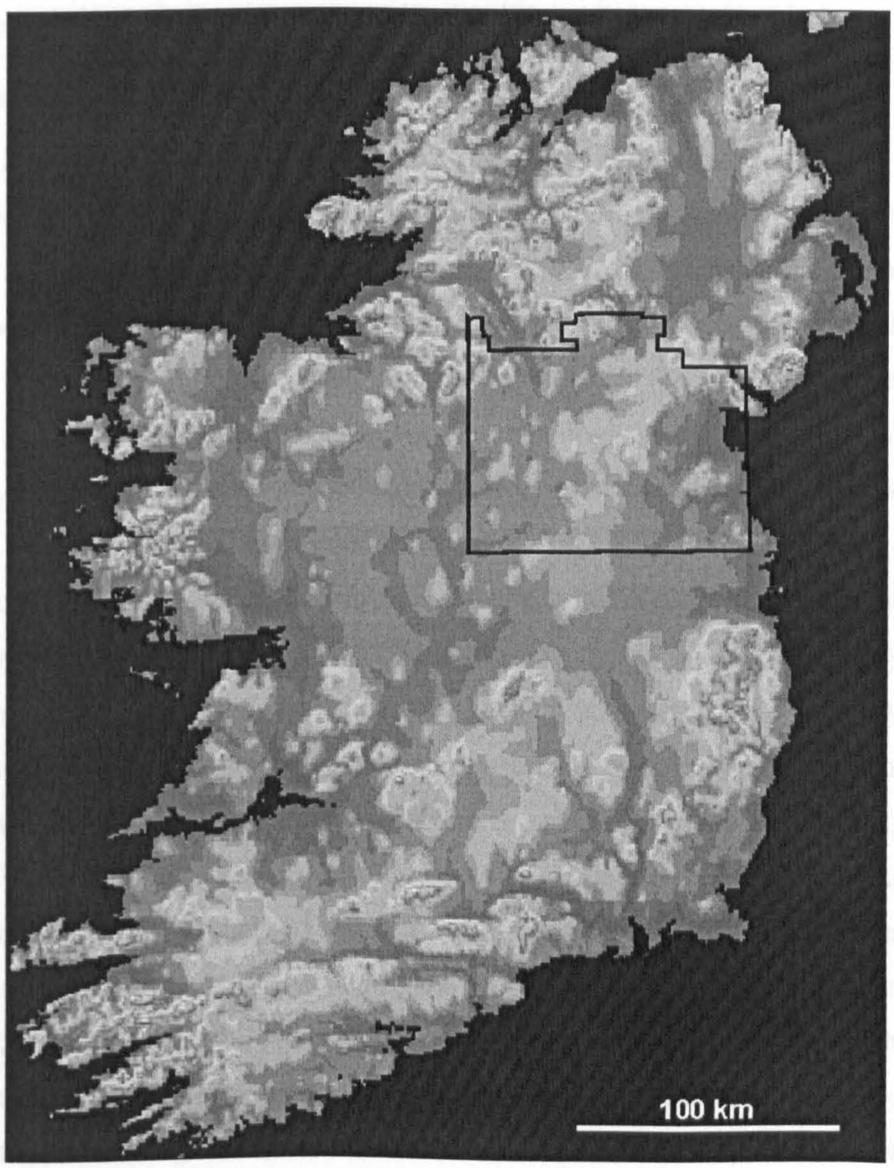

Figure 7.1. General location map showing the limits of the DEM used to map the Irish ribbed moraine ridges.

7.2. Data sources and methodology

The ribbed moraine in this part of Ireland were comprehensively mapped by Clark and Meehan (2001) who used a 25 m grid resolution, 1 m vertical accuracy DEM that was derived from digital photogrammetry. These authors conducted the mapping by on-screen digitising directly into a GIS, with large-scale ribbed moraine ridges portrayed as polygons drawn at the break of slope defining the ridge and smaller scale ridges by digitising the ridge crest. It was not necessary to re-map the area, as this author was given access to Clark and Meehan's original ARC coverage.

7.3. Results from mapping

7.3.1. Large-scale pattern

Figure 7.2 shows the general orientation of the ribbed moraine fields in this area from which three distinct flow patterns can be identified. These patterns were also recognised by Clark and Meehan (2001), who interpreted the ribbed moraine as belonging to three distinct bedforming events that occurred at separate times during the evolution of the Irish Ice Sheet (Fig. 7.3). Clark and Meehan interpreted the ribbed moraine between points A and B as belonging to the earliest bedforming phase in the area (which they arbitrarily termed rm-2) and was produced when the Irish Ice Sheet was centred over the northeast of the country. The small field at point C (termed rm-g) post-dates rm-2 and records ice discharge towards the northwest from a north-south ice divide at the Last Glacial Maximum (LGM). The other ribbed moraine fields were produced by ice flow in a south-easterly direction (termed rm-1). These were interpreted as belonging to the latest phase of ice flow in the region and were produced when the ice divide migrated to the northwest after the LGM. In this position, the ribbed moraine fields rm-2 and rm-g would have been close to the ice divide and as a consequence would have experienced low ice velocities. These authors state this as a likely explanation for their preservation given that other subsequent ice flow phases are known to have occurred. Compared to the ribbed moraine sites in Québec, where the orientation patterns indicate synchronous formation, the Irish ribbed moraine is unique because it is the only place where ribbed moraine of different ages and orientations have been observed juxtaposed within the same area.

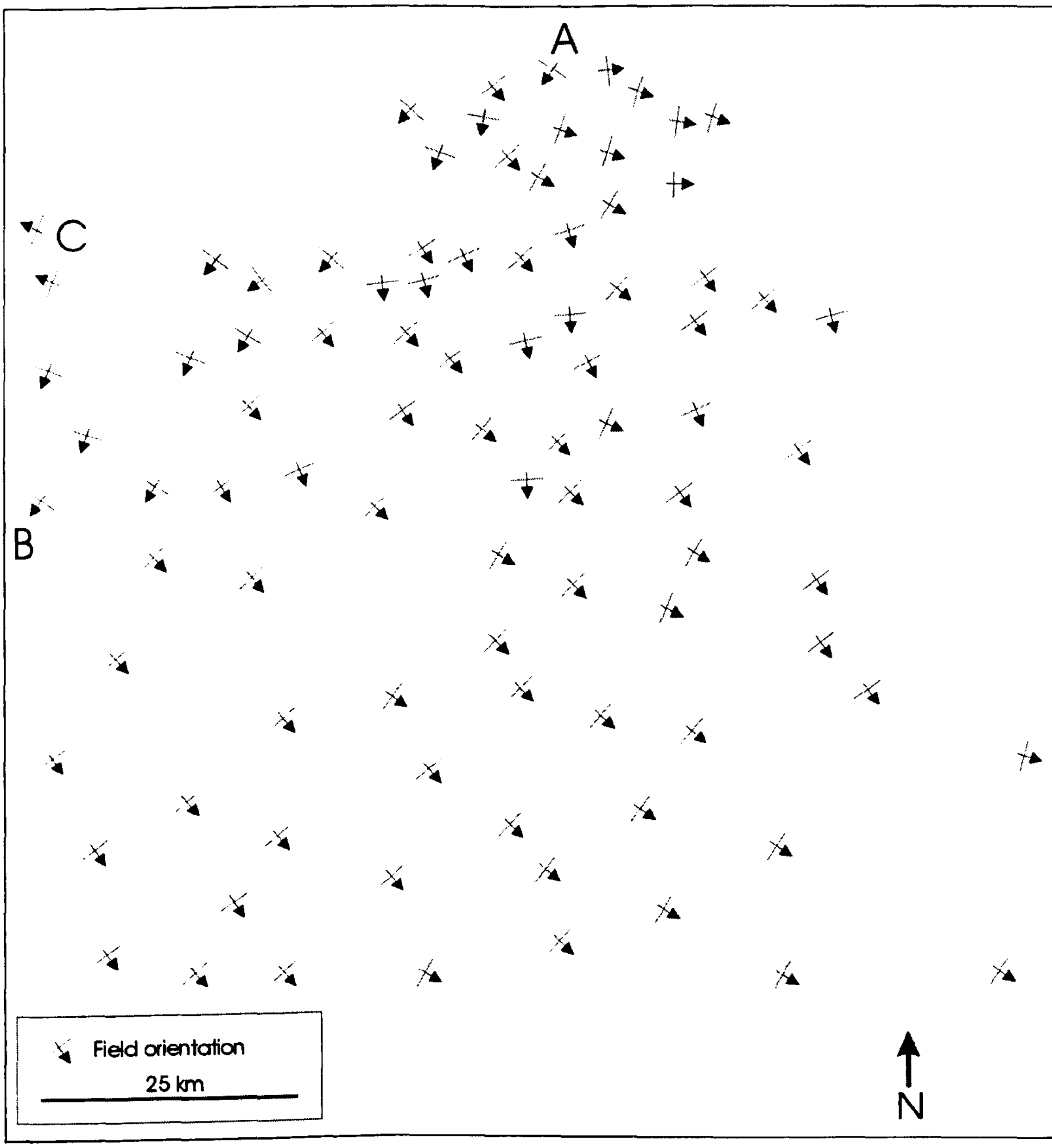

Figure 7.2. Ribbed moraine field orientation map in relation to the regional ice flow pattern. The lines show the general orientation of the ribbed moraine ridges in each field and the arrows the direction of ice flow. Note that the ridges are not uniformly oriented across the site. This is because the site contains ribbed moraine that were formed at three separate times during the evolution of the Irish Ice Sheet.

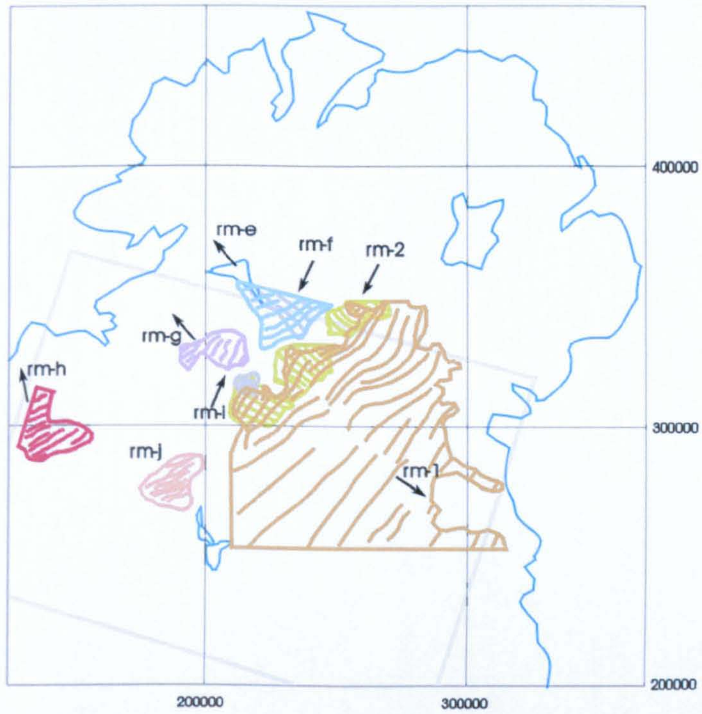

Figure 7.3. Showing the known spatial distribution of ribbed moraine in Ireland (After Clark and Meehan, 2001). Clark and Meehan grouped the ribbed moraine into 8 flow sets, which they arbitrarily named rm-1, rm-2, rm-e, rm-f, rm-g, rm-h, rm-i and rm-j. The area covered by the DEM contains the ribbed moraine fields rm-1, rm-2 and the eastern portion of rm-g. The other ribbed moraine fields were mapped using a Landsat TM image and are not included in this study.

Approximately 2500 ribbed moraine ridges were mapped using the DEM and the resulting ARC coverage can be seen in Figure 7.4 and Map 7.1. A striking pattern is the abrupt transition from large-scale ribbed moraine in the north, to much smaller ribbed moraine in the south. To illustrate this difference, ribbed moraine ridges from both areas, marked A and B in Figure 7.4, are compared. In the southern region, the ribbed moraine are made of ridges that typically range between a few hundred metres to several kilometres in length and 50 m to several hundred metres wide (i.e. the typical scale range of ribbed moraine ridges, see Table 7.1 and Sections 5.6 & 6.6). For example, all of the ridges in the area marked A are between 400 m to 1 km in length and 60 m to 80 m wide and the ridge at point C, which is the longest in the southern region, measures just over 3 km by 250 m. Clark and Meehan (2001) originally classified this area as containing only minor ribbed moraine, which is normally 100 m to 500 m in length by 25 m to 75 m wide (Hättestrand, 1997b). However, the wide-spread prevalence of ridges whose dimensions and characteristics are akin to the classical forms (see Figure 7.5) means it is more accurate to reinterpret this area as a zone containing both minor and classical type ribbed moraine.

In comparison, the ribbed moraine in the northern area is made of much larger landforms and at point B, many of the ridges range between 7 km and 16 km long and can be up to 1.1 km wide. As Clark and Meehan (2001) previously noted, these are the biggest ribbed moraine ridges ever reported. In order to distinguish them from the more usual scale ridges they are herein referred to as mega-scale ribbed moraine ridges and entire fields as mega-scale ribbed moraine.

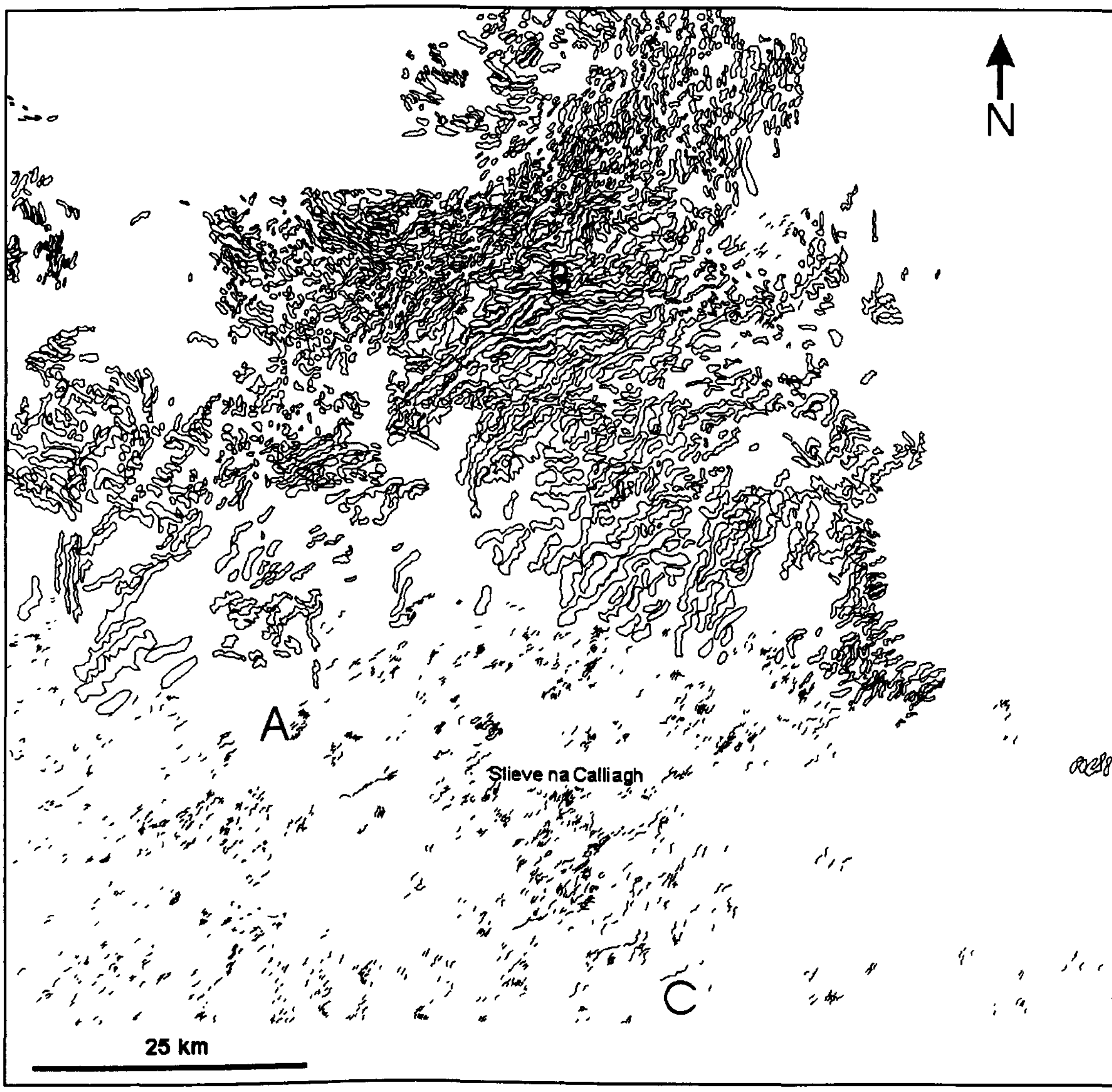

Figure 7.4. Distribution and pattern of ribbed moraine as mapped from the DEM by Clark and Meehan (2001). Polygons mark the break of slope of individual mega-scale ribbed moraine ridges and single lines mark the crests of smaller scale ribbed moraine ridges. Note the abrupt transition from mega-scale ribbed moraine in the north to the more typical scale ribbed moraine in the south. See Map 7.1 for a more detailed view.

Table 7.1. Typical dimensions of ribbed moraine ridges reported in Hättestrand and Kleman (1999)

Length (m)	300 – 1200
Width (m)	150 - 300
Height (m)	10 - 30

Figure 7.5. Ribbed moraine just south of Slieve na Calliagh (7° 06 w & 53° 44 N). All of the ridges in this area were originally interpreted by Clark and Meehan (2001) as being minor ribbed moraine. However, the ridges marked A, B and C are between 1 km to 1.5 km long and 100 m to 150 m wide and are much larger than the typical dimensions of minor ribbed moraine, which range between 100-500 m in length and are between 25 -75 m wide (see Hättestrand, 1997b). Their morphology and size indicates that these ridges belong to the classical category of ribbed moraine, which are larger scale versions of the landform. The picture is a relief image made using the DEM.

To obtain an idea of the dimensions of the ribbed moraine coverage in this area the ribbed moraine fields were divided into their separate flow sets (Fig. 7.6). This was necessary because each belongs to a separate bedforming event and treating the area as one large field would lead to erroneous conclusions. As Figure 7.6 shows, flow set rm-1 covers the widest area and is approximately 5000 km^2 in extent. The mega-scale ribbed moraine in the northern parts of this field have a continuous coverage measuring approximately 3000 km^2, which makes it the largest known uninterrupted ribbed moraine field (maximum size observed in Québec 2300 km^2 and in Sweden 1000 km^2; Hättestrand, 1997b). In the south, the smaller-scale ribbed moraine are less continuous and are distributed in dispersed clusters (e.g. A & B) and isolated fields (e.g. C & D). These are periodically broken by gaps, some of which can be quite sizeable. For example, the nearest ribbed moraine downstream from the field marked B is 17 km. The mega-scale ribbed moraine in field rm-2 covers a much smaller area (approximately 900 km^2) but nonetheless is still comparable to fields found in Canada and Sweden. The ribbed moraine belonging to rm-g appears small in comparison to the other two fields (65 km^2). However, it must be remembered that this is only the eastern portion of a much larger field that extends off the coverage of the DEM that is estimated to be approximately 170 km^2.

In several places along the northern parts of site, there are areas of overlap between rm-1 and rm-2 (see Figure 7.6). Where this occurs the ribbed moraine ridges form an orthogonal pattern of intersection, which is illustrated in Figure 7.7. Clark and Meehan (2001) correctly interpreted both sets of ridges as being ribbed moraine and argued that superimposition relationships reveal that rm-1 post-dates the orthogonal pattern of rm-2, which is oriented to the southwest. This is only one of two examples where cross-cutting ribbed moraine have been observed (preliminary observations in Newfoundland also show ribbed moraine in a cross-cutting relationship see Figure 10.18) and is significant as it provides a record of shifting flow patterns and the position of ice divides over time.

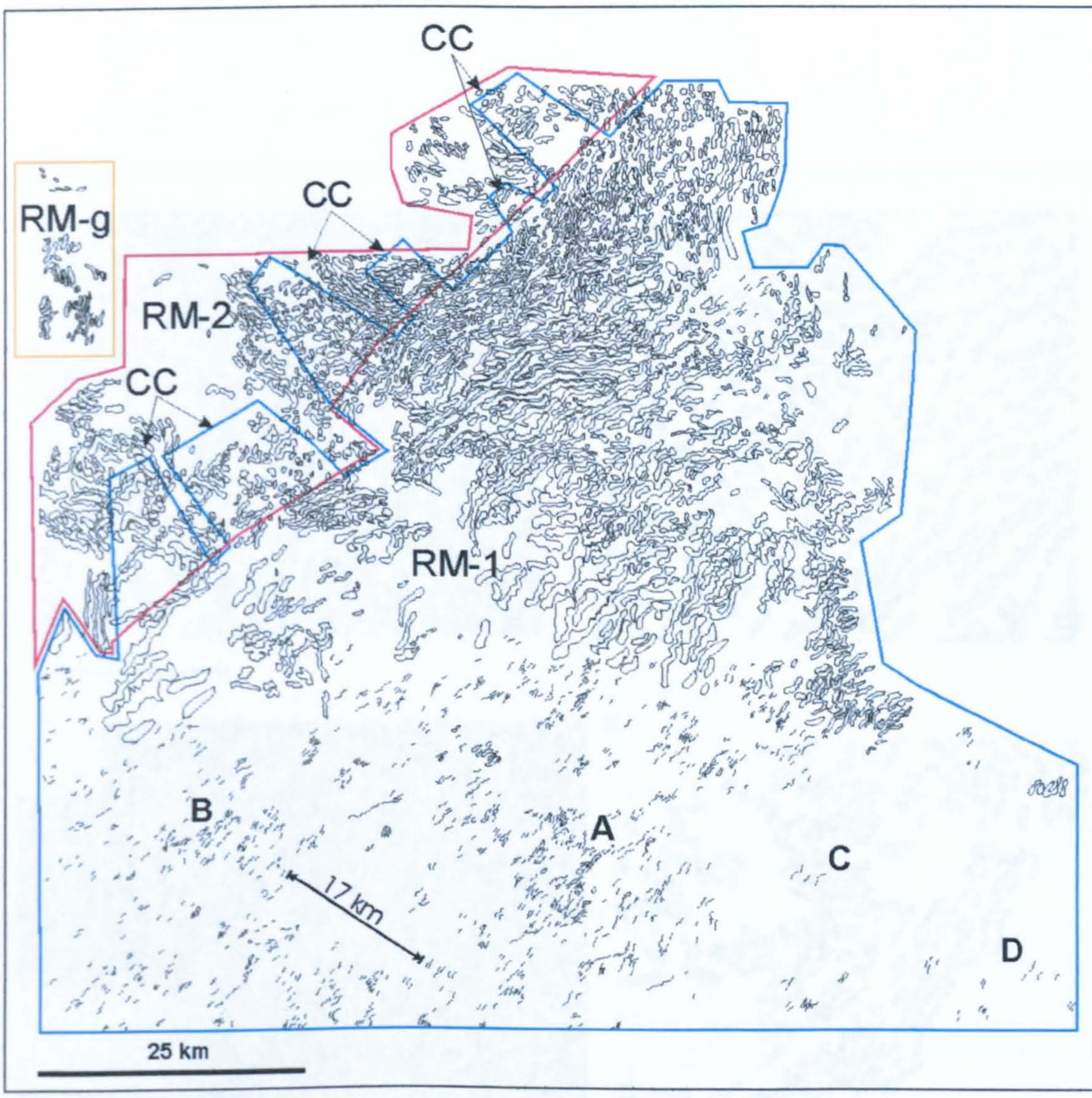

Figure 7.6. Showing the aerial coverage of each ribbed moraine in the study area. The flow set termed rm-1 is bounded in blue and covers an area measuring approximately 5000 km^2. Flow set rm-2 is bounded in red and measures approximately 900 km^2 and rm-g, which is bounded in yellow, covers 65 km^2. Note how in places rm-1 overlaps with rm-2. These are areas of cross-cutting ribbed moraine (marked CC) and are shown in greater detail in Figure 7.7.

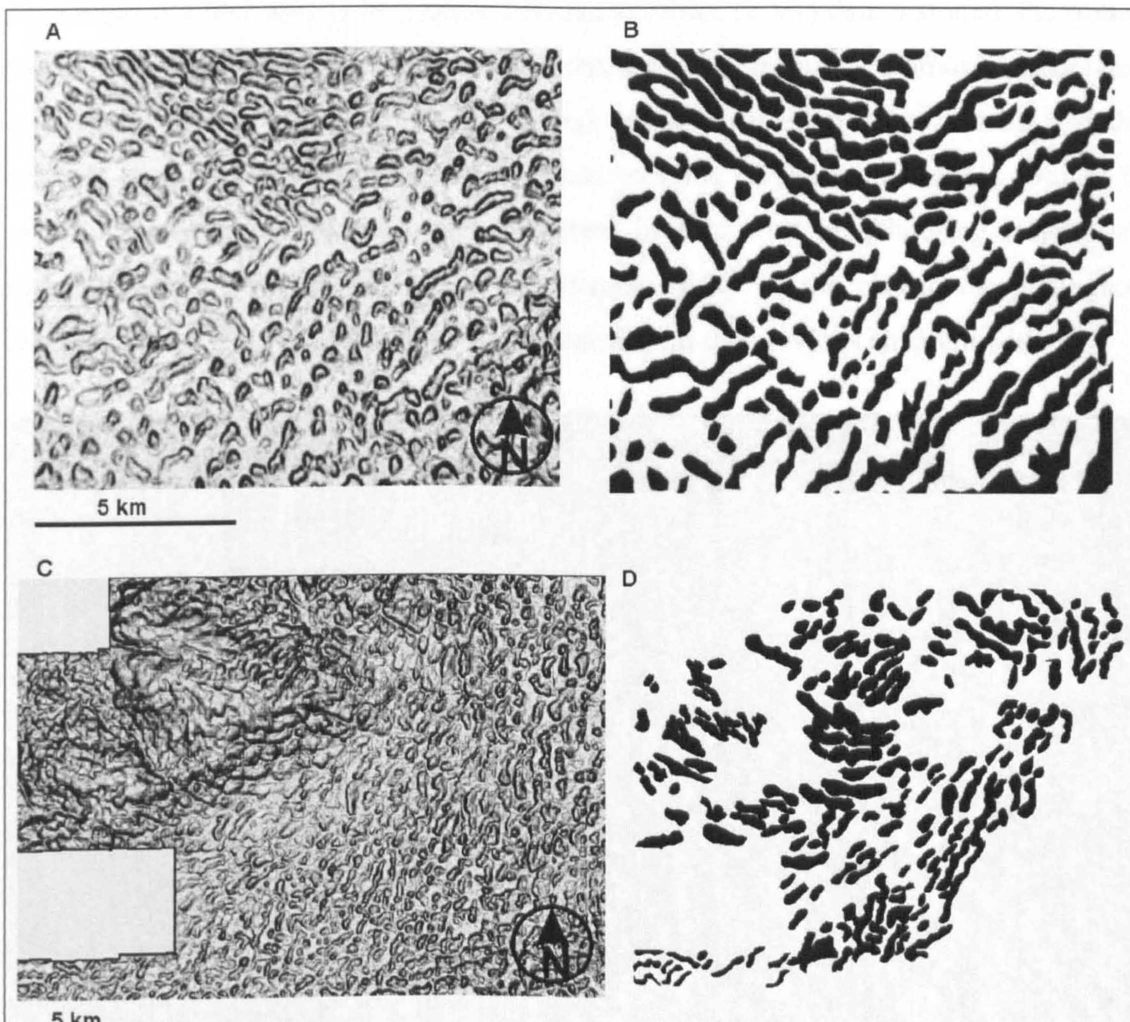

Figure 7.7. Illustrating ribbed moraine fields in a cross-cutting relationship. The area shown in Figure 7.7a is to the southeast of Upper Lough Erne, west of Clones (7° 10 W & 54° 11 N). Figure 7.7b is an interpretive map of the ribbed moraine ridges and clearly shows their intersecting orthogonal pattern (After Clark & Meehan, 2001). Figure 7.7c and 7.7d shows cross-cutting ribbed moraine 7 km northwest of Monaghan town (7° 04 & 54° 18). In both examples, the ribbed moraine pattern that records flow towards the southeast belongs to rm-1 and post dates the orthogonal pattern that records ice flow towards the southwest and belongs to rm-2.

7.4. Morphological characteristics of the ribbed moraine in the northeast midlands of Ireland

7.4.1. Plan view morphology

As Knight and McCabe, (1997) and Clark and Meehan, (2001) demonstrated, the ribbed moraine in Ireland exhibits many of the characteristic features commonly associated with this bedform. This is true of the various scales of ribbed moraine found across the region. In the case of the mega-scale ribbed moraine ridges, many have a straight to arcuate planform morphology, are consistent in size with neighbouring ridges, are regularly spaced across the terrain and display many of the classic morphological features (Fig. 7.8). However, as was demonstrated in the previous chapters with

Figure 7.8. Oblique view of the mega-scale-scale ribbed moraine landscape illustrating the classic features associated with ribbed moraine (After Clark and Meehan, 2001). Note the contiguous nature of the bedforms, their arcuate planform shape, consistent size in relation to neighbouring ridges, regular spacing of the ridges, anastomosing ridges, downstream pointing horns and undulating ridge crests; all features associated with classical type ribbed moraine. Ice Flow is from the top left (northwest). Image is approximately 30 km across in the foreground and is looking northwards across Co. Monaghan. These are the largest ribbed moraine ridges ever reported, with ridge lengths up to 16 km and widths up to 1.1 km. The picture is a relief image made using the DEM. (After Clark and Meehan, 2001).

classical type ribbed moraine, close inspection of the mega-scale ribbed moraine ridges also reveals variations in morphology. For example, in Figure 7.9 it is possible to identify drumlinized ridges, curved ridges that are concave up-ice, straight rectangular ridges and barchan shaped ridges. In some regions, the mega-scale ridges have a very heavily drumlinized surface. Where this is the case, the ridges have multiple breaches along the entire ridge length, many of which cut right through to the base of the ridge.

This gives them a rather broken appearance and many of the ridges appear like transversally aligned mounds of sediment rather than proper ridges (Fig. 7.10).

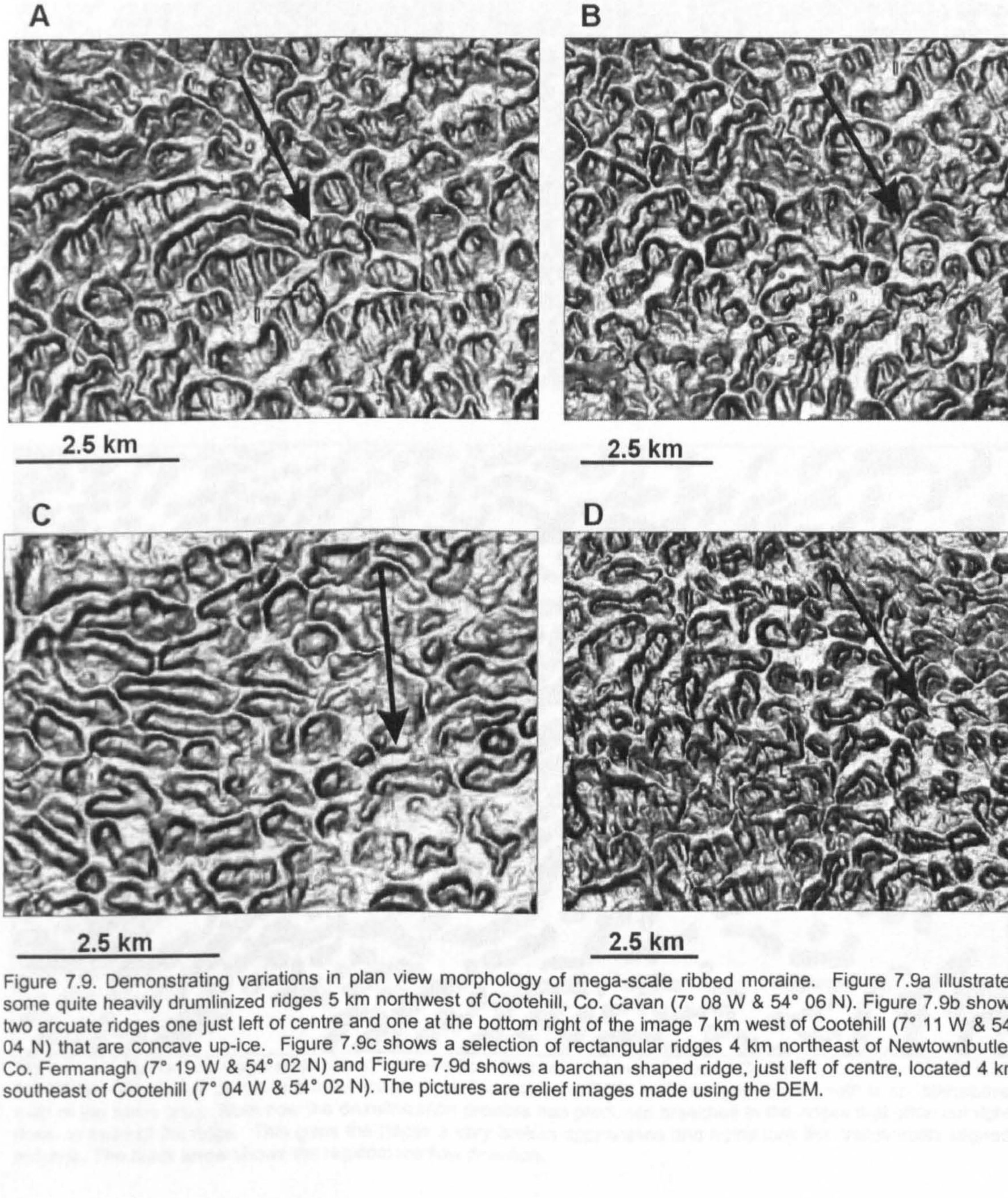

Figure 7.9. Demonstrating variations in plan view morphology of mega-scale ribbed moraine. Figure 7.9a illustrates some quite heavily drumlinized ridges 5 km northwest of Cootehill, Co. Cavan (7° 08 W & 54° 06 N). Figure 7.9b shows two arcuate ridges one just left of centre and one at the bottom right of the image 7 km west of Cootehill (7° 11 W & 54° 04 N) that are concave up-ice. Figure 7.9c shows a selection of rectangular ridges 4 km northeast of Newtownbutler, Co. Fermanagh (7° 19 W & 54° 02 N) and Figure 7.9d shows a barchan shaped ridge, just left of centre, located 4 km southeast of Cootehill (7° 04 W & 54° 02 N). The pictures are relief images made using the DEM.

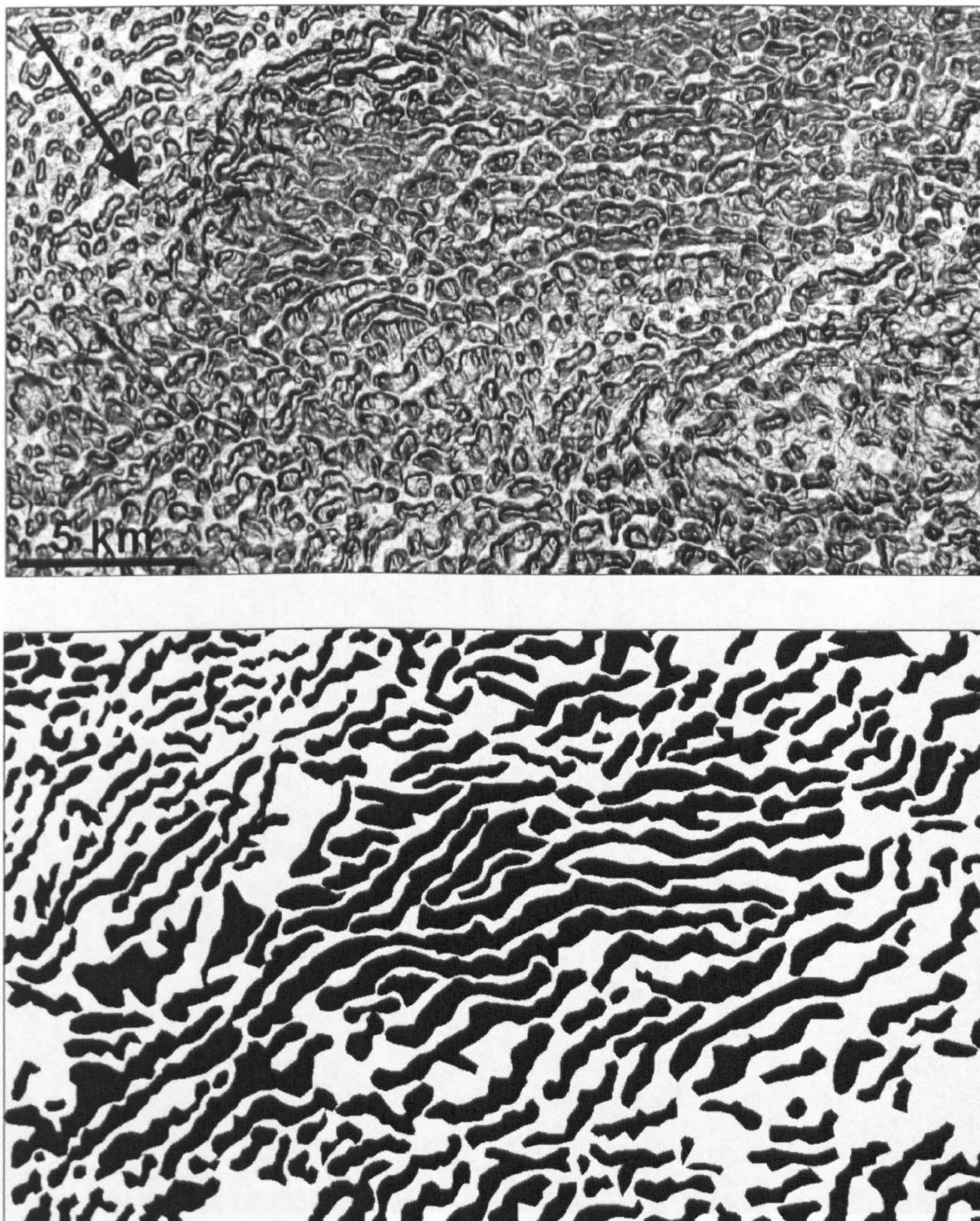

Figure 7.10. Broken up mega-scale ribbed moraine from flow set rm-1 in and around Cootehill, Co. Cavan (7° 05 W & 54° 03 N). The image on top is a relief image produced using the DEM and the figure underneath is an interpretive map of the same area. Note how the drumlinization process has produced breaches in the ridges that often cut right down to base of the ridge. This gives the ridges a very broken appearance and many look like transversely aligned mounds. The black arrow shows the regional ice flow direction.

The smaller ribbed moraine ridges in the southern region also vary in form. As was previously noted, classical type ridges are located immediately south of Slieve na Calliagh (see Figure 7.5). Here, sequences of narrow sinuous ribbed moraine ridges that are arcuate in plan form, many of which curve downstream, liberally cover the landscape (Fig. 7.11). However, just like other ribbed moraine there are variations in form within the same field and in this area, it is possible to identify elongate straight ridges, ones that are rectangular and a few which are gently curved with their concave side facing upstream. The minor ribbed moraine ridges generally tend to be much shorter in length and as a result are usually straighter in form. They are found in a variety of settings but are more usually located next to, or between classical scale ridges (see white spot in Figure 7.11). However, they have also been observed in small isolated fields far from major areas of ribbed moraine and also superimposed on top of other bedforms (Fig. 7.12).

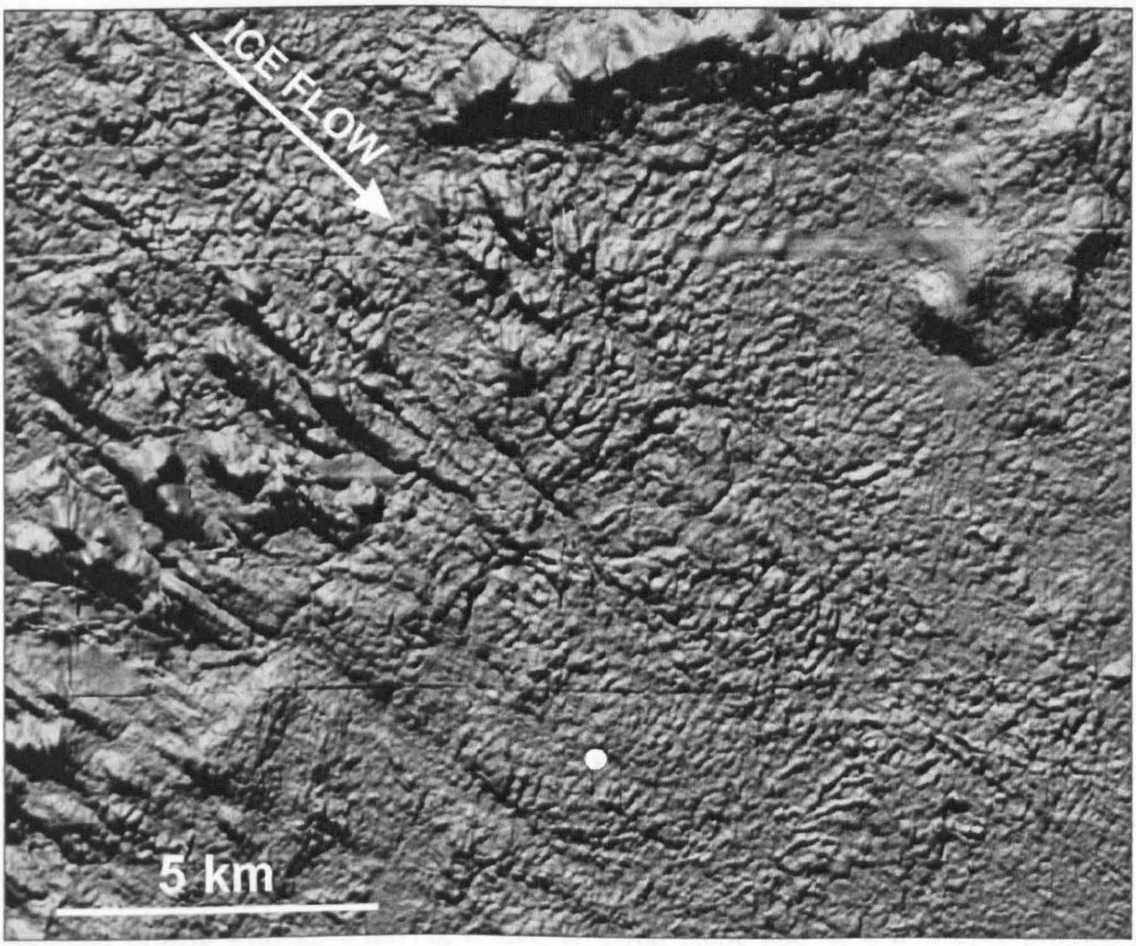

Figure 7.11. Showing examples of classical type ribbed moraine ridges south of Slieve na Calliagh (7° 06 w & 53° 44 N). Many of the ridges are sinuous, arcuate and curve downstream. Note however, the wide variation in morphology and that many diverge from the classic form. Note also the area of minor ribbed moraine marked by the white spot, which are shorter in length and are more rectangular in shape. The picture is a relief image made using the DEM.

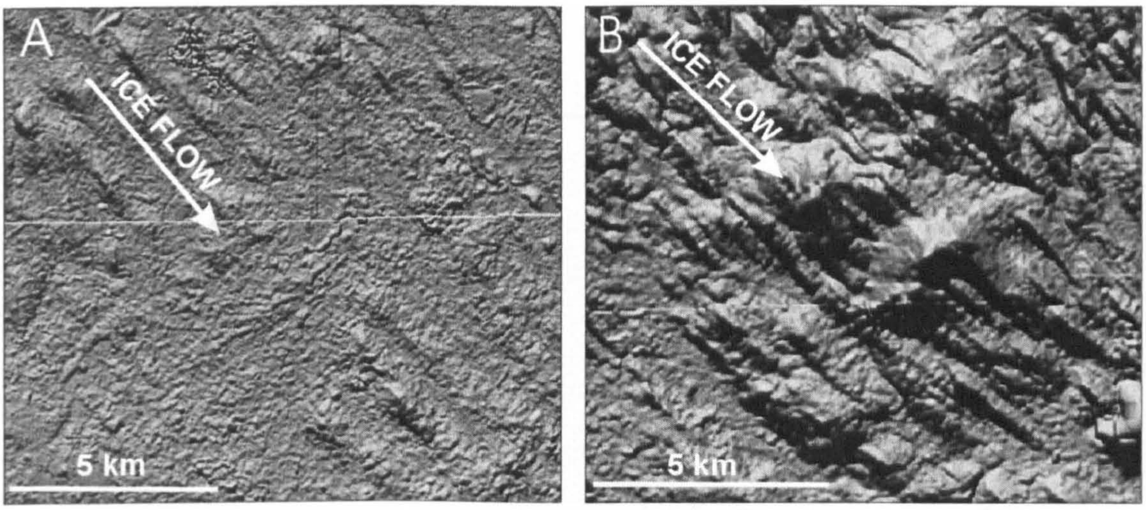

Figure 7.12. Showing an isolated field of minor ribbed moraine (A) situated in the southeast of the site (7° 32 W & 53° 34 N) and minor ribbed moraine superimposed on drumlinoid bedforms and glacially streamlined hills (B) 10 km northwest of Slieve na Calliagh (7° 10 W & 53° 50 N). Images are relief images made using the DEM.

7.4.2. Individual ridge morphology

Using the DEM it was possible to build a picture of the topographic morphology of the ribbed moraine ridges at this locality. This was done by taking cross sections over entire ribbed moraine fields and longitudinal profiles along the length of individual ribbed moraine ridges. As noted previously, several authors assert that ribbed moraine ridges are generally asymmetric with the distal (down-ice) slope being much steeper than the proximal slope (Shilts *et al.*, 1987; Aylsworth and Shilts, 1989; Bouchard, 1989; Hättestrand and Kleman, 1999). To investigate whether this was the case in Ireland, transects totalling 100 km in length were taken across a random sample of ribbed moraine ridges. Each profile was then visually assessed to determine the symmetry of the ridge and to investigate whether the distal or proximal side had the steepest slope. All of the ridges sampled were found to have an asymmetric cross sectional profile with 52% having a steeper distal slope and 48% a steeper proximal slope.

To explore the longitudinal profile of the ribbed moraine ridges in this locality 50 randomly selected ridges were chosen and profiles were taken along the crest of the ridges. In this sample it was found that all of the ridges had undulating crests. This was similar to what was found in the Lac Naococane region (see Section 5.4.2) and appeared to be a typical characteristic of the ribbed moraine ridges in the region (Fig. 7.13).

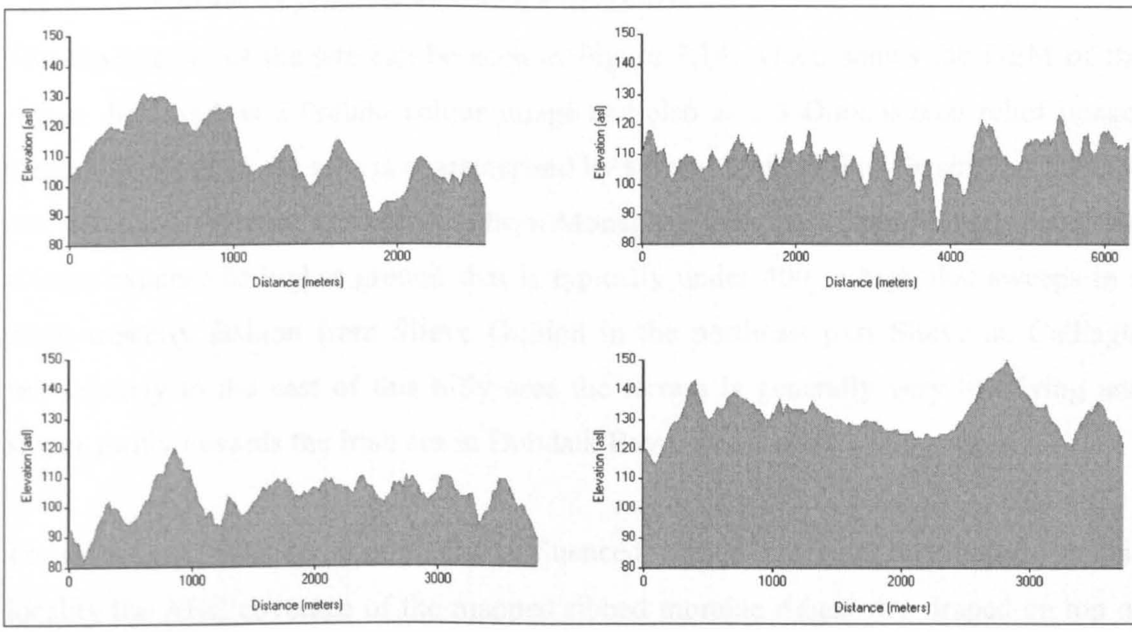

Figure 7.13. Examples of longitudinal profiles taken along the entire length of ribbed moraine ridges on the DEM. Note how the ridge crests are all undulating, which appears to be a common individual characteristic of the ribbed moraine ridges in Ireland.

The DEM was also used to investigate whether the ribbed moraines in Ireland had accordant summits. To test this, ten transects totalling 225 km in length were taken randomly across both the mega-scale and classical scale ribbed moraine at this site. Following the procedures described previously, regression analysis was then applied to these data to derive the R Squared value. As Table 7.2 shows, all of the transects have low R Squared values, which meant that in the areas sampled the ridge summits can not be described as accordant. These results are similar to those found in the Lac Naococane region and contradict the assertions made by Bouchard (1989) and Hättestrand and Kleman (1999) that ribbed moraine fields have accordant summits.

Table 7.2. R Squared values for transect data totalling 225 km in length taken across the Irish ribbed moraine fields. Note how all of the transects in the sample have low R Squared Values, meaning all of ribbed moraine ridges sampled in this study did not have accordant summits.

R Squared	R Squared
0.19	0.24
0.01	0.57
0.29	0.28
0.00	0.08
0.13	0.12

7.5. Topography

7.5.1. Topographic setting of ribbed moraine

The topography of the site can be seen in Figure 7.14, which shows the DEM of the region displayed as a Pseudo colour image and also as a 3-Dimensional relief image. Generally speaking the area is characterised by several large shallow basins, such as the one that runs northeast to southwest from Monaghan town past Upper Lough Erne, and a large expanse of higher ground that is typically under 400 m high that sweeps in a south-westerly fashion from Slieve Gullion in the northeast past Slieve na Calliagh. Immediately to the east of this hilly area the terrain is generally very low lying and slopes gently towards the Irish sea in Dundalk Bay.

To investigate whether topography influenced ribbed moraine distribution at this locality the ARC coverage of the mapped ribbed moraine ridges was draped on top of the DEM (Fig. 7.15). What became immediately apparent was that the distribution of ribbed moraine from the different flow sets was not influenced by variations in topography. Ridges from the three flow sets can be seen to have formed in a variety of topographic settings including hilltops (e.g. A, B & C), basins (e.g. D, E & F) and on the slopes running in and out of the basins (e.g. G, H & I). If a transect is taken across the site, the resultant profile clearly illustrates these observations. Figure 7.16, shows the profile of a transect that was taken across a portion of the mega-scale ribbed moraine field in the north, starting from the slopes of Doocarn and running through the valleys and over the hills just south of Monaghan town, to a position 8 km northeast of Corraweelis. This graph clearly shows the undulating nature of the terrain and the cross-sectional profiles of the mega-scale ribbed moraine ridges and lucidly illustrates that the ribbed moraine distribution was not influenced by changes in topography. In this case, ribbed moraine ridges can be seen running along the entire length of transect over a wide range of topographies, including valleys, hill slopes (both proximal and distal) and also on hilltops.

Topography also does not appear to have influenced the occurrence of cross-cutting ribbed moraine as they too are found in various topographic positions including hilltops (A) slopes running into basins (J) and within the regions major depressions (K). Furthermore, the ribbed moraine ridges of rm-1, which is the largest field in the area, encounter wide variations in topography across the site, yet this has not affected their orientation as most maintain a uniform south-easterly orientation.

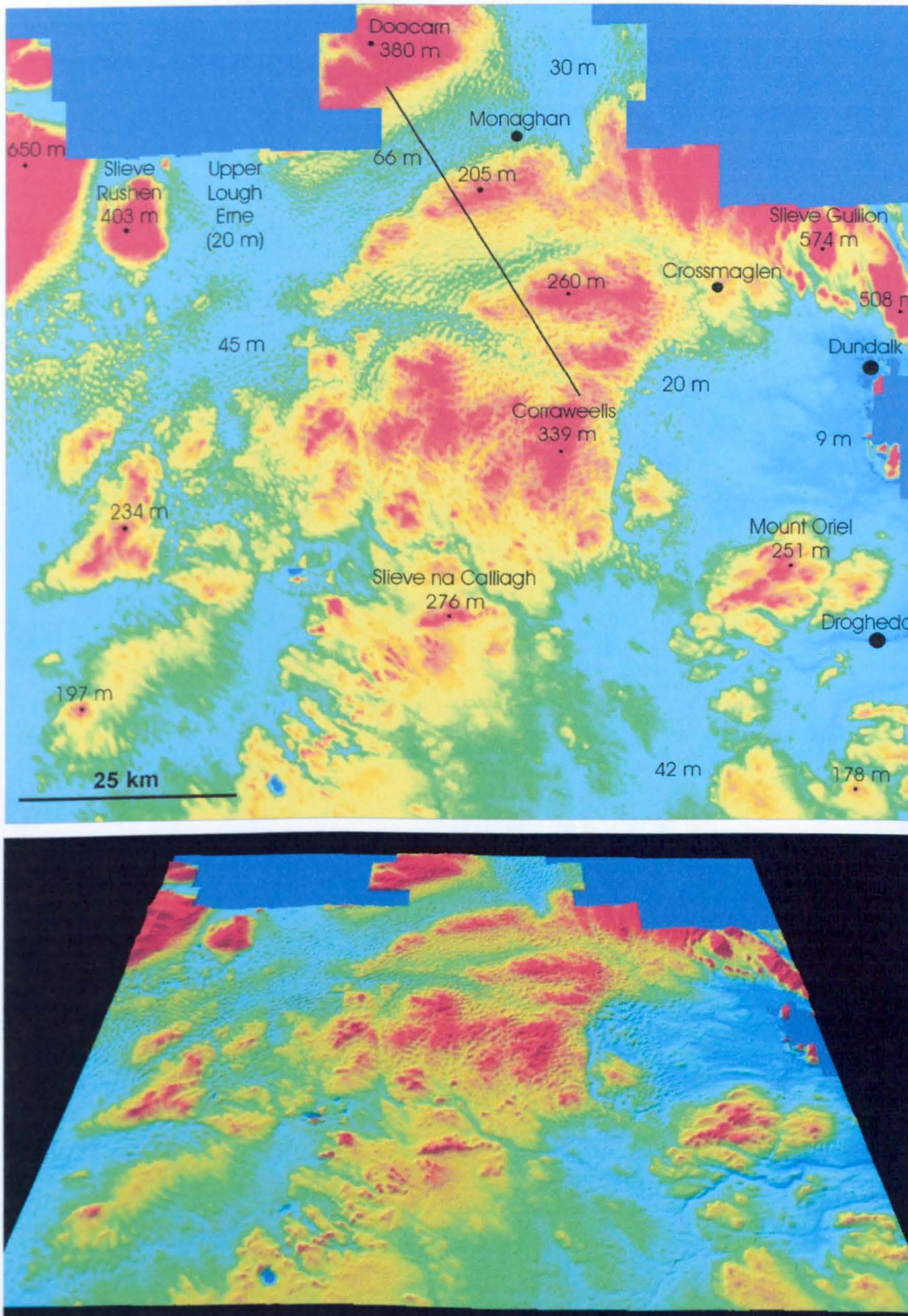

Figure 7.14. The figure on top is the DEM of the study site displayed as a Pseudo colour image. Elevation is coded to show the highest elevations as red, grading down to orange, yellow, green to blue, which represents the lowest elevation. Regions coloured dark blue are areas where there is no elevation data. The relief image at the bottom was made using the DEM and gives the viewer a 3-Dimensional oblique view of the site. The black line that runs from the slopes of Doocarn towards Corraweelis shows the path of the transect taken to show the profile of the terrain illustrated in Figure 7.16.

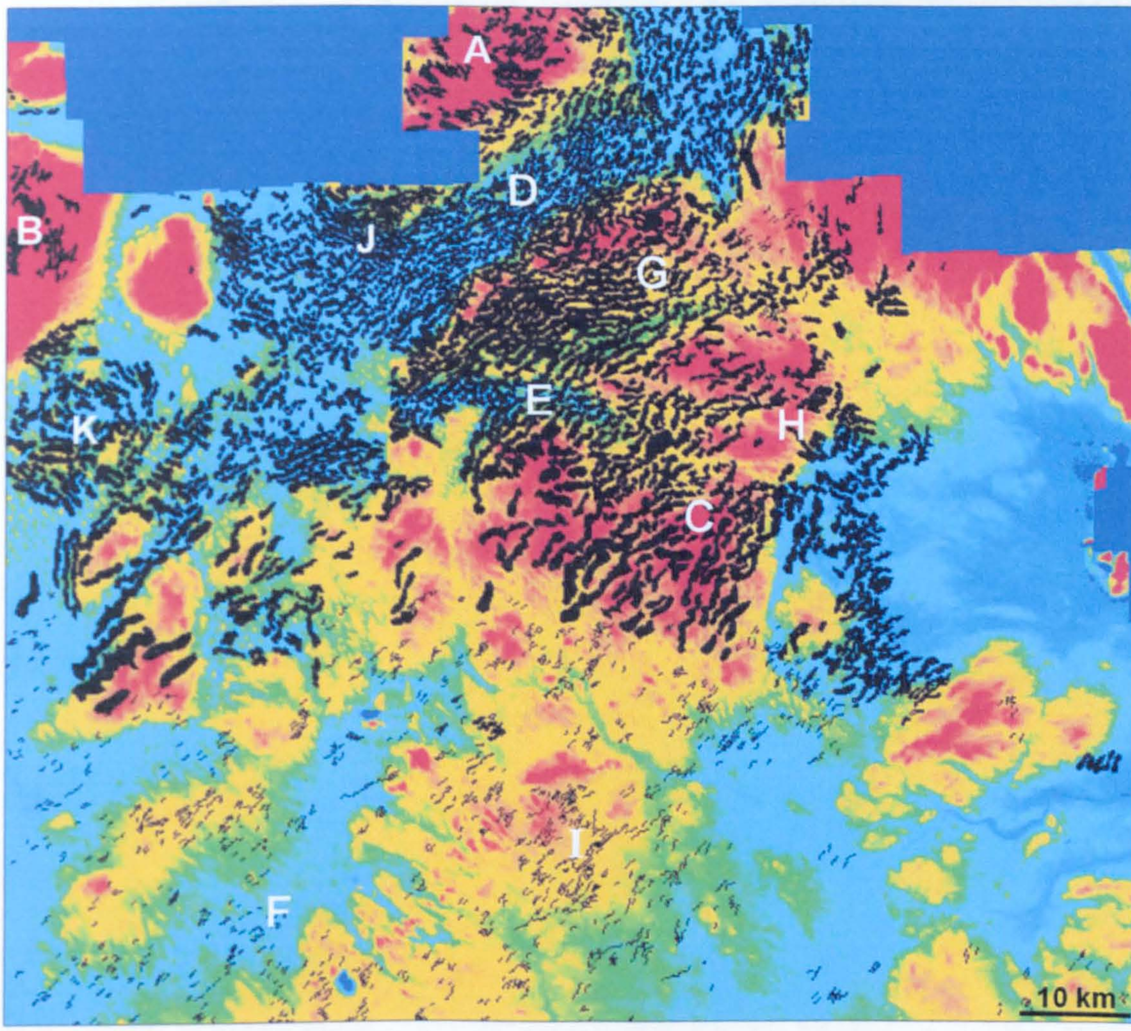

Figure 7.15. Showing the DEM with the ARC coverage of the mapped ribbed moraine draped on top. Note how the distribution of all scales of ribbed moraine and cross-cutting ribbed moraine in the region has not been influenced by variations in topography as all types are found in a variety of topographic settings.

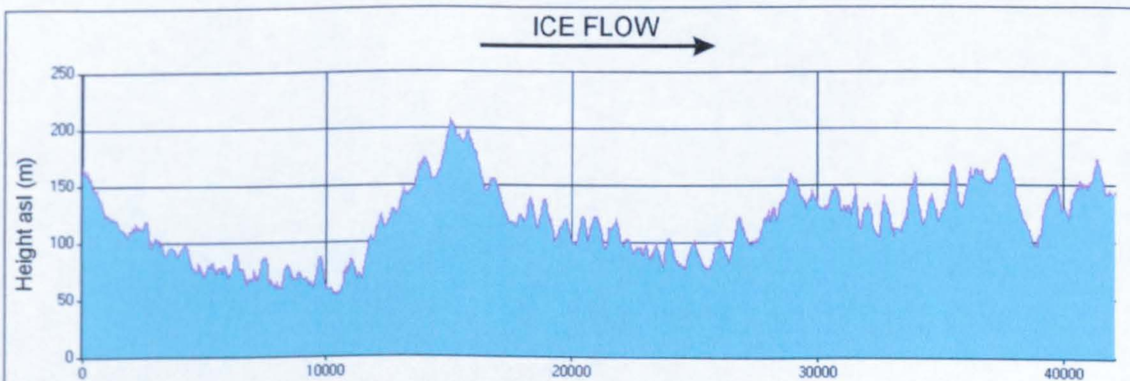

Figure 7.16. The profile of the transect taken from the slopes of Doocarn (7° 11 W & 54° 17 N) to a position 8 km northeast of Corraweelis (6° 51 W & 53° 58 N). The cross-sectional profile of the ribbed moraine ridges are clearly visible along the entire length of the transect. Note how the ribbed moraine ridges ignore changes in topography and can be seen distributed in a wide variety of topographic settings. In this example, the ribbed moraine field runs across valley floors, up and down hill slopes and over the tops of hills.

7.6. Morphometric measurements

To add to the quantitative database of ribbed moraine characteristics, measurements were conducted on four aspects of ribbed moraine morphometry. These were ridge height, ridge length, ridge width and ribbed moraine wavelength. The following sections report the findings for this study site.

7.6.1. Ribbed moraine wavelength

The wavelengths of the ribbed moraine in this region were calculated following the procedures set out in Section 4.3.5. This involved taking transects across the ribbed moraine fields and then using the elevation and distance data to make graphs that showed the topographic profile of the terrain. These graphs were then used to determine the exact location of every ribbed moraine ridge crest along each transect from which the wavelength could be then calculated. In this locality, data from transects totalling 2000 km in length were used to extract the wavelength data and a histogram showing the wavelength distribution in this region was made (Fig. 7.17). The majority of ribbed moraine ridges in the area have wavelengths ranging between 250 m and 1850 m, which represents 95.79 % of the population. The other 4.2 % have wavelengths ranging between 150 m to 200 m (0.48 %), which is the typical wavelength range for minor ribbed moraine, and 1900 m to 5800 m (3.73 %), which are longest wavelengths yet recorded (the maximum wavelength recorded in Québec was 1800 m). To summarise, the smallest wavelength recorded in the area was 125 m, the longest was 5800 m, the average was 834 m and the most frequently occurring wavelength, the mode, was 550 m.

7.6.2. Ribbed moraine ridge length

Information on the length of the ridges in this region was obtained by using the same methods described in Section 5.6.2 and by also manually measuring the length of the megascale-ribbed moraine ridges. The mega-scale ridges had to be measured using this method because the attribute table belonging to the ARC coverage does not record the length of polygons (i.e. the method used to map mega-scale-scale ribbed moraine). At this site a randomly chosen sample of one thousand ridges were taken. The sample ensured that all scales of ribbed moraine were included and that the ridges were sampled from the three flow sets rm-1, rm-2 and rm-g. In this sample, 88 % of the ridges are between 100 and 2000 m long (Fig. 7.18), which is comparable to the ribbed moraine

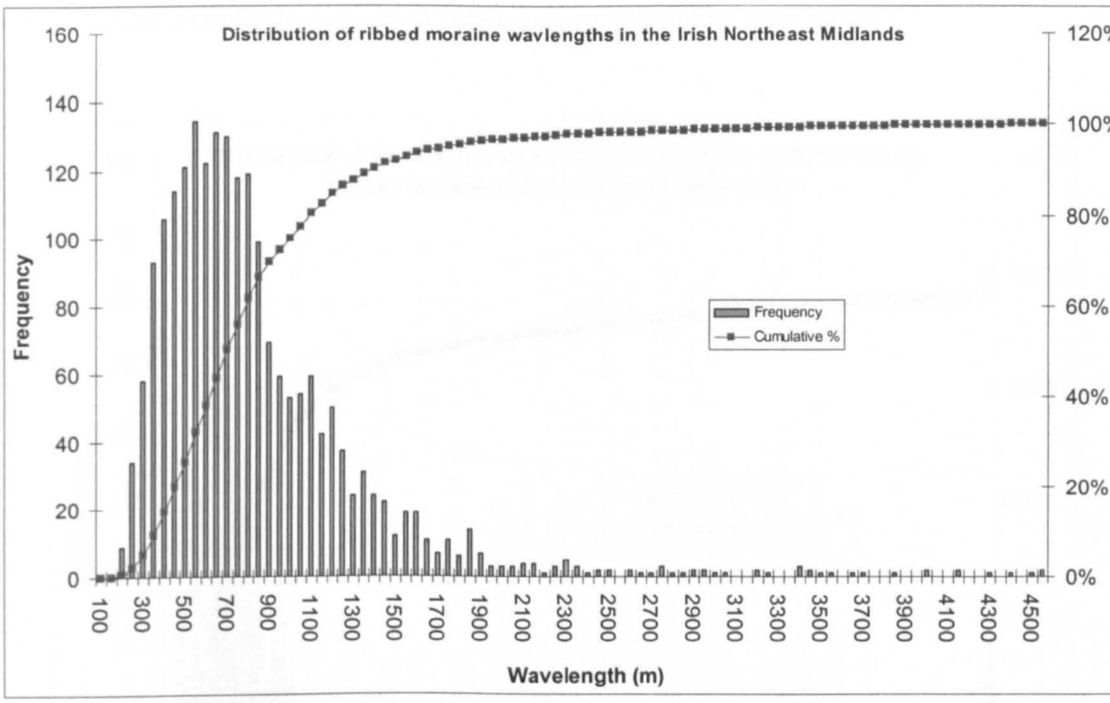

Figure 7.17. Distribution of ribbed moraine wavelength determined from transect data totalling 2000 km.

ridges measured in the two areas in Québec (Sections 5.6.2 & 6.7.2). What is different about the ribbed moraine in this area though, is the number of ridges that are much longer than this and many are greater in length than the maximum observed in the Kaniapiskau region (2993 m) and at the Lac Naococane (5967 m), which makes them the longest ribbed moraine ridges thus far observed. In this region the minimum ridge length was found to be 103 m, the maximum 16.2 km and the mean ridge length 1091 m.

7.6.3. Ribbed moraine ridge height

Information on the height of the ribbed moraine ridges in this area was obtained following the same procedures set out in Section 5.6.3. Transects were taken across 300 randomly sampled ribbed moraine ridges and once the height of each ridge was determined a histogram showing the height distribution was made (Fig. 7.19). This showed that just over 99% of ridges are between 8 m and 53 m high, which is a much larger height range than was found in Québec, where the majority of ridges in the sample were between 1 m and 22 m high (see Section 5.6.3). The average height of the ribbed moraine ridges in Ireland was also much larger, in Québec the average height was 12 m, however in Ireland, the average height is more than double this at 26 m. The minimum ridge height measured at this site was 6 m, the maximum height was 63 m and the most frequently occurring ridge height, the mode, was 28 m.

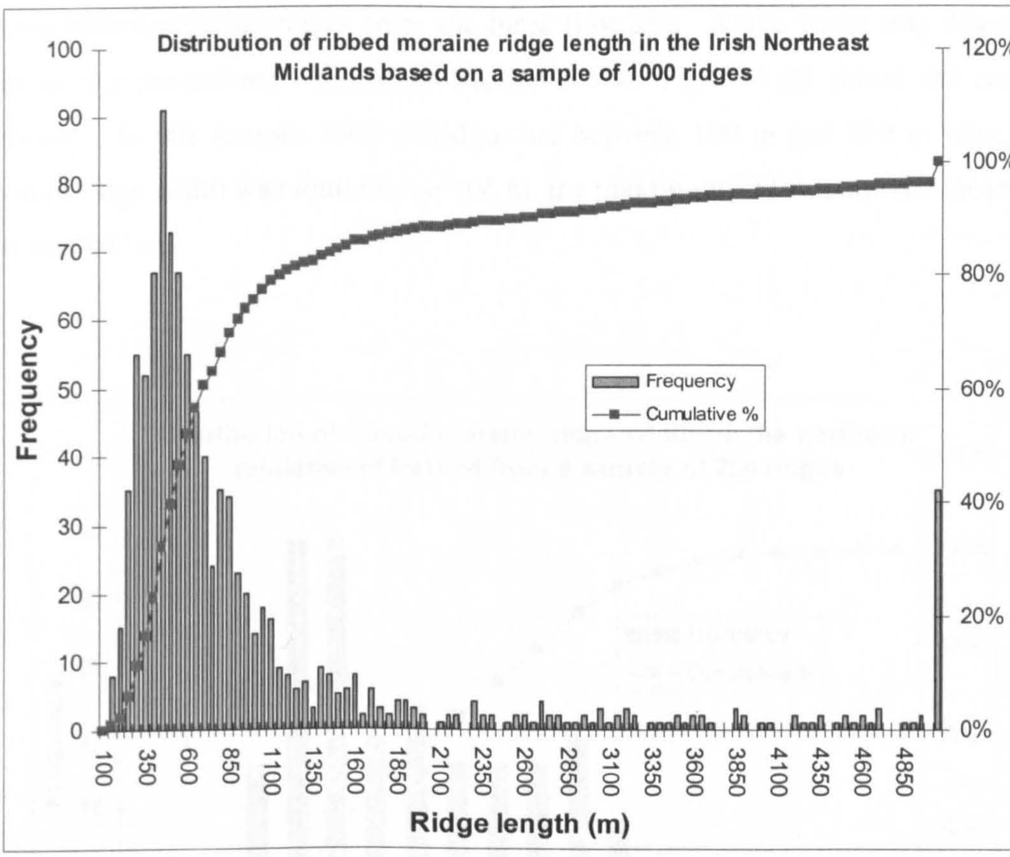

Figure 7.18. Distribution of ribbed moraine ridge length from a sample of 1000 ridges. 88 % of the ridges have lengths between 100 and 2000 m, with the maxima at 450 m. Note however that many of the ridges are much longer than this and are the longest ribbed moraine ridges observed to date.

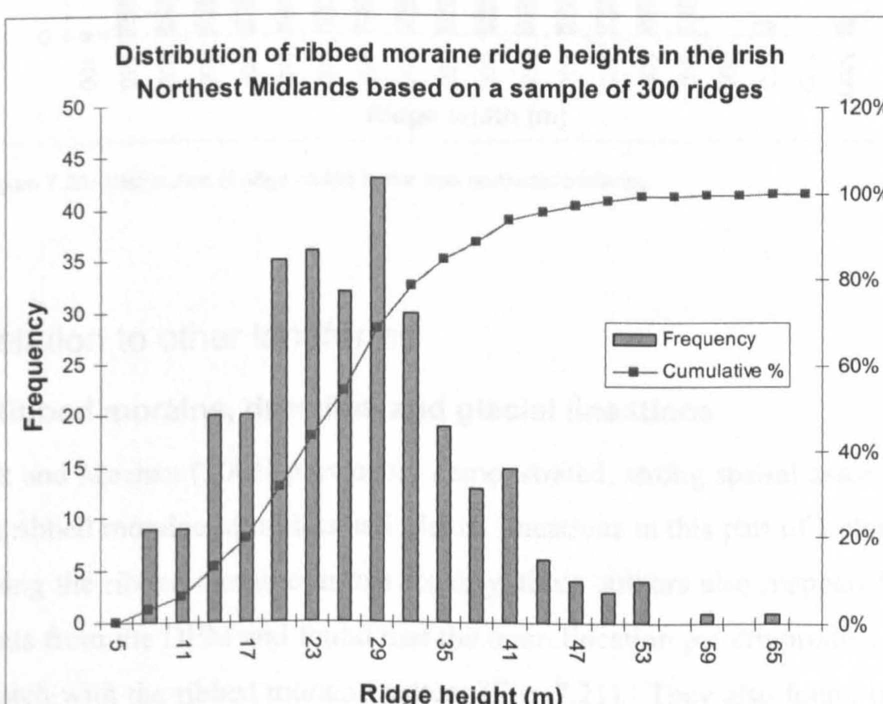

Figure 7.19. The distribution of ribbed moraine ridge height based on a sample of 300 ribbed moraine ridges.

7.6.4. Ribbed moraine ridge width

To investigate the width of the ribbed moraine ridges in this region a sample of 250 ridges were chosen randomly from various locations across the site. The sample included ribbed moraine ridges from the three flow sets. Ridge width was determined following the procedures outlined in Section 5.6.4. Figure 7.20 shows the resultant histogram. In this sample, 99% of ridges are between 100 m and 850 m wide. The minimum ridge width was found to be 105 m, the maximum 1116 m and the mean ridge width was 443 m.

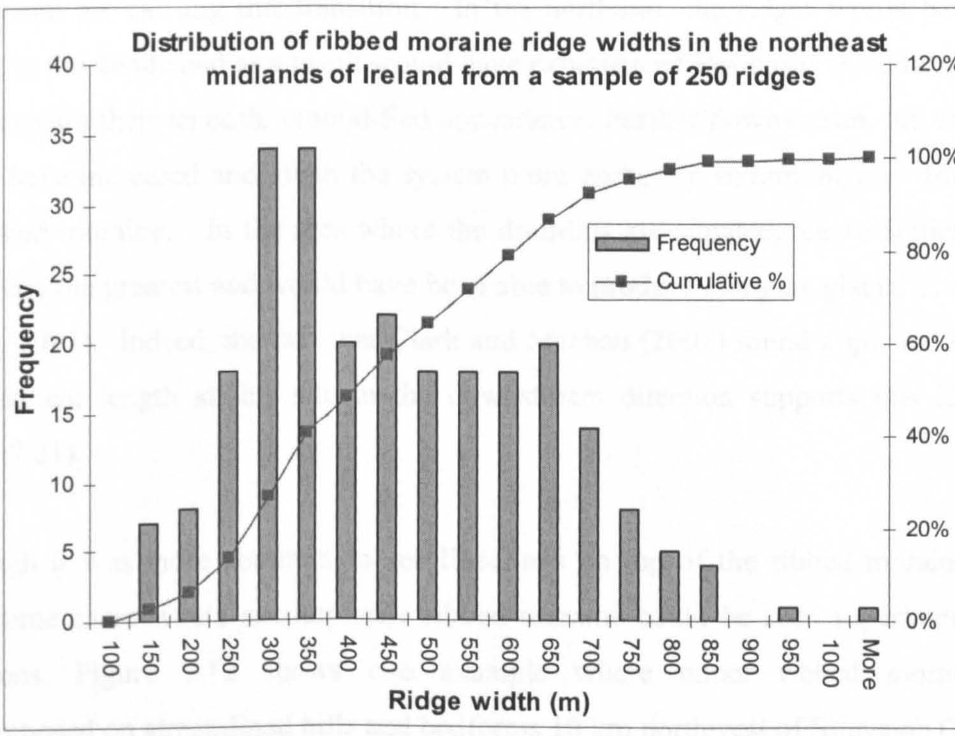

Figure 7.20. Distribution of ridge widths in the Irish northeast midlands.

7.7. Relation to other landforms

7.7.1. Ribbed moraine, drumlins and glacial lineations

As Clark and Meehan (2001) previously demonstrated, strong spatial associations exist between ribbed moraine, drumlins and glacial lineations in this part of Ireland. As well as mapping the ribbed moraine in this locality, these authors also mapped 5600 glacial lineaments from the DEM and found that the main lineation pattern produced an almost exact match with the ribbed moraine pattern (Fig. 7.21). They also found that many of the drumlins are superimposed on the ribbed moraine and that the drumlins are nearly always orthogonal to the ridges. Clark and Meehan (2001) cite these facts as evidence that the generation of the two bedforms are highly related, with drumlinization closely following the formation of the ribbed moraine. As discussed previously, many of the mega-scale ribbed moraine ridges show various degrees of drumlinization (see Figure 7.9 and 7.10). If the mega-scale ribbed moraine belonging to rm-1 is viewed in its entirety, it is possible to see that the drumlinized ridges appear to be part a transitional phase whereby the ribbed moraine was gradually broken up and streamlined into drumlins further downstream (Fig. 7.22). If the location of the landforms in Figure 7.22 is considered in relation to their position to the ice divide, it would appear that increasing basal velocities away from the ice divide may have been the likely mechanism for causing this transition. In the northeast, the ridges would have been closest to the divide and as a result would have experienced low basal velocities and this helps explain their smooth, unmodified appearance. Further downstream, ice velocities would have increased and given the system more energy to streamline and drumlinize the ribbed moraine. In the area where the drumlins are situated, ice velocities would have been the greatest and would have been able to produce elongate glacial lineaments (Clark, 1993). Indeed, the fact that Clark and Meehan (2001) found a gradual increase in lineament length at this site in the downstream direction supports this idea (see Figure 7.21).

Although it was more common to see lineations on top of the ribbed moraine, there were some cases where smaller scale ribbed moraine could be seen superimposed on lineations. Figure 7.12 shows one example where minor ribbed moraine are superimposed on streamlined hills and bedforms 10 km northwest of Slieve na Calliagh. However, they were also observed superimposed on more subtle streamlined lineations in the western portion of the site 15 km southeast of Edgeworthstown in Co. Longford (Fig. 7.23). A more unusual example of lineations being "ribbed" into small-scale ribbed moraine ridges was also observed near Castlepollard, Co. Westmeath. In this case, the drift tail of a crag-and-tail feature appears to have been reworked to form a short sequence of minor ribbed moraine ridges (Fig. 7.24). In all the cases where superimposition was observed the ribbed moraine were oriented in the same direction as the lineations, indicating they are related to the same ice flow event (rm-1). It appears that in this area there were multiple phases of ribbed moraine formation operating during this bedforming phase.

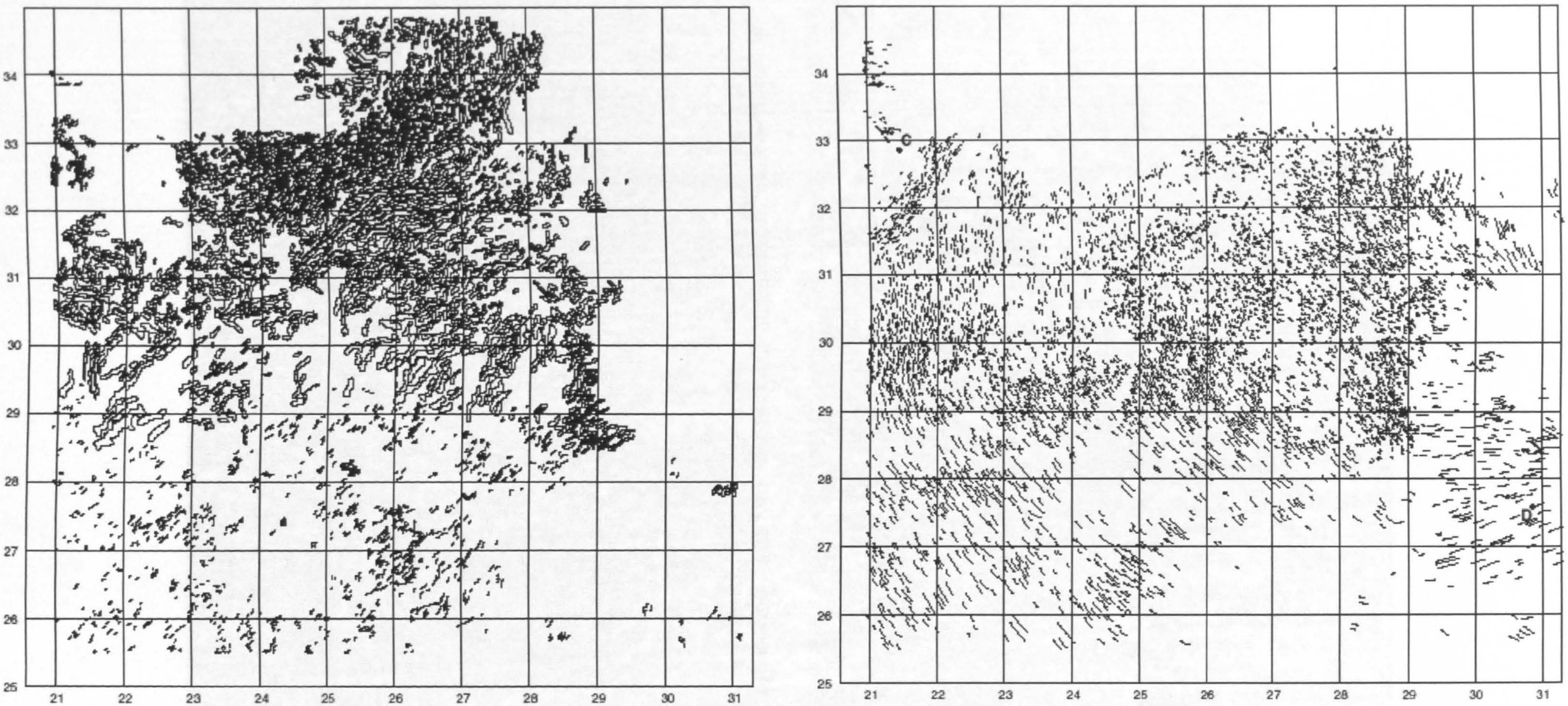

Figure 7.21. Comparison of ribbed moraine (left) and glacial lineation coverage (right) in the northeast midlands of Ireland (After Clarke and Meehan, 2001). Note how the ribbed moraine has been overprinted with glacial lineations and that the main lineation pattern closely matches the ribbed moraine pattern. Grid squares are 10 by 10 km.

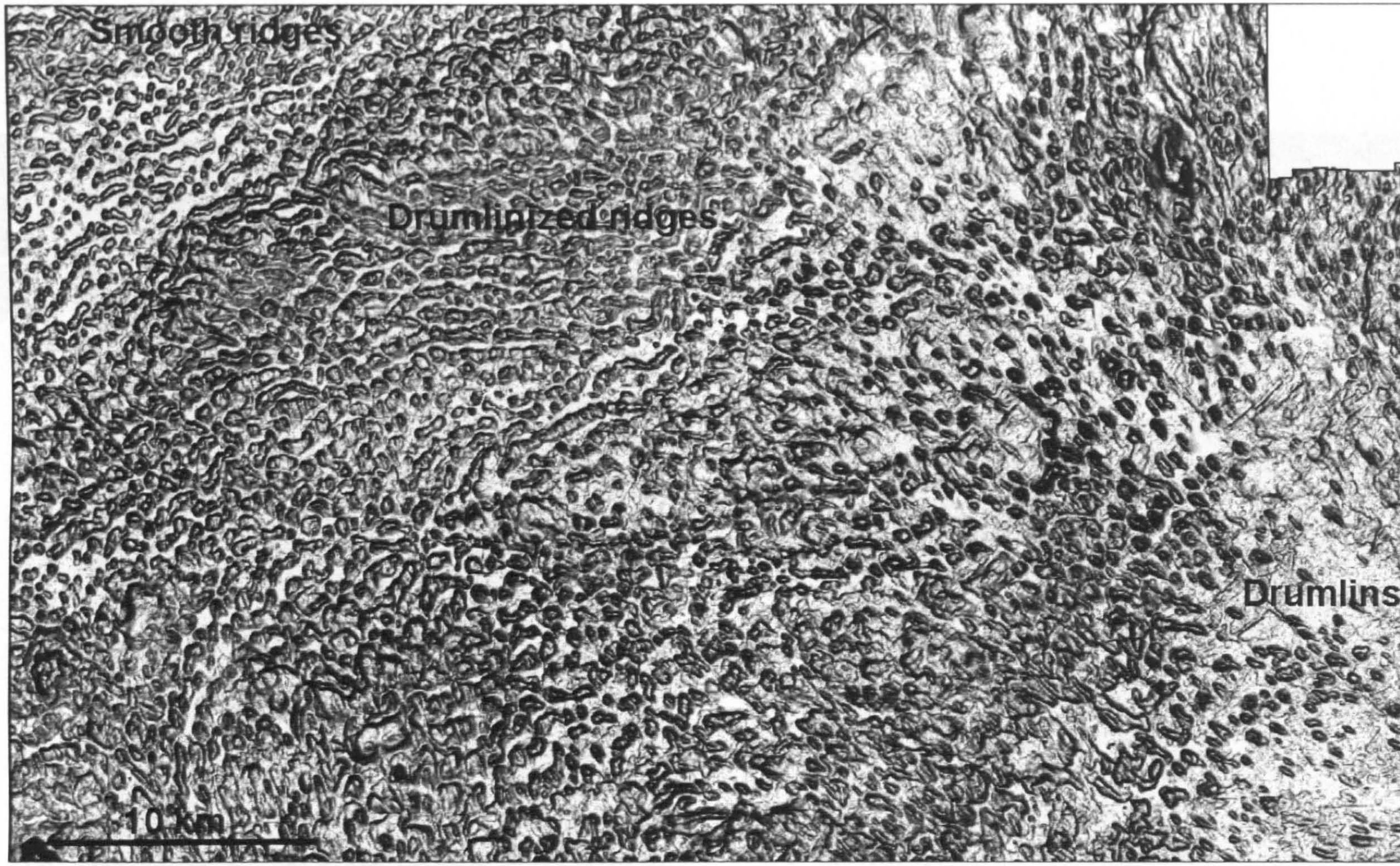

Figure 7.22. Demonstrating the down stream transition from mega-scale ribbed moraine in the northwest to classical type drumlins in the southeast. The smooth ridges are located to the southeast of Upper Lough Erne, west of Clones (7° 10 W & 54° 11 N). The drumlinized ribbed moraine is situated in and around Cootehill, Co. Cavan (7° 05 W & 54° 03 N) and the swarm of drumlins are 16 km northwest of Dundalk Bay (6° 35 W & 54° 00 N). Regional ice flow was from the top left towards the bottom of the image. Image is a relief image made from the DEM.

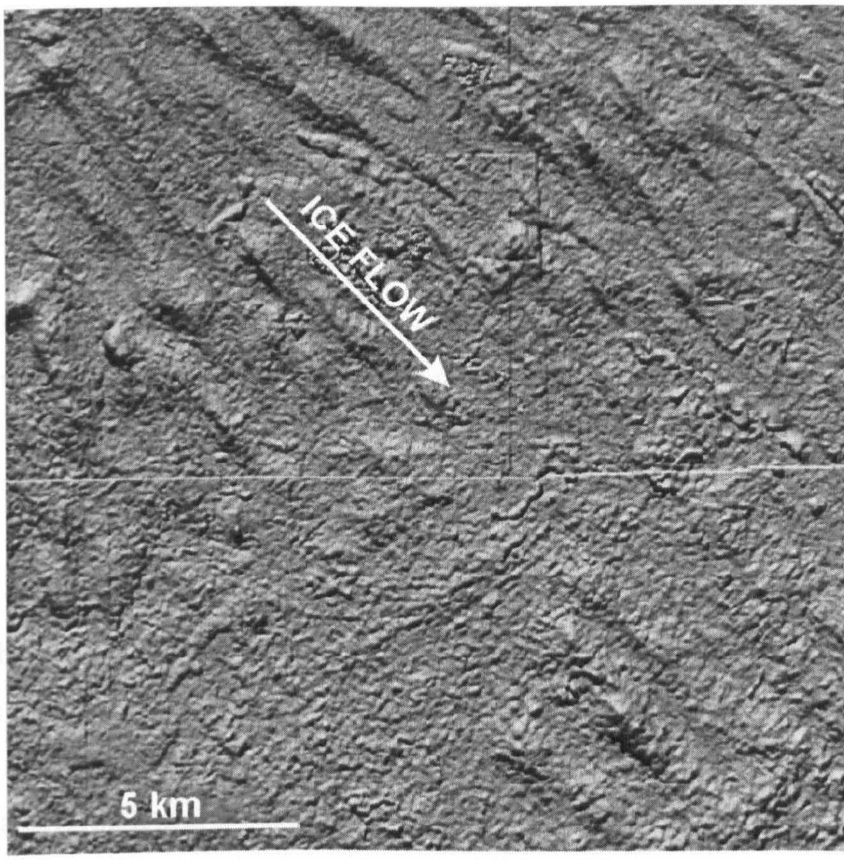

Figure 7.23. Showing a situation where minor ribbed moraine is superimposed on subtle glacial lineations near Edgeworthstown at (7° 31 W & 53° 33 N). Note that the lineations in the bottom left of the image are entirely covered with minor ribbed moraine ridges. Image is a relief image made using the DEM.

Figure 7.24. Some crag-and-tail features near Castlepollard Co. Westmeath (7° 11 W & 53° 42 N). Note how the tail at the top right has been "ribbed" into a sequence of minor ribbed moraine ridges.

7.8. Summary and conclusions

Using the DEM to map ribbed moraine in this region revealed the ridges were not formed synchronously but by three separate bedforming events. This pattern was first recognised by Clark and Meehan (2001) who termed the ribbed moraine flow sets rm-1 (*southeast flow*), rm-2 (*southwest flow*) and rm-g (*northwest flow*). These authors argue that the ribbed moraine belonging to rm-2 were formed during the earliest bedforming phase when the Irish Ice Sheet was centred over the northeast of the country. Flow set rm-g postdates these ribbed moraine and was produced by ice discharging towards the northwest from a north-south ice divide at the LGM. The ribbed moraine fields termed rm-1 were formed by the latest phase of ice flow in the region and were produced by ice flowing from the northwest after the LGM. In the northern parts of the site it was observed that the flow sets overlap in places (see Figure 7.6). Where this occurs, ribbed moraine in a cross-cutting relationship were found (see Figure. 7.7). This is interesting because it shows the formational process can both create and preserve landforms in the same area and formational theories need to explain this phenomenon.

The ARC coverage showed that very large ribbed moraine ridges covered the landscape in the northern half of the site (see Figure. 7.4). These bedforms are the largest ribbed moraine ridges found to date and to distinguish them from the more usual scale of ribbed moraine, they were classified as mega-scale ribbed moraine. In this area the mega-scale ribbed moraine belonging to rm-1 has a continuous coverage that was estimated to be approximately 3000 km^2 in extent, making it the largest known uninterrupted ribbed moraine field. The southern half of the site contains fields of smaller scale ridges. This region was originally classified by Clark and Meehan (2001) as containing only minor ribbed moraine, however, many of the ridges are much larger than this and are also morphologically akin to classical forms (see Figure 7.5). In light of this evidence, it was thought best to reclassify the southern region as an area containing both minor and classical type ribbed moraine. In this location, the smaller scale ribbed moraine is less continuous and patchier in nature and the ribbed moraine is distributed in dispersed clusters and isolated fields, (see Figure 7.4). The discovery of mega-scale ribbed moraine and the juxtaposition of such widely differing scales of ridge within the same bedform suite have quite important implications for formational theories. Not only must they explain the mechanisms responsible for producing mega-scale ribbed moraine, they also have to explain how the process can make both mega-scale and smaller scale ridges in the same region during one flow event, as this is what seems to have happened during the formation of rm-1.

As was shown in Section 7.4.1, both the mega-scale and smaller scale ridges display many of the characteristic features often associated with this landform (see Figures 7.5 and 7.8). However, like the ribbed moraine studied in Québec, the ridges in Ireland also diverge somewhat in morphology. For example, among the smaller scale classical type ribbed moraine in the south it was possible to identify elongate straight ridges, rectangular forms and ridges that were arcuate and concave in an up ice direction (see Figure. 7.11). The same was also true of the mega-scale ribbed moraine and as well as seeing many classical features it was possible to see rectangular ridges, barchan forms and very heavily drumlinized ridges (see Figure 7.9).

Using the DEM to investigate whether topography influenced ribbed moraine distribution concluded that the ridges were not confined to any particular topographic setting. Ribbed moraine ridges from the three flow sets were found distributed on hilltops, hill slopes, and also in the large basins in the region (see Figures 7.15 & 7.16). Topography also appears not to have interfered with the orientation of the ridges. For example, the ribbed moraine produced by the bedforming event rm-1 all have a uniform southeasterly orientation, regardless of their elevation or topographic setting. This indicates that the ice was thick enough during this bedforming phase that ice surface slope rather than topography controlled the ice flow directions.

Morphometric measurements conducted on ribbed moraine length, height, width and wavelength again showed a wide variation in all four parameters (see Section 7.6 and Table 7.3). These were important findings because it confirms the conclusions of Clark and Meehan (2001) that the Irish ribbed moraine are the largest ever found and also has implications for formational theories which need to explain this wide variation in scale.

Table 7.3. Average value and the range for each measured ribbed moraine parameter in the study area.

Parameter	Min	Max	Mean
Length (m)	103	16214	1091
Height (m)	6	63	26
Width (m)	105	1116	443
Wavelength (m)	125	5800	834

Finally, the relationship between ribbed moraine, drumlins and glacial lineations was considered. This was partly done by Clark and Meehan (2001), who found a lineation pattern superimposed on the ribbed moraine that closely matched the ribbed moraine pattern. This they argued, was evidence that the generation of the bedforms was highly related, with drumlinization closely following the formation of the ribbed moraine. When the ribbed moraine field rm-1 was viewed in its entirety it became evident that there is a downstream transition from ribbed moraine to drumlins in this region (see Figure 7.22). It was hypothesised that increasing basal velocities away from the ice divide may have been responsible for this transition. If one considers the further away from the divide the ridges were the more drumlinized they appeared and that the lineaments also tended to increase in length downstream away from the divide (Clark and Meehan, 2001), then the idea seems plausible. It may also add further support to the idea that ribbed moraine, drumlins and glacial lineations are genetically linked and form part of a bedform continuum. Although it was more common to see glacial lineation on top of ribbed moraine, there were some cases where minor ribbed moraine was found superimposed on glacial lineations (see Figure 7.12 & 7.23). A more unusual case was observed where a crag-and-tail feature had been "ribbed" into a series of minor ribbed moraine (see Figure 7.24). In all the cases where superimposition was observed the minor ribbed moraine pattern matched that of the lineations, indicating they are related to the same ice flow event, which in this case is rm-1. It appears that in this area there may well have been multiple phases of ribbed moraine formation operating during this bedforming phase.

***

Map 7.1. Distribution of Ribbed Moraine, Northeast Midlands Region, Ireland

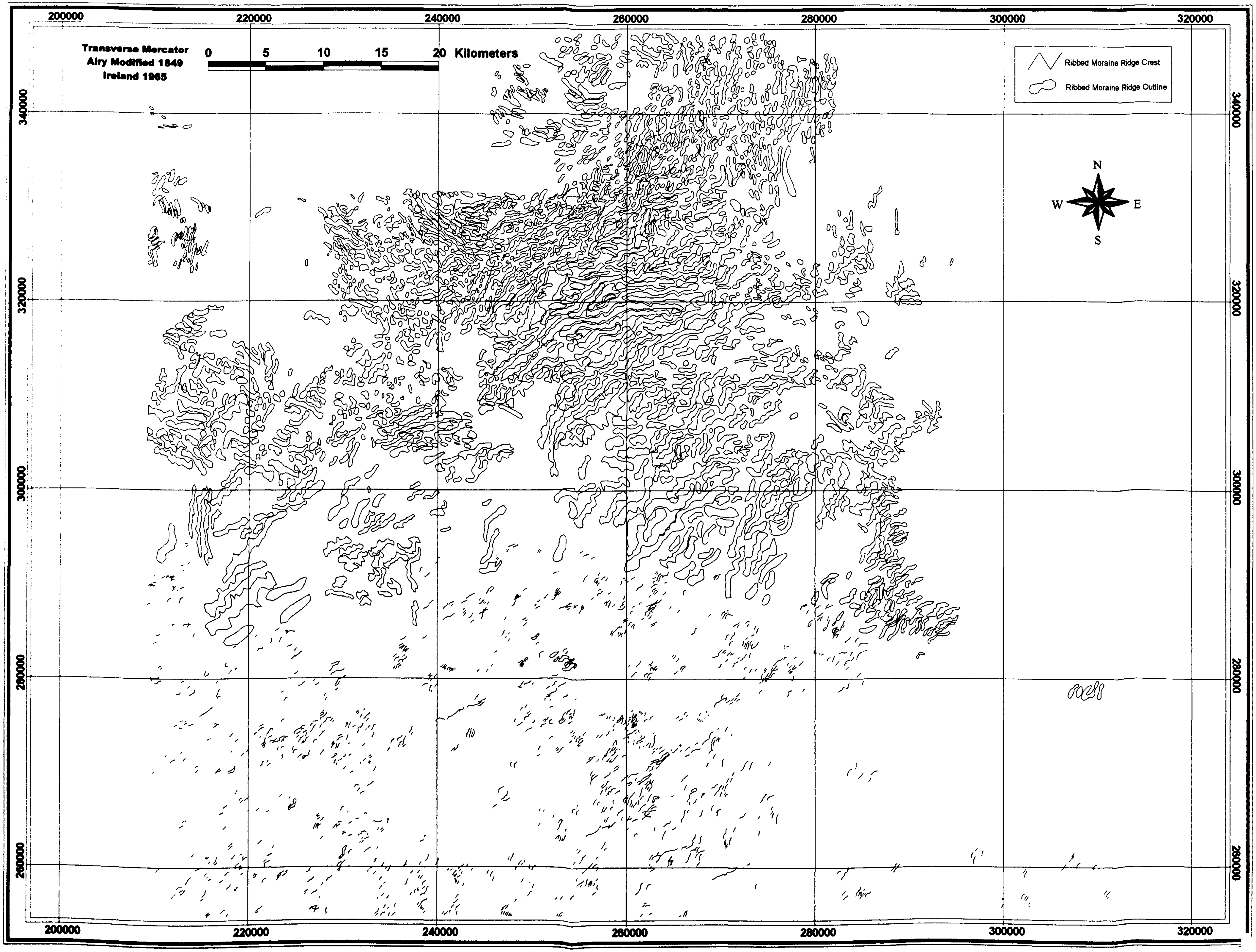

Chapter 8: The Characteristics of Ribbed Moraine in the Lake Rogen area, Härjedalen, Central Sweden

8.1. The study site

The Lake Rogen study site is situated in the mountainous province of Härjedalen in central Sweden (Fig. 8.1). It is a well-known region, because it is the type locality for the so-called "Rogen moraine" and much has been written about the ribbed moraine in this region (e.g. Lundqvist, 1969; Lundqvist, 1989; Hättestrand, 1997b).

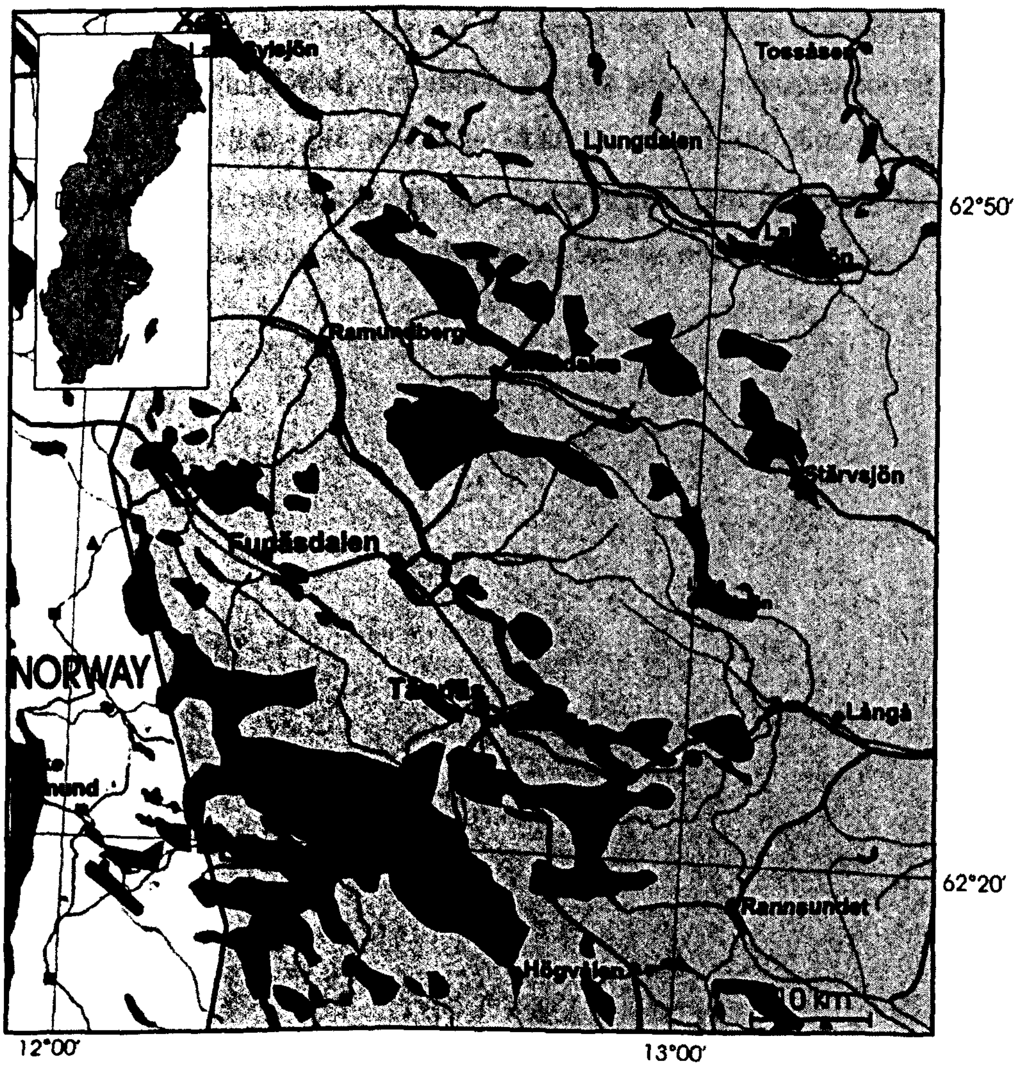

Figure 8.1. Location map showing the Lake Rogen study site. The dark grey areas mark the approximate location of the ribbed moraine fields in this region.

8.2. Data Sources and methodology

For the purpose of obtaining information on the wavelength of the ribbed moraine ridges in this region, 1:60 000 aerial photographs covering approximately 3600 km^2 of the Lake Rogen area were acquired. The ridges were mapped and their wavelength determined following the procedures outlined in Chapter 4 (see Section 4.3.4). To make a digital map of the ribbed moraine one Advanced Spaceborne Thermal Emission and Reflectance Radiometer (ASTER) scene (15 m, 60 × 60 km) was acquired and geocoded. All the ribbed moraine ridges that could be identified from the image were mapped, which was accomplished by visual interpretation of the landforms and on-screen digitising directly into Erdas Imagine (see Section 4.3.4). To obtain an indication of the general topography of the study site a 30-arc second (ca 0.5-1 km) Digital Elevation Model (DEM) was obtained. This allowed visualisation of the general topography of the study site and was used to investigate relationships between topography and ribbed moraine distribution in the region. The following sections report on the results of the mapping and morphometric analysis of the landforms.

8.3. Results from mapping

8.3.1. Large-scale pattern

The general orientation of the ribbed moraine is shown in Figure 8.2. As can be seen, the area is covered by ribbed moraine that records a southeast to northwest ice flow and owing to the strong conformity of orientation across the site, it is hypothesised that these ribbed moraine were generated isochronously during a single phase.

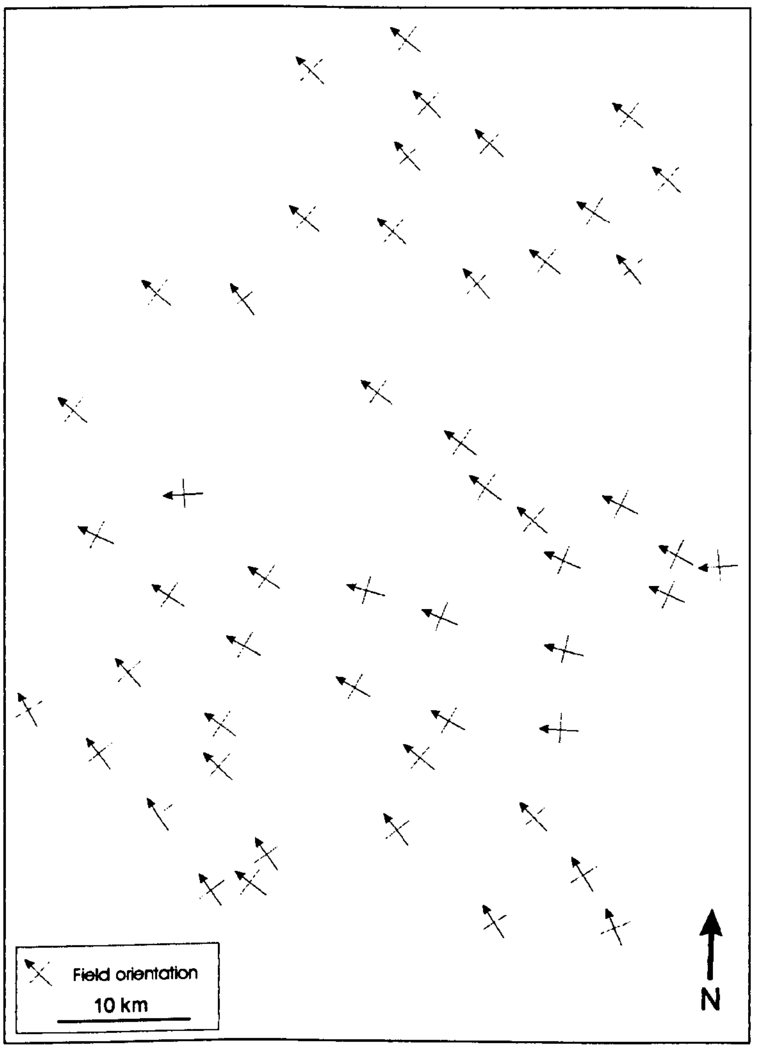

Figure 8.2. Ribbed moraine field orientation map in relation to the regional ice flow pattern. The lines show the general orientation of the ribbed moraine ridges in each field and the arrows the direction of ice flow. Note the strong conformity of field orientation across the region, which strongly indicates the ribbed moraine were formed isochronously during a single ice flow event.

In total, 5637 ribbed moraine ridges were mapped from the ASTER image and the resulting ARC coverage can be seen in Figure 8.3 and Map 8.1. At this locality, the ribbed moraines were found to be concentrated in the southern and northern parts of the site, with the central region conspicuously lacking significant coverage.

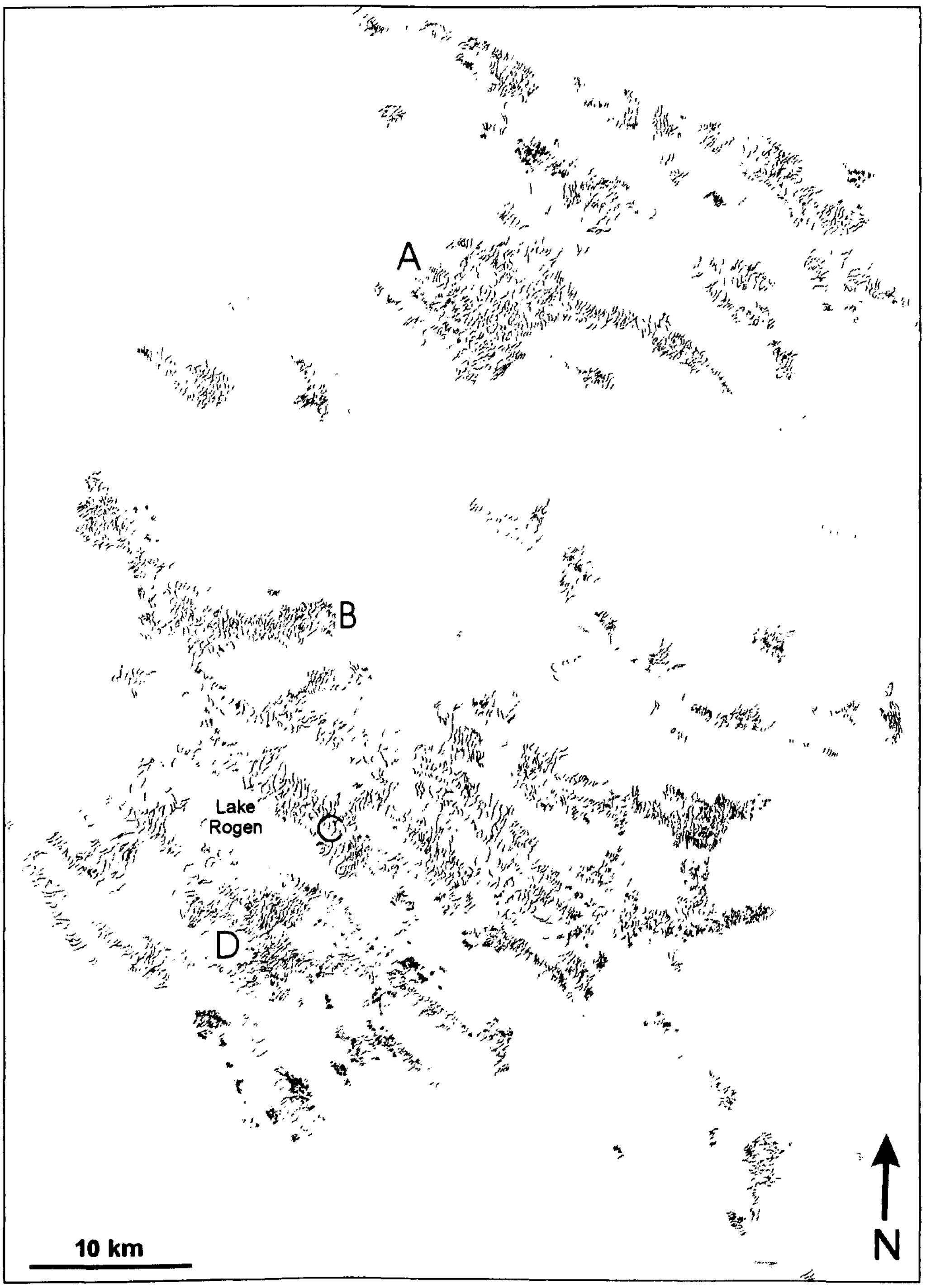

Figure 8.3. Ribbed moraine ridges mapped in the Lake Rogen area from the ASTER image. The fields at locations A, B C and D mark the largest uninterrupted fields in the area and are referred to later on. See Map 8.1 for a more detailed view.

Generally, the ribbed moraine fields in this region tend to be much smaller than those observed in Canada and Ireland, where fields measuring more than 40 by 50 km were observed (e.g. Sections 5.3.1 & 7.3.1). In this region, the largest uninterrupted ribbed moraine fields were less than half this and all were approximately between 13 km to 21 km long and 3 km to 11 km wide (Fig. 8.4).

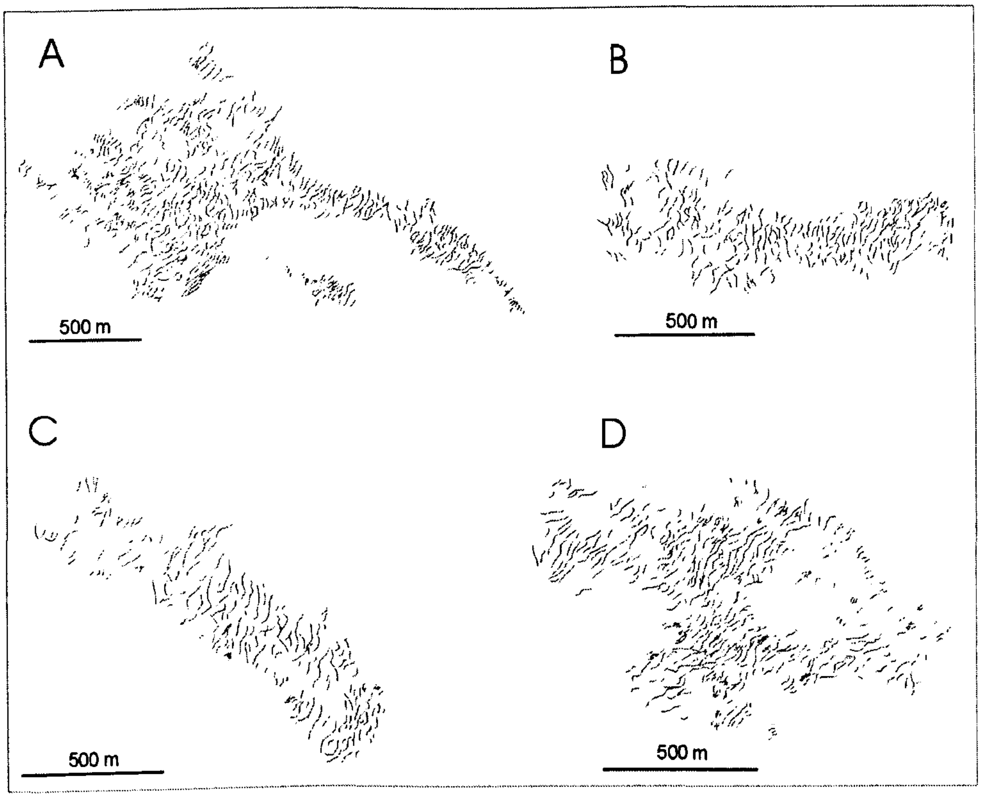

Figure 8.4. In the Lake Rogen area the ribbed moraine fields tend to be smaller than those found at the other three sites. This diagram shows four of the largest fields in the region marked A, B, C and D in Figure 8.3. The ribbed moraine marked A is situated just south of Mittådallen (12° 38 E & 62° 39 N) and is the largest continuous field in the area measuring 21 by 11 km. The field marked B is situated 11 km north of Lake Rogen (12° 20 E & 62° 27 N) and measures 13 by 3 km. Field C is situated on the northern shores of Lake Rogen (12° 24 E & 62° 21 N) and measures 14 by 4 km. The ribbed moraine at D is situated immediately south of Lake Rogen (12° 22 E & 62° 16 N) and measures 14 by 7 km.

The distributional pattern of ribbed moraine in the Lake Rogen area was classified into the following categories:

1. Elongate ribbons and narrow tracks
2. Clusters
3. Isolated fields

8.3.2. Elongate ribbons and narrow tracks

In the Lake Rogen site many large linear ribbon type fields were clearly evident running through the area (Fig. 8.5). These elongate ribbons have a range of morphologies and also vary in scale across the region. The fields marked A and B in the diagram show two examples of broad type ribbons which are approximately 14 km long and 4 km wide.

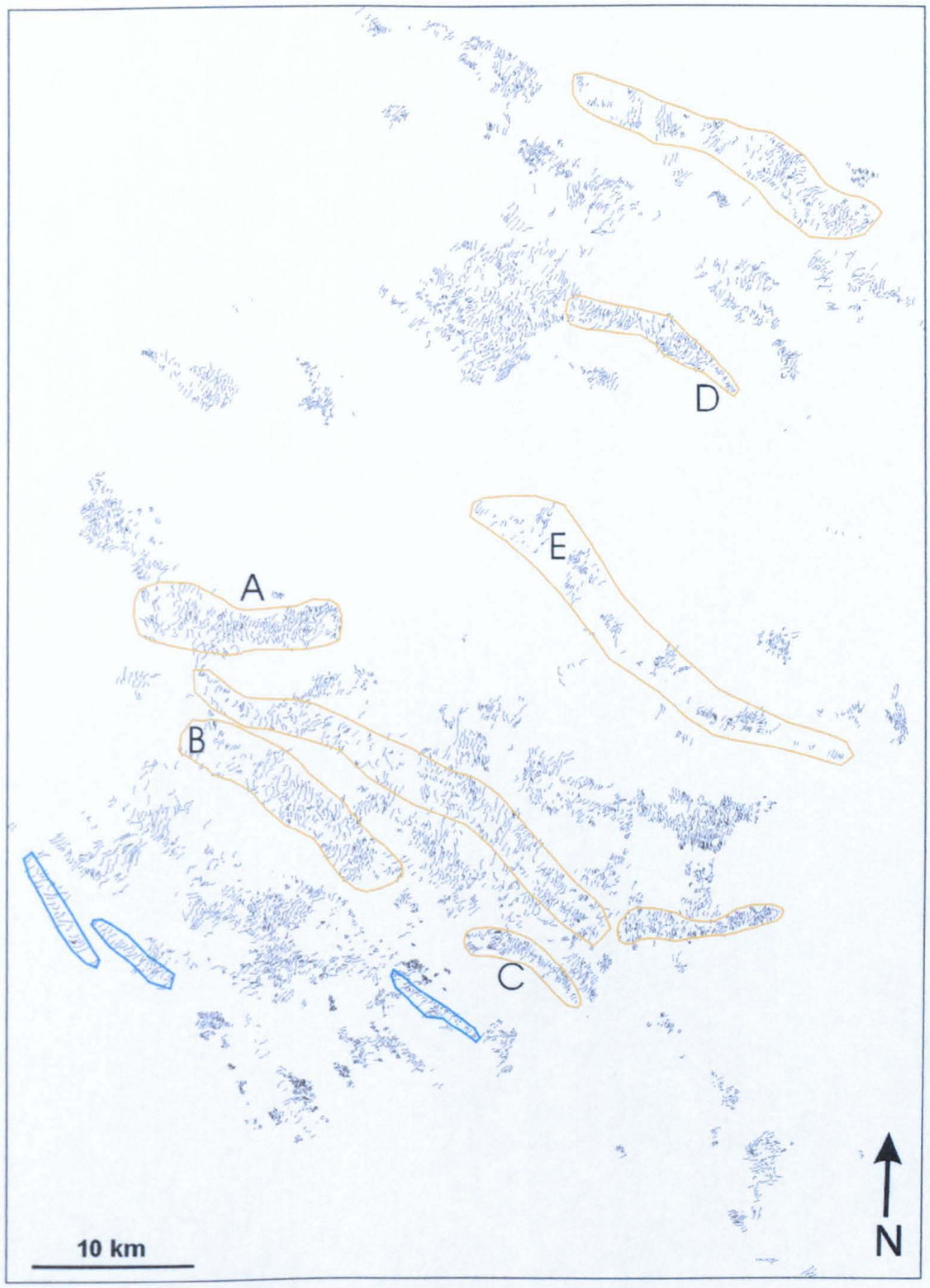

Figure 8.5. Examples of ribbon and narrow track type ribbed moraine fields in the Lake Rogen study area. Ribbons are bounded in yellow and the narrow tracks in blue.

The narrower ribbons are of a similar length as the broader ribbons, however they are much thinner features and the two examples marked D and E are only a few hundred metres at their narrowest points. Although most of the ribbons are made of sequences of ridges that are largely uninterrupted, some examples of broken ribbons were also observed. These ribbons are not a single field, but rather a collection of fields, separated by sizable gaps that have been distributed in a linear fashion and it is the spaces between the fields that give the ribbon a rather broken appearance (e.g. E). Visual inspection of the site established the majority of these ribbon type fields were located in the valleys that run through this region and this helps explain their linear pattern (see Section 8.5.1 and Figure 8.14 below). As well as having large-scale linear fields, this site also contained some narrow ribbed moraine tracks that were similar to those observed in Québec, (see Sections 5.3.2 & 6.3.2). Compared to ribbon type fields, these are much narrower and shorter features and typically consisted of a single line of ridges. In Québec, the narrow tracks tended to be made of smaller scale ribbed moraine ridges that had a much shorter wavelength than ribbed moraine in their immediate surrounds. This was not the case in the Lake Rogen site. Here, the ridges are between 500 m and 1.5 km long and a few hundred metres wide, which is the typical scale range of classical type ribbed moraine ridges. They also have a similar wavelength as the surrounding ribbed moraine.

8.3.3. Clusters

Ribbed moraine in this region were also found to be distributed as clusters (Fig. 8.6). These clusters tend to cover much smaller areas than those observed in Québec, where some were found to be as large as 300 km^2 (see Section 6.3.3). The largest cluster observed at this site, marked A in Figure 8.6, measures only 80 km^2. Generally, the clusters tend to be quite dense having high concentrations of ribbed moraine ridges. However, dispersed clusters were also evident in the area, the cluster marked B being a good example. As well as having both dispersed and dense clusters, this area also had number of very dense clusters of ribbed moraine. These clusters are all very small and are all less 5 km^2. Visual inspection of these clusters revealed these areas were made of what Hättestrand (1997b) terms minor ribbed moraine (Fig. 8.7), which explains the very dense appearance on the landscape because minor ribbed moraine ridges are typically much closer together than the ridges of larger forms.

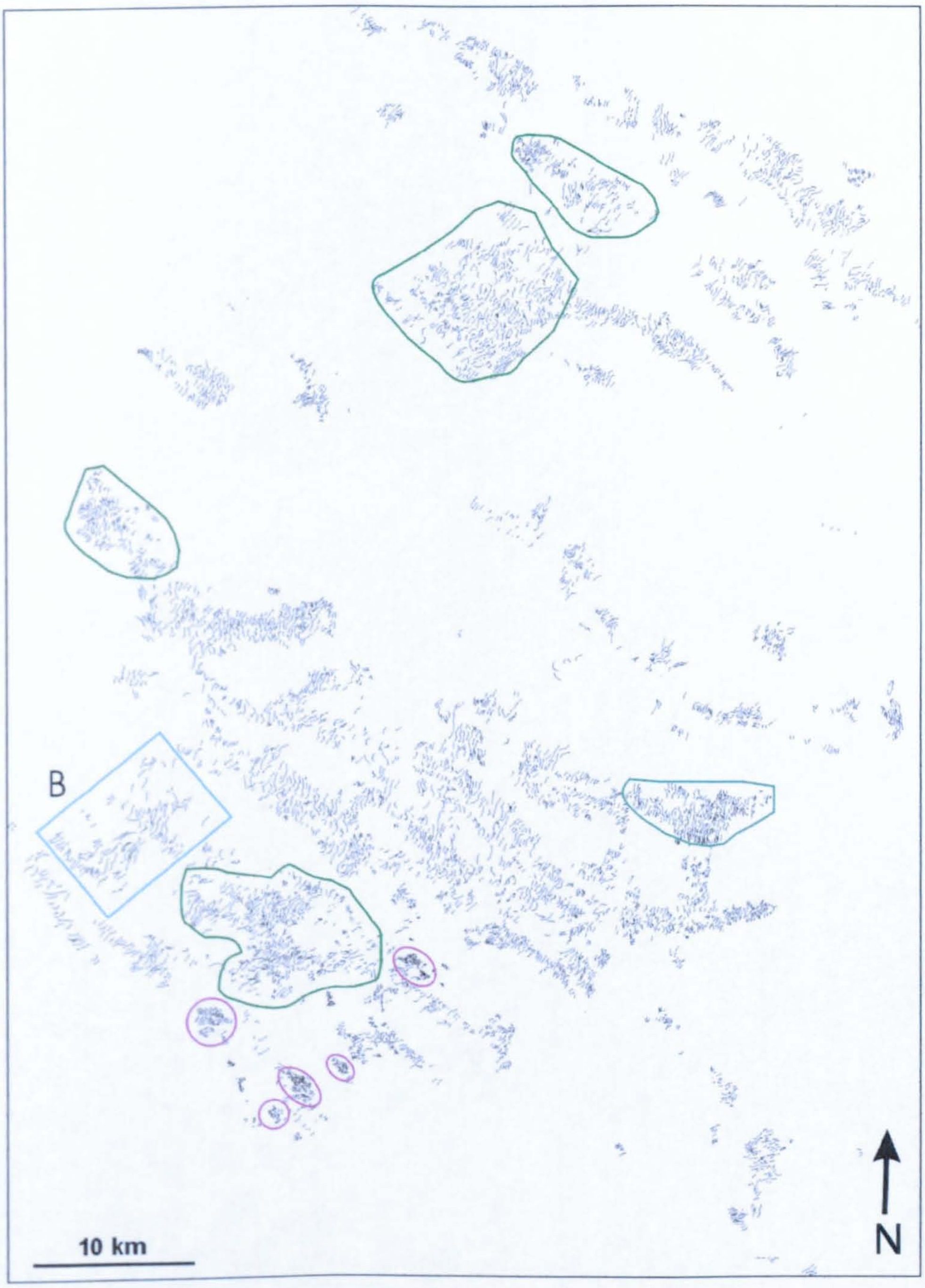

Figure 8.6. Examples of ribbed moraine clusters in the Lake Rogen study area. The green outlines mark some examples of dense clusters in the area. Small, very dense clusters have been ringed in purple and an example of a dispersed cluster had been outlined in blue.

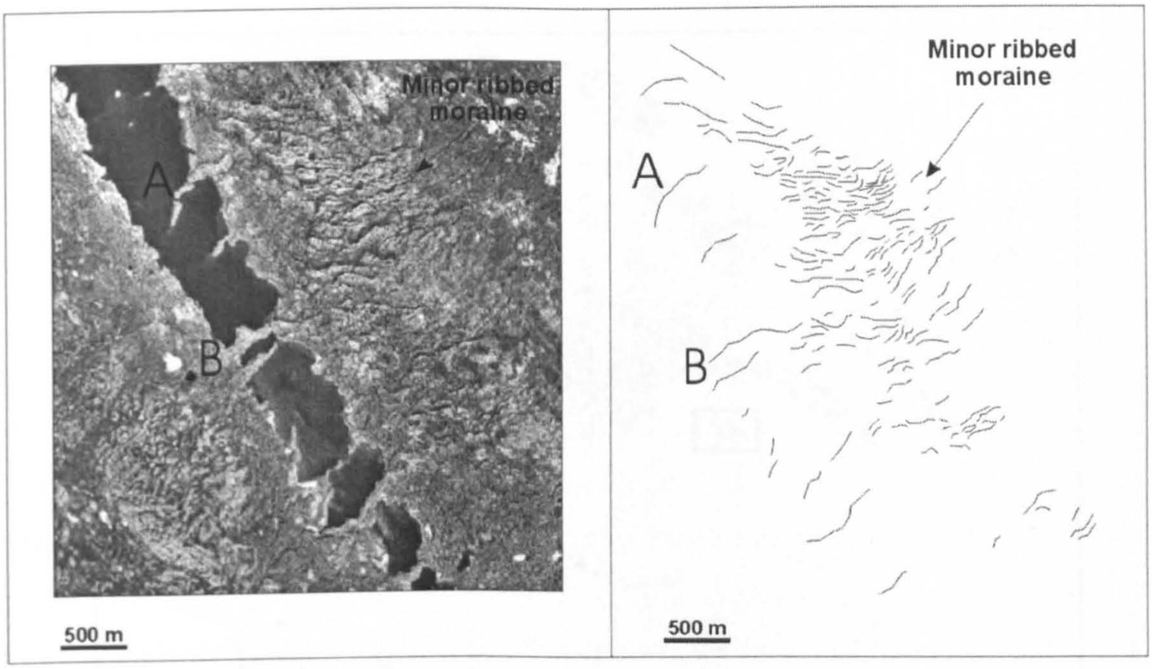

Figure 8.7. In the southern parts of the Lake Rogen site, some small very dense clusters of ribbed moraine were observed. All of these were found to contain minor ribbed moraine, such as the one shown above, which is situated 9 km southwest of Lake Rogen (12° 25 E & 62° 11 N). Note their small-scale compared to some larger classical type ridges, marked A and B that bridge the lake. This minor ribbed moraine can be seen in greater detail in Figure 8.12. Image taken from 1:60 000 scale aerial photograph.

8.3.4. Isolated fields

Elsewhere across the region, many isolated ribbed moraine fields can be seen dotted across the landscape (Fig. 8.8). They tend to be rather small and normally range between a few hundred metres in length (e.g. A) to several kilometres long (e.g. B) and are usually spatially isolated from other areas of ribbed moraine. Generally, the fields in this area are isolated by only a few kilometres (e.g. C) however, there are some instances where fields are more removed from the general population and the field marked D is one example.

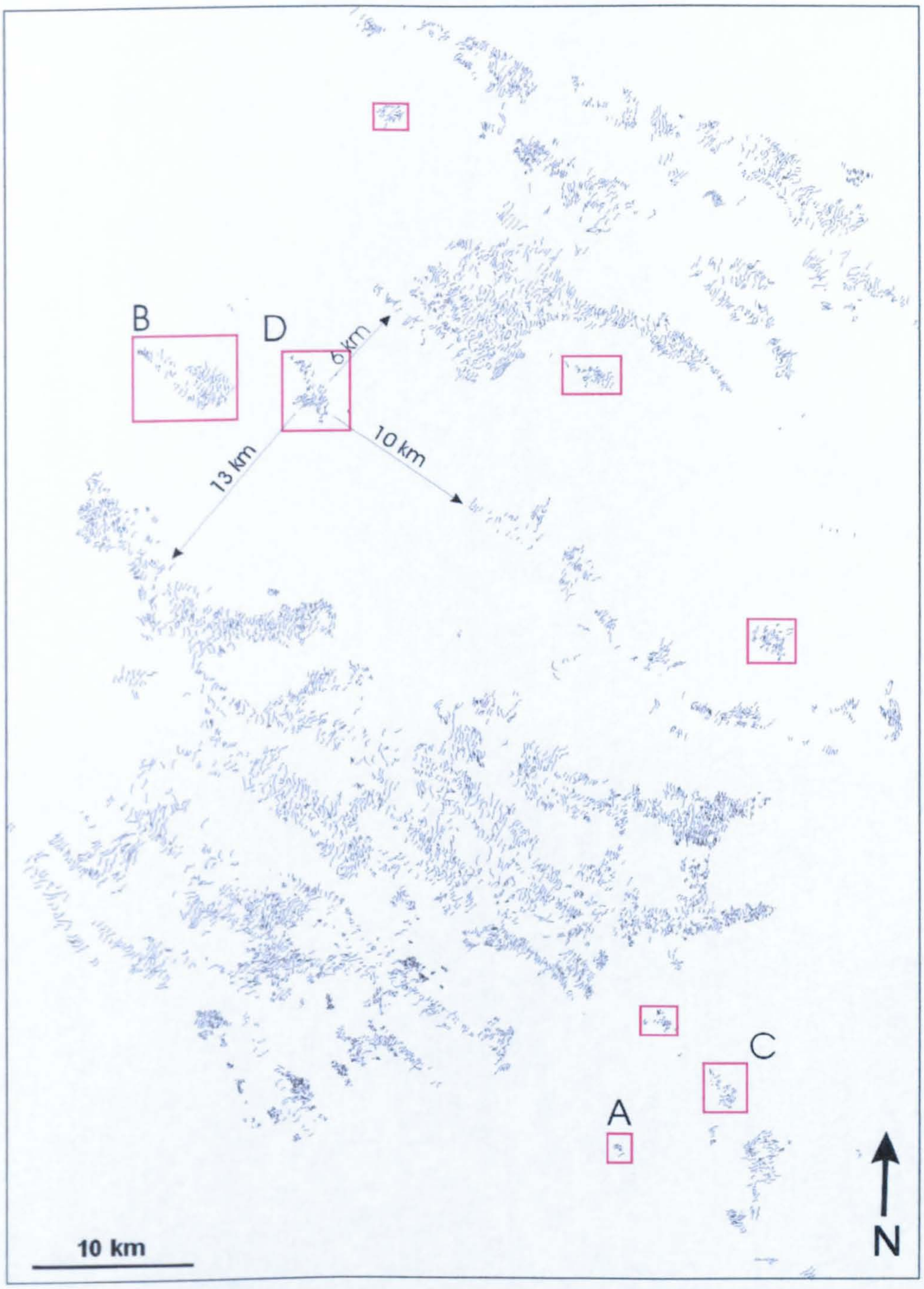

Figure 8.8. Some examples of isolated ribbed moraine fields. Note that they are usually quite small and are spatially isolated from other ribbed moraine fields.

8.4. Morphological characteristics of the ribbed moraine in the Lake Rogen region

8.4.1. Plan view morphology

In the Lake Rogen site many examples of classical type ribbed moraine ridges are clearly evident across the region and a large proportion of the fields in this locality contain ridges that match the classic morphological description discussed in Section 5.4.1. However, just like the ribbed moraine fields observed in Québec and Ireland, close scrutiny of ridge morphology exposed variations in form (Figs. 8.9 & 8.10). In both examples, it is possible to identify ribbed moraine ridges displaying the classic traits associated with this landform i.e. ridges with horns at their ends, anastomosing ridges and ridges whose ends curve downstream. However, there are also examples of ridges that curve upstream and are concave up ice, barchan shaped ridges and both fields also contain broad ridges that are twice the width of the other ridges in the field.

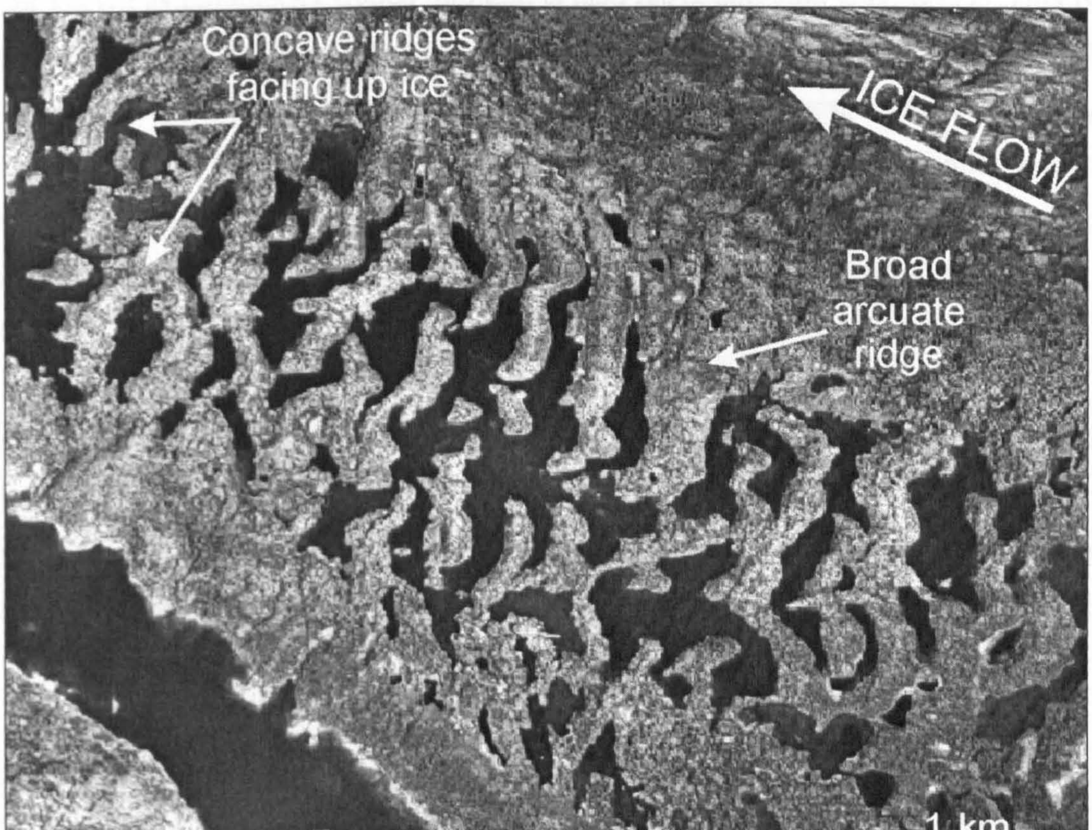

Figure 8.9. Showing classical type ribbed moraine ridges at Lake Rogen (12° 25 E & 62° 21). Note how many of the ridges display the classic morphological characteristics of ribbed moraine such as being anastomosing and curved downstream and having horns at their ends. Note also however, that some of the ridges differ somewhat from the classical description of ribbed moraine given in the literature. Image taken from 1:60 000 scale aerial photograph.

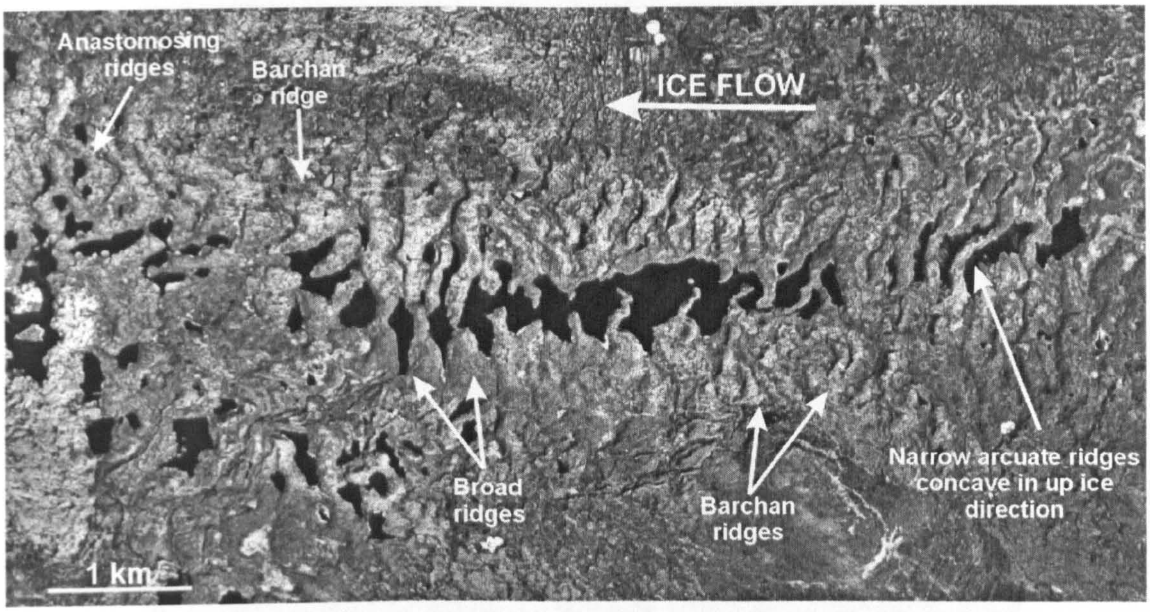

Figure 8.10. Showing another ribbed moraine field 11 km north of Lake Rogen (12° 22 E & 62° 27 N) where ridges of mixed morphology are found together. Note the variety of forms within this field, including ridges that are concave in an up ice direction, very broad ridges and barchan shaped ridges. Image taken from 1:60 000 scale aerial photograph.

Although fields of classical type ribbed moraine are widespread in this region, another kind known as hummocky ribbed moraine is also fairly common (Fig. 8.11). This type of ribbed moraine has been recognised for some time in this area (e.g. Lundqvist, 1989; Hättestrand, 1997b) and is described as a poorly developed form of the classical type ribbed moraine. Hättestrand (1997b) found that hummocky ridges are similar in size to classical forms, however they are commonly shorter in length and are also less constant in height and spacing. Although they are clearly transverse to ice flow they are not as parallel as is generally the case with classical type ribbed moraine.

In the southern parts of the site, some small fields of minor ribbed moraine were also identified (see Figures 8.6 & 8.7). In this area, the minor ribbed moraine consists of small closely spaced ridges that often have sharp crests and as is the case with the larger scale forms, these too display a range of morphologies within the same field (Fig. 8.12).

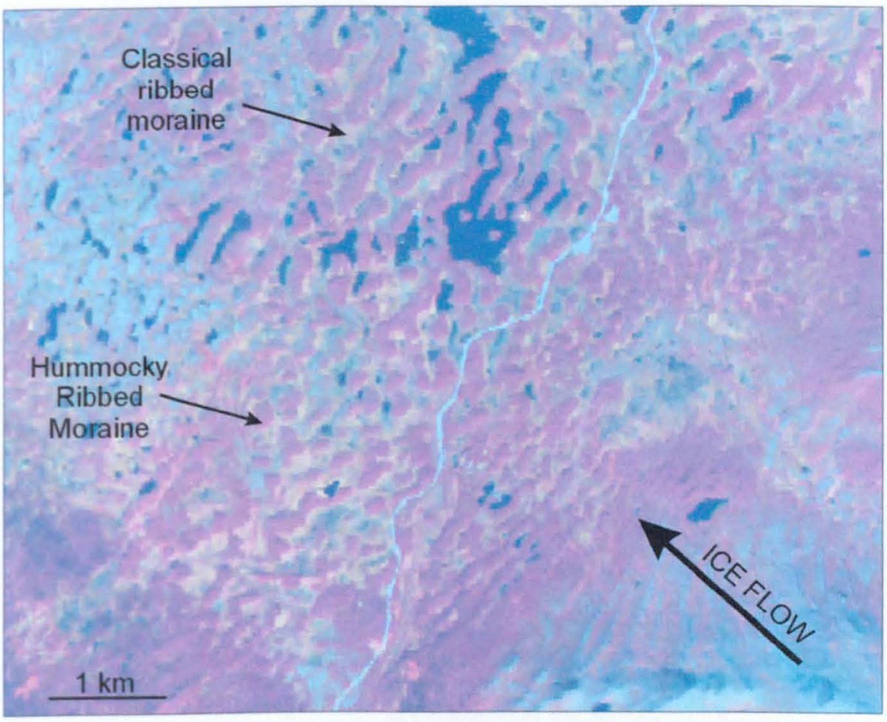

Figure 8.11. An ASTER satellite image showing some hummocky ribbed moraine situated immediately south of Mittådallen (12° 36 E & 62° 37 N). Note the difference in form from the classical type ridges at the top of the picture. The hummocky ribbed moraine is composed of rounded or drumlinized mounds that are aligned transverse to ice flow.

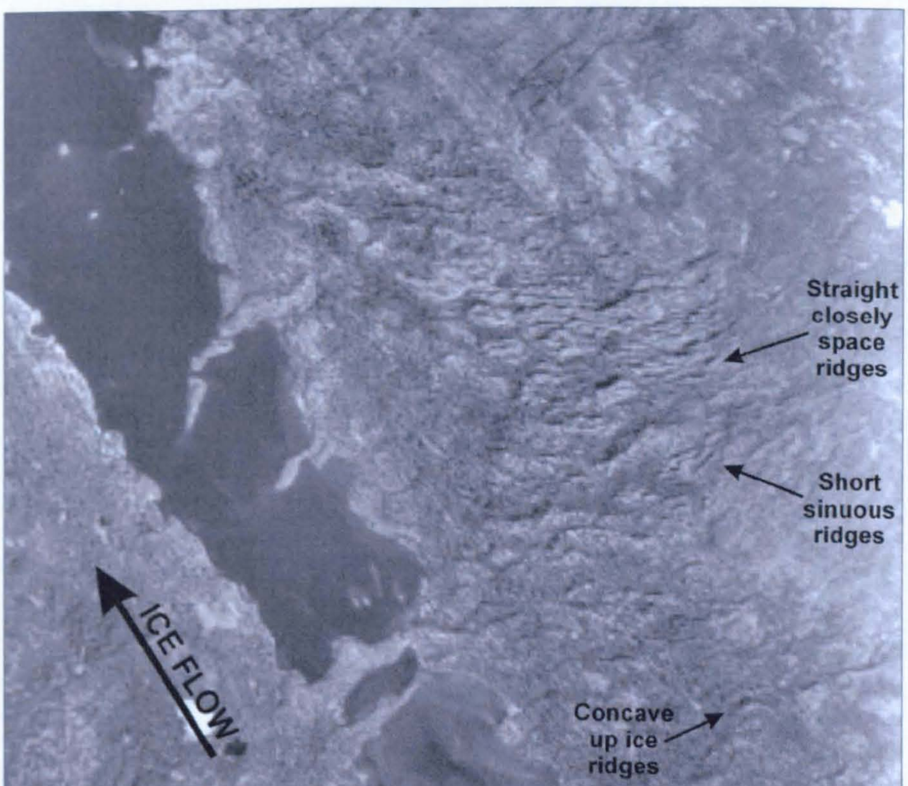

Figure 8.12. A detailed view of the minor ribbed moraine field situated 9 km southwest of Lake Rogen (12° 25 E & 62° 11 N). Note the range of morphologies within the same field including both short and sinuous ridges and ones that are curved and are concave up ice. Image taken from 1:60 000 scale aerial photograph.

8.5. Topography

8.5.1. Topographic setting of ribbed moraine

The general topography of the site is depicted in Figure 8.13, which shows a GTOPO30 DEM and a 3-D relief image of the site. As is illustrated, the terrain in this part of Sweden is quite rugged and within the confines of the site, many of the peaks are over 1000 m high. Like all mountainous terrain, numerous broad valleys and depressions can be seen meandering through the landscape between the hills. Some of these valleys are quite long and the one containing Lake Lossen, which dissects the site in a northwesterly fashion, measures over 70 km in length. Above the lower valleys, large expanses of open undulating topography can be seen. The area immediately east and west of Lake Rogen is a good example of this type of terrain and as Figure 8.14 shows these regions are typically quite open and are characteristically flat or gently undulating.

To investigate the topographic setting of the ribbed moraine at this locality, the ARC coverage of the mapped ribbed moraine crests was draped on top of the DEM (Fig. 8. 15). Viewed in this fashion, it was immediately apparent that the highest mountainous terrain lacked significant coverage of ribbed moraine. However, it was possible to see fields of ribbed moraine distributed lower down on mountain slopes (e.g. A, B & C) however, these fields tended to be small and account for a small percentage of the entire population. The rest are located in the valleys and valley slopes (e.g. D, E & F) and on the areas of open undulating topography (e.g. G, H & Figure 8.14). The small fields of minor ribbed moraine that are situated just south of Lake Rogen, were found to be restricted to areas of higher elevation and are found exclusively high up on hill slopes in the southern part of the site.

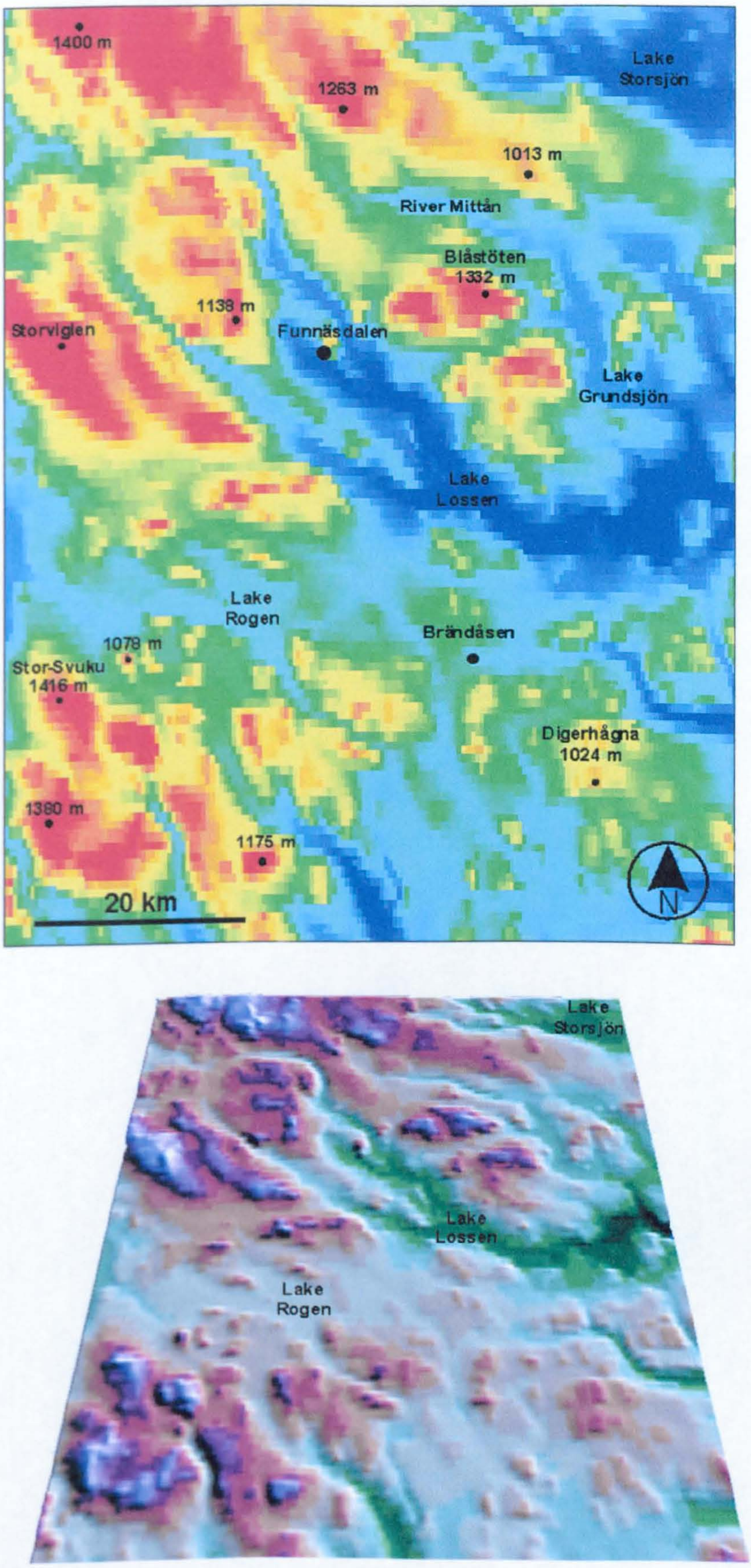

Figure 8.13. The figure on top is a GTOPO30 DEM of the Lake Rogen region. Elevation is coded to show the highest elevations as red, grading down to orange, yellow, green, blue to purple, which represents the lowest regions. The relief image at the bottom was produced using the DEM and gives a 3-Dimensional impression of the general topography.

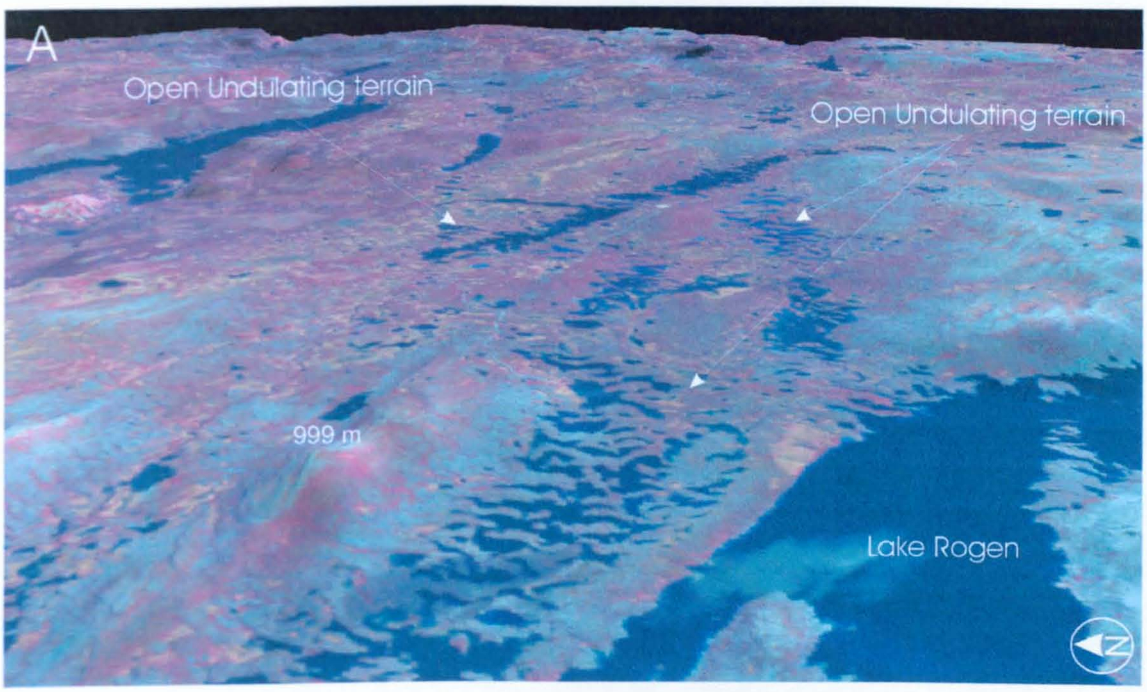

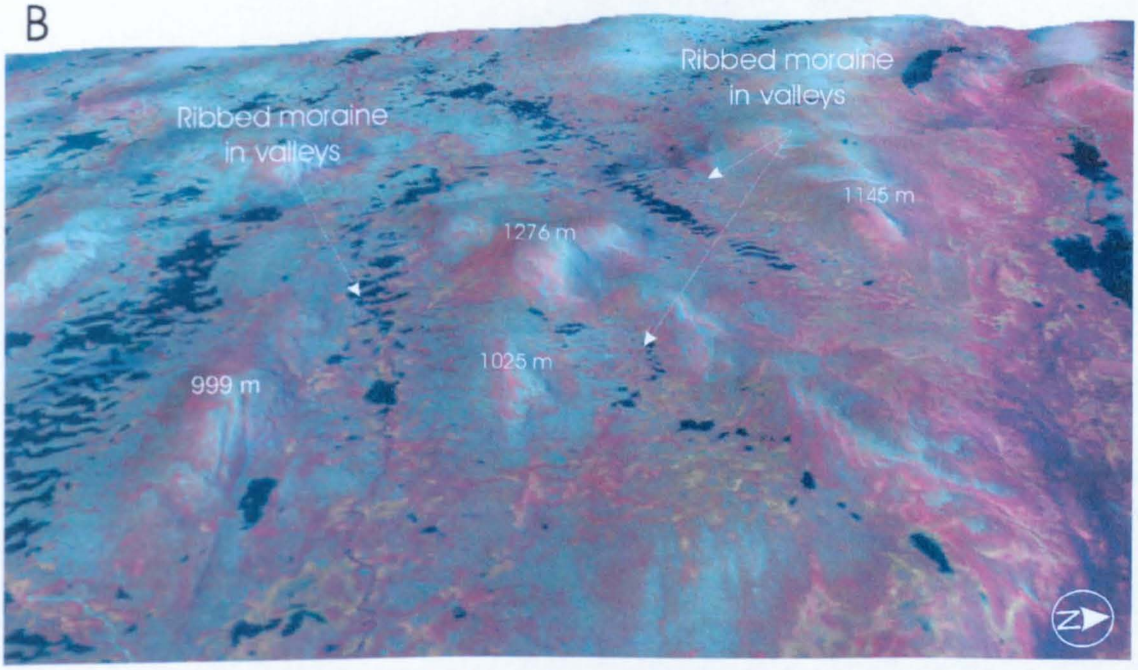

Figure 8.14. Two oblique views of the region in and around Lake Rogen. Figure 8.14a shows the terrain looking eastwards across Lake Rogen. Note the large open expanses of undulating ground and that ribbed moraine is liberally distributed on this type of terrain. Figure 8.14b is an oblique view of the site looking westwards from a position just north of Lake Rogen. Note the many broad valleys in the area and that the ribbed moraine in this area is found exclusively in these and not on the hills. Both images are approximately 10 km across in the foreground and are 3-D renderings of the GTOPO30 DEM with the ASTER satellite image draped on top.

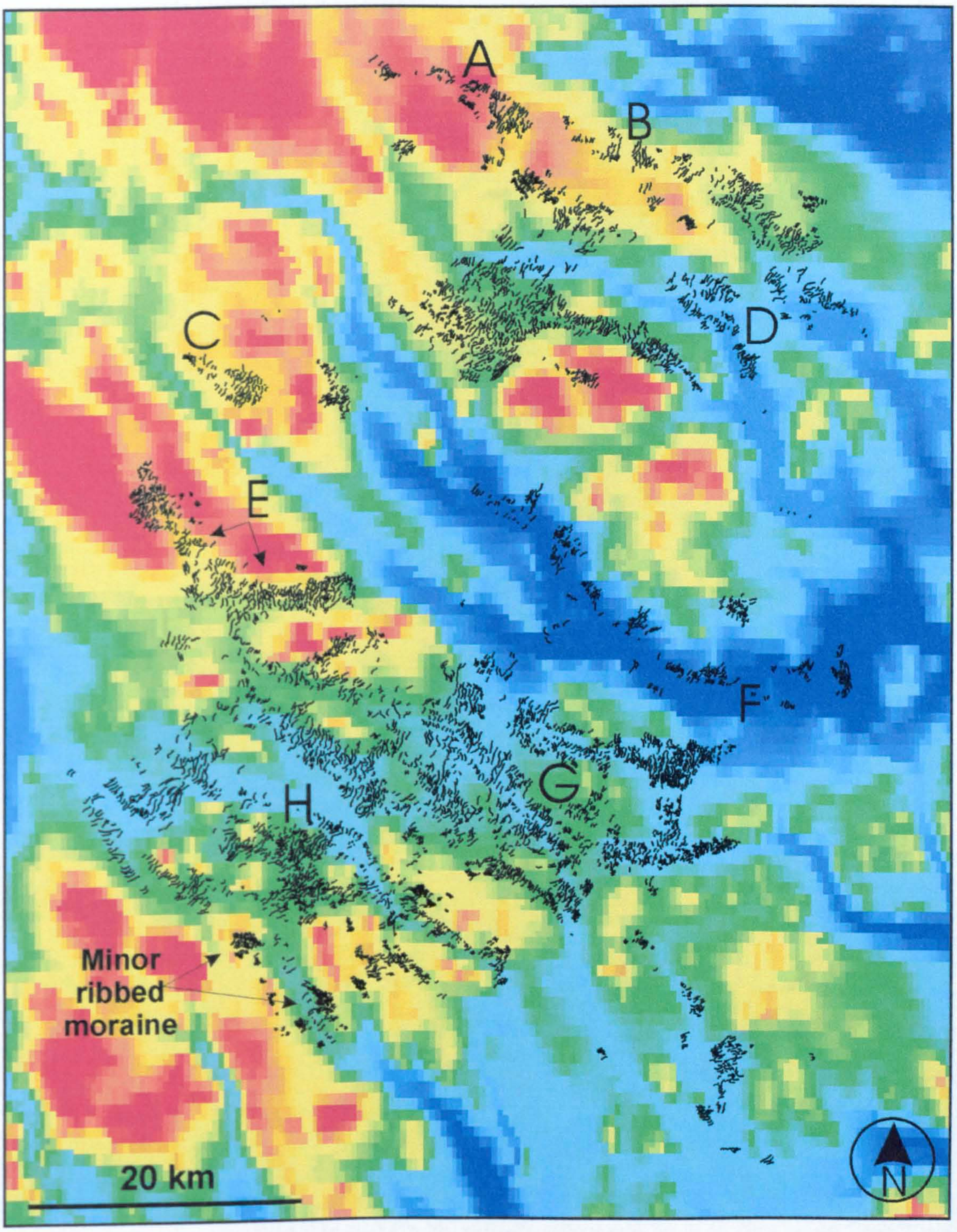

Figure 8.15. DEM of the region with the ARC coverage of the ribbed moraine ridges draped on top. Note how the ribbed moraine is not distributed on the mountains in this region but largely in the broad shallow valleys and areas of open undulating countryside.

8.5.2. Relationship to slope aspect

In the Lake Rogen area ice flowed from the southeast in a northwesterly direction across the site (see Figure 8.2). This meant that slopes facing the southeast would have experienced compressive glacial stresses as the ice flowed against them and slopes facing the northeast would have been zones of extending glacial flow as the ice flowed over them. To investigate whether the different glacially imposed stresses influenced ribbed moraine distribution in this area some detailed analysis was conducted in a GIS using the same procedures outlined in Section 5.5.2. By defining compressive slopes as those facing between 45° to 215° and extensional slopes as those facing between 235° to 35° the GIS was used to map the area of both categories and assess the relative proportion of ribbed moraine found in category (Fig. 8.16). The results of the compressive slope test showed that 47 % of the ribbed moraine population was formed on slopes that would have experienced compressive stresses (Fig. 8.17a) and areas that experienced extending glacial flow had 43 % of the ribbed moraine population (Fig. 8.17b). Again, this is contrary to some published accounts (e.g. Bouchard, 1980,1989; Minell, 1980; Sollid & Sørbel, 1984) as no preferential relationship was found between ribbed moraine occurrence and compressive slopes for this sample of 5637 ribbed moraine ridges.

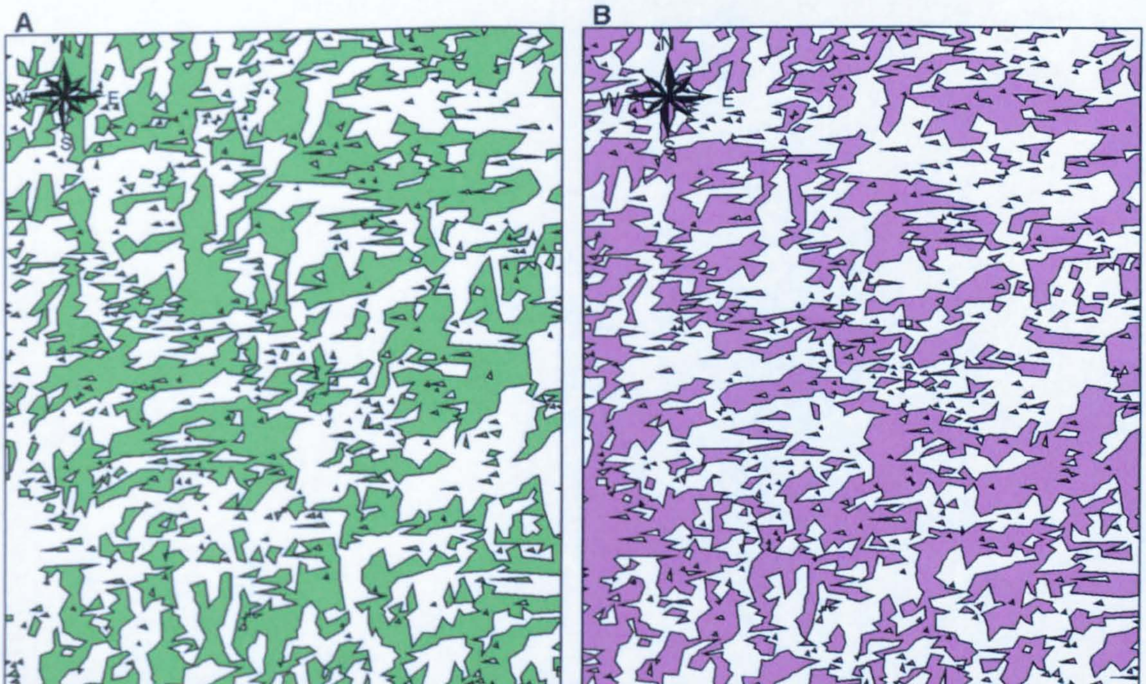

Figure 8.16. The polygon layers created in ArcView GIS, which show the total area of slopes that would have experienced compressive glacial flow (A) and extending glacial flow (B) in the Lake Rogen region.

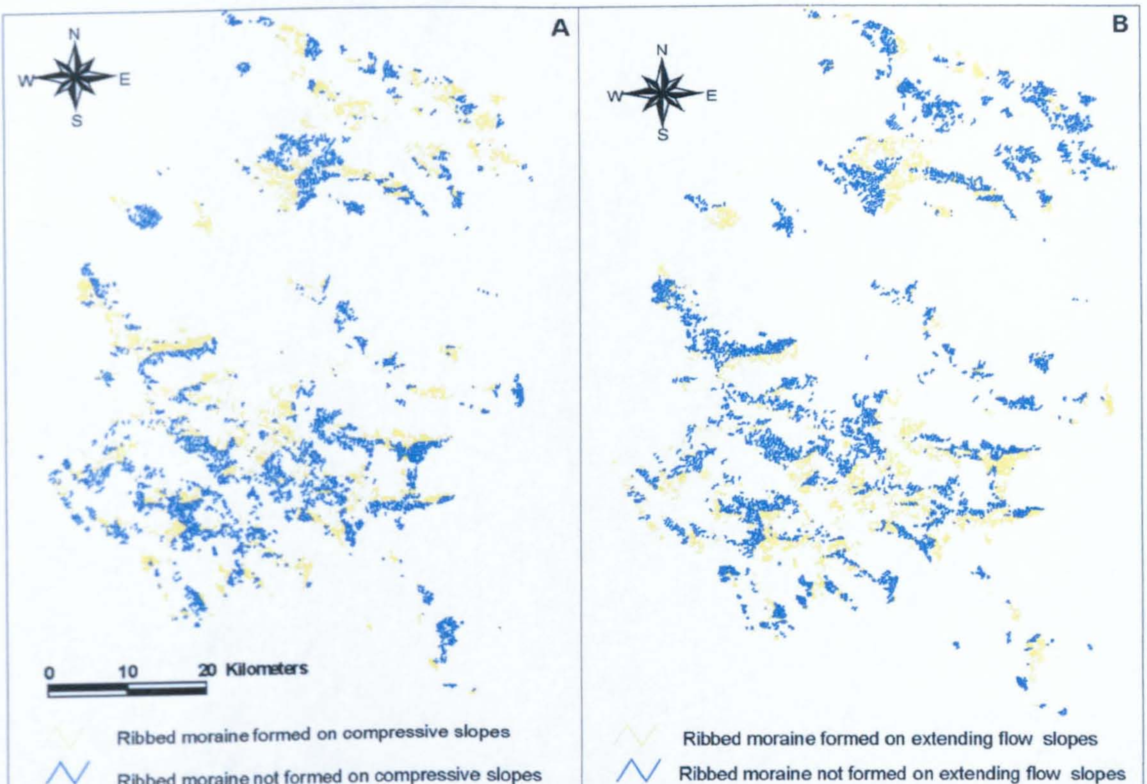

Figure 8.17. Using the GIS to calculate the percentage of ribbed moraine ridges formed on compressive and extending slopes determined that 43 % of the ribbed moraine population was formed on compressive slopes (A) and 47 % on regions that would have experienced extending glacial flow (B).

8.6. Morphometric measurements

To complete the quantitative database of ribbed moraine characteristics for this thesis, measurements were conducted on three aspects of ribbed moraine morphometry. These were ridge length, ridge width and ribbed moraine wavelength. The following sections report the findings for this study site.

8.6.1. Ribbed moraine wavelength

The wavelength of the ribbed moraine ridges in this region were calculated following the procedures set out in Section 4.3.4. This involved mapping the ribbed moraine ridges from stereo aerial photographs to produce a map from which the wavelength was measured manually. In this area, 2666 individual wavelength measurements were taken and a histogram showing the wavelength distribution was made (Fig. 8.18). This showed that the majority of ribbed moraine ridges in this region had wavelengths ranging between 50 m and 475 m, which is 96 % of the population. The other 4 % had wavelengths ranging between 500 m and just over 800 m. The smallest wavelength recorded was only 12 m, the largest was 817 m, the average wavelength was 202 m and the most frequently recurring wavelength, the mode, was 117 m.

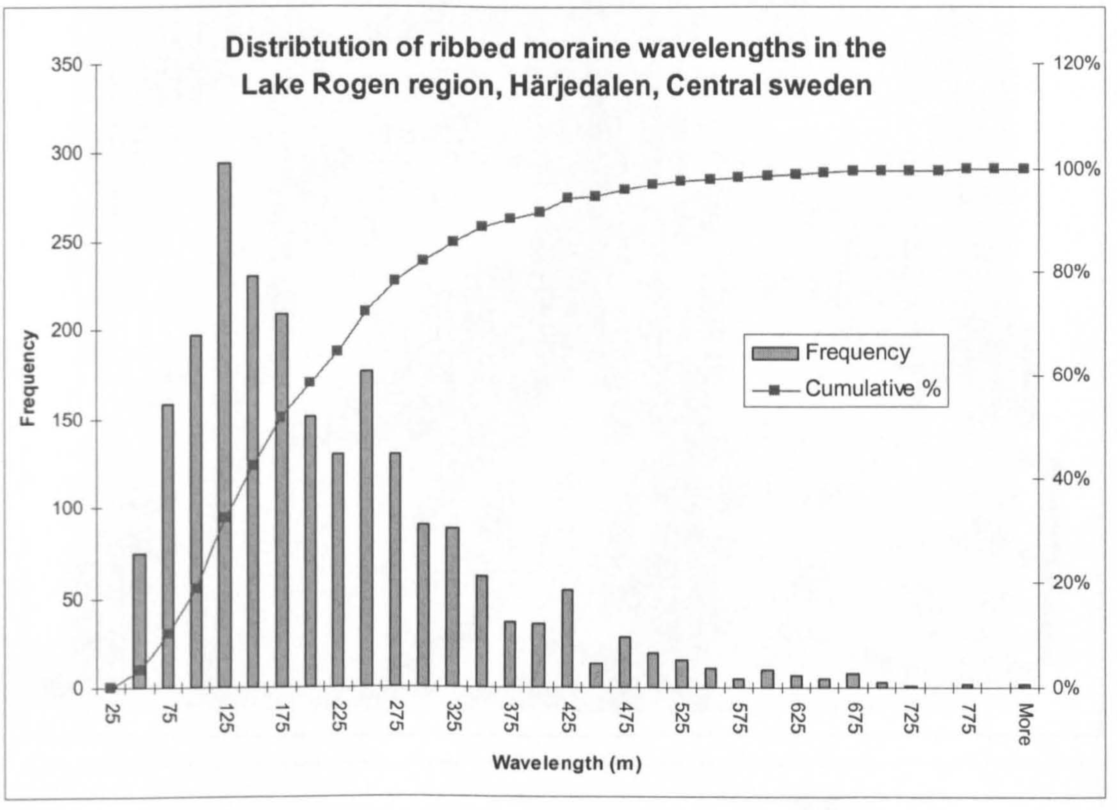

Figure 8.18. Distribution of ribbed moraine wavelength in the Lake Rogen region made from a sample of 2666 individual measurements.

The spatial distribution of ribbed moraine wavelength was examined using a GIS. Using the same methods as those in Lac Naococane and River Kaniapiskau regions (see Section 5.6.1), a density map was produced which showed the locations of the various ribbed moraine wavelengths across the site (Fig. 8.19). In general, this showed that most ribbed fields had ridges of mixed wavelength (e.g. A, B & C). Saying this though, there were some large tracts of ribbed moraine that did appear to be made of ridges of a similar wavelength and some good examples can be seen in an around Lake Rogen, marked by a red spot in the diagram (e.g. D, E & F). Draping the density map on top of the DEM showed that except for the minor ribbed moraine, which was always situated on mountain slopes, there was no specific topographic setting where one could find ribbed moraine of a certain wavelength. For example, it was possible to find ribbed moraine with long wavelength in valleys (e.g. G) as well as high up on mountain slopes (e.g. H). The same was the case with ribbed moraine with shorter wavelengths.

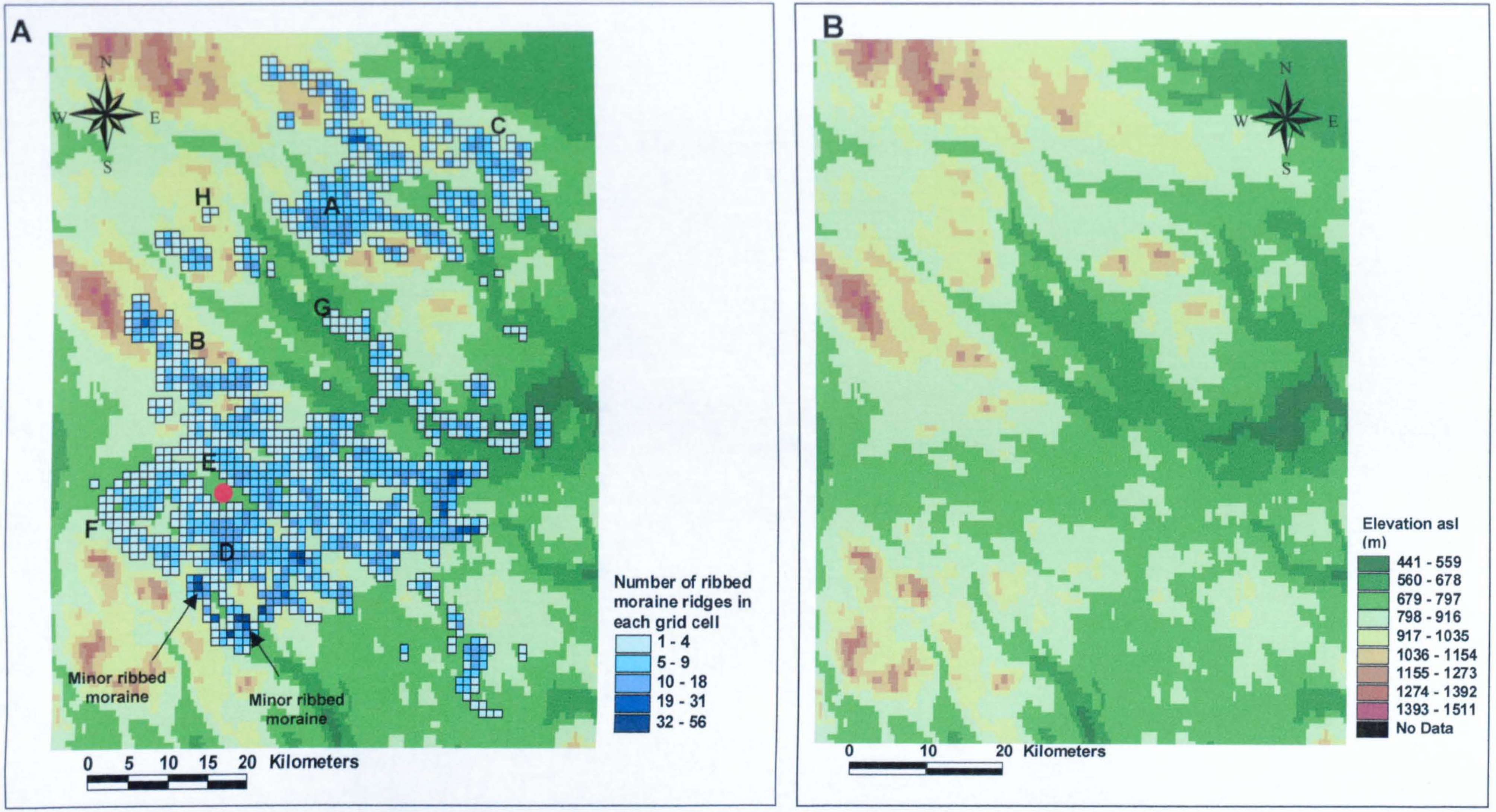

Figure 8.19. Showing the ribbed moraine density map draped on top of the DEM (A) and the DEM on its own (B) to allow visual comparison between wavelength and topographic setting. This analysis firstly showed that most fields were made of ribbed moraine ridges of mixed wavelength, although some large tracts of ribbed moraine ridges with similar wavelengths are located in and around Lake Rogen. It also showed that topography did not appear to control ribbed moraine wavelength, as ribbed moraine with both short and long wavelengths can be observed in a variety of topographic settings.

8.6.2. Ribbed moraine ridge length

Data on the length of the ribbed moraine ridges was obtained by the methods described previously in Section 5.6.2. Figure 8.20 shows the histogram made using these length data in this study area and it can be seen that 95 % of the ridges are between 100 m and 1250 m. The shortest ridge measured was 40 m long, the longest ridge was 2344 m, the mean length of the ridges was 393 m and the mode was 193 m.

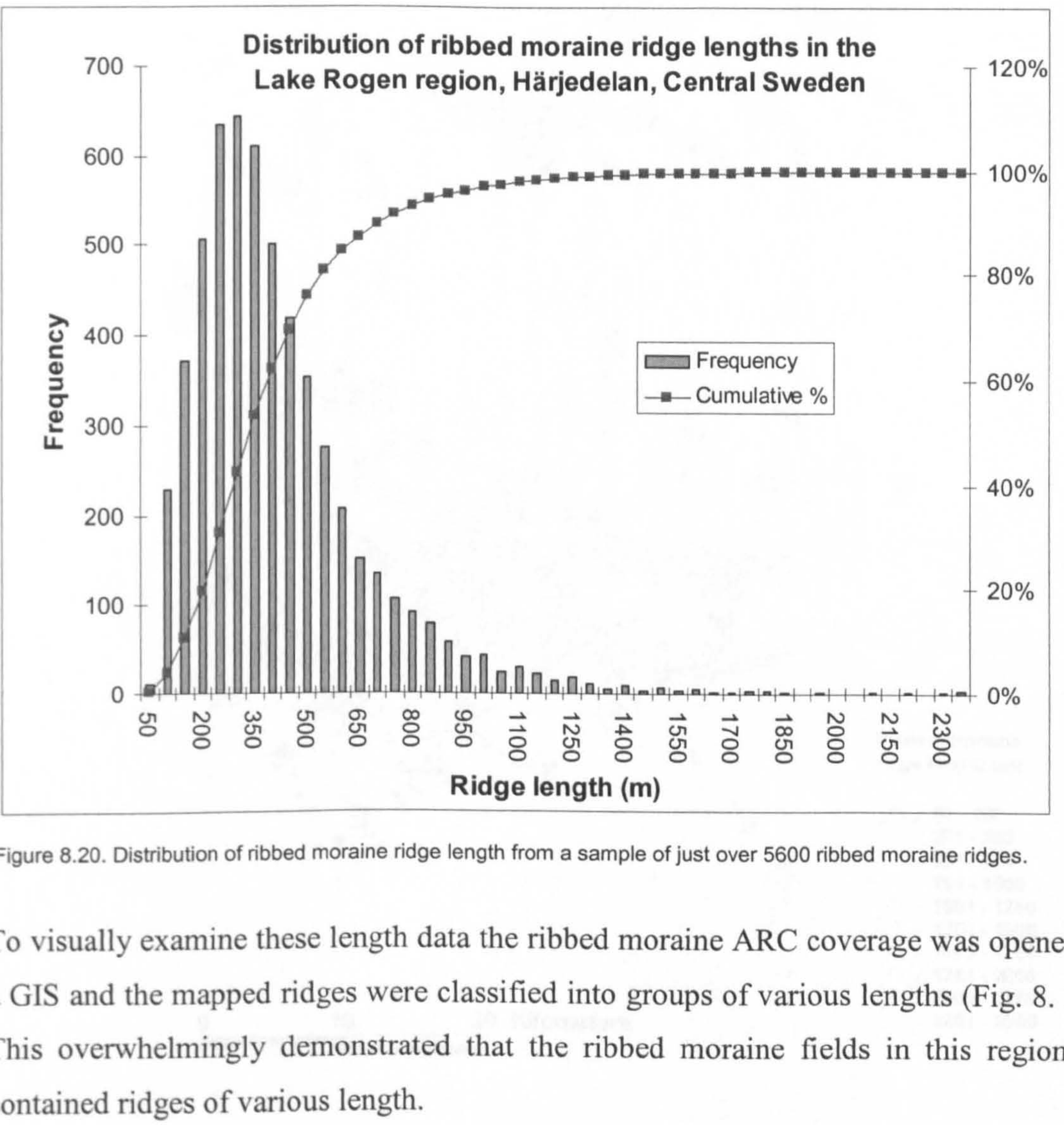

Figure 8.20. Distribution of ribbed moraine ridge length from a sample of just over 5600 ribbed moraine ridges.

To visually examine these length data the ribbed moraine ARC coverage was opened in a GIS and the mapped ridges were classified into groups of various lengths (Fig. 8. 21). This overwhelmingly demonstrated that the ribbed moraine fields in this region all contained ridges of various length.

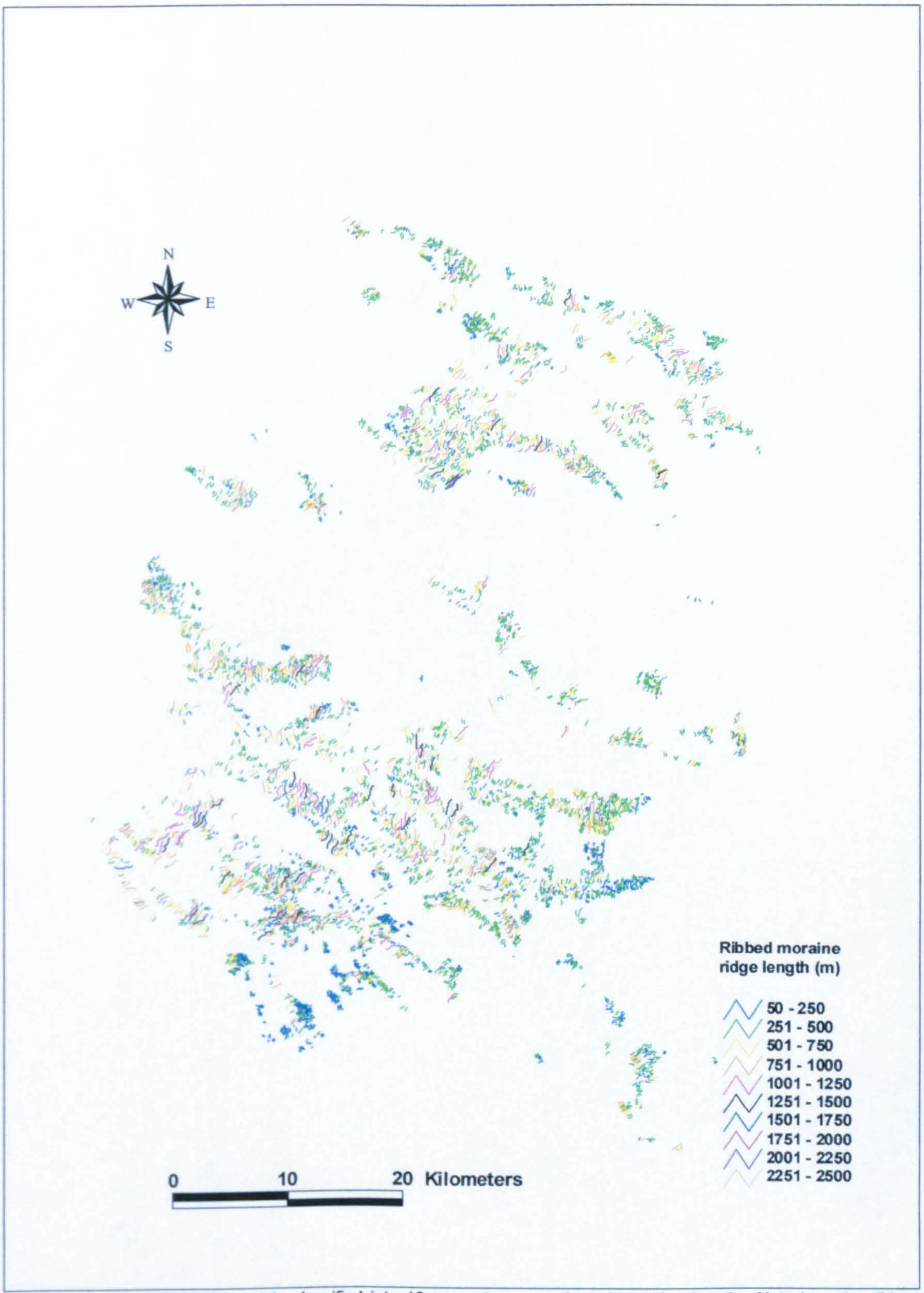

Figure. 8.21. Ribbed moraine crests classified into 10 separate groups based on ridge length. Note how the ribbed moraine fields are made of ridges of different length and that there is no particular area in the site where one can observe ridges of a standard length.

8.6.3. Ribbed moraine ridge width

To investigate the width of the ribbed moraine ridges in this locality 250 ridges were randomly sampled from various locations across the site. The width of the ridge was measured following the procedures outlined in Section 5.6.4. Figure 8.22 shows the resultant histogram. In this sample, 99% of ridges are between 30 m and 285 m wide. The minimum ridge width was found to be 17 m, the maximum 334 m and the mean ridge length was 143 m.

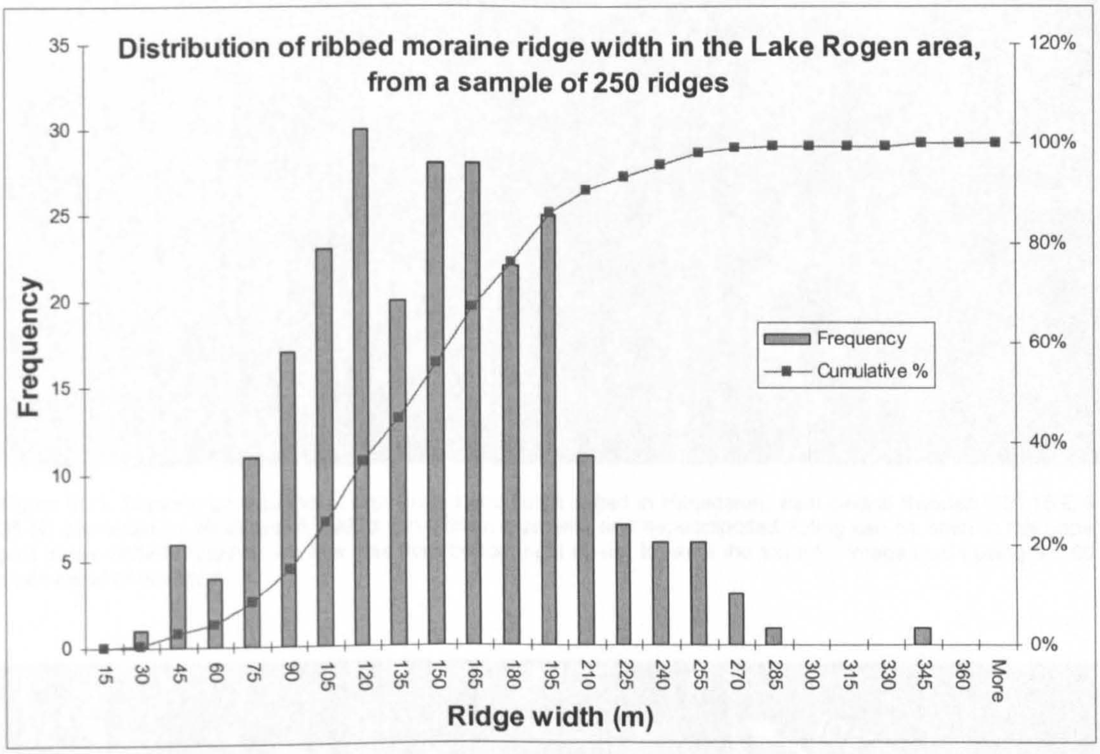

Figure 7.22. Distribution of ridge width in the Lake Rogen region. 97% of the ridges in this area are between 40 and 500 m wide, with the Maxima being 250 m.

8.7. Relation to other landforms

8.7.1. Ribbed moraine, drumlins and glacial lineations

Ribbed moraine in Härjedalen has been studied for some time now and the relationships between ribbed moraine and other subglacial bedforms are well documented (Lundqvist, 1969; Lundqvist 1989; Markgren and Lassila, 1980; Hättestrand and Kleman, 1999). All of these authors state the presence of drumlinoid elements within ribbed moraine fields and fluting of the ridges as being common characteristics of the ribbed moraine in this region (Fig. 8.23). Visual inspection of the ribbed moraines in this site supports these observations. However, most ridges were not drumlinized to the same degree as those presented by Hättestrand and Kleman (1999) (Fig 8.23), the more usual case was to observe ribbed moraine fields with small drumlinoid elements and weakly fluted ridges (Fig. 3.24).

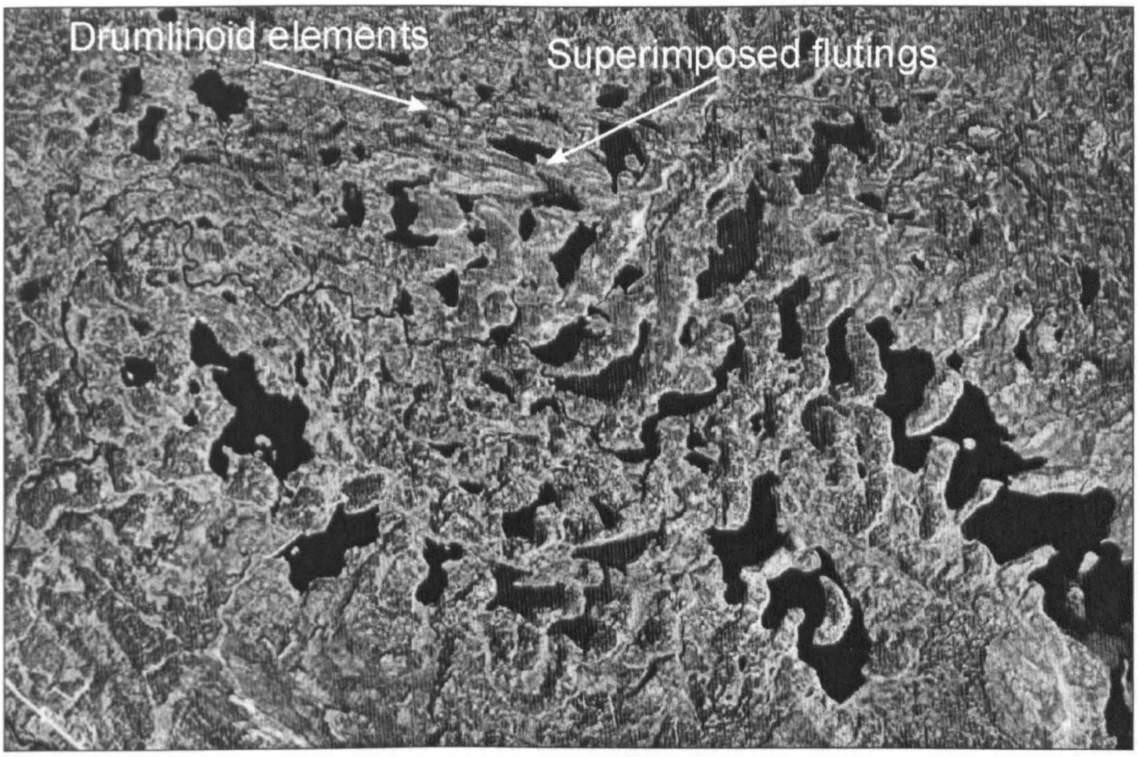

Figure 8.23. Showing an example of drumlinized and fluted ribbed in Härjedalen, west-central Sweden (12° 16 E & 62° 35 N) presented by Hättestrand, 1997b. Drumlinoid elements and superimposed fluting can be seen in the upper left part of this ribbed moraine. Ice flow was from bottom right corner towards the top left. Image made using a 1:60 000 scale aerial photograph.

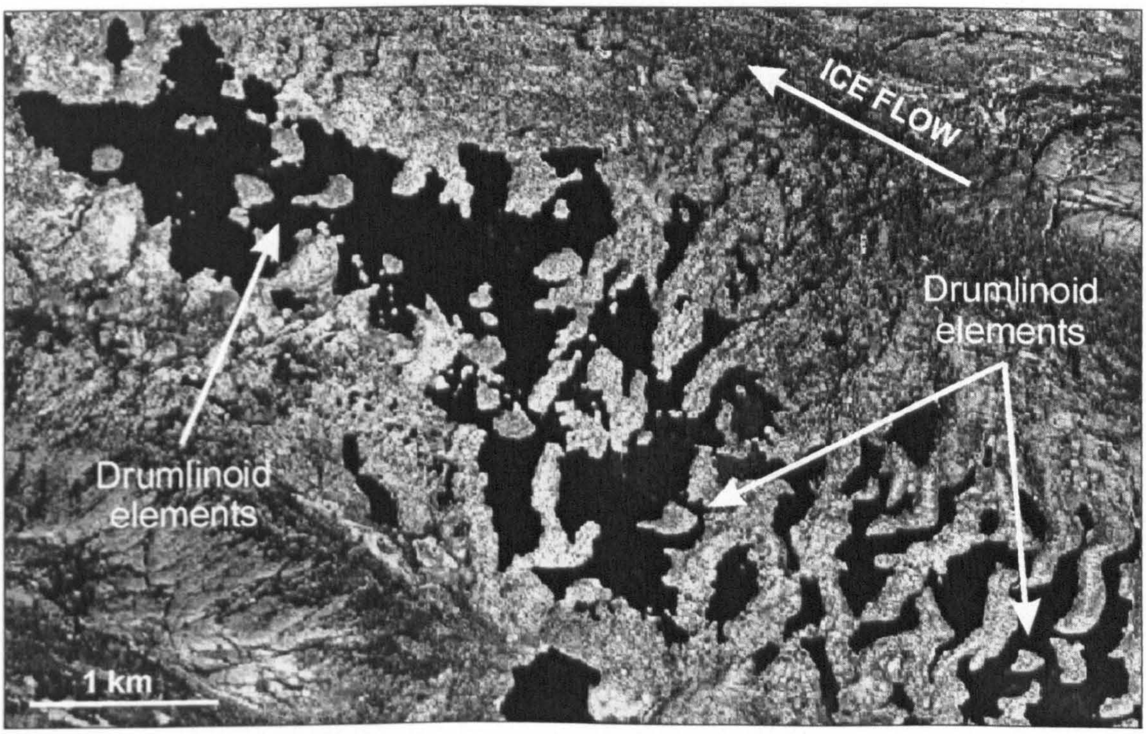

Figure 8.24. This ribbed moraine field situated on the northern shores of Lake Rogen (12° 21 E & 62° 22 N) contains some examples of drumlinoid features. Note, that they are usually quite small compared to the ribbed moraine ridges. Image made using a 1:60 000 scale aerial photograph.

Regarding the relationship to drumlins, Lundqvist (1989) argues the most characteristic feature of the ribbed moraine at Lake Rogen is their gradual transition into drumlins. In areas where this transition occurs, Lundqvist (1989) insists that the landforms be referred to as "Rogen moraine", named after the type locality at Lake Rogen, as he sees this drumlin/ribbed moraine relationship as being rather unique. However, it has been convincingly argued by Hättestrand (1997b) that the various types of ribbed moraine reported in the literature, for example Blattnick moraine and Rogen moraine, are in fact one genetic landform and therefore do not warrant a special category. According to Lundqvist (1989), the transition is not necessarily seen in every individual ridge, but in each tract of Rogen moraine there should always be streamlined forms, flutings and transitions into drumlins. He argues that the transition between Rogen moraine and drumlins may take place in different ways, but the most important one is where short crescent-shaped drumlins line up side by side to form ridges at right angles to the drumlins (Fig. 8.25). He further states that the Rogen moraine is found essentially in valleys (in the direction of ice flow) while drumlins occur on convex ground between the valleys and on valley slopes above the Rogen moraine, and that this takes place repeatedly from one valley to another. However, extensive observations conducted at this site do not support these assertions as this topographic sequence was only observed in one place across the entire site (Fig. 8.26). Although some fields contained drumlinized ribbed moraine and fluted ridges and a few fields did have glacial lineations nearby, it was more usual just to see ribbed moraines on their own (Fig. 8.27). It is not certain whether this study site covers the same area as that used by Lundqvist (1989) where he reports seeing the transition. However, considering the imagery used for this site covers an extensive area around Lake Rogen (3600 km^2), and that this area is the type locality for Rogen moraine, then one would expect to see many examples of this transition. However, it was only observed once at this site (see Figure. 8.26). Therefore, based on this investigation, it is apparent that there is not the strong relationship between ribbed moraine and lineations that Lundqvist reports, and that this relationship should not be taken as a valid generalisation as it is based on too few occurrences.

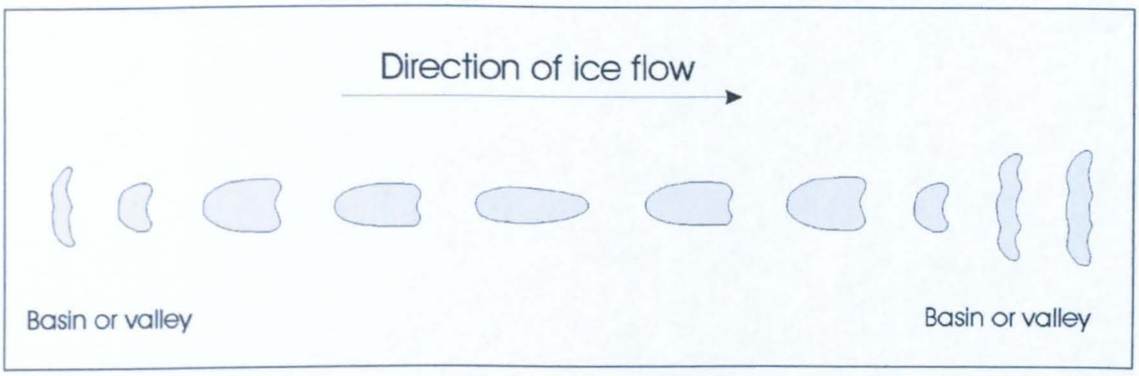

Figure 8.25. Schematic representation of the most important transition between Rogen moraine and drumlins (After Lundqvist, 1989). According to Lundqvist, the transition takes place repeatedly upglacier as well as downglacier, following the terrain forms.

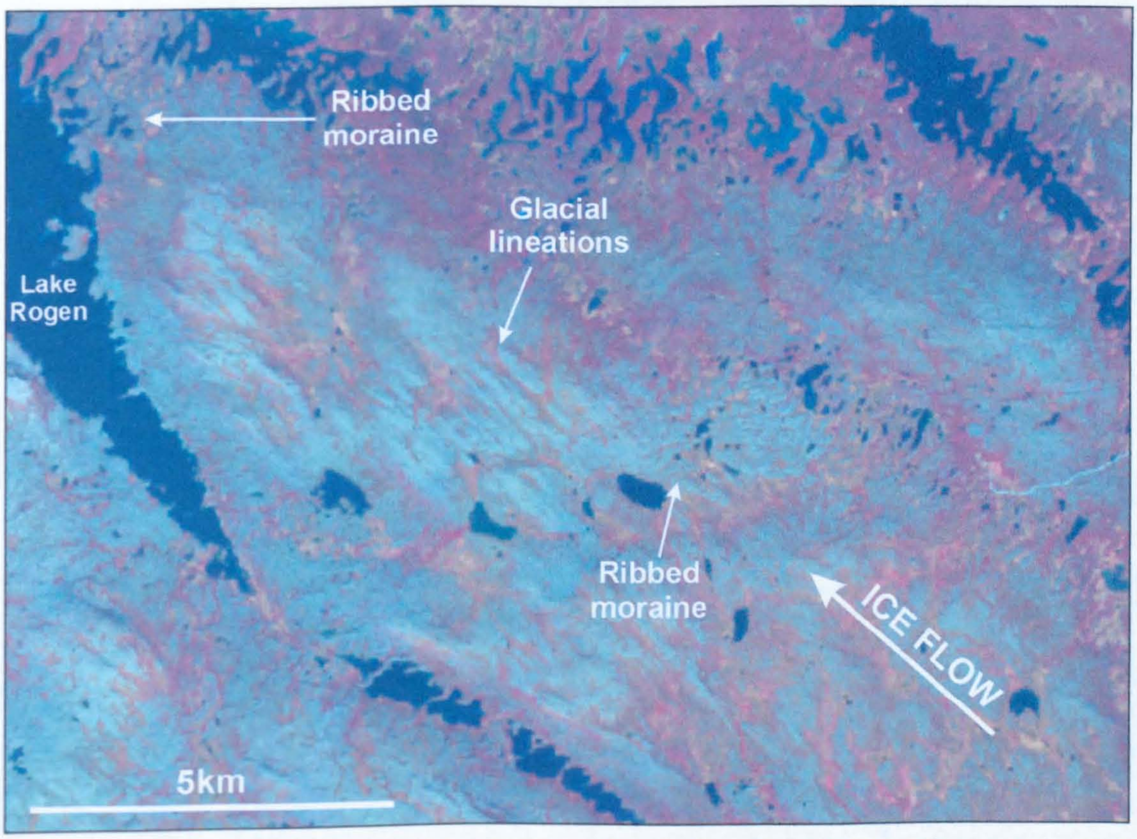

Figure 8.26. The area immediately east of Lake Rogen was the only place where glacial lineations were observed. Considering that ribbed moraine fields are situated in both a downstream and upstream position in relation to the lineations, it could be argued that this is an example of the transition described by Lundqvist (1989) whereby ribbed moraine in valleys are replaced by glacial lineations on convex ground. Picture taken from ASTER satellite image.

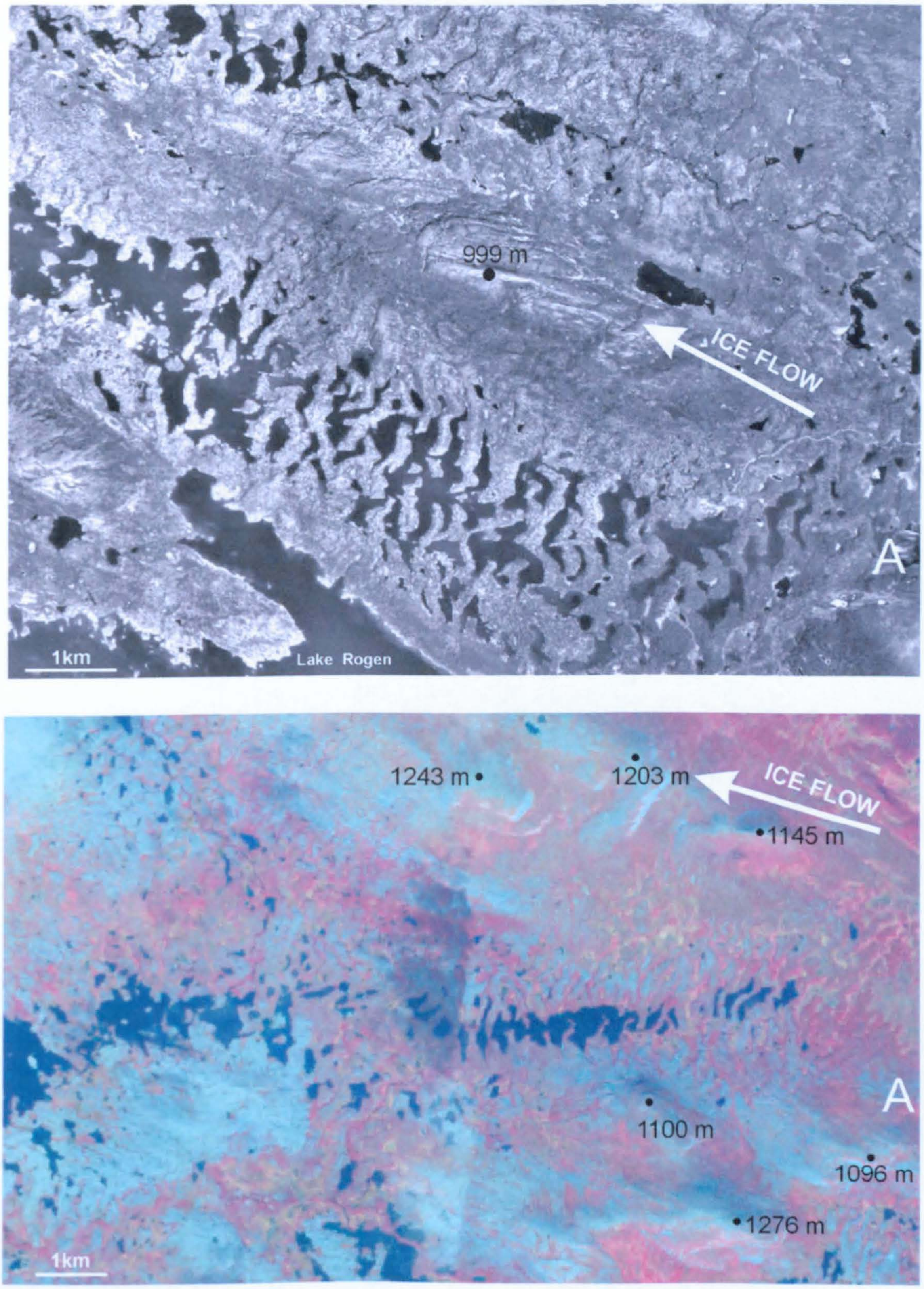

Figure 8.27. Showing two large tracts of ribbed moraine running along valleys in quite mountainous terrain in Härjedalen. According to Lundqvist (1989), drumlins should be seen at the start and at the end of each valley and also on the slopes above the ribbed moraine. The image at the top is a 1:60 000 scale aerial photograph showing the ribbed moraine located at Lake Rogen (12° 21 E & 62° 22 N). The image at the bottom is an ASTER image of a long valley 10 km north of Lake Rogen (12° 20 E & 62° 26 N). The start of each valley is marked by the letter A. Note that in both cases there are no drumlins at the start of each valley, but rather well formed ribbed moraine ridges. Note also that although there are some drumlinized ridges and some fluting on the hillsides, drumlins are not located on the hill slopes above the ribbed moraine and there are no drumlins in the downstream end of each valley.

8.8. Summary and conclusions

Mapping the ribbed moraine ridges in the Lake Rogen area established that the ribbed moraine was produced synchronously during a single ice flow event (see Figure 8.2). The large-scale distributional pattern demonstrated that the fields were concentrated in the southern and northern parts of the site and that the central region lacked significant numbers of ribbed moraine. The ribbed moraine fields in this locality were generally small and the largest fields in the Lake Rogen area were found to be approximately half the size of the largest fields observed in Canada and Ireland.

Close inspection of the site revealed that the ribbed moraine was distributed in a similar fashion as the ribbed moraine fields observed in Québec. These were elongate ribbons and narrow tracks, clusters and isolated fields. The field types were not restricted to any particular part of the study site and examples of each field type could be seen at various locations across the site.

As was shown in Section 8.4 the ribbed moraine in this region displays many of the characteristic morphological features of ribbed moraine (see Figures 8.9 & 8.10). However, just like the ribbed moraine ridges observed at the other three sites, the ridges in this region also display a range of morphologies that conflict with the classic description. In the examples presented above, which also included the smallest known ridges called minor ribbed moraine, it was possible to identify a wide range of ridge morphologies including barchan ridges, broad straight forms, and ridges that were concave in the up ice direction.

Using a DEM to investigate the topographic setting of the ribbed moraine in this region concluded that the majority of ribbed moraine fields were located in areas of open undulating terrain and in the valleys and valley slopes that run through the site. Generally, ribbed moraine was lacking high up on mountain slopes and none were found on mountaintops. Visual inspection of the site using stereo aerial photographs concluded that the tops of the mountains in this region were mainly rocky and lacked even a thin covering of till. It may have been the case that these higher elevations would have been subject to aerial scouring leaving a limited sediment supply for the process to work efficiently. The valleys and areas of open ground on the other hand would have acted as sediment sinks and an abundant sediment source in these areas would allow the process to work more effectively. The fact that the majority of ribbed moraine are found in these areas lends support to this idea (see Figures 8.14 & 8.15). The slope aspect tests that were conducted showed that the distribution was not influenced by the direction the slopes were facing in relation to the regional ice flow. It concluded that 47% of the ribbed moraine population was formed on slopes that experienced compressive glacial stresses and 43 % of the population were formed on slopes that would have experienced extending glacial flow (see Section 8.5.2). Again, this contradicts the assertions made by several authors (e.g. Bouchard, 1980,1989; Minell, 1980; Sollid & Sørbel, 1984) as no preferential relationship was found between ribbed moraine occurrence and compressive slopes in this sample of 5637 ribbed moraine ridges.

Morphometric measurements conducted on ribbed moraine length and wavelength showed a wide variation in both parameters (see Section 8.6 & Table 8.1). Again, these were important findings, because formative theories need to account for this variation if they are to be considered credible.

Table 8.1. Showing the average value and the range for each measured ribbed moraine parameter in the study area

Parameter	Min	Max	Mean
Length (m)	40	2344	393
Width (m)	17	334	143
Wavelength (m)	12	817	202

Analysis conducted using a GIS, concluded that most fields contained ridges of mixed length and that ribbed moraine of both short and longer wavelengths was spread across the entire region. Procedures carried out in the GIS also showed that, apart from minor ribbed moraine which were always found on mountain slopes, there was no specific topographic setting where one could find ribbed moraine ridges of a certain wavelength, as ridges of various wavelengths were found in a range of topographic settings (see Figure 8.19).

Finally, the relationship between ribbed moraine and other glacial landforms was investigated. Several authors who have studied the ribbed moraine in Härjedalen state that the presence of drumlinoid elements within ribbed moraine fields and fluting of the ridges as being common characteristics. Visual inspection of the ribbed moraines in this site supports these observations. However, most ridges were not heavily drumlinized and the more usual case was to observe ribbed moraine fields with small drumlinoid elements and weakly fluted ridges (see Figure. 8.24). According to Lundqvist (1989), it should have been possible to observe ribbed moraines and drumlins in a variety of spatial relationships as well as seeing transitional forms. However, detailed visual inspection of the site failed to find many noteworthy examples. It seems that the strong spatial associations reported as being so characteristic in this region, may not be as strong as suggested by Lundqvist, and as such, should not be taken as a valid generalisation as they appear to be based on too few occurrences.

***

Map 8.1. Distribution of Ribbed Moraine, Lake Rogen, Sweden